Spring 2023

Selecting Consolidation Procedures for Making Concrete Specimens

Paige Marie Toebben
Missouri University of Science and Technology

Department:

SELECTING CONSOLIDATION PROCEDURES FOR MAKING CONCRETE SPECIMENS

by

PAIGE MARIE TOEBBEN

A THESIS

Presented to the Graduate Faculty of the

MISSOURI UNIVERSITY OF SCIENCE AND TECHNOLOGY

In Partial Fulfillment of the Requirements for the Degree

MASTER OF SCIENCE IN CIVIL ENGINEERING

2023

Approved by:

Dr. Dimitri Feys
Dr. Mohamed ElGawady
Dr. Thomas Schuman

ABSTRACT

The goal of this research was to reevaluate ASTM C31 Standard Practice for Making and Curing Concrete Test Specimens in the Field, as well as deepen our understanding of the relationship between the consolidation process, concrete composition, and workability. An improved understanding of this area will help to reduce variability in concrete quality. The project involved evaluating the effect of different consolidation methods on concrete specimens with changing levels of workability. To do this, concrete cylinders were created with varying viscosities by adjusting the water-to-cement ratio (w/c) and water-reducing agent. More cylinders were created with varying paste volumes while keeping the paste composition and aggregate gradation constant. Then cylinders with different gradations were created. The consolidation methods used in this experiment were rodding and vibrating. Both methods were used, with a wide range of amounts of consolidation energy, on all concrete mixtures. All cylinders were tested for segregation, which indicates over-consolidation. They were also tested for saturated surface-dry (SSD) density and compressive strength, as an indication of if the cylinders were under-consolidated.

ACKNOWLEDGMENTS

I would like to express my gratitude to all those who have helped me in some way to write this thesis.

Firstly, I would like to thank my advisor Dr. Dimitri Feys, who introduced me to research as an undergraduate and has consistently supported me in my research journey. I am very grateful for everything he has taught me both academically and professionally.

In the same manner, I would like to thank Dr. Thomas Schuman and Dr. Mohamed ElGawady. Even though our meetings were less regular, your feedback and guidance have been of value to me.

My appreciation also goes out to many individuals from the civil engineering department of Missouri University of Science and Technology who have aided me in this research.

Lastly, I would like to thank my husband, family, and friends for their personal support.

TABLE OF CONTENTS

Page

LIST OF ILLUSTRATIONS

Page

LIST OF TABLES

Page

NOMENCLATURE

Symbol	Description
w/c	Water-to-Cement Ratio
ASTM	American Society for Testing Materials
VMP	Vibrations per Minute
SCC	Self-Consolidating Concrete
SCMs	Supplementary Cementitious Materials
MCR	Modular Compact Rheometer
ACI	American Concrete Institute
τ	Shear Stress
Pa	Pascal
$\tau 0$	Yield Stress
μ	Plastic Viscosity
s	Second
$\dot{\gamma}$	Shear Rate
PC	Portland Cement
C_3S	Tricalcium Silicate
C_2S	Dicalcium Silicate
C_3A	Calcium Aluminate
C_4AF	Calcium Aluminoferrite
Ca^{2+}	Calcium
OH^-	Hydroxide

SO_4^{2-}	Sulfate
SiO^{4-}	Silicate
$C_6AS_3H_{32}$	Ettringite
C-S-H	Calcium Silicate Hydrates
CH	Calcium Hydroxide
nM	Nanometer
C_3ASH_{12}	Monosulfoaluminate
kg	Kilogram
m	Meter
hr	Hour
lb	Pound
Ca	Capillary Number
mm	Millimeter
VMA	Viscosity Modifying Admixture
HRWRA	High-Range Water-Reducing Admixture
CaO	Calcium Oxide
SiO_2	Silicon Dioxide
AL_2O_3	Aluminum Oxide
ft	Foot
Nm	Newton Meter
lbf	Pound-Force
Tmax	Maximum Torque
K	Constant Relating Torque to Vane Geometry

r	Radius of Vane
psi	Pounds per Square Footpounds per square foot (
CSV	Control Speed Vibrator
ACML	Advanced Materials Characterization Lab
SSD	Saturated Surface Dry (SSD)
RDSSD	Saturated Surface Dry Relative Density
MSSD	Mass of Saturated Surface Dry Sample
MSSD	Mass of Sample in Water
HRC	Hardness Rockwell C
mL	milliliter
SO_3	Sulfur Trioxide
$CaCO_3$	Calcium Carbonate
CO_2	Carbon Dioxide
CO_3^{2-}	Carbonate
Na_2O	Sodium Oxide
K_2O	Potassium Oxide
LOI	Loss on Ignition
T	Torque
Ri	Radius of Inner Cylinder
h	Height of Material
k	Constant Relating Radius of Inner and Outer Cylinder
Ω	Omega
N	Velocity

n	Constant Relating Slope of Natural Log of Torque and Omega
c	Fitting Constant
Ro	Radius of Outer Cylinder
G	Intercept of T-N Relationship
H	Slope of the T-N Relationship
τRo	Shear Stress Calculated from Torque
R_p	Radius of Plug

1. INTRODUCTION

1.1. PROBLEM STATEMENT

In 1914 Committee C-9 was formed to address the need for concrete standardization requirements [1]. In 1920, during the twenty-third annual meeting of the American Society for Testing Materials (ASTM) the tentative methods for making and storing specimens of concrete in the field was proposed. It was then adopted and published in 1921 [2]. This makes the procedure used to create concrete specimens over 100 years old. Furthermore, the vibration procedure for concrete specimens is at least 50 years old, having been presented in the 1966 version of ASTM C31 [3]. The vibration description in the ASTM is vague, outdated, and easily misinterpreted. The standard requires at least 9,000 vibrations per minute (VPM). However, recent research has shown that high frequency can cause fresh concrete to bleed [3].

These standards were written at a time when slump was a good representation of the strength of concrete. Historically, high slump was indicative of concrete with low strength and low performance. This is because, in the past, water was the only way to increase workability. However, concrete technology has evolved over the last century. Modern concrete is more intentionally designed with respect to paste volumes, water-to-cement ratios, aggregate gradations, and air contents. Chemical admixtures and supplementary cementitious materials have also been developed that can render a concrete mixture more workable without affecting its strength or performance. Furthermore, certain concrete mix designs have been developed that require completely different consolidation standards, such as self-consolidating concrete (SCC) which should

not be consolidated to avoid segregation [4]. On the other hand, roller-compacted concrete requires a much larger amount of consolidation energy, with some needing a vibrating hammer with a mass of 19 to 30 pounds and with 2000 ± 200 impacts per minute in order to be properly compacted [5]. As more carefully designed concrete, supplementary cementitious materials (SCMs), and admixtures become increasingly common, a re-evaluation of the optimum consolidation efforts is needed. The required consolidation energy should be dependent on the concrete characteristics, as insufficient consolidation will result in entrapped air and over-consolidation can cause segregation.

1.2. PROJECT OBJECTIVE

The objective of this research work is to revise the required consolidation efforts used to create concrete specimens and to perform fresh concrete tests to appropriately reflect the influence of workability. The goal of this project is to create different fresh concrete classifications and assign an ideal consolidation effort to each of them.

1.3. PROJECT SIGNIFICANCE

The significance of this research project is a better understanding of the relationship between consolidation, concrete composition, and workability. It reassesses the required consolidation needed for concrete specimens while taking into account the advances in concrete technology. This will reduce the variability associated with concrete testing and construction. In the future, knowledge from this project can be extrapolated to provide more specific requirements on consolidation energy for concrete placement. For example, based on the concrete specifications, it could be suggested which type of

vibrator should be used along with the amplitude, frequency, and duration. This could increase the practical implementation of different concrete types. It could also increase our understanding of consolidation efforts required in new construction techniques, such as 3-D printing. It would aid in predicting the concrete properties based on the consolidation history. The information generated by this project and subsequent research is essential to facilitate concrete consolidation automation or robotization.

1.4. PROJECT OVERVIEW

Consolidation is the process of reducing the voids in freshly mixed concrete by some sort of mechanical means. This process is needed because freshly placed concrete usually has entrapped air voids that, if not properly removed through consolidation, will cause the concrete to be porous, non-uniform, and have reduced strength and durability. If the concrete is over-consolidated, it is at risk of segregation and bleeding. It has been suggested that concretes with different levels of workability respond best to different amounts of consolidation energy [6]. This idea is what is being explored through this research project.

An indication of insufficient consolidation is an excessive amount of entrapped air. In order to quantify the amount of air that remained in the hardened cylinders, density and compression tests were performed in accordance with ASTM C127 and ASTM C39 respectively. An indication of over-consolidation is segregation. To check for segregation, an SCC penetration apparatus was used in accordance with ASTM C1712. Bleeding was also monitored visually.

For the purpose of characterizing the workability of the concrete, for every mixture, a representative paste sample was evaluated in the Anton Paar Modular Compact Rheometer (MCR) 72 for plastic viscosity. Additionally, as soon as the concrete was mixed and sampled, standard fresh concrete tests were conducted. These tests included temperature, slump, density, air content, and a static yield stress test. In order to evaluate the consequences of consolidation on concrete mixtures with different levels of workability, fourteen different mix designs with different water-to-cement ratios, paste volumes, aggregate gradations, and admixture types and quantities were produced. For every individual mixture, 54 cylinders in total were created. 18 different consolidation strategies were used, with the same consolidation strategy being used on three consecutive cylinders to determine statistical significance. The results for segregation, density, and compressive strength were compared to each other.

2. LITERATURE REVIEW

2.1. CONCRETE

Since its advent in 1824, the year of the patent, Portland cement concrete (PCC) has become the most used building material in the world [7]. Applications for the use of PCC range from roadways to parking lots, and structural members. The caliber of the concrete structures is dependent on the quality and quantity of each element in the concrete. These include coarse and fine aggregates, cement, and any admixtures or SCMs. It also relies on a proper consolidation effort being employed when the concrete is placed. The ideal level of consolidation is dependent on certain characteristics of the fresh concrete, including its workability. When using PCC, it is imperative to understand the relationship between the workability of the concrete and the ideal level of consolidation.

2.2. WORKABILITY AND RHEOLOGY

Concrete must be made at suitable consistencies, or it could result in an inability to properly place, consolidate, or finish the concrete. Inadequate consolidation could lead to many undesirable effects such as cold jointing and honeycombing if the concrete is under-consolidated, or segregation and bleeding if the concrete is over-consolidated. Therefore, having appropriate workability and rheological properties is imperative for creating concrete structures [7]. These properties are influenced by almost every aspect of the physical and chemical components in the concrete mix design. Some of these factors include the grading and shape of the fine and coarse aggregate, percentage of entrained

air, temperature, the quantity of cementitious material, SCMs, admixtures, and of course, the amount of water [8].

2.2.1. Workability. Workability is often described with qualitative and subjective terms such as consistency, cohesiveness, and flowability. Generally, it is a representation of how easily the concrete can be placed [9]. The American Concrete Institute (ACI) Standard 116R-90 (ACI 1990b) defines it as "that property of freshly mixed concrete which determines the ease and homogeneity with which it can be mixed, placed, consolidated, and finished."

2.2.2. Rheology. The rheological properties are based on the same forces that impact workability, such as the stability, mobility, and compatibility of the concrete [10]. However, the rheological properties are described with more quantifiable parameters, such as viscosity and yield stress. The term rheology was coined by Professor Bingham of Lafayette College, Indiana. It means "the study of the deformation and flow of matter" [11].

Rheology can be used to study many materials, both Newtonian and non-Newtonian. Concrete is a non-Newtonian material, meaning its viscosity is affected by the force being applied to it [12]. Through the study of rheology, quantifiable data on the workability of concrete such as the viscosity, yield stress, and thixotropy can be gathered.

The material's viscosity is its ability to resist an increase in flow rate after the flow has been initiated [11]. The viscosity affects the rate at which air can rise out of the concrete and how quickly aggregates can sink when the yield stress is exceeded. Dynamic yield stress is the minimum stress needed to maintain flow or transition from a

liquid-like behavior to a solid-like behavior [2]. These two rheological properties can be measured with a flow curve. To obtain a flow curve, the material is subjected to a high shear rate that progressively decreases to a lower rate [13]. When this method is used, an additional measurement, known as a pre-shear, is generally applied directly before the flow curve. The purpose of the pre-shear is to confirm that the material is in a uniform state and has the same shear history as samples it may be compared to [13]. It also breaks down structures that may have built up within the cement paste and ensures the material is in an equilibrium state when the flow curve is applied. The rate of the pre-shear is done at the same rate as the maximum shear rate of the flow curve [13]. After the flow curve is measured, the Bingham model is typically used to calculate the dynamic yield stress and plastic viscosity of concrete. This model draws a linear correlation between the shear rate and shear stress applied to the concrete. The most common way to collect the data needed for this model is by slowly decreasing from a high to low shear rate while monitoring the material's shear stress response [14]. The equation for this model can be seen below in Equation (1):

$$\tau = \tau_0 + \mu\dot{\gamma} \quad (1)$$

In this equation τ represents the shear stress applied in Pascals (Pa), τ_0 represents the dynamic yield stress in Pa, μ is the plastic viscosity in Pa*s and $\dot{\gamma}$ is the shear rate in s^{-1} [15]. Rheology can also be used to calculate static yield stress. The static yield stress can best be described as the point at which the stress applied to a system is enough to overcome the structure and induce flow [16]. This parameter can be determined by applying an increasing amount of low-shear stress. Initially, the concrete will not move

and the shear stress within the material will increase until enough force is applied to induce flow.

The yield stress is determined by the amount of internal structure within the concrete. The internal structure originates from a network of particles that are connected through flocculation and hydration. It builds up over time and has both a reversible and non-reversible component. The reversible component is caused by attractive interparticle forces that cause cement particles to flocculate, as well as the formation of weak hydration bonds that can be broken by shear. The irreversible component is caused by the formation of hydration bonds that are permanent [17]. Reiter et al. [18] found that the yield stress is dominated by flocculation for about the first five minutes into hydration. Roussel et al. [16] suggested that the reversible effects including flocculation and weak hydration bonds growing in the pseudo-contact points between cement particles may dominate for the first hour. Irreversible effects due to cement hydration dominate in later stages [19]. The rate of the yield stress evolution is dependent on the distance between the cement particles, which can be altered by dispersing admixtures, and the number of cement grain contact points, which can be influenced by the cement particle sizes and volume fraction [18].

2.2.3. History of Testing Workability and Rheology. Many test methods attempting to quantify workability have been developed over the years. Some testing methods have evolved to be very accurate in a laboratory setting but are physically impractical to be used in the field. Others have evolved to provide a great deal of information in the field but are not as accurate as laboratory techniques or are difficult to compare across testing methods [20].

Concrete has been used in the U.S. since the mid-1800s. Although some test methods for determining workability have been developed, during this time period, it was most common to use just enough water to allow the concrete to be rammed into place [21]. Trautwine described the consistency as “just sufficient to make a plastic paste” in order to fill the voids between the coarse aggregate [22].

In the 1920s, the slump test was used to measure the workability of concrete. This test method was first published by the American Society of Testing and Materials (ASTM) in 1922 as ASTM D138-22T. It is currently referred to as ASTM C143. However, slump only describes one aspect of workability, consistency [15]. While slump, or slump flow can be related to the yield stress of the concrete, another vital component affecting workability is plastic viscosity, which is not indicated by the slump test [15].

Powers tried to overcome the deficiencies in the slump test by developing the “remolding test” which is able to better measure the dynamic component of workability. In this test, a drop table is used. The number of drops needed to change the shape of a concrete cylinder into a wider cylinder is measured [15,21]. This test was adapted into other testing methods such as the flow table test, which was developed by Graf in 1933 [23]. In this test, a mold is filled with concrete and the sample is allowed to slump when the mold is removed. The table is then jolted in a controlled manner. The Vebe consistometer was another empirical testing apparatus that was developed from the remolding test. It was developed into a standard test method by ASTM C1170. In this test, a slump cone sample is placed within a cylinder on a base plate. When the cone has been filled with a sample it is removed, and the plate vibrates. The amount of time needed for the sample to conform to the shape of the cylinder is recorded [20]. This was

followed by test methods such as the V-funnel and L-box, which were intended to be used for highly flowable concrete [7].

The Wigmore consistometer was also developed to gain a clearer image of workability [15]. It consists of a container, compaction table, and a two-inch ball that is attached to a stem. The stem is mounted on the lid of the container. The container is filled with concrete and the compaction table is dropped eight times to consolidate it. The ball is lowered so that it is resting on the surface of the concrete. The table is then repeatedly dropped, and the number of drops required to lower the ball into the concrete is counted [8]. In the 1950s another apparatus that attempted to quantify aspects of workability such as consistency was developed. Known as the Kelly-Ball test, the apparatus consists of a six-inch diameter ball and stem that slides through the center of a stirrup. The legs of the stirrup rest on the concrete. The ball is slowly lowered onto the surface of the concrete. It is then released, and the depth of penetration is measured. It was adopted as ASTM C360 "Test Method for Ball Penetration in Fresh Portland Cement Concrete" in 1955 and discontinued due to lack of use in 1999 [8]. One huge benefit of this test was that it was able to be used in the field.

In the 1960s the Federal Highway Administration developed the Vibrating Slope Apparatus. This testing method attempts to evaluate the workability of low-slump concrete. To perform this test, a sample of concrete is placed on an inclined box. The box is then subjected to vibration, and the amount of concrete that falls off the box is measured. This is done at two different slopes and this information is used to calculate a workability index [20].

In the 1970s, tests that were able to be used in the field gained increasing interest and led to the development of the K-slump tester. It is a tube with a disk attached in the middle. The lower half of the tube is slotted and made of metal, while the upper part of the tube is plastic and has a measuring rod. The metal part of the tube is inserted into the concrete up to the disk. Concrete is able to enter the tube through the slots. After a minute has elapsed the measuring rod is slid down until it rests on the concrete within the tube. This reading is the K-slump. The device is then removed from the concrete, allowing some of the concrete to fall from the slots. The measuring rod is then lowered to the concrete that is still in the tube, this reading represents the workability of the concrete [8].

While the first commercial control strain viscometer was created by MacMichael in 1915, it took some time for this technology to be applied to concrete. The first attempt at using a rotational viscometer on concrete was made by Powers and Wiler in 1941 [21]. They attempted to test the dynamic component of concrete with a coaxial-cylinder rotational viscometer. In this test, the concrete was placed between two cylinders. The inner cylinder was closed and suspended in a bucket. The bucket acted as the outer cylinder, which contained concrete. The outer cylinder was rotated back and forth by a small angle [7]. The amount of torque necessary to prevent the rotation of the inner cylinder was measured. However, this was never developed into a standard test practice [15].

In 1983, Tattersall and Banfill classified concrete workability test methods into empirically and rigorously defined tests. Empirical tests were classified as those that only give results that can be interpreted in the context of the test method. These test results include slump, compaction factor, Vebe time, and flow table spread. Rigorously defined

methods were classified as those that give results in standard units of measurement such as viscosity and yield stress [24]. They believed workability should only be described with rigorously defined methods. They strove to develop rheological principles to measure the workability of concrete [15]. Tattersall initially used a modified food mixer to extract rheological measurements [7]. It was a modified version of the rotational viscometer, but it was larger and able to measure the viscosity of concrete, even given its heterogeneous nature. It did this by measuring the torque required to turn an impeller at different speeds while that impeller is submerged in the sample [15]. They used the Bingham model to represent the rheological behavior of concrete. This configuration became known as the Mk I. It was further developed into the Mk II and is used for highly workable mixtures. The Mk II was developed into the Mk III and was intended for lower workability concretes [7]. These devices used calibration techniques to extract ‘g’ and ‘h’ values, representing the intercept and slope in a torque (T) vs. rotational speed (N) diagram, respectively. These values can be converted into fundamental physical quantities such as yield stress and plastic viscosity, if the geometry is sufficiently simple [7]. These devices became known as two-point workability apparatuses [15]. Over the years this instrument has been revised into the rotational viscometers that are commercially available today such as the IBB rheometer, developed in 1994, and the RheoCad rheometer, developed in 1997 [25].

Some modifications of the MK III device have adapted the inner and outer cylinder surfaces to be serrated in order to avoid slippage. In the late 1980s, it was determined that the shear stress generated at the bottom of the inner cylinder was throwing off the measurements. To counteract this effect, the bottom of the inner cylinder

was altered so that it no longer registered torque [7]. This became the BML viscometer. Over the years the viscometer has been continuously improved on, with enhanced software, such as FreshWin, controlling the viscometer [7]. The successor of the BLM viscometer, the ConTec Viscometer 5, is still used today, as are other rheometers based on coaxial cylinder rheometers that have also been developed for testing concrete, mortar, and cement paste. A few of these include the FANN 35 Viscometer, Brookfield BF35 Viscometer, Anton Paar rheometer, 8-speed viscometer, and the NXNQ Rotational Viscometer [25].

2.3. FACTORS AFFECTING RHEOLOGY AND WORKABILITY

The consistency, cohesiveness, flowability, yield stress, and viscosity of concrete are dependent on a wide variety of factors such as the concrete mix proportions, the properties of each constituent, the amount of mixing time, the hydration age of the concrete, and additional ingredients such as admixtures and SCMs. This section will discuss only a few of these elements including hydration age, w/c, paste volume, aggregate shape, and gradation, as well as select admixtures and SCMs.

2.3.1. Time. Fresh concrete loses workability as time progresses. This is due to a combination of factors such as water loss due to evaporation and water absorption into the aggregate. However, the predominant cause is the chemical reactions that cause cement to hydrate. To recognize how the hydration process impacts the yield stress and viscosity of the cement, it is important to understand how cement hydrates.

The hydration process begins as soon as Portland cement (PC) is mixed with water. Directly after the cement and water have been mixed, the system is in a purely

dispersed state where chemical reactions do not have an impact on the yield stress or viscosity. Within a fraction of a second, the cement grains begin to dissolve. The cement grains are made up of compounds such as tricalcium silicate (C_3S), dicalcium silicate (C_2S), calcium aluminate (C_3A), and calcium aluminoferrite (C_4AF). These are also intermixed with a sulfate source such as gypsum. The surface of cement grains, composed of a variety of compounds, is charged both negatively and positively in different areas of the grain. This contributes to cement grains being attracted to one another. Within a few seconds of water being added, colloidal attractive forces encourage cement particles to flocculate. As the grains and sulfate ions dissolve, they release Calcium (Ca^{2+}), Hydroxide (OH^-), Sulfate (SO_4^{2-}), and silicate (SiO^{4-}) ions. This leads to an increase in the ion concentration of the paste [26]. As the water reacts with (C_3A), an aluminate-rich gel is formed within the flocculated cement particles. The gel reacts with calcium sulfate in the solution to form ettringite ($C_6AS_3H_{32}$). Ettringite is a long crystalline material that is only stable in a solution with gypsum [26]. While ettringite is being formed, the C_3S is dissolving and releasing additional ions. After the initial C_3A reaction, ions from the C_3S begin to react with water to form calcium silicate hydrates (C-S-H) and calcium hydroxide (CH) compounds [27].

As the Ca^{2+} concentration in the system exceeds 1 nM the pH level rises above 10. C-S-H is less soluble than C_3S, and as the solution becomes supersaturated with respect to C-S-H, it begins to precipitate [28]. During this time, the cement particles continue to flocculate. The probability of C-S-H growth is higher in areas that are supersaturated with the ions released by the C_3S [29]. Due to the proximity of multiple ion-releasing cement grain surfaces, the pseudo-contact zones between the grains within

the flocculants become an ideal place for C-S-H to nucleate [16]. Roussel et al. [16] states that this begins happening within a couple of tenths of seconds after water has been added to the cement. The C-S-H nuclei begin to grow within the aluminate-rich gel from the C_3A reaction. The gel is elastic, cohesive, and porous. It gains its strength partially through attractive forces. During this time colloidal surface interactions determine the strength of the network. At this point, the hydration products are not forming rigid bonds. However, they do fill the pore space that was previously occupied by water [16].

After the initial desolvation, the precipitation rate decreases, and the concrete enters the dormant stage. It is during this dormant state that most concrete is placed, consolidated, and finished. During this phase the concrete hydration is still progressing, just much more slowly.

The C-S-H is highly charged and able to adhere to other C-S-H bonds, partially due to electrostatic interactions. Because the C-S-H is charged, as it precipitates it forms on the C-S-H nuclei that already exist within the system, as well as the gel around the cement grains [30]. C-S-H grows out from these points and starts to form a complex system of C-S-H bridges between the particles in the paste. This turns the soft colloidal interactions into C-S-H bridges. While this is happening, attractive forces within the cement paste are causing the cement particles to continue to flocculate. As C-S-H grows on and around these flocculated cement particles, compact sub-microstructures, often referred to as agglomerations, are formed. After about 30 seconds, the network of particles within the agglomerations starts to become connected [16]. This is referred to as a percolation path. These networks can resist stress. As the size and number of bridges increases, the yield stress and viscosity also increase.

After about 100 seconds the system can be seen as cement particles interacting through rigid connections due to the C-S-H that has nucleated in the contact zones between these particles. The diameter of these bridges is in the size range of a couple of nanometers, whereas the cement particles are in the order of 10 micrometers [16]. Stress and strain forces concentrate in the bridges, making them easy to break. As C-S-H continues to precipitate, the gel agglomeration evolves. It becomes a stronger, denser, structure that shares many contact points with neighboring particles. The interparticle network grows and thickens, providing more and more structure to the paste. The C-S-H particles continuously create new, stress-bearing, links between the cement grains that increase the connectivity of the microstructure [27]. This is why even within this dormant period; the yield stress and viscosity continue to increase. This was verified by Roussel et al. [16] who observed an increase in critical strain and proved this can be linked to the increase in the size of the C-S-H particles. The study looked at the same cement paste for times between 10 to 60 minutes after the initial mixing. They found that the C-S-H particles increased in size from 150 nanometers to 600 nanometers over 50 minutes. The critical strain needed to disrupt the formations increased as C-S-H particles grew in size [16].

After the end of the dormant period, the dissolution rate of C_3S increases, and the acceleration period begins. There are a couple of different ideas to explain this accelerated dissolution. Juilland et al. [31] observed the formation of etch pits on the surface of C_3S at the end of the dormant period. They suggest that this increased surface area may help explain the increased dissolution rate. During this time the yield stress and viscosity of the cement paste begin to rapidly increase. This implies that the system is

becoming more rigid. Bogner et al. [26] suggests that this is caused by the C-S-H bridges beginning to thicken and fully span the interparticle distances between cement particles. According to Bellotto et al. [27] this increase can also be associated with pore refinement. The C-S-H particles create linkages between the cement grains which forces the agglomerates to decrease in size. On a microscopic level, this means that the pores are refining, with large pores decreasing in volume and the number of small pores increasing. The evolving network becomes stronger and has an increased ability to transmit stresses, which causes an increase in yield stress.

After the acceleration period, the hydration of the cement enters the deceleration period. During this time all the gypsum has been consumed, and the ettringite becomes unstable. It reacts with any remaining C_3A to form monosulfoaluminate (C_3ASH_{12}). The C_2S also hydrates to form additional C-S-H and heat. The pore size distribution becomes even denser as more C-S-H precipitates onto it. The microstructure of the paste becomes more refined, and pores in the cement decrease in volume [32]. The C-S-H is ultimately what binds everything together, and its microstructure controls the mechanical properties of the hardened concrete. The concrete will now finish the hydration process and reach its final strength over the course of a few weeks.

2.3.2. Water to Cement Ratio. The w/c used in concrete has a huge impact on the fresh and hardened properties. For cement to completely hydrate only a w/c between 0.22 to 0.25 is needed [33]. Typically, more water is present to ensure the concrete has adequate workability [34].

The addition of water greatly alters the rheological characteristics of the concrete, decreasing both the yield stress and the viscosity. This is because as more water is added

to the system, the cement particles are spaced further apart. This increases the time needed for the cement particles to flocculate. For a given time there will be less flocculation-induced connections formed in a cement paste with a higher w/c. The presence of fewer flocculation connections means that there are fewer interparticle interactions. This is what causes the lower yield stress. Furthermore, the increase in water will result in the volume fraction of particles being lower, which will directly result in a decrease in viscosity [35]. The physical distance between the particles will also cause the hydrates to take more time to overlap. This will not slow down the rate of hydrate production, but it will decelerate the increase in yield stress and viscosity due to the lower number of connections [36].

The w/c also has an impact on the characteristics of the hardened cement paste. Reducing the amount of water will cause the paste to have a higher density. This, in turn, will result in specimens having higher compressive strength and lower permeability [34, 37]. One reason for this is that the strength of concrete is proportional to the gel/space ratio in the fresh concrete, which is controlled by the water-to-cement ratio [38]. Additionally, as the w/c is increased, there are fewer cement particles in a given volume of concrete, and therefore, less hydrates in that volume. This creates more water-filled pore space between the grains. This water will eventually evaporate and become pores that increase the permeability of the concrete, thereby decreasing its strength.

The aggregates used can also influence the final w/c of the concrete. When dry aggregates are used to make concrete, they absorb some of the water, leading to a loss of workability over time. About 70-80% of the volume of concrete is made up of aggregates, making their impact on the properties of concrete substantial. Most

aggregates absorb an amount of water that is equivalent to 1-2% of their weight [39]. The water absorption rate is high when the water is first introduced to the aggregate. However, after about 15 minutes the effect substantially decreases. This is partially because the dry aggregates become coated with cement paste, which prevents the water from continuing to absorb into the aggregate [39]. The amount of water the aggregates absorb in 24 hours can be calculated by ASTM C127. However, this is not entirely reflective of how much water is absorbed by the aggregate between the time water is added to the concrete and the concrete setting. According to ASTM C192, the amount of water that is absorbed by the aggregate before the concrete sets is about 80% of the difference between ASTM C127 and ASTM C566, which is used to calculate the amount of water in the pores of the aggregate in their room-dry state.

Evaporation can also alter the w/c of the concrete, leading to a loss in workability over time. The rate of evaporation increases as the temperature increases and is proportional to the amount of exposed surface area of the concrete. Some evaporation is unavoidable, however too much can have a detrimental impact on the concrete. According to ACI 308, if the rate of evaporation exceeds 1 $kg/m^2/hr$ (0.2 $lb/ ft^2/hr$), action must be taken to slow the evaporation, or the concrete is at risk of plastic shrinkage [40].

2.3.3. Paste Volume. The volume of cement paste can have a large impact on the properties of concrete. Cement paste is the lubricating medium between aggregates which facilitates flow. Different paste volumes are used for various purposes. If the paste volume is high, the concrete will be more flowable and will be well-suited for placement around dense reinforcement [37]. A low-paste volume concrete may be used for improved dimensional stability and sustainability [10, 37]. In an even lower paste

volume, voids between aggregates may not be adequately filled. This reduces the hydrate bonds between the aggregates and will lower the strength of the specimen. However, this is ideal for pervious concrete [11, 37].

Paste volume affects the rheological characteristics of fresh concrete. Providing all other factors remain constant, as the volume of cement paste decreases so does the workability [41]. Changing the paste volume also has an impact on the compressive strength of concrete specimens. The lower the paste volume is, the smaller the mean distance between two adjacent aggregates is, and therefore, the higher the strength is. Chu [41] found that with an increase in cement paste volume, the 28-day strength of the concrete decreases. This is attributed to the fact that cement paste contributes greatly to the porosity of the concrete [42]. If a volume of aggregate is replaced by a volume of cement paste the concrete as a whole becomes more porous. Furthermore, cement paste has a lower elastic modulus than aggregate, making it a weak point. The paste-aggregate interface is often where the concrete will fail. In concrete specimens with a very low paste volume, when the cylinder is breaking, the crack that forms must follow a longer path around a greater number of aggregates. This makes the energy absorption higher. When the volume of the paste is higher, the volume of the aggregates decreases and the length the crack has to travel is straighter and thus shorter. This causes the energy absorption to decrease [42].

The paste volume may also influence the amount of consolidation that is ideal for a given concrete. This is because paste volume impacts the vibrational energy transfer between the aggregates [41]. A study done by Chu [41] compared the uncompacted wet density of various concrete mixtures to the compacted wet density. The uncompacted wet

density refers to the mass of the partially compacted concrete sample in the container divided by the capacity of the container. The compacted wet density is the mass of the fully consolidated concrete sample in the container divided by the capacity of the container. The difference increases as paste volume decreases, emphasizing the importance of the consolidation process at low paste volumes [41].

When determining the appropriate paste volume for a given concrete it is important to keep in mind that paste demand is heavily impacted by variables associated with the aggregates, such as the gradation, texture, size, and angularity. All of these factors influence the void content between the aggregates, which in turn affects the amount of paste needed to maintain the same level of workability [43].

2.3.4. Aggregate Characteristics. The characteristics of the aggregates such as shape, size, gradation, and surface texture all have a significant impact on the rheology and workability of the fresh concrete [43]. Not only do these factors alter the paste volume needed to fill the voids between the particles, but they also influence how the aggregates are able to move through the concrete, the degree of friction between the aggregates, and the ability of the aggregates to interlock [43].

The angularity of the coarse aggregates is one of the factors that play a role in the workability of the concrete. Angular aggregates contribute to a higher degree of friction and aggregate interlock. This reduces the motion of the aggregate in fresh concrete and consequently leads to higher yield stress and viscosity [43]. This property also contributes to the amount of sand needed to maintain the same level of workability. Flaky, angular, elongated, or rough particles create more voids within the concrete. Therefore, more sand is needed to fill the voids. These additional voids also contribute to

increased water demand [20]. Similarly, smooth and spherically shaped coarse aggregates decrease yield stress and viscosity and improve workability [44].

The shape of the sand particles also has a significant impact on the workability of the concrete. Spherical particles have significantly less surface area than elongated particles [20]. Therefore, they have a lower paste demand [20]. Much like coarse aggregate, more angular sand particles will increase the friction in concrete as well as the amount of voids [20]. This will increase the water demand of the concrete.

The gradation of the aggregates used also has a large impact on the yield stress and viscosity of concrete. This has to do with the packing density that can be achieved. Packing density refers to the amount of space in a given volume that is filled with particles. For particles that are all the same size, only a certain amount of space can be filled, this is the maximum packing density. As a wider range of particle sizes is incorporated into the volume the smaller particles are able to fit in the gaps left by the larger ones, and the maximum packing density increases. An optimal aggregate gradation has a well-graded size distribution, where there is a wide range of aggregate sizes, allowing for a high maximum packing density to be achieved. In this situation, there is enough sand to separate the coarse aggregates and fill the voids between them, but not enough to increase paste demand [45]. In this gradation, the yield stress is the lowest. The yield stress increases as the gradation becomes more one-sided [44]. This is because the yield stress and viscosity of the concrete increase as the amount of uncompacted voids increase [43]. More narrow gradations can result in a higher void content and consequently a lower level of workability [43]. As the gradation drifts from a well-graded size distribution to one with a majority coarse aggregate, both yield stress and viscosity

increase [46]. This is because the more coarse aggregates are present in the concrete, the less mortar is available to coat them for better flow [43]. Furthermore, more coarse aggregates lead to more aggregate interlock. As the gradation becomes majority sand the yield stress and viscosity also increase [43]. The gradation can also affect the strength of the hardened concrete, with well-graded mixtures leading to more dense and less permeable concrete due to the better packing of the aggregates [20]. These mixtures also require less paste, leading to less bleeding, shrinkage, and creep [20].

Within the same gradation, the size of the particles also affects the workability of the concrete, with smaller particles requiring more water to maintain the same level of workability [46]. This could be because smaller aggregates create more surface area within the concrete and therefore, more paste is required to coat the particles [46]. When a well-graded aggregate size distribution is used, the change in aggregate size has less of an impact on yield stress and viscosity. This could be attributed to the smaller differences in surface area and void content [43]. The size of the aggregates also affects the final strength of the concrete, with some studies reporting that as coarse aggregate size increases the concrete strength increases [46].

2.3.5. Air Content. The air content can alter the workability of fresh concrete as well as decrease the compressive strength and increase the porosity of hardened concrete. Air is known to make concrete more cohesive, reducing the tendency to bleed or segregate [35]. The air content can be affected by the type of cement, w/c, mixing procedure, as well as the type and amount of admixtures used [47]. More air voids in the concrete can decrease the compressive strength as well as the elastic modulus and density. As a general rule, if the air content is increased by 1%, the compressive strength

will decrease by 4-6% [47]. Higher air contents can also increase the permeability of the hardened concrete [47].

Rheologically, air behaves differently in concrete than in cement paste. This is because air can behave either like hard spheres or deformable particles depending on the Capillary number (Ca) [48]. The Ca is the ratio of viscous forces to interfacial forces. It is based on the size of the air bubbles, the viscosity of the material, the shear rate used in the rheological test, and the surface tension. A Ca below 1 would indicate the bubbles are acting like hard spheres, and above 1 would indicate they are acting like deformable particles. The capillary number of bubbles in cement paste is typically around 0.1. At this number, the bubbles will act like hard spheres, increasing the volume fraction, and leading to an increase in viscosity. In concrete, the typical Ca is about 10, meaning the bubbles would be deformable. In rheological studies on concrete, a high capillary number is observed as a decrease in yield stress and viscosity [48].

Because of the high capillary number, increased air content improves the workability of concrete. In concrete, the deformable bubbles are able to reduce friction while improving particle mobility [35]. A higher air content can also decrease the water demand needed to maintain the same level of workability, making the concrete more sustainable [47]. It has been well established that as air content increases, so does the slump. According to ACI 211.1, “Standard Practice for Selecting Proportions for Normal, Heavyweight, and Mass Concrete”, as a rule of thumb, slump increases 10 mm (.4 inches) per 1% air. An increasing slump is an indication that yield stress is decreasing [35]. Therefore, in concrete, as air content increases yield stress and viscosity should decrease.

Air-entraining admixtures are chemicals used to better control the air content in concrete. They work by incorporating many small air bubbles into the concrete matrix and stabilizing the bubbles during the hydration process [35]. They are used to improve the freeze-thaw resistance of concrete because they relieve expansive pressure during the freezing of pore water [35]. Different types and amounts of air-entraining admixture can cause variations in the air bubble volume, which in turn changes the amount of air incorporated into the internal structure of the suspension and therefore, the amount of air voids in the hardened concrete [47]. Air-entraining agents usually create bubbles that are in the size range of 0.1 to 1 mm in diameter. As the amount of air-entraining admixture increases so does the air content, up to the saturation point [35]. The water-to-cement ratio also has an impact on the degree of effectiveness of the air-entraining agents. At a given dosage of admixture, slightly higher air contents are seen in pastes with higher w/c values. This indicates that air content increases with increased fluidity. As w/c increases the yield stress and viscosity become less sensitive to the air content [35].

A study done by Struble et al. [35] found that during a rheological test of cement pastes with air-entraining admixture, as the air content increased the yield stress increased but the viscosity decreased. An argument could be made that the behavior difference was due to the different ways air behaves in cement paste than it does in concrete. However, if this were the solution to the strange behavior seen, the viscosity would have increased [35]. The decrease in viscosity led researchers to believe the air was behaving like deformable bubbles. One possible explanation is the theory that entrained air bubbles can be attracted to cement particles and form bridges through interparticle interactions [49]. The cement particles can absorb calcium ions and become

positively charged. Air bubbles are negatively charged because of the anionic surfactants from the admixture. Cement particles are smaller than most of the air bubbles, so the bubbles become coated in cement particles. This causes the formation of bubble bridges between cement particles, increasing the degree of bonding. For the cement to flow, these bridges need to be broken, leading to an increase in the yield stress. Once the bridges are broken, the paste becomes flowable, and the bubbles reduce the plastic viscosity. This theory was proposed by Edmeades and Hewlett in 1999 [49].

2.3.6. Admixtures. Admixtures are ingredients that can be used to improve the properties of concrete to better fit the purpose of the concrete. They are added before or during mixing. Some common admixtures include air-entraining admixtures, high-range water-reducing admixtures, retarders, and viscosity-modifying admixtures (VMA).

2.3.6.1. High-range water-reducing admixtures. One of the most commonly used admixtures is high-range water-reducing admixtures (HRWRA). These admixtures are also known as superplasticizers, water-reducing admixtures, or dispersive admixtures. They are able to make the concrete more workable without increasing the w/c [50]. When they are used, water content can be reduced by as much as 40%. This enables the creation of highly workable, yet strong concrete. They can also aid in optimizing the cement content, making the concrete more economical and sustainable.

In the 1930s, E.W. Sikely discovered that sulfite pulp waste could increase the workability of concrete while enhancing its strength and durability [51]. This became the first dispersive admixture. In the 1960s analogous naphthalene was developed in Japan and sulphonated melamine formaldehydes were developed in Germany [50]. With the advent of these polymers, superplasticizers began to be used more. Naphthalene sulfonate

formaldehyde was patented in 1984 [52]. In this polymer, sulfonate contains a hydrophilic group and naphthalene contains a hydrophobic group. These two groups form a polymer chain that is negatively charged on both sides and attaches to the positive regions of the cement particle, producing more negative surface potential on cement grains [35]. When this occurs, the cement particles electrostatically repel each other [53]. Admixtures based on poly-carboxylate were developed in the late twentieth century [50]. Polycarboxylate ethers work through the use of steric hindrance. The polymer consists of a main chain with carboxylate and ether groups branching laterally off it. The backbone of the main chain has a negative charge, allowing it to attach to the positively charged sections of the cement particle. The branching groups physically block the cement particles from getting too close to each other. The duration of the effectiveness of the concrete fluidity is directly related to the length of the chains. The longer the branching chains are, the more long-lasting the fluidization effect is [54]. In both forms of superplasticizer, a reduction in the formation and interconnection of flocculation results in reduced yield stress [50]. The reduction in yield stress can be as much as 70%. While the goal of these admixtures is not to reduce viscosity, a small drop in viscosity is sometimes seen. This is because water that was trapped in flocculants is released into the system [55]. Superplasticizers do not slow the rate of hydrate precipitation. However, depending on the dosage used, they may slow the effects of hydration by physically separating the cement particles, causing the hydration products to take longer to overlap [50]. This slows the increase of yield stress and viscosity.

The effectiveness of this admixture is dependent on how much of the superplasticizer is adsorbed onto the surface of the cement particles or hydration

products. Adsorption is affected by many factors, including the molecular weight of the polymer, the specific surface area of the cement particles, and the possible competition with other anions, such as sulfate ions. The admixture appears to become more effective if it is added a few minutes after the concrete has already been mixed. There are a few theories to explain this phenomenon. Some authors have speculated that this admixture may adsorb onto C_3A more readily than to C_2S and C_3S [54]. C_3A and sulfate start reacting with water to form ettringite as soon as they come in contact [56]. After this occurs, there is a decrease in C_3A in the concrete and the admixture is better able to evenly adsorb onto all parts of the cement particle [56]. Other studies have indicated that while the polymers do absorb onto the surfaces of C_3S, they absorb especially well onto C-S-H hydrates. Naphthalene sulfonate, the superplasticizer used in this research project, has shown considerable adsorption ability onto C-S-H hydrates, particularly the C-S-H gel [57].

Studies such as the one done by Puertas, et al. [50] show that superplasticizer does not have a significant impact on strength values. However, if a high dosage is used, and there is a delay in hydration, the morphology and microstructure of the concrete may be altered [50]. When Puertas, et al. [50] used Fourier transformation infrared spectroscopy on concrete with a high dosage of superplasticizer, they found that the C-S-H gel appeared less condensed and had a higher Ca^{2+}/ SiO^{4-} ratio. After two days of hydration, the total porosity of the concrete declined, and the pore structure became more refined as the superplasticizer content was increased [50]. Furthermore, the fact that less water can be used to achieve the same slump inherently improves strength. In mix designs that are

identical in terms of aggregates, cement, and level of workability, but with water reduced and superplasticizer added, the strength can increase anywhere from 10-25% [58].

When performing rheological tests on concrete containing superplasticizer, shear thickening is sometimes seen. This is because the superplasticizer can cause the particles to repel each other. As the shear rate increases and the force of the particles being pushed together increases, the force of the electrostatic repulsion pushing away from particles also increases [59].

2.3.6.2. Hydration stabilizers. Hydration stabilizers are used to delay the setting rate of concrete. They work by coating cement particles, blocking the water needed for hydration from accessing the cement grain. This reduces the rate of calcium and sulfate dissolution. As a consequence, it also reduces the rate of hydrate precipitation, thereby inhibiting the nucleation of C-S-H and CH [60]. This causes the slump, yield stress, viscosity, and air content to remain stable. Eventually, the admixture is chemically consumed, at which point the hydration reaction returns to its normal rate [61]. This means that the higher the amount of admixture added, the longer the initial setting time will be postponed [60].

In a study performed by Vieira et al. [60] by analyzing 1500 tests on the compressive strength of concrete made without any admixtures and one containing stabilized concrete, it was found that the compressive strengths were similar. However, some studies have suggested the delay caused by the hydration stabilizer produces a superior microstructure and improves strength [61].

2.3.6.3. Viscosity modifying admixtures. Many concrete applications require that the concrete remain highly cohesive during transportation, pumping, and placing. This can be achieved through the use of a viscosity-modifying admixture (VMA). These admixtures can also be used to keep highly fluid mixtures, such as self-consolidating concrete, stable and resistant to segregation [8].

Modifying the viscosity of concrete can be accomplished with a few different types of admixtures. Most are made from large synthetic polymer chains that sit between cement particles. When shear stress is applied, the polymer chains align with the flow direction. They then tend to stretch out and elongate, causing shear thinning. This is a temporary effect as they are colloidal and return to their original shape after the shear stress is removed. This shear thinning can be helpful in construction because under low shear rates, the VMA increases the viscosity and stabilizes the suspension. Under high shear rates, like when it is being mixed or pumped, the shear thinning helps reduce the resistance to flow.

2.3.7. Supplementary Cementitious Materials. Concrete production greatly contributes to greenhouse gas emissions. Including SCMs like slag, silica fume, and fly ash can help reduce the amount of cement needed in concrete production, which in turn will aid in sustainability.

2.3.7.1. Slag. Slag is used as a supplement in concrete to enhance workability, increase strength, reduce permeability, and improve chemical attack resistance. It is a byproduct of the production of steel. The particles are fine, non-crystalline, and glassy. When mixed with PC, it has very good binding abilities. Concrete containing slag may hydrate slower, but it has improved durability [62].

As previously stated, slag improves the workability of concrete. As the percentage of slag increases the yield stress decreases. Slag has a high surface area and fine particles that are able to fill spaces made by the larger cement particles. They lessen friction within the system which increases flowability. However, at very high dosages it may lower the workability and increase yield stress [62].

2.3.7.2. Silica fume. Silica fume is a byproduct of the production of elemental silicon or alloys containing silicon in the ferrosilicon industry. It is a very fine, noncrystalline silica that is pozzolanic [63]. It is used in concrete to increase durability and resistance to chloride attack [63].

The effect silica fume has on workability varies depending on the dosage. In moderate amounts, it can decrease viscosity. This is because the particles are very fine and adding it to concrete will increase the maximum packing density. Reports such as Wallevik et al. [52] indicate this only helps up to a certain dosage, around 5%. If the system is not well dispersed the silica fume may flocculate causing an increase in viscosity. If plasticizer is used along with silica fume, to ensure the system stays well dispersed, the viscosity will go down even at higher doses of silica fume [52].

Silica fume is known to increase yield stress. This is because it adds surface area to the system, which corresponds with more interparticle interactions such as repulsive and attractive forces. These forces increase the likelihood that the particles will flocculate [15]. Brownian motion is also much more pronounced on tiny particles, causing them to move more. This further increases the possibility they may come in contact with other particles and increases the flocculation rate. The size of the particles could also increase

the structural build-up due to hydration because the small particles would provide more surface area for the hydrates to precipitate onto.

2.3.7.3. Fly ash. Fly ash is the smoke residue that is collected after coal is burned [64]. Using fly ash to supplement concrete can improve strength, durability, and workability. Fly ash is also effective at lowering the heat of hydration, lowering the cost of the concrete, improving the resistance to sulfate attack, lowering shrinkage, and lowering the porosity and permeability of the concrete [8]. Fly ash has a positive impact on workability because of the morphological effect it has on concrete. The particles are between 1 and 100 micrometers, and spherical in shape, similar to microbeads. They work like ball bearings in fresh concrete to improve workability [64].

There are two different classifications of fly ash listed in ASTM C618-08a, Class C and F. These classes are based on the type of coal that was burnt to produce the ash. Fly ash that was created during the burning of bituminous coal is known as Class F. This type of fly ash typically contains less than 18% Calcium oxide (CaO) and behaves more like a pozzolan [21]. When C_3S reacts with water it forms C-S-H and CH. The fly ash contains silicon dioxide (SiO_2) and aluminum oxide (AL_2O_3) compounds which react with the CH. This leads to more hydrated C-S-H gel being produced. The additional C-S-H fills in the capillary space in the concrete paste microstructure [64]. It improves long-term strength but may have a negative impact on short-term strength. A study by Coa et al. [64] showed that at very early curing ages, increasing the amount of fly ash decreased the strength of concrete. However, the strength developed rapidly. By day seven, the fly ash had a positive effect on strength and by day 90 strength approached a 50% increase when compared to the reference concrete.

Class C Fly ash is created from the burning of sub-bituminous coal and lignite. As a result, it contains more than 18% CaO and behaves more like hydraulic cement [21]. Hydraulic cement is a material that chemically reacts with water to form a compound with cementitious properties. Class C Fly Ash is able to react with water to produce hydration products in the absence of a source CH. This type has both good short term and long-term strength gain.

Both forms of fly ash have a microaggregate effect, meaning the fly ash particles disperse well into the concrete and combine with the gel products during the cement hydration. This promotes concrete density. A study done by Nath et al. [62] found that as fly ash increased, the pore diameter decreased. Furthermore, the use of fly ash also decreases the total pore volume and porosity of the concrete. Consequently, the permeability of the concrete was also reduced [62].

2.3.8. Self-Consolidating Concrete. ACI Committee report ACI 237R-07 (2007) defines self-consolidating concrete (SCC) as "...highly flowable, non-segregating concrete that can spread into place, fill the formwork, and encapsulate the reinforcement without any mechanical consolidation". The Australian Standard (AS 1012.3.5:2015, 2015) describes it as "Concrete that is able to flow and consolidate under its own weight, completely fill the formwork or borehole even in the presence of dense reinforcement, whilst maintaining homogeneity and without the need for additional consolidation." It was first developed at the University of Tokyo in Japan in 1986 by Ozawa and colleagues [10]. It was further developed by large Asian construction companies and discussed in ACI Conferences throughout the 1990s. The goal of developing SCC was to increase the quality and safety of concrete structures while also saving on labor and construction

costs. In SCC, the yield stress must be close to zero, so that the concrete can flow and consolidate under its own weight. The plastic viscosity must be high enough to maintain stability but low enough to facilitate flow. It must be able to flow through confined areas such as reinforcement in the concrete, have good segregation resistance, and be able to remain a homogenous mass during transporting and placement [10].

2.4. CONSOLIDATION

When a concrete mix design is created, there is an assumption that the concrete will be homogeneous, dense, and have filled all sections of the formwork. However, concrete that has been freshly poured does not immediately take the shape of its container and may contain an excessive amount of air voids, which can have a detrimental impact on the performance of the structure. This is why proper consolidation is so essential. This section will elaborate on what consolidation is, why it is necessary, the tools used in concrete consolidation, what happens during consolidation, a few factors that influence how much consolidation is ideal, and the negative effects of both over and under-consolidating.

2.4.1. What Consolidation is. According to ACI Concrete terminology, consolidation is: “The process for reducing the volume of voids, air pockets, and entrapped air in a fresh cementitious mixture, usually accomplished by inputting mechanical energy.” It has also been described as causing a denser arrangement of solid particles during concrete placement [65].

2.4.2. Why Consolidation is Necessary. Consolidation is needed because the freshly placed concrete contains an excessive amount of entrapped air voids. If the

concrete is left to harden in this condition, it will have a high air content, low compressive strength, high permeability, and reduced durability. However, when the correct amount of consolidation is applied, the concrete is able to reach its design strength and density [12].

The amount of consolidation applied to fresh concrete has a direct effect on the amount of pores in the hardened concrete. Concrete is expected to have some pores. The type, size, and number of these pores have a direct effect on the concrete's compressive strength, freeze-thaw resistance, and resistance to chemical attack [12]. Some of these pores are necessary. Capillary pores, which are less than five micrometers in diameter and are filled with water in fresh concrete, supply water to the cement and become filled with hydration products [66]. Entrained air voids are intentionally added to the concrete through the use of air-entraining agents. The admixture gives them a high surface tension which protects them from aggregates and keeps them spherical. They are usually less than one millimeter in diameter. Providing they can be evenly distributed, they prevent the pressurization caused by the expansion of water as it freezes, reducing the risk of freeze-thaw damage. They can also help to increase the workability of the fresh concrete [66] However, some voids can be harmful to the properties of the hardened concrete. Entrapped air voids negatively affect the compressive strength of hardened concrete and must be eliminated during the consolidation process. They are typically larger than one millimeter and are formed by air or water pockets [66]. The elimination of entrapped air voids increases the strength of the concrete by about 5% for every 1% of entrapped air removed during consolidation [67].

When concrete is initially mixed, the friction between coarse aggregates keeps the concrete stable. Immediately after mixing, most concrete contains 5%-20% by volume entrapped air. Large air voids are trapped beneath the surface of the concrete and the mixture exhibits poor fluidity, low slump, and a low degree of bonding. The entrapped air voids are protected by the yield stress of the concrete. One of the main contributing factors to yield stress within the concrete is the friction from the aggregates, and their ability to interlock. These factors cause the aggregates to form structures within the concrete that prevent the concrete from releasing voids. [68]. The formation of the structures is also dependent on the packing density of the mixture. As the volume fraction of aggregates increases, the aggregate skeleton has greater friction, and thus a higher static yield stress [45]. Consolidation is the best way to break these structures and release the entrapped air.

2.4.3. Tools and Methods Used in Consolidation. Consolidation is typically achieved through the use of rodding or vibrators, with vibration being the most common method. There are many different types of vibrators, but typically they consist of an off-centered weight attached to a rotating shaft. They generate compressive (P) waves and shear (S) waves of energy that emanate out perpendicularly from the vibrating shaft [69]. Amplitude and frequency are both important elements of consolidation. The amplitude is described as the linear displacement the weighted head will move from its axis; this is typically two millimeters [70]. Frequency is the speed at which the vibrator head moves within the confined amplitude. It is measured in the number of cycles a vibrator completes per minute, typically around 6,000-13,000 VPM [69]. The energy of the vibrator is governed by the mass and offset of the rotating weight. The energy is typically

expressed as the acceleration of the particles as the waves cause them to move back and forth. This acceleration is proportional to the frequency. The energy is reduced as the distance from the shaft of the vibrator increases. This causes there to be a radius around the shaft within which sufficient energy is delivered to the system [70].

Rodding and tamping are also used to consolidate concrete. Rodding is simply packing the concrete down by repeatedly inserting and removing a metal rod. It is done over the complete area to ensure the large, entrapped air voids are completely removed. This method also forces the yield stress to be exceeded. The internal structure of fresh concrete can be described as chains of aligned aggregate grains that are in direct contact with each other and compress to support the load of the fresh concrete [71]. Rodding and tamping forces these chains to be broken which in turn releases air from the concrete and causes it to become denser. These methods are, however, less effective than vibration at reducing the amount of entrapped air [12].

2.4.4. What Happens During Consolidation. Consolidation is used to exceed the yield stress of the concrete. It is typically done by vibration, rodding, tamping, or some combination of these actions [1]. The use of vibration is often needed to enable concrete to flow around reinforcement and formwork. However, it is also used to reduce the volume of voids, air pockets, and entrapped air. When vibration is used, it causes the particles to be set in motion. In this state, the concrete behaves like a Newtonian fluid and can flow under its weight [72]. The concrete is then able to fill the mold through liquefaction. Liquefaction is when particles that are already saturated act as a liquid under vibration. In fresh concrete, there is water adsorbed onto, and weakly bound to, the ionic surface of the aggregates. The vibrational impulses cause the bound water to separate

from the ionic surface of the aggregates and become free water. This free water is released from a large number of tiny, interconnected channels within the mixture. This damages the bonding forces between the aggregates [73]. The water mixes with the gel of the cement and fine aggregates to form a slurry. The slurry is heavily affected by the increased pore pressure caused by the vibrational impulses. This pressure increases the most at the points of contact between particles, where there is the largest restriction to flow [73]. The pressure causes the spacing between the particles to increase. This causes the internal flocculated structures of the cement paste to suffer damage. The static yield stress of the cement is overcome, and the shear resistance of the concrete decreases [73]. This is similar to cohesionless soil where an increase in pore water pressure results in a decrease in shear strength. As pressure increases, the shear stress continues to decrease until it becomes lower than the normal stress caused by gravity [74]. This results in flow behavior similar to a liquid. As can be applied from soil mechanics, as the void pressure increases, the angle of internal friction decreases, the shear strength is reduced, and the concrete stays in a temporary liquid state [73]. This phenomenon typically occurs in the first 3-5 seconds and causes a dramatic reduction in the internal friction between the aggregate particles [45]. The coarse aggregates then start to experience a further reduction in friction in the concrete. The vibration generates a fluctuating acceleration which makes the solid particles come in and out of contact with each other, rearranging the aggregate distribution. During this stage, the yield stress of the concrete is exceeded, and the bubbles move upwards, resulting in entrapped air rising to the surface [75]. If the vibration is removed, the yield stress is fully regained. A study conducted by L’Hermite

and Tournon [76] indicated that when vibrated, the internal friction of concrete is reduced to about 5% of the value at rest [77].

The fluidization of the concrete allows air bubbles to rise out of the system. Larger bubbles rise out of the system faster than smaller bubbles [69]. However, the larger bubbles can become trapped by the framework of the coarse aggregates. Vibration can cause the bubbles to split, reducing them in size, and making it easier for them to rise to the surface. The coarse aggregate and mortar matrix have different densities than the bubbles. Because of this, during vibration, the internal forces of the materials are different. The large inertia forces acting on the aggregates can sometimes cause bubbles to split. This can cause the diameter of the bubbles to become smaller [75]. As concrete loses entrapped air, it becomes denser. If the vibrator is removed too soon the smaller bubbles will not have enough time to rise to the surface [12].

2.4.5. Factors that Influence How Much Consolidation is Ideal. The degree of consolidation needed varies across concrete mixtures depending on many factors including slump, admixtures, supplementary cementitious materials, w/c, the properties of the aggregates, paste volume, air content, and concrete placement method [78]. As the w/c increases, the risk of segregation due to over-consolidation also increases [79]. In a study done by Arslan et al. [79], the group subjected some samples of fresh concrete to 240 seconds of vibration time and other samples to 60 seconds of vibration time. The group found that samples subjected to 240 seconds had approximately a 36% reduction in compressive strength, with concretes with higher water-to-cement ratios being more adversely affected [79]. The group also determined that concrete containing superplasticizer required a reduced vibration time. Air content also influences the amount

of consolidation that is needed. According to Ling et al. [70] due to the lower degree of energy transfer, when consolidating concrete with higher air content, more energy is required to induce particle movement. Therefore, the vibration time should be extended. Ling et al. [70] also determined that mixtures with a low slump (2.5 cm) required more energy to mobilize the mixture due to the higher yield stress [70]. The lower slump mixtures required more time to reach stability, due to the fact that more energy was needed to send vibration through the rigid systems [80].

The degree of consolidation needed cannot be based on slump alone. Ling et al. [70] compared the effect of consolidation on two mixtures with similar slumps. One had a higher water content. The other had a lower water content but also included a water-reducing admixture. The purpose of this was to explore the fact that slump only measures yield stress, and mixtures with comparable slumps may have different levels of workability depending on how the slump was achieved [70]. The mixture with water-reducing admixture reached stability faster. This is because water-reducing admixture only changes the yield stress of the mixture, but more water will change the yield stress and viscosity [70]. The loss of air was also lower in mixtures with water-reducing admixture, most likely due to the higher viscosity [70].

2.4.6. Risks of Under-Consolidating. In concrete that has been adequately consolidated, all entrapped air is removed, and an optimal packing of particles is achieved. Concrete is able to consolidate, maximizing its strength, density, and durability. However, if the concrete is under-consolidated, the density is diminished, the air content is increased, and the resistance to degradation is diminished [78].

If concrete is under-consolidated, air segregation can occur. Air segregation is when concrete is partially consolidated, and entrapped air rises near the surface, but consolidation is ended before the entrapped air is fully able to escape the concrete. If the concrete is allowed to harden in this state, it will contain a large percentage of entrapped bubbles near the surface, which will have a detrimental impact on the compressive strength and density of the concrete [12]. Empirical data obtained by Ojala et al. [12] shows that if the top of the layer has 3% entrapped air, the density of the concrete specimen will be roughly 70 kg/m^3 lower when compared to a properly consolidated sample.

2.4.7. Risks of Over-Consolidating. Concrete contains cement, water, sand, and coarse aggregate, all of which have different densities. The differences in densities can lead to segregation. Aggregate particles, which have a higher density than cement paste, tend to move downward. While air, which has a lower density than cement paste, tends to move upward. Some level of segregation is unavoidable, but excessive segregation can have significant negative impacts on the properties of hardened concrete [12]. Concrete is at a more acute risk of segregation when vibration is the method of consolidation being used. Vibration sets all the particles into motion and causes the concrete to momentarily liquify, sometimes leading to aggregate segregation [78]. Fresh cement paste has a porosity of 40-50%, while the porosity of the aggregate is significantly less. When aggregate segregation occurs, there is a change in the volume share of the cement paste and aggregate. The cement paste, containing the majority of the air, rises to the top. The coarse aggregate, containing the smallest degree of porosity, sinks to the bottom. This phenomenon is known as laitance [78]. It dramatically increases the porosity of the top of

the cylinder which contains a higher volume share of cement paste, forming a plane of weakness that has a higher potential for failure [12].

The risk of over-consolidation is higher when vibration is being used. Previous studies have indicated that if too high of a vibration frequency is used, the S waves can cause the free water to move away from the vibrator and toward form walls, which can cause holes and voids on the faces of forms [69]. A study done by Taylor [69] found that the permeability of the concrete increases as the distance from the vibrator tip increases. This occurs more dramatically in mixtures with higher w/c [69]. Other studies have indicated that using high frequencies, such as 13,000 VPM, can cause a more rapid loss of entrapped air than moderate frequencies, such as 6,000 VPM [81]. However, these high frequencies can also cause segregation to occur more rapidly.

2.5. ASTM C31

ASTM C31 provides the procedures for making and curing concrete specimens. It contains specifications on the tools that should be used such as the molds, tamping rods, vibrators, mallets, and placing and finishing tools. It contains directions on casting specimens including consolidation through both rodding and vibration. It also contains information on curing, storing, and transporting specimens.

This specification has evolved very little since its initial creation. ASTM Committee C-9 proposed ASTM C31 in 1920 [2]. When it was proposed, instructions for making cylinders were as follows: “The test specimens shall be molded by placing the concrete in the form in layers approximately four inches in thickness. Each layer shall be puddled with 25 to 30 strokes with 5/8 to ¾ inches. bar about two ft. long, tapered

slightly at the lower end." [2] This procedure has not changed in over 100 years, despite the advances in concrete technology.

In later additions of ASTM C31, instructions on the use of vibration were added [3]. These instructions were vague and have not significantly improved since then. The current version states "The duration of vibration required will depend upon the workability of the concrete and the effectiveness of the vibrator. Usually, sufficient vibration has been applied as soon as the surface of the concrete has become relatively smooth and large air bubbles cease to break through the top surface. Continue vibration only long enough to achieve proper consolidation of the concrete." It also includes in Note 7 that no more than five seconds should be required for concrete with a slump higher than three inches, and that ten seconds of vibration rarely should be exceeded for any mixture. This vibration description does not take into account how different concrete mixtures are affected by vibration. Furthermore, the standard requires at least 9,000 vibrations per minute (VPM). However, recent research has shown that high frequency can cause fresh concrete to bleed [3].

The approaches to concrete consolidation outlined in ASTM C31 have worked well in the past. However, there have been many advances in concrete technology over the past 100 years. These include self-consolidating concrete, high-performance concrete, concrete with admixtures, and concrete with supplementary cementitious materials. They also include concrete with more intentionally designed paste volumes, water-to-cement ratios, aggregate gradations, and air contents. Because of all these factors, a better understanding of the necessary levels of consolidation in modern concrete mixtures is needed.

2.6. CONCLUSION

The goal of this literature review was to point out the wide variety of factors that can influence the workability of concrete, and consequently alter the ideal level of consolidation. The review started by discussing the qualitative nature of the term workability and the quantitative term rheology as well as how these ideas are linked. In an attempt to illustrate why the slump test is still being used, despite its weaknesses, a brief history of testing workability and rheology was provided. Many, but by no means all, of the factors that impact workability were then discussed, with an explanation of how these factors alter the yield stress and viscosity of the concrete as well as the strength. This was followed by a discussion on consolidation that included what consolidation is, why it is necessary, the tools used in concrete consolidation, what happens during consolidation, factors that influence how much consolidation is ideal, and the negative effects of both over and under-consolidating. Finally, ASTM C31 and a few of its current shortcomings were discussed.

3. EQUIPMENT AND TEST METHODS

This section contains the details of the equipment and test methods used to conduct the research in this project. It first discusses the preparation for casting cylinders, the fresh concrete tests, the cylinder creation method and needed equipment, the segregation test, the details of how the cylinders were cured, and finally the density and compression tests done on the hardened cylinders.

3.1. CYLINDER MOLD PREPARATION

When casting cylinders for every mixture, the first step was preparing the cylinder molds. Reusable molds that conformed with the standards set in ASTM C470/ C470M-15 Standard Specification for Molds for Forming Concrete Test Cylinders Vertically, were used to save on costs and limit waste. They were constructed in the form of a right circular cylinder. The dimensions of the molds were four inches in diameter and eight inches in height. The molds were reusable, with nonabsorbent ¼ inch-thick heavy plastic walls. The molds were labeled with an oil-based marker to ensure the cylinder ID was known. They were then all laid out in sets of three, as can be seen in Figure 3.1. The molds were coated with demolding oil, also known as form oil, so that the cylinders could be easily extracted from the molds. The molds have a small hole at the bottom that pressurized air can be sent through for demolding. A small piece of paper was placed over this hole to ensure that the concrete did not seep out.

Figure 3.1 Cylinder Molds

3.2. MIXING PROCEDURES

For every mix design, the amount of concrete that needed to be made was divided into two separate batches. The first 24 cylinders were made from the first batch and the next 30 were made from the second. The mixer used had a six cubic foot capacity. However, it struggled with the amount of energy needed to mix 4.5 cubic feet at a time adequately. Furthermore, separating the mixture into two separate batches decreased the amount of slump loss while making cylinders. To verify that both batches of concrete had the same proportions and properties, the slump test and static yield test were both performed for each batch.

A Multiquip Whiteman electric-powered concrete mixer was used to mix the concrete. It is a drum mixer that was in compliance with ASTM C192/C192M-19.13 Standard Practice for Making and Curing Concrete Test Specimens in the Laboratory. It can be seen in Figure 3.2. The order in which the materials were added was deemed significant. As such, every time the coarse aggregate was added first, followed by the sand, a small portion of the water, the cement, then the remaining water. In cases where fly ash was used, it was added at the same time as the cement. The timer used to track hydration age was started when the cement was added. When the hydration stabilizer was

used, it was mixed in with the water before the water was incorporated. When the HRWRA was used, it was added approximately two minutes after the water had been mixed into the mixture. This is so the admixture would have time to bind to a portion of the hydration products. The concrete was then mixed for approximately five minutes before being sampled.

Figure 3.2 Concrete Mixer

3.3. SAMPLING PROCEDURES

Correct sampling procedures are important for ensuring that a representative portion of the entire batch is being sampled. In this research project, the sampling procedure was very straightforward. ASTM C172: Standard Practice for Sampling Freshly Mixed Concrete was followed when sampling the mixture. The majority of the batches were 2.25 cubic feet. This was below the capacity of the wheelbarrow being used. Therefore, after the sample was thoroughly mixed, the wheelbarrow was simply

placed under the mixer, and the entire contents of the mixture were deposited into the wheelbarrow. Once the concrete was in the wheelbarrow it was then remixed with a scoop until it was uniform.

3.4. TEMPERATURE

The temperature has an impact on the workability of the concrete. When temperature increases, the time window in which the concrete is workable decreases. This is because heat accelerates both the water evaporation from the concrete and the rate of hydration [8]. The quick evaporation may cause shrinkage and make the concrete prone to cracking [40]. The temperature of the fresh concrete will also affect the way the concrete sets. If the concrete is mixed at too high of an internal temperature, it will set faster and may experience a loss of entrained air. If the internal temperature is too low, the concrete may harden more slowly and gain strength at a slower pace. If the temperature is low enough it may even freeze, which will make it brittle and have a low compressive strength.

Therefore, the first test performed was to find the temperature, which was done in accordance with ASTM Standard C1064: Temperature of Freshly Mixed Hydraulic Cement Concrete. The thermometer used was able to measure within +-1°F, had a measuring range of 30-120°F, and had a five-inch stem. An image of this type of thermometer can be seen below in Figure 3.3.

Figure 3.3 Thermometer

To obtain an accurate reading, the sample was mixed thoroughly in the wheelbarrow and the thermometer was placed in the middle of the wheelbarrow. The stem of the thermometer was submerged three inches into the concrete. It was ensured that the stem of the thermometer was at least three inches away from the sides or bottom of the wheelbarrow and that there were no large air voids around the stem. The nominal aggregate size used in the concrete for this project was less than three inches, therefore the thermometer was allowed to rest in the concrete for three minutes, between the recommended two and five minutes. The temperature was recorded to the nearest ˚F.

3.5. SLUMP

The slump of the fresh concrete can be used as a measure of its consistency. After mixing the concrete and testing the temperature, the test used to determine the slump was performed. The slump test was repeated near the end of the batch, prior to filling the final set of molds consolidated with the reference procedure. This was done to evaluate the workability loss. The duration between both slump tests was in the order of one hour. This test was done for both batches of concrete. Any large deviations in the slump could

alert us to a possible mistake when weighing the materials, uncorrected changes in aggregate moisture contents, changes in aggregate gradations, or incomplete mixing of the concrete [8].

All equipment used to conduct the slump test conformed to ASTM C143 - Slump Test of Hydraulic Cement Concrete and was supplied by MS&T construction and materials lab. To perform the test, a standard metal slump cone with a four-inch diameter top, eight-inch diameter base, and 12-inch height was used. It was clean, free of dents and deformities and had a thickness of more than 0.06 inches. The tamping rod used had a 5/8-inch diameter, was 24 inches in length, and both ends were rounded with a hemispherical tip. The scoop used to fill the cone was large enough to obtain a representative sample of the concrete, but small enough that concrete was not spilled while placing the layers. The measuring device used was a tape measure that was longer than 12 inches and had measuring increments of 1/16-inch. In place of a slump test base plate, a large slump flow test plate was used. This plate is typically used in a slump-flow test for self-consolidating concrete. However, it complied with the specifications laid out in ASTM C143. It was made from a stiff, nonabsorbent material, and was larger than the 27.5 inch length requirement. The use of this plate made the cleanup process more efficient and improved the accuracy of the test when working with high-slump concrete mixtures. An image of the slump cone and base plate can be seen below in Figure 3.4.

Figure 3.4 Slump Cone and Base Plate

The slump test was performed in accordance with ASTM C143 - Slump Test of Hydraulic Cement Concrete. Before the test began, the cone, plate, rod, and scoop were all moistened. The cone was placed at the center of the slump flow test plate. The wings of the slump cone were stood on to ensure that the cone would not shift or lift. The volume of the cone was divided into three sections, one for each lift. The first lift was filled to 2⅝-inches in height, a third the volume of the cone, and rodded 25 times through the depth of the lift. While rodding, it was ensured that the compaction was evenly

distributed over the entire surface area and that the tamping rod was slightly angled on the edges of the cone. The second lift was filled to 6 1/8-inches, two-thirds the volume of the cone. It was rodded 25 times, an inch into the underlying lift. The third lift slightly exceeded the top of the cone and was again rodded 25 times, an inch into the underlying layer. After the third lift was rodded, the excess material was screened off the top with the tamping rod. Excess material was removed from the base of the cone. The cone was then held down by pushing down on the handles of the cone to keep it steady while the researcher stepped off. The cone was then gently pulled straight up, away from the concrete, over the course of about five seconds. The cone was then flipped upside down and the tamping rod was set on top of the cone and over the slumped concrete. The tamping rod and a measuring tape were used to find the distance from the base of the cone to the center of the displaced concrete. The result was recorded to the nearest quarter inch. This was all performed within two and a half minutes.

3.6. STATIC YIELD STRESS

The static yield stress refers to the amount of force needed to initiate the flow of concrete. The static yield stress of concrete is typically found using a rheometer. However, these are large machines that are less practical for use in the field. One method for determining the static yield stress while in the field is by using a portable vane test.

The portable vane test was originally designed to test the shear stress of clay soils [82]. In that context, a borehole is made. The vane, which is attached to a torque meter, is inserted inside the borehole. The vane is then slowly turned, and the torque meter records the torsional force needed to shear the material [82]. Bauer et al. [83] reported the vane

test could be used on mortars. It was then adopted by Omran, Naji, and Khayat [82] who altered the vane geometry to better capture the torque values needed to break down the structure of the material. The intended purpose of the altered device was to test the thixotropy of SCC on-site as a quality control measure. There is currently no ASTM on this testing method.

The device consists of a vane, a square container with a lid, and a torque meter. The vane has four blades, which are configured in a cross shape, and affixed to a stainless-steel shaft. The vane is 22 mm (7.87 inches) in height and the radius of the vanes are 37 mm (1.46 inches) across [82]. The container is 210330 mm (8.2713 inches) and has a bolt attached to the bottom center. The purpose of the bolt is to elevate and stabilize the vane, as well as aid in keeping the vane centered [82]. The lid of the bucket has a hole drilled in the center that is 0.08 inches larger than the diameter of the vane's shaft. The purpose of this is to maintain the vane in the center of the bucket, in a vertical position, without restricting the vane while it is being turned. The torque meter is attached to a socket that allows it to be attached to the shaft of the vane [82]. The device can be seen in Figures 3.5 and 3.6.

Figure 3.5 Inside of Portable Vane Test Device

Figure 3.6 Outside of Portable Vane Test Device

To perform the test, the vane was placed in the center of the bucket resting on the bolt. Around the vane, the bucket was filled with concrete until the concrete reached just over the top of the vane. The lid was placed on top, and the torque meter was attached to the shaft of the vane. The torque meter was then rotated 90° at the recommended speed of 10-15 seconds for the quarter turn. The torque meter recorded the maximum torque needed to break the inter-structural bonds in the cement, overcoming its yield stress. It had a precision of 0.5 Nm or 0.44 lbf in. and a capacity of 18 Nm or 160 lbf in. This test was done at the start of every batch of concrete.

The static yield stress was calculated according to Equation (2):

$$\tau_0 = \frac{T_{max}}{K} \tag{2}$$

where τ_0 is the static yield stress, T_{max} is the maximum recorded torque, and K is a constant that relates the torque to the geometry of the vane. K is calculated according to Equation (3):

$$K = 2\pi r^2 \left(H + \frac{2}{3}r\right) \quad (3)$$

where h represents the height of the concrete in the bucket, and r is the radius of the vane in meters. The concrete was systematically filled to a height of 9.75 inches, or 0.248 meters. The radius of the vane was 1.46 inches or 0.037 meters. Therefore, the K used to calculate all yield stresses were .002345 m^3.

3.7. DENSITY

The aggregate gradation and characteristics, w/c, air content, and consolidation method all impact the density of the concrete. The density of the concrete was calculated with the results from the unit weight test. The unit weight was found per ASTM C138: Unit Weight, Yield, and Gravimetric Air Content of Concrete. To prepare for this test, a unit-weight container was needed, to save time the container from the pressure meter was used. The container from the pressure meter was a cast aluminum case with a known volume of 0.2504 ft^3 (0.0071 m^3). The container was checked for wear and damage before each test. The mass of the empty container was found on a scale and was recorded to the nearest 0.1 lbs.

To begin the test, the inside of the container was dampened, and any excess water was poured out. A scoop was used to fill the container. The scoop was large enough to obtain a representative sample of the concrete, but small enough that concrete was not spilled while placing the layers. The layer was then consolidated through the use of

rodding. The container was filled with three layers of concrete of equal volume. Each layer was rodded 25 times. The tamping rod was 5/8th inch in diameter, 24 inches long, with hemispherical tips. The bottom layer was rodded all the way through. When the next two layers were rodded, the rodding depth was about one inch into the underlying layer. After each layer, the sides of the container were struck with a mallet 12 times, three times at an increment of 90˚. The rubber mallet used had a mass of 1.25 lbs. After the consolidation of the third layer was finished the container was checked to not have any excess or deficiency of concrete. The surface of the container was then leveled with the strike-off plate. The strike-off plate was a half inch thick and was checked to be at least two inches greater lengthwise and widthwise than the diameter of the pressure meter container. It was also checked for cracks, bumps, and deformations. The plate was placed two-thirds the way over the top of the container. It was moved side to side in a sawing motion while being pulled backward off the container. The plate was then replaced on the top of the concrete and pushed forward in a sawing motion until the backside of the plate passed over the remaining third of the container completely. Finally, the strike-off-plate was angled and swept back and forth across the top of the container. Any excess concrete was cleaned off the sides of the container. The full container was placed on the scale, and the unit weight was recorded. The density of the concrete was then calculated with Equation (4).

$$Density = \frac{(\text{Weight of Container with Concrete}) - (\text{Weight of Empty Container})}{\text{Volume of the Container}} \qquad (4)$$

3.8. AIR CONTENT

The amount of air in concrete can have an impact on its strength and ability to endure freeze-thaw cycles and weathering. It can also influence concrete workability [8]. The air content of the concrete was found in accordance with ASTM C231: Testing Air Content of Concrete with a Type B Pressure Meter. To prepare for this test, a pressure meter was checked for dents and cleanliness. The components include an air pressure gauge, stainless steel clamps, a built-in pump, brass petcocks with stainless steel ball valves, and the container. It was ensured that the gauge had been recently calibrated and the container of the pressure meter was watertight without any dents or deformities. An image of the pressure meter used can be seen below in Figure 3.7.

Figure 3.7 Pressure Meter

The concrete from the density test was kept inside the container. The cover of the air meter was then clamped onto the bowl, and it was ensured that the bowl had an air-tight seal. The leavers of the petcocks were opened by pushing the levers into the upright position. The water dropper was then used to squeeze water into one petcock until water flowed out of the other. The container was jostled while doing this to ensure that the only air present was air inside the concrete. Air was pumped into the pressure meter until the gauge read the initial pressure. Both petcocks were then closed and the lever at the top of the meter was used to release the pressure in the measuring bowl. Simultaneously the side of the bowl was struck with a mallet. The gauge was then lightly tapped until it appeared stabilized. The air content value shown on the gauge is known as the apparent air content. To find the actual air content an aggregate correction factor of 0.3% had to be subtracted.

3.9. CASTING CYLINDERS

For every mixture 4.5 cubic feet of concrete was made. 54 cylinders in total were created from each mixture. 18 different consolidation strategies were used, with the same consolidation strategy being used on three consecutive cylinders to determine statistical significance. The process of creating these cylinders required significant time, therefore, two 2.25 cubic feet batches were made for each mixture. To further control the slump loss as the cement hydrated, all mixtures were retarded.

As soon as the concrete was mixed and sampled, standard fresh concrete tests were conducted. These tests included temperature, slump, density, and air content. The concrete's static yield stress was also evaluated at this time. With the remaining concrete, nine sets of three cylinders were cast, each set with a different consolidation procedure.

The first set created was used as a reference set, which was consolidated by following ASTM C31 for rodding. The cylinders were filled with a scoop in two layers. The first layer was approximately four inches high. It was rodded with a tamping rod 25 times throughout the layer. The tamping rod was 3/8-inch in diameter and 12 inches long. The roddings were distributed uniformly over the cross-section of the cylinder. The outside of the mold was then tapped 15 times, three times each 72˚ to close voids left by the tamping rod. The second lift was created and was rodded an inch into the underlying lift. It was then tapped an additional 15 times. The surface of the mold was struck off using the tamping rod to produce a flat, even surface. The hydration age at which they were created was then recorded. This reference set procedure was done at the beginning and end of each batch. This is to account for the variation in fresh properties of the batches, as, despite the addition of a retarder or hydration stabilizer, a slump loss is observed for all mixtures. Because two batches of concrete were created for each mixture, the reference set was created four times for each mix design.

The next consolidation procedure used was dependent on if the slump indicated that the mixture was highly workable or stiff. For more fluid mixtures, the next six sets were made in two layers with the number of roddings increased from 5, 10, 15, to 20 per layer. A two-layer set was then rodded fifty times and a four-layer set were rodded 25 times. After each layer, the cylinder mold was tapped 15 times. For stiff mixtures the next six sets were also made in two layers with the number of roddings increased from 10, 20, 30, 40, to 50 times per layer. Then a four-layer set was made with 25 roddings per layer.

At this point, a second slump test was performed to determine the degree of slump loss over the casting period. Immediately afterward, an additional reference set was

created following ASTM C31. All equipment was then cleaned, and 2.25 cubic feet of the same mix design was produced. The temperature, slump, and static yield stress were re-evaluated for this second batch, and another reference set following ASTM C31 was created, followed by a single layer set with 25 roddings total. The next several sets of cylinders were all cast by varying the power and frequency of the vibrator, as well as vibration time.

When the cylinders were vibrated, a Control Speed Vibrator was used. Minnich Manufacturing, the industrial partner in this project, donated a Control Speed Vibrator (CSV). The CSV is a lightweight, durable, electric flex shaft concrete vibrator. It is controlled by Bluetooth and connects to the Minnich app. Through the app, a frequency of 6,000, 8,000, 10,500, or a custom VPM could be selected. VPMs of 6,000, 8,000, and 12,000 were used in this project. The vibrator attachment had a flexible shaft that ended in a head that was 1 1/8-inches in diameter.

The cylinders were filled in two layers with each layer vibrated once. A layer was vibrated by first turning on the CSV, slowly lowering it into the center of the concrete near the bottom for the first lift and an inch into the underlying lift for the second. The CSV was allowed to remain stationary in the center of the cross-section of the cement for a predetermined number of seconds before slowly being raised. It was turned off only when completely outside of the sample. After each layer was vibrated, the side of the mold was tapped 15 times. The first four vibrated sets were made at a frequency of 8,000 VPM with the duration ranging from one, three, six, to 12 seconds. The next set was made at 6,000 VMP for three seconds, and the last was made at 12,000 VPM for three seconds.

When this was concluded, the last slump was measured, an additional reference set was created. With the remaining concrete, a set with no consolidation was produced. It should be noted that the cylinders without rodding or vibrating were still tapped 15 times after the filling of each layer. For the first two mixtures, a single batch was made. In this mixture, there were only three reference sets. One in the beginning, one in the middle, and one at the end. Table 3.1 shows the detailed procedures for each of the 18-cylinder sets for the two-batch procedure.

Table 3.1 List of compaction methods. L is the number of layers, R is the number of roddings per layer, s is seconds, and VMP is vibration per minute.

Cylinder #	**Fluid**	**Stiff**	**Cylinder #**	**Vibration**
1, 2, 3	2L, 25 R	2L, 25 R	25, 26, 27	2L, 25 R
4, 5, 6	2L, 5 R	2L, 10 R	28, 29, 30	1L, 25 R
7, 8, 9	2L, 10 R	2L, 20 R	31, 32, 33	2L, 3s, 8000 VPM
10, 11, 12	2L, 15 R	2L, 30 R	34, 35, 36	2L, 1s, 8000 VPM
13, 14, 15	2L, 20 R	2L, 40 R	37, 38, 39	2L, 6s, 8000 VPM
16, 17, 18	2L, 50 R	2L, 50 R	40, 41, 42	2L, 12s, 8000 VPM
19, 20, 21	4L, 25 R	4L, 25 R	43, 44, 45	2L, 3s, 6000 VPM
22, 23,24	2L, 25 R	2L, 25 R	46, 47, 48	2L, 3s, 12000 VPM
			49, 50, 51	2L, 25 R
			52, 53, 54	2L, 0 R

3.10. PENETRATION TEST

Segregation can be the result of over-consolidating concrete. To determine if the concrete was experiencing segregation a self-consolidating concrete (SCC) penetration apparatus was used. The SCC penetration apparatus is typically used to assess the static stability of a sample during an inverted slump cone test. However, it is capable of giving an indication of the degree of segregation in the sample. To conduct this test, ASTM C1712 Standard Test Method for Rapid Assessment of Static Segregation Resistance of Self-Consolidating Concrete Using Penetration Test was used. Its components include a hollow cylinder affixed to a rod. The rod is surrounded on the lower end with a protective hollow sleeve which is attached to the frame of the apparatus. An adjustable set screw is used to hold the rod in place. A reading scale is attached to the frame of the apparatus adjacent to the rod. This reading scale measures in increments of one mm. A slider is attached to, and overhangs, the reading scale. It can be raised and lowered on the reading scale to line up with the top of the rod to make the readings more accurate. An image of this apparatus can be seen in Figure 3.8. This test was performed on every cylinder. The cylinders that were rodded were tested after the top layer of the cylinder was finished. However, for the cylinders that were vibrated, the penetration test was done before the final finishing.

To prepare this apparatus for use, it was first placed on a level surface free of vibration. The hollow cylinder was dampened, and the apparatus was held in the horizontal position as the set screw was released. The penetration head was then gently spun to ensure no obstructions were between the rod and the inner sleeve. The set screw was then tightened to the hold rod in the sleeve. To use the apparatus, it was first set on

top of the mold of a freshly made cylinder. Care was taken to ensure the cylinder was placed on top of a flat surface. The metal rod was held as the set screw was released. The hollow cylinder was carefully lowered to the point where it was barely touching the surface of the concrete. The set screw was tightened and the initial reading on the reading scale, which was the mark that was in line with the top of the metal rod, was taken. The apparatus was left in place for the concrete to stabilize for 90 seconds after finishing. After the stabilization period, the set screw was released, and the hollow cylinder was allowed to penetrate the concrete. The cylinder was allowed to continue to sink for ten seconds, and the final depth was recorded. The depth of penetration was calculated to the nearest 0.5 mm. The cylinders were also visually inspected for signs of bleeding that could be used to indicate segregation.

The measurements obtained in this test allowed the team to investigate if the consolidation procedure used was too impactful and caused segregation. This aided in identifying an upper limit to the consolidation energy. However, there were a few downfalls in this assessment. Firstly, the measurement is very subjective, as it depends on how easily the hollow cylinder can be placed level with the top surface, potentially impacting the measurement. Additionally, despite extremely fluid mixtures being created with nearly a ten-inch slump and obvious visual signs of bleeding, no significant penetration was assessed. The maximum value of penetration seen was eight mm. These values are indicative of stable concrete, as ten mm penetration is deemed the upper boundary for static stability. When specimens were consolidated through the use of vibration, the head of the vibrator could at times cause concrete to flow over the top of the mold. When the vibrator head was removed it would result in substantial subsidence

of the surface. It was determined that refilling the mold would impact the results of the segregation test. Therefore, we performed the segregation test before the final finishing of the concrete. Furthermore, when vibration is used, particularly at higher frequencies or durations, it is noted that the top surface of the concrete becomes “creamier”, indicating potential paste movement. However, the segregation apparatus does not capture this, as the aggregates are right below the surface and relatively immobile. As such, a more qualitative note is made on this paste migration aspect.

Figure 3.8 Penetration Apparatus

3.11. INITIAL CURING AND DEMOLDING

For every cylinder, immediately after the penetration test was concluded, the cylinder was placed back in the row and column it had been taken from. Once all the cylinders were finished and placed back in their original spots, they were covered in a sheet of plastic. The cylinders were left in the MS&T construction materials lab. This lab was climate controlled and maintained at a consistent 69˚ F, well between the 60-80˚ required. They were left to harden for 24-48 hours. After this time had elapsed, they were placed on a cart and moved to the demolding area. An air compressor and rubber-tipped air blow gun were used to extract the cylinder from the mold by sending a stream of compressed air into the hole at the bottom of the mold. The cylinders were labeled with the ID number written on the mold, the date they were created, and the researcher's initials. The cylinders were then carefully transported to the moisture-curing chamber and the cylinder molds were cleaned.

3.12. CURING THE CYLINDERS

The cylinders were cured in a moisture-curing chamber. The chamber is built into the MS&T Advanced Materials Characterization Lab (ACML). Conditions of the room followed ASTM C511 Mixing Rooms, Moist Cabinets, Moist Rooms, and Water Storage Tanks Used in the Testing of Hydraulic Cements and Concretes. The room was maintained at 72.6 °F and a relative humidity of 98%. The humidity was maintained by an Aqua Fog humidity machine. The cylinders were kept stationary in this room until 28 days had elapsed.

3.13. SURFACE SATURATED DRY RELATIVE DENSITY

The main consequence of insufficient consolidation is entrapped air. The amount of entrapped air can be quantified with a Bulk Saturated Surface Dry (SSD) Specific Gravity assessment, also known as an SSD relative density assessment. To do this, ASTM C642 Standard Test Method for Density, Absorption, and Voids in Hardened Concrete was followed, with the exception that the drying and boiling portions were omitted due to the potential impact on strength.

For this assessment, a balance was needed that could accurately read the weight of the cylinder. A submerged weighing apparatus and a wire mesh sample basket that was eight inches in diameter and eight inches deep were also needed, as was a large absorbent cloth and a tank large enough to submerge the specimen.

This assessment was performed after the cylinders had been in the curing room for 28 days. Groups of 18 cylinders at a time were removed from the curing room, and a damp towel was placed over the cylinders that had been removed. This diminished the extent to which the cylinders were impacted by evaporation. The cylinders were patted with a towel until the surface was dry. They were then weighed in their saturated surface dry condition and their weight was recorded to the nearest 0.1 grams. The basket was submerged in room temperature water and suspended from a hook attached to the balance. The balance height was adjusted to appropriately weigh the specimens. The balance was zeroed, and the samples were then placed in the wire mesh basket. This can be seen in Figure 3.9. The weight of the specimens underwater was recorded. The SSD relative density, represented by RD_{SSD} was calculated with Equation (5):

$$RD_{SSD} = \frac{M_{SSD}}{M_{SSD} - M_{water}} \quad (5)$$

where M_{SSD} is the mass of the surface dry samples and M_{water} is the mass of the immersed samples. Once the cylinders had been weighed they were returned to the cure room until the compression test could be performed.

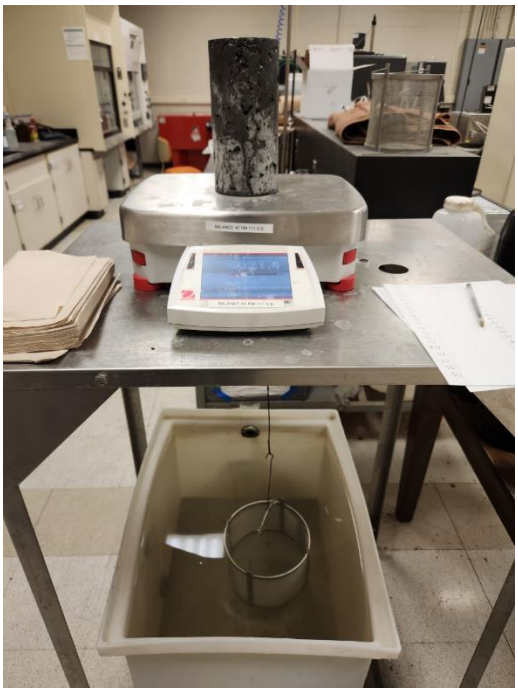

Figure 3.9 Scale used for Surface Saturated Dry Specific Density

3.14. COMPRESSIVE STRENGTH

The compression test was used to determine if the concrete specimen had been under-consolidated. If the compressive strength was significantly lower than the reference cylinder, it was an indication the specimen was under-consolidated.

A Tinius Olsen hydraulic tension/compression machine with a maximum capacity of 200,000 lbs was used to determine the compressive strength of the concrete specimens. This machine followed the specifications required in ASTM C39 Concrete Cylinder Compression Testing. It was ensured that the equipment had been calibrated within the past 18 months. The machine was power operated and applied the load smoothly and continuously. Our research did not include high-strength concrete; however, a protective fragments guard was still used for safety purposes. The machine is powered by hydraulic fluid and uses a piston to lift a lower steel bearing block and push the specimen into an upper steel bearing block. This applies an increasing compressive axial load to the specimen until failure occurs. The compression machine itself is operated by a dial to retract, hold, or advance the lower bearing block. However, the computer system attached is more accurate and was predominantly used. The software program MTESTWindows Materials Testing System made by ADMET is used to monitor the load being applied, the stress in psi, the peak compressive strength, and the stress-strain curve. The spacing blocks were measured to ensure that the diameter was at least 3% greater than the diameter of the concrete specimens. The bearing surface had no gouges or deformities that caused the bearing surface to depart from the plane by more than .001 inches. They also had a Rockwell hardness of more than 55 HRC. A bottom spacer was used to raise the elevation of the specimen to accommodate the fragment guard. It was made of steel, cylindrical in shape, and wider than the specimen. Other equipment needed to perform this test included a ruler to measure the cylinder diameter and carpenter square the check for perpendicularity. Cylinder wraps were also used. These are rectangular pieces of canvas with velcro on the ends that wrap around the cylinder. Retaining rings were used

as the capping method for the specimens. These are caps that contain neoprene pads that distribute the load more evenly over the cast concrete surface. An image of the equipment used can be seen in Figure 3.10.

To perform a compression test, specifications in ASTM C39: Compressive Strength of Concrete Cylinders were followed. Groups of 18 cylinders were transported from the moisture room at one time. While they were being transported and waiting to be tested a wet towel was placed over them to keep them moist. The first specimen was placed on a nearby table and checked for defects. A straight edge was used to check for planeness. The height of each cylinder was measured, and the diameter was measured twice. This was needed to calculate the surface area of the cylinder to find its strength. It was important to measure multiple diameters on the same cylinder to ensure they were deviating by less than 2%. A carpenter's square was then used to check the perpendicularity of the cylinder's axis. The cylinders could not depart from the vertical axis by more than 0.5˚. The cylinder was then wrapped in a cylinder wrap. This is a safety precaution used to keep concrete fragments contained. The cylinder was placed between the top and bottom retaining rings, being careful to center the cylinder inside the rings as much as possible. The power to the machine was then turned on so that the tables could be manually raised and lowered. The tables were positioned so that the cylinder could be placed in the center of the spacer on the lower bearing block. The fragment guild was then placed around the cylinder.

The computer was turned on and the software package MTESTWindows was opened. The hydraulic pumps of the machine were then turned on. The machine was switched from being operated manually to being operated by the computer. Information

about the cylinder such as the size, diameter, and file name were entered. The definition of a cylinder break, 75% of the peak load, was then entered into the computer. This instructs the machine to ignore any breaks or edge crumbling that may occur before this point. The machine was positioned so that the specimen was close to the upper table, but not touching it. The load on the machine was then zeroed out. The next step was to preload the machine. The pounds being applied were displayed on the screen, after 100 lbs, the computer had to be manually told to continue. The load was then applied at full advance by the machine at a constant loading rate of 40 psi/s. When the stress dropped below 75% of the peak load, it indicated the cylinder had been broken, and the machine automatically turned off. The pieces were placed in the wheelbarrow. The breaking pattern was determined according to ASTM C39 [84]. The diagram used can be seen in Figure 3.11. The strength of the cylinder was recorded to the nearest 10 psi. The compressive strength of the cylinder was calculated by dividing the maximum load achieved during the test by the cross-sectional area of the cylinder.

Figure 3.10 Tinius Olsen Hydraulic Tension/Compression Machine

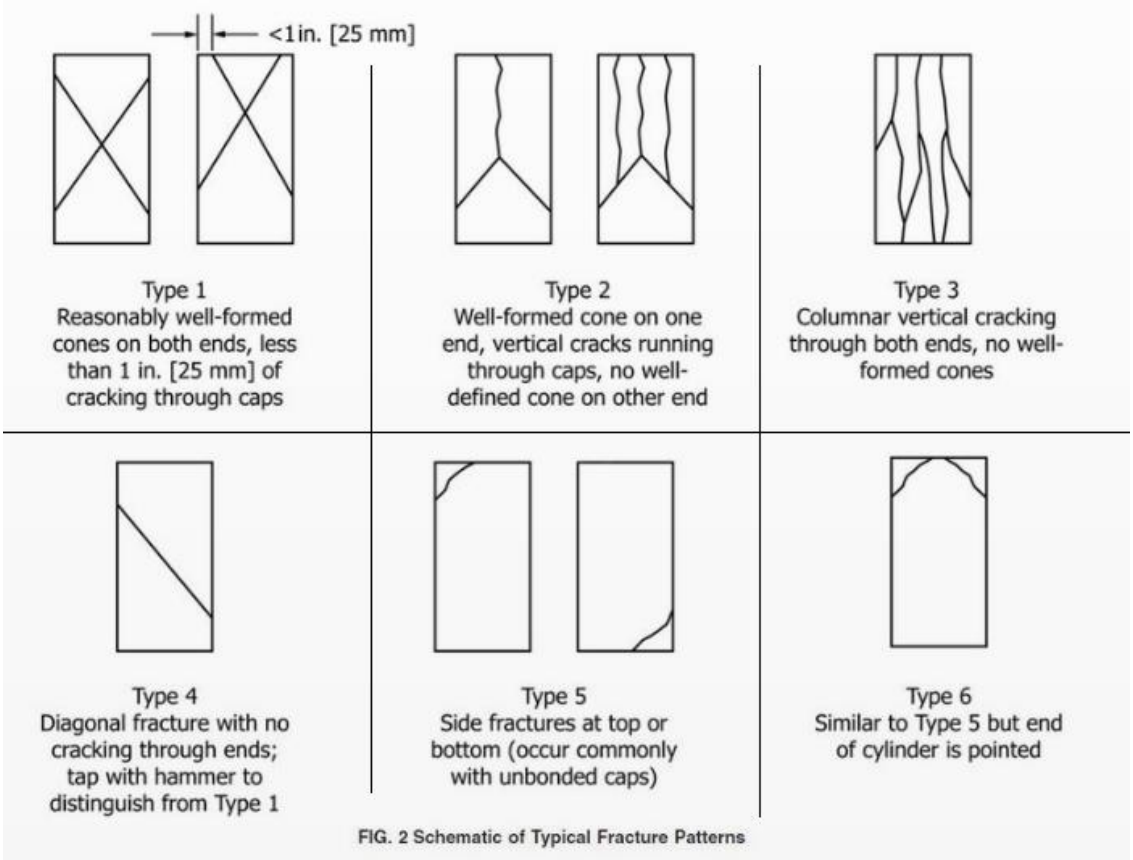

Figure 3.11 Fracture Patterns ASTM C39

3.15. RHEOLOGY

An Anton Paar MCR 72 was used to study the rheological characteristics of the cement. This rheometer uses an electrically computed motor, low-friction bearings, and an optimized normal force sensor to ensure accurate and precise results. With this piece of equipment, the viscosity and dynamic yield stress of each mix design could be calculated. The Anton Paar RheoCompass software is used for control of the system. With this software, text files could be customized to ensure the desired material characteristics are displayed. Data could be collected from the software package in the

form of text files or graphs. An image of the Rheometer can be found below in Figure 3.12.

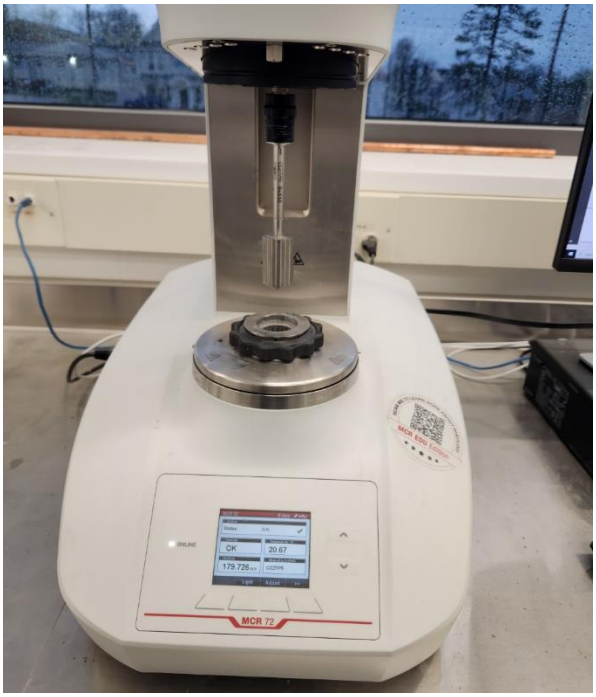

Figure 3.12 Anton Paar MCR 72 Rheometer

Additional equipment was used when conducting rheological tests, such as a precise balance to measure the mass of samples being tested, a small mixer to mix the sample in, and deionized water to create the cement paste. A pipette that could be set to administer water in the range of 100 to 1000 microliters was also used. This ensured that a precise amount of water was added to the paste. The measuring cylinder, CC27/P6 number 5916, was the bob used to measure the sample. This cylinder had a diameter of

26.6 mm and was sandblasted. The measuring cup, C-CC27/T200/XL/SS/P number 253703, was used to contain the sample. The cup had a diameter of 28.93 mm and was ribbed.

To prepare for the test, the cement, water, and utensils were all heat conditioned overnight so there would be no temperature fluctuations that could impact the test. Before the tests were conducted, the rheometer was initialized and set to 20˚C. Files for measuring the dynamic yield stress and viscosity were then created in the software. When the software and rheometer were ready to perform the test, the sample was prepared. Based on the volume of the space between the cup and the bob, a sample size of 40 grams was selected for each test. To avoid the adverse effects of an excessive shear history, for every batch, enough cement paste was made for at least two tests. To do this, one large batch of cement paste was made, and 40 grams was removed from the bowl, tested, and immediately thrown away. Then the other 40 grams were removed from the mixing bowl, tested, and thrown away. The first test was done 15 minutes into hydration and the next at 60 minutes. This was intended to mirror when the first and second slump test was performed when casting cylinders.

The mixtures that were tested matched the paste compositions of the mix designs. For example, when cylinders were made based on Mixture 12, 28.863 kg of cement, 11.545 kg of water, 30 mL of hydration stabilizer, and 150 mL of HRWRA were used. The total amount of cement paste used when casting cylinders was 40.41 kg or 40410 grams. This was divided by 100 so that when weighing out materials the amount of cement paste totaled 404.1 grams, containing 288.6 grams of cement and 115.5 grams of water. Then 0.3 mL of hydration stabilizer and 1.5 mL of high-range water-reducing

admixture were added. This was far more than was needed for two tests but ensured the ratio of cement paste to admixture could remain accurate. A table of the cement paste compositions that were rheologically tested can be seen below in Tables 3.2 and 3.3. It should be noted that in mixtures where the paste composition remained constant, and another variable was adjusted the cement paste was not retested.

Table 3.2 Paste compositions for rheological tests Mixtures 1-6.

	Mixture 1	Mixture 2	Mixture 3.1	Mixture 3.2	Mixture 4	Mixture 5	Mixture 6
Cement Paste (g)	462.5	426.4	300.9	300.9	361.2	391.2	404.1
Portland Cement (g)	308.3	294.1	207.5	207.5	249.1	269.8	288.6
Fly Ash (g)	0.0	0.0	0.0	0.0	0.0	0.0	0.0
Water (g)	154.2	132.3	93.4	93.4	112.1	121.4	115.5
w/c	0.50	0.45	0.45	0.45	0.45	0.45	0.40
Recover (mL)	0.0	1.75	2.75	5.49	0.0	0.0	0.0
Daracem 19 (mL)	0.0	0.0	0.0	0.0	0.0	0.0	0.0
Delvo (mL)	0.0	0.0	0.0	0.0	1.5	1.0	1.5

Table 3.3 Paste compositions for rheological tests Mixtures 7-14.

	Mixture 7	Mixture 8	Mixture 11	Mixture 12	Mixture 13	Mixture 14
Cement Paste (g)	391.2	380.0	421.8	404.1	404.1	404.1
Portland Cement (g)	179.9	253.3	288.9	288.6	288.6	288.6
Fly Ash (g)	89.9	0.0	0.0	0.0	0.0	0.0
Water (g)	121.4	126.7	132.9	115.5	115.5	115.5
w/c	0.45	0.50	0.45	0.40	0.40	0.40
Recover (mL)	0.0	0.0	0.3	0.3	0.3	0.3
Daracem 19 (mL)	0.0	0.0	1.5	1.5	0.5	0.75
Delvo (mL)	1.0	1.0	0.0	0.0	0.0	0.0

When preparing the materials, the cement paste was carefully weighed on a precise balance. Water was weighed in a separate bowl. After the majority of the water

had been added to the bowl a pipette was used to administer the rest of the water one gram at a time. This was also done on the precise balance to check for accuracy. If hydration stabilizer was used, it was added to the water with a pipette 0.1 grams at a time. The water was then poured into the cement and a stopwatch was started. The sample was then combined in a mixer and mixed for two minutes. If HRWRA was used, it was then added to the paste with the pipette 0.1 gram at a time. The sample was then mixed in the mixer for two additional minutes. 40 grams of the sample was then scooped into the cup, the cup was loaded and secured into the rheometer, and the bob was attached. The bob was lowered into the cup, and the measuring file for viscosity and dynamic yield stress was opened. The measuring file had two separate components, a pre-shear, and a shear rate ramp. The pre-shear measured a data point every 0.1 seconds for 60 seconds, measuring 600 points total. It was done at a constant shear rate of 100 s^{-1}. The shear ramp started immediately after the pre-shear. It collected information on the shear stress, shear rate, strain, torque, and rotational speed. It took a measurement every 0.1s for 30 seconds, measuring 300 points in total. The ramp started at a shear rate of 100 s^{-1} and decreased to 0.1 s^{-1}. After this had concluded the sample was removed and thrown away. The equipment was cleaned, and the next sample was removed from the mixer and loaded into the cup. At 60 minutes into hydration the test was done again.

4. MATERIALS

4.1. CEMENT

The exact proportions of the C_3A, C_2S, C_3S, C_4AF, the quantity of the minor compounds, the sulfate source, the amount of additives, and the fineness of the cement grains can vary widely across cement types, brands, and even batches. Because of these differences, it was important that all the cement used in this research was obtained from the same manufacturer. The cement used in this study was supplied by Holcim (US) inc. It was selected based on its consistent cement qualities. The cement was batched from the St. Genevieve MO, plant. The cement used in this project is Type 1L- Portland limestone cement. It is made of calcium silicate-based clinker, limestone, and gypsum. It meets the requirements defined in ASTM C 595 Standard Specification for Blended Hydraulic Cement. The following sections describe some of the elements in cement as well as a few of its characteristics.

4.1.1. Sulfur Trioxide Content. Sulfur trioxide (SO_3) is the main component of gypsum. The SO_3 content reported includes both the amount in the cement, as well as the amount added while the clinker is ground. As discussed in Section 2, gypsum helps control the C_3A reaction, which is why there are upper and lower limits on how much SO_3 can be added to the cement. If too little is added, it can result in flash setting. If too much is added, the cement hydration can be retarded. The SO_3 content in the cement used in this research was 3.18%, with typical values being about 3% [85].

4.1.2. Calcium Carbonate Content. The cement used in this research contained calcium carbonate ($CaCO_3$). Limestone cement has been gaining popularity for its

positive environmental benefits as well as its impact on the mechanical properties of concrete. The process of making cement creates a large amount of carbon dioxide (CO_2) emissions. Replacing a percentage of this clinker with ground limestone reduces the amount of CO_2 emitted to produce cement. While regular Portland cement is only allowed to contain 5% limestone, limestone Portland cement can contain up to 15%. The environmental benefits are not the only reason to use limestone PC. Limestone's average particle size is 0.7 micrometers, while Portland cement's is 12 micrometers. The finer particles help to improve the particle size distribution and fill in the spaces between the larger cement grains. It is also thought that limestone can improve the mechanical properties of concrete by contributing to the "filler effect". The filler effect occurs because of the increase in surface area. Limestone is not only finer than cement but also has more defects on the surface of the grains than cement, meaning it provides considerably more surface area. When surface area is added, C-S-H is able to nucleate on it, forming a larger quantity of C-S-H nuclei, and accelerating hydration. Additionally, when C-S-H grows on limestone, the contact angle made on the surface of the limestone is very low. This improves the wetting of C-S-H and means more is able to grow on the surface. Furthermore, limestone can raise the pH level of the paste. This is because limestone is not completely inert. It partially dissolves, releasing Ca^{2+} and carbonate (CO_3^{2-}) ions. C-S-H acts like a magnet for negative ions and attracts the CO_3^{2-} ions. When it attracts these ions, it releases 2 Hydroxide (OH^-) ions into the solution. This increases the pH and gives rise to even more C-S-H nuclei [86]. Most of these positive benefits come from the $CaCO_3$ in the limestone, which is the majority of the limestone. However, limestone also contains various impurities such as magnesium carbonate, or

dolomite. For this reason, the minimum amount of $CaCO_3$ that must be in the limestone added to cement is 70%. The limestone in this research was 89% $CaCO_3$.

4.1.3. Alkali Content. The alkali content is expressed as the equivalent alkali percentage. This is the combined percentage of sodium oxide (Na_2O) and potassium oxide (K_2O). The amount of alkali can impact how effective air-entraining agents are, the reactivity of SCMs, the pH of the mix water, and the possibility of alkali-silica compounds reacting with the aggregate. [87]. A low-alkali cement is below 0.6%. The cement used in this project was 0.52%.

4.1.4. Loss on Ignition. The loss on ignition (LOI) test is used to determine the amount of volatile substances in the cement. The LOI is determined by heating a sample of the cement at a specified temperature and allowing the volatile substances to escape until the mass no longer changes. The upper limit for how much of the mass could be lost was 10%. However, only 4.6% of the cement used was determined to be volatile.

4.1.5. Blaine Fineness. The fineness of the cement has a huge impact on the reactivity of the cement. The finer the cement particles are, the more surface area they have. The amount of surface area the cement particle has is a leading factor that controls the hydration kinetics, with more surface area contributing to faster the dissolution of cement particles and faster precipitation of hydration products [21]. The fineness will not only impact how fast the cement will hydrate, but it will also influence the water demand, with finer cement needing more water for the same level of workability [87]. The Blaine fineness is determined by how fast air can move through a compacted pellet of cement [87]. Type 1L PC typically has a Blaine fineness of around 380-470 m^2/kg, with higher

numbers indicating finer particles. The cement used in this project had a Blaine fineness of 470 m^2/kg [88].

4.1.6. Initial Vicat. A Vicat apparatus can be used to determine how much time a sample of concrete takes to set. The Vicat test follows ASTM C191 Standard Test Methods for Time of Setting of Hydraulic Cement by Vicat Needle. It is performed on a sample of cement with an extremely low w/c, around 0.25. The acceptable range for the setting time is between 45 to 420 minutes, with the cement used in this research setting in 89 minutes.

4.1.7. Compressive Strength. The compressive strength values of a sample of the cement used in this research were provided by Holcim. However, it should be noted that the results can be influenced by a wide variety of factors. For example, these tests are done at a fixed w/c and will not reflect changes in the strength from adjusting this value, or any other adjustments to the mix design [85]. The three-day compressive strength for the cement used in this project was 4590 psi, with 1890 being the minimum value allowed, the seven-day was 5370 psi, with 2900 psi being the minimum, and the 28-day was 6460 psi, with 3620 psi being the minimum.

4.2. AGGREGATES

The aggregates used in the concrete were composed of limestone, supplied local suppliers, and complied with ASTM C33 Standard Specification for Concrete Aggregates. To accurately calculate a mix design for the concrete, it was important to have a good understanding of the characteristics of the aggregates, such as the specific gravity and bulk density.

Aggregates contain pores that are both permeable and impermeable. The absolute specific gravity is the volume of the aggregate excluding all pores. It is defined as the ratio of the mass of the solid to the mass of an equal volume of water. The only way to mitigate the effect of the impermeable voids is to pulverize the aggregates. However, to avoid pulverizing the material, the apparent specific gravity can be found instead [21]. This is the ratio of the dried mass of the aggregate to the equal volume of the water. Equation (6), seen below, can be used to determine this.

$$Apparent\ Specific\ Gravity = \frac{D}{B-A+D} \tag{6}$$

D represents the mass of the oven-dried sample. B is the mass of the vessel full of water. A is the mass of the vessel with the water and sample.

When finding the specific gravity of aggregate that will be used in concrete, it is important to consider that the water contained in all the pores in the aggregate does not take part in the chemical reaction. They can therefore be considered part of the aggregate. Because of this, many calculations are based on saturated surface-dry (SSD) relative densities, also commonly known as the gross apparent specific gravity. The only change in that calculation is that C represents the mass of the saturated surface dry aggregate [21]. This can be seen in Equation (7).

$$Gross\ Apparent\ Specific\ Gravity = \frac{C}{B-A+C} \tag{7}$$

Throughout the research project, two separate sources of aggregates had to be used. These were very comparable in size and gradation; however, the specific gravities were slightly different. For the aggregates used in Mixtures 1 through 10, the coarse aggregates and sand had a gross apparent specific gravity of 2.72 and 2.62 respectively. For

aggregates in Mixtures 11-14, the coarse aggregates had a gross apparent specific gravity of 2.78 and the sand had a specific gravity of 2.6.

The density of a material is numerically equal to its specific gravity multiplied by the density of the water. The specific gravity is a dimensionless ratio, while density is expressed in either kilograms per cubic meter or in lbs per cubic foot. If the American system is being used, the specific gravity must be multiplied by the unit mass of water (62.4 lb/ft^3) to retrieve density. Absolute density refers to the volume of the individual particles. However, it is not possible to pack particles in a way that eliminates all voids. The bulk density, however, describes the mass of aggregate that actually fills a volume. This is the density used to convert quantities of mass to quantities of volume. The bulk density depends on the size distribution and shape of the particles. Therefore, the degree of compaction must be known. There are two separate bulk densities, loose and compacted. To determine the loose bulk density, dried aggregate is gently placed in a container overflowing and then leveled. For the compacted bulk density, the container is filled in three lifts and each lift is compacted with a rod. The container is then leveled. The mass of the aggregate in the container is divided by the container's volume. When this was done for the first set of aggregates used in this research, the loose bulk density of the coarse aggregate was 94.3 lb/ft^3, and the compacted was 107.12 lb/ft^3. The sand's loose compacted density was 102.432 lb/ft^3 and the compacted was 116.4 lb/ft^3. When this was done for the second set of aggregates used in this research, the loose bulk density of the coarse aggregate was 86.3 lb/ft^3, and the compacted was 98.07 lb/ft^3. The sand's loose compacted density was 91.77 $lb/ft^3$and the compacted was 104.28 lb/ft^3.

4.3. ADMIXTURES

The admixtures that were used in this research project were Delvo hydration stabilizer Type B and D, Recover hydration stabilizer Type B and D, and Daracem 19 high-range water-reducing admixture Type A and F. These admixtures work in similar ways and have alike effects. They are all classified by ASTM C 494 Standard Specification for Chemical Admixtures for Concrete, [53]. In this classification system there are seven different types of these admixtures:

- Type A Water-reducing admixtures
- Type B Retarding admixtures
- Type C Accelerating admixtures
- Type D Water-reducing and retarding admixture
- Type E Water-reducing and accelerating admixtures
- Type F Water-reducing, high-range, admixtures
- Type G Water-reducing, high-range, and retarding admixtures

Type A admixture is a water-reducing agent. Its purpose, as defined by ACI Committee 212.3R, is to reduce the water requirement of the mixture for a given slump, produce concrete of higher strength, obtain specified strength at lower cement content, or increase the slump of a given mixture without an increase in water content." To be classified as such, the admixture must reduce the need for water by a minimum of 5%. The initial and final set times must not be accelerated by more than one hour or reduced by more than 1.5 hours. However, typically this admixture has little effect on the setting time. They must also not cause a reduction in flexural strength [53]. The effectiveness of this admixture is dependent on the characteristics of the concrete it is in. Factors such as

concrete temperature, cement content, cement composition, and fineness, and the presence of other admixtures can impact the extent to which the effects of the admixture are seen [58].

Type B and D admixtures are known as conventional retarding admixtures. They are used to diminish the effects of high-temperature concrete and to maintain the workability of concrete while it is being placed. Both admixtures contribute to the water demand reduction, however, type D does this particularly effectively. This is related to the amount of (C_3A) and alkalis (Na_2O and K_2O) in the cement. When high doses of this admixture are used it can cause rapid stiffening and slump loss in some cements [53].

Type F is a high-range water-reducing admixture that reduces the water demand by up to 30% without causing retardation. There are three categories of this admixture based on the ingredients: sulfonated melamine-formaldehyde condensate, sulfonated naphthalene-formaldehyde condensate, and polyether-polycarboxylates. The admixture used in this research was a sulfonated naphthalene-formaldehyde condensate. These are not designed to entrain the air. However, they may change the air-void systems. One possible problem with this kind of admixture is that it is only effective at increasing slump for 30-60 minutes. When it loses effectiveness, the slump reverts to its original level. The duration of the admixture's effectiveness is impacted by the concrete’s temperature, the type of cement, the type of admixture, the dosage, the mixing time, and the initial slump [53].

4.3.1. High-Range Water-Reducing Admixture. Daracem 19 is a high-range water-reducing admixture Type A and F. It is used to decrease the amount of water needed to achieve a similar slump [58]. While adding this to concrete did increase the

slump, it did not decrease the rate of slump loss. It may have even increased it, reducing the time available to cast the cylinders. To overcome this, it was paired with a hydration stabilizer.

4.3.2. Hydration Stabilizers. Recover and Delvo are hydration stabilizers Type B and D. They were used to delay the setting rate of the concrete. Type D admixture is designed to both retard and be a water reducing agent, meaning Recover and Delvo were able to increase slump and postpone hydration [89]. They work by coating cement grains, slowing the hydration process. They are effective until the admixture is incorporated into the hydration product's microstructure, at which point the hydration reaction returns to its normal rate. This means that the effectiveness of the admixtures is dependent on the dosage. If too small an amount is added it may increase the rate of slump loss [89]. The more that is added, the longer the initial setting time will be postponed [60]. In the case of Mixture 3, the cylinders were created with a high dosage of Recover. The cylinders were not set enough to be taken out of the molds for nine days. This led to a high degree of variability. Another disadvantage of both Delvo and Recover is that they can increase the bleeding rate of concrete [60].

4.4. FLY ASH

The fly ash used in this project was a Class C fly ash that complied with the standards set in ASTM C618-15 Standard Specification for Coal Fly Ash and Raw or Calcined Natural Pozzolan for Use in Concrete. It was used in Mixture 7 to replace 25% of the cement. Fortunately, we acquired the Fly Ash from a research team at Missouri University of Science and Technology studying the use of alkali-activated concrete in 3-

D printing. They used X-ray Fluorescence to break down the chemical composition of the Fly Ash by percent weight [90]. This can be seen in Table

Table 4.1 Chemical composition of fly ash using x-ray fluorescence.

Composition	SiO_2	Al_2O_3	Fe_2O_3	CaO	MgO	Na_2O	K_2O	TiO_2	P_2O_5	MnO	LOI*
wt.%	36.9	14.0	3.52	37.0	4.80	1.62	0.62	0.87	0.70	0.03	0.50

*Loss on ignition

4.5. MIX DESIGNS

When creating the mix designs that would be evaluated, we started with a relatively high paste volume of 39%, a w/c of 0.5, and a gradation that consisted of 57% coarse aggregate and 43% sand. The paste volume was the first variable analyzed. Therefore, in the next mixtures, after reducing the w/c to 0.45, all variables were held constant, except the paste volume. The paste volume was lowered to 35%, 32.5%, 30%, and finally 25%.

The standard paste volume was selected to be 32.5%. The next variable considered important to look at was the w/c due to its impact on paste viscosity. The standard paste volume was used, along with the previously described gradation, but the w/c was lowered to 0.40, and in Mixture 8 was raised to 0.50. The 0.45 was selected as the standard ratio that would be used throughout the remainder of the project, except for the mixtures with increased slump, as high slump with minimal segregation can only be created at sufficiently low w/c when no SCMs or mineral fillers are used.

The coarse aggregate content was the next variable looked at. It is considered important because it can have a significant influence on the static yield stress by

impacting the interparticle friction. Moreover, aggregate can increase vibration transfer, so the degree of compaction may need to be adjusted based on this variable. The preselected paste volume of 30% and w/c of 0.45 were used while the gradation was changed to 65% coarse aggregate and 35% sand.

The effects of fly ash and plasticizer were also studied in this project. When fly ash was investigated in Mixture 7, a w/c of 0.45 was used with a gradation of 57% coarse aggregate and 43% sand. The paste volume used was 32.5%. Of the cementitious material used, 75% was Portland cement and 25% was fly ash. When plasticizer was evaluated 150 mL was used with 30 mL of retarder, a paste volume of 32.5%, and a w/c of 0.40. This was then reduced to 75 mL, and then further reduced to 50 mL.

The effect of consolidation efforts on an extremely stiff and extremely fluid mixture was also evaluated. For the extremely stiff mixture, a paste volume of 25%, w/c of 0.45, and a gradation of 65% coarse aggregate and 35% sand was created. For the extremely fluid mixture, a w/c of 0.45, a paste volume of 35%, and gradation of 57% coarse aggregate and 43% sand were used. This extremely fluid mixture also contained 30 mL of Recover hydration stabilizer and 150 mL of the high-range water-reducing admixture. These mix designs can all be found in Table 4.2.

Table 4.2 Mix designs used in the project. Coarse aggregate % is the percentage of the aggregates that were coarse. Similarly, sand % refers to the percentage of the aggregates in the mixture that were sand. Fly ash % is the percentage of cement that was replaced with fly ash.

Mix #	w/c	Paste Volume	Coarse Agg	Sand	Delvo	Recover	Daracem 19	Fly Ash
1	0.5	39%	57%	43%				
2	0.45	35%	57%	43%		175 mL		
3	0.45	25%	57%	43%		275 mL 550 mL		
4	0.45	30%	57%	43%	150 mL			
5	0.45	32.5%	57%	43%	100 mL			
6	0.4	32.5%	57%	43%	150 mL			
7	0.45	32.5%	57%	43%	100 mL			25%
8	0.5	32.5%	57%	43%	100 mL			
9	0.45	30%	65%	35%	100 mL			
10	0.45	25%	65%	35%	100 mL			
11	0.45	32.5%	57%	43%		30 mL	150 mL	
12	0.4	32.5%	57%	43%		30 mL	150 mL	
13	0.4	32.5%	57%	43%		30 mL	50 mL	
14	0.4	32.5%	57%	43%		30 mL	75 mL	

5. RESULTS AND DISCUSSION

5.1. RHEOLOGY

To begin the rheological data analysis, the data was retrieved from the Anton Paar RheoCompass software. The software provides values for torque, rotational speed, shear stress, shear rate, viscosity, and many other parameters. However, only torque and rotational speed are directly measured and are therefore the only values trusted by the software. To check the results of this test, the shear stress was calculated from the torque per Equation (8).

$$\tau = \frac{T}{2\pi R_i^2 h} \tag{8}$$

In this equation, τ represents shear stress, T is torque, R_i represents the radius of the inner cylinder, and h represents the height of the cement paste in the cup.

Calculating the shear rate is a little more complicated. The first step was determining what formula to use, which depended on if the rheometer was a wide, narrow, or intermediate gap rheometer. This is determined based on the value of k, which is calculated with Equation (9).

$$k = \frac{\text{Radius of the Inner Cylinder}}{\text{Radius of the Outer Cylinder}} \tag{9}$$

For this rheometer, the inner cylinder radius was 0.0133 m, and the outer cylinder radius was 0.01446 m. Therefore, the k value was 0.91978, making it a wide-gap rheometer. The next step was converting velocity in rotations per second, to velocity in radians per second, represented by Omega (Ω). This was done by using Equation (10):

$$\Omega = \mathrm{N}2\pi \tag{10}$$

where N is the velocity in rotations per second. The next step was calculating n, which was done with Equation (11).

$$n = \frac{\text{Slope of Natural Log of Torque}}{\text{Slope of Natural Log of } \Omega} \tag{11}$$

Once all this was known, the equation for shear rate ($\dot{\gamma}$) was used as seen below in Equation (12).

$$\dot{\gamma} = \frac{2\Omega}{n(1-k\frac{2}{n})} \tag{12}$$

When the values for shear stress and shear rate were calculated, the shear rate (x-axis) verses shear stress (y-axis) graphs were created. To calculate the dynamic yield stress and viscosity, the shear stress ramp was plotted against the shear rate applied to the paste. This can be seen in Figure 5.1.

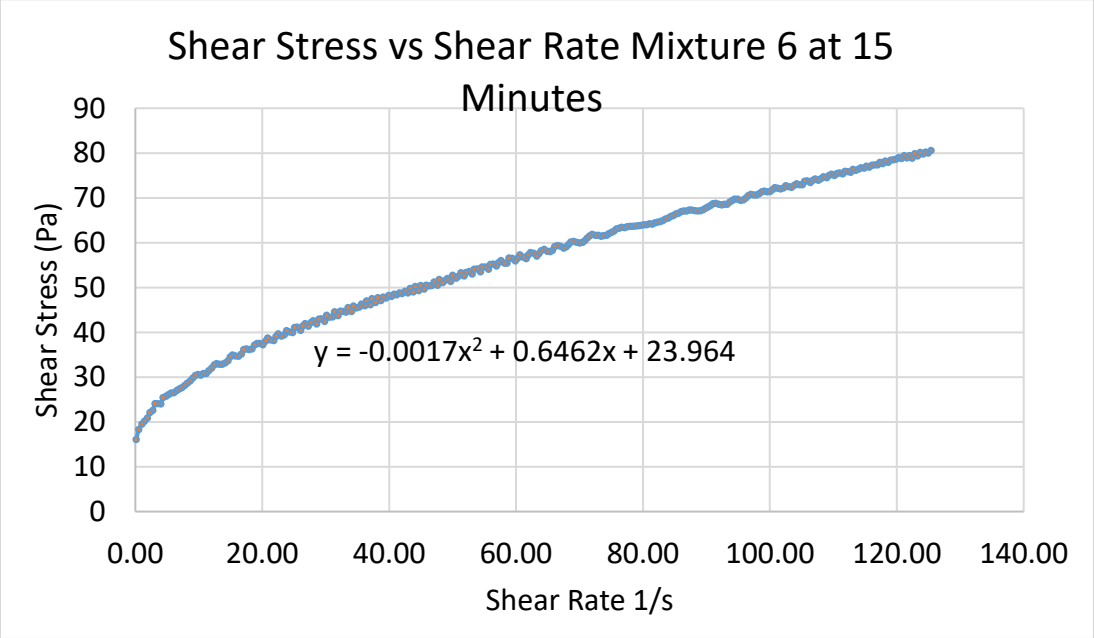

Figure 5.1 Shear Stress vs Shear Rate

The material showed non-linear behavior; therefore, the modified Bingham model was applied. This equation is very similar to the Bingham equation, except it fits the data in a non-linear manner by incorporating a second-order term $c\dot{\gamma}^2$, where c is a fitting constant. It can be seen in Equation (13).

$$\tau = \tau_0 + \mu\dot{\gamma} + c\dot{\gamma}^2 \tag{13}$$

The y-intercept of the very curved section was taken to be the yield stress. The derivative of the slightly curved line was calculated, with 50 s^{-1} being the value of $\dot{\gamma}$ used. The value of the derivative equation at 50 s^{-1}, which is the slope of the resulting line, is the viscosity.

The Reiner-Riwlin equations were used to validate this approach. To do this, velocity in rotations per second (N) was plotted against torque in Nm (T). The Modified Bingham equation was applied to the T-N curve in the form seen in Equation (14).

$$T = G + HN + CN^2 \tag{14}$$

Based on Equation 12, the Reiner-Riwlin equations were used to calculate dynamic yield stress and viscosity. These can be seen in Equations (15), (16), and (17).

$$\tau_0 = \frac{\frac{1}{R_i^2} - \frac{1}{R_o^2}}{4\pi h * \ln\left(\frac{R_o}{R_i}\right)} G \tag{15}$$

$$\mu = \frac{\frac{1}{R_i^2} - \frac{1}{R_o^2}}{8\pi^2 h} H \tag{16}$$

$$c = \frac{\left(\frac{1}{R_i^2} - \frac{1}{R_o^2}\right)}{8\pi^3 h} \frac{(R_o - R_i)}{(R_o + R_i)} C \tag{17}$$

In these equations, dynamic yield stress is represented by τ_0 and viscosity is represented by μ. R_i represents the radius of the inner cylinder of the rheometer in meters and R_o

represents the radius of the outer cylinder in meters. The height of the coaxial zone, also known as the height of the inner cylinder submerged in the sample in meters, is represented by h. G is the intercept of the T-N relationship in Nm, H is the slope of the T-N relationship in Nms and C is the second-order term in the T-N relationship.

When performing rheological tests with cub-and-bob geometries, it is sometimes possible for plug flow to occur. This can happen when the shear stress at the inner cylinder is high enough to overcome the yield stress of the sample, but the shear stress on the outer cylinder is below the yield stress. When this happens, the sample in the zone does not exceed the yield stress and acts like a solid plug. If the plug zone is not considered, dynamic yield stress and viscosity can be miscalculated. To determine if plug flow may have occurred, the shear stress at the outer cylinder was calculated according to Equation (17):

$$\tau_{Ro} = \frac{T_{min}}{2\pi R_o^2 h} \tag{17}$$

based on the lowest torque value. If τ_{Ro} was larger than the dynamic yield stress found by the Reiner Riwlin equations, there was no plug flow. If it was less it was an indication that plug flow had occurred.

A plug flow analysis was done to calculate the dynamic yield stress and viscosity with the plug flow zone corrected. To determine how much of the measurement was affected by plug flow, the new yield stress was used to find the radius of the plug (R_p) for multiple sections of the curve. If the R_p was smaller than the radius of the outer cylinder, the data was affected. It was determined that plug flow was seen in some of the measurements. However, in cases where plug flow was seen, it was only observed in the

last section of the measurement. This last section contained the shear rates of approximately 0-18 s^{-1}.

As previously mentioned, the cement pastes in this study showed consistent non-linearity at shear rates below 20 s^{-1}. This is a phenomenon that is commonly seen when analyzing rheological measurements on cement paste. Haist et al. [91] conducted an extensive study on cement pastes in the shear rate range between 0-90 s^{-1}. They used multiple devices and many different measurement geometries, including five different-sized parallel plates, cone and plate, three different sized coaxial cylinders, nine types of paddles, and five unique geometries such as a sphere probe. They found that non-linear behavior consistently occurred in the shear rate range of 0-20 s^{-1}.

A direct consequence of applying a non-linear model such as the Modified Bingham or Modified Reiner-Riwlin equations, is that the value for viscosity that is calculated is dependent on the shear rate. This effect can leave the final calculation of viscosity slightly misrepresented. However, a linear model such as the Bingham model does not accurately capture the yield stress in the case of non-linear behavior [92]. In this project, the yield stress of the concrete was already being captured by other test methods such as the slump and static yield stress test. Furthermore, the purpose of the rheological measurements was to obtain the value of the viscosity. Therefore, the decision was made to forgo the dynamic yield stress calculation and not incorporate the last 20 s^{-1} of the measurement. This enabled the use of the Bingham model and a more accurate calculation of the viscosity. Table 5.1 below contains the viscosity values that were calculated. The viscosities for Mixtures 9 and 10 were not calculated because the paste composition for these mixtures was identical to the paste composition of Mixture 5. From

these results, it was observed that the viscosity increases with time. Furthermore, both high quantities of hydration stabilizer and HRWRA had the effect of reducing viscosity. When analyzing the effect of viscosity on the test results, only mixtures with a paste volume of 32.5% or greater were considered. Mixtures 7, 8, and 11 were considered to have low viscosity, Mixture 5 had mid-level viscosity, and Mixtures 6, 12, 13, and 14 were considered to have high viscosity.

Table 5.1 Viscosity results.

Viscosity (Pa*s)							
Time (min)	Mixture 1	Mixture 2	Mixture 3.1	Mixture 3.2	Mixture 4	Mixture 5	Mixture 6
15	0.27	0.37	0.12	0.09	0.25	0.28	0.40
60	0.33	0.48	0.27	0.11	0.40	0.42	0.61

Viscosity (Pa*s)						
Time (min)	Mixture 7	Mixture 8	Mixture 11	Mixture 12	Mixture 13	Mixture 14
15	0.23	0.17	0.20	0.36	0.48	0.44
60	0.32	0.25	0.26	0.48	0.55	0.51

5.2. FRESH TEST RESULTS

The test results from the fresh concrete can be seen as summarized in Table 5.2. All results were obtained by following the procedures outlined in Section 3.

Table 5.2 Fresh concrete test results. S1, S2, S3, and S4 refer to the slumps in the order in which they were done. YS1 and YS2 are the first and second static yield stress.

Mix #	S1 (in)	Temp ˚F	YS1 (Pa)	Density (lb/ft^3)	Air	S2 (in)	S3 (in)	YS2 (Pa)	S4 (in)
1	7	75	660.1	148	1%	7.5	3	602.3	
2	7.75	75		148.6	2.4%	7	5.5		
3	3	65	2910.1	151.4	3.1%	0.5	2	3310	1
4	1	70	5116.8	150.8	3%	0	1.5	3974.9	.5
5	7	70	1040.7	149.8	1.9%	3.5	7	1093.7	3
6	1	72	5622.7	151.8	2.9%	0	3	3974.9	0.5
7	8.5	70	240.9	151.6		5	8.5	409.5	5
8	7.5	70	563.7	150.7	1.7%	6.5	8.25	1252.7	6.5
9	4	71	1821.2	151.7	2.5%	0.5	4.5	2042.9	2.5
10	0	70	4707.3	151.9	3.6%	0	1.5	5849.2	0
11	9.25	68	53	151.8	1.1%	8	9.75	183.1	8
12	8.5	70	91.5	152.8	1.9%	3.75	8.25	780.5	4.75
13	4.25	70	5511.9	150.7	1.8%	2	4.25	4008.7	1.5
14	6	70	101.2	151.1	2.1%	2	5.5	1744.2	2

5.3. RESULTS OF SEGREGATION EVALUATION

5.3.1. Analysis Procedure. Segregation can be used to indicate over-consolidation. As discussed in Section 3, one approach to evaluating segregation was the

use of the penetration apparatus. According to ASTM C1712 Standard Test Method for Rapid Assessment of Static Segregation Resistance of Self-Consolidating Concrete Using Penetration Test, the concrete is considered to not be resistant to segregation if the penetration is above 25 mm. Between 10-25 mm the concrete is considered moderately resistant to segregation, and any amount of penetration under 10 mm is considered resistant to segregation [93]. None of the cylinders in the project showed this extent of penetration depth. The maximum penetration was seen on Mixture 11, which had a slump of 9.75 inches. The penetration depth was 8 mm after the consolidation method 6s 8000 VPM was applied. The highest average penetration depth was also seen in Mixture 11. It was 6.33 mm after the consolidation method 12s 8000 VPM was applied.

Though none of the consolidation methods showed what ASTM C1712 classifies as being unstable, the penetration depth of the cylinders was still analyzed to determine if a pattern of unusually high penetration could be identified. Because every mix design has a different level of workability, the analysis had to be done for each mix design individually. Furthermore, because of evaporation and hydration, the level of workability was actively decreasing as the cylinders were being created. To normalize the results for time, the average hydration age of each cylinder in a given set and the average penetration depth was plotted. A sample of this can be seen in Figure 5.2.

A trendline between the reference set cast at the beginning of the batch, and the reference set that was cast at the end of the batch was then inserted. The equation of the trendline was used to find the time evolution of the penetration based on the penetration of the references. The difference between this expected value and the actual value was then calculated. This is referred to as the delta.

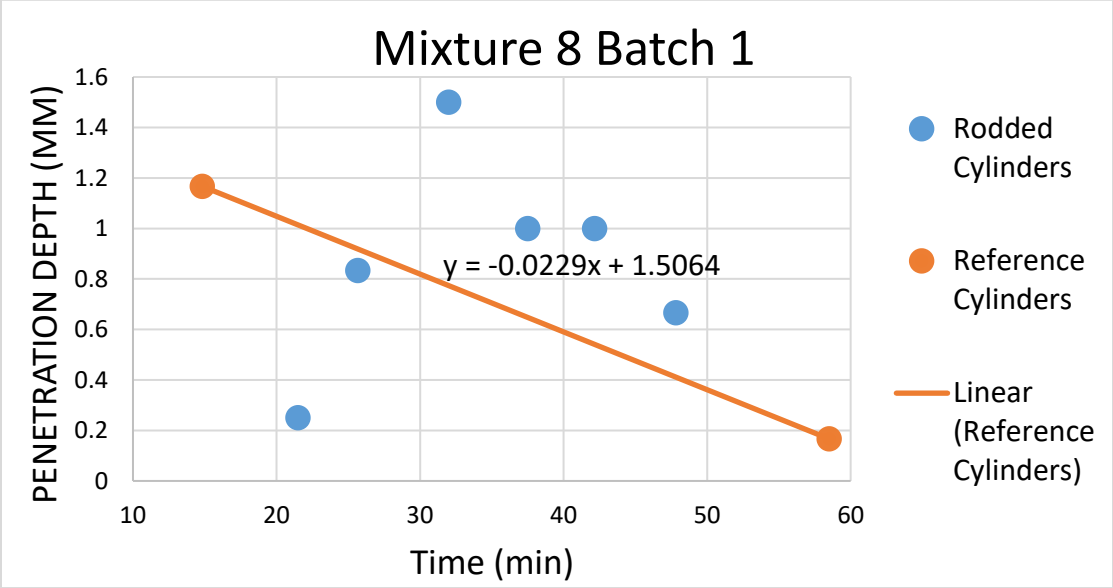

Figure 5.2 Penetration Depth Reference Trendline

The standard deviation was then calculated. A t-value of 1.886 was used to calculate the 90% confidence interval. This value corresponded with one-tail and two degrees of freedom for the three cylinders in the reference sets. The confidence interval was used to find the upper and lower limits. The deltas and upper and lower limits were then plotted to enable better visualization of the data. An example of this can be seen in Figure 5.3. The sets of cylinders and corresponding consolidation methods that fell outside of these limits were identified. As can be seen in Figure 5.3, some cylinders exhibited less penetration than the references and were below the lower limit, while some exhibited more and were above the upper limit. Because the cylinders were being evaluated for over-consolidation, only data points that were identified as being above the upper limit were considered.

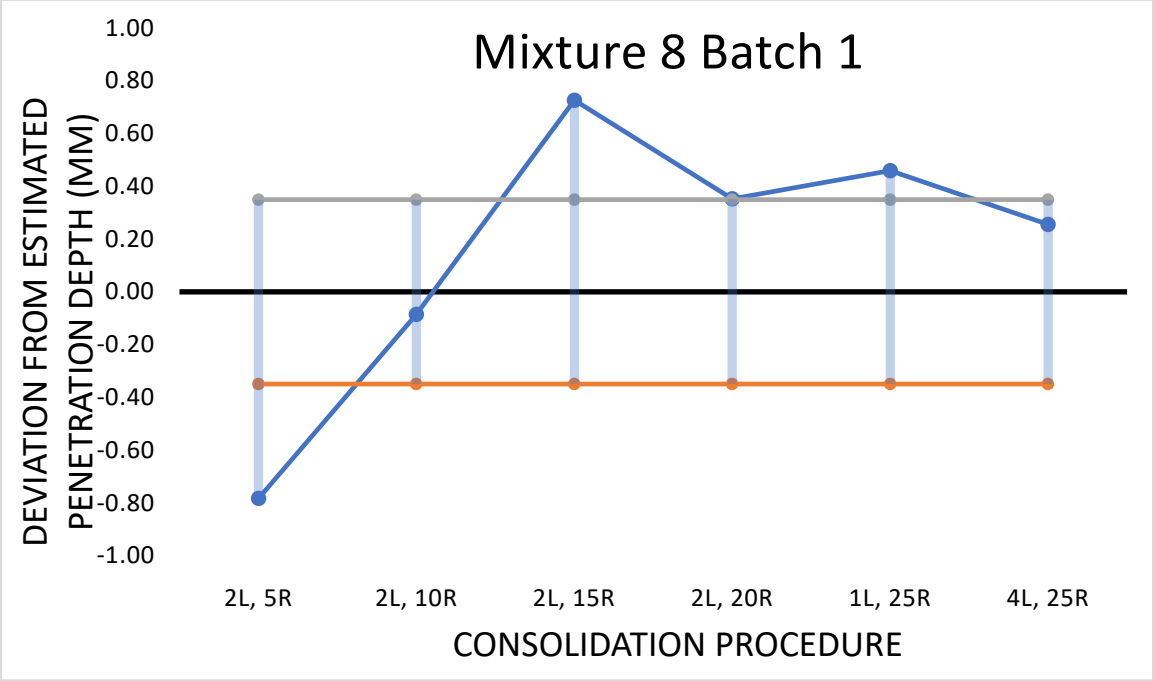

Figure 5.3 Deviation from Reference Set

This procedure was completed for both batches of every mix design. These graphs can all be found in Appendix A. The data was used to create a matrix, in which every consolidation method that fell above the upper limit was highlighted. The percentage of sets for each consolidation method that was above the limit was calculated. The mix designs were split into two groups based on if the cylinders were created with the fluid or stiff procedure. The percentage of sets for each consolidation method that were above the limit was also calculated. This matrix can be found in Appendix B and seen in Table 5.3. In the matrix, the mix designs are in order of workability, with the stiffest mixtures at the top and the most fluid mixtures at the bottom. The compaction methods are in order from lowest to highest amount of consolidation energy applied by rodding, followed by lowest to highest amount of consolidation energy applied by vibrating. Mixtures highlighted in

yellow were created with the stiff consolidation procedure, and mixtures highlighted in blue were created with the fluid consolidation procedure.

Table 5.3 Penetration deltas. Orange highlighted values are above the 90% confidence interval.

	Paste Vol	w/c	2L, 0R	2L, 5R	2L, 10R	1L, 25R	2L, 15R	2L, 20R	2L 30R	2L 40R	2L, 50R	4L 25R	1s, 8000 vpm	3s, 6000 vpm	3s, 8000 vpm	6s, 8000 vpm	3s, 12000 vpm	12s, 8000 vpm
Mix 10	25%	0.45	0.0		0.0	0.0		0.0	0.0	0.0	0.0	0.0	0.0	0.0	0.0	0.0	0.0	0.0
Mix 3	25%	0.45	-0.1		0.0	0.0		0.0	0.3	0.7	0.7	0.3	0.6	0.3	0.7	0.5	0.2	0.7
Mix 4	30%	0.45	0.0		0.0	0.0		0.0	0.0	0.0	0.0	0.0	0.0	0.0	0.0	0.0	0.0	0.0
Mix 9	30%	0.45	-0.1		-0.8	-0.3		-0.1	0.7	0.3	0.4	0.3	-0.4	-0.5	-0.5	-0.1	-0.6	0.5
Mix 6	32.50%	0.4	0.0		0.0	0.0		0.0	0.0	0.0	0.0	0.0	0.0	0.0	0.0	0.0	0.0	0.0
Mix 13	32.50%	0.4	0.0		0.0	0.2		-0.2	0.0	-0.1	0.1	-0.1	0.0	0.2	0.0	0.0	0.0	0.0
Mix 14	32.50%	0.4	0.0	-0.2	-0.3	-0.1	-0.1	0.0			0.3	0.4	0.0	-0.1	0.0	0.2	0.1	0.4
Mix 5	32.50%	0.45	0.0	0.2	0.1	-0.1	0.6	0.2			-0.3	0.1	-0.2	0.2	-0.2	-0.1	-0.1	0.3
Mix 1	39%	0.5	0.1	-1.0	-0.6	-0.1	-0.9	-0.1			0.3		-0.1	-0.2	-0.5	0.0	-0.1	0.4
Mix 8	32.50%	0.5	-0.1	-0.8	-0.1	0.5	0.7	0.4			0.2	0.3	-0.1	-0.4	-0.2	0.1	-0.5	0.7
Mix 2	35%	0.45	0.5	-0.8	-1.0	-1.0	-0.7	-0.7				0.0	-0.6	0.0	-0.4	0.2	0.1	1.0
Mix 12	32.50%	0.4	0.1	-0.4	-0.4	0.0	-0.3	-0.1			-0.8	-0.2	-0.8	-0.3	-0.5	-0.5	-0.2	-0.4
Mix 7	32.50%	0.45	-0.1	-0.2	-0.1	0.5	0.2	-0.1			0.2	0.0	-0.1	-0.3	-0.9	-0.3	0.2	0.3
Mix 11	35%	0.45	-1.5	-0.6	-0.7	-0.7	-0.7	-0.6			1.7	-0.5	-1.3	-1.9	-1.7	0.1	-1.7	2.2
Total % above limit			7	13	0.0	21	38	0.0	33	17	29	14	7	21	7	14	14	50
Stiff mixtures above limit			0		0.0	17		0.0	33	17	33	17	17	33	17	17	33	33
Fluid mixtures above limit			13	13	0.0	25	38	0.0			25	13	0	13	0	13	0	63

5.3.2. Discussion of Results. Based on studying the matrix, certain patterns could be identified. For example, for 50% of the mixtures, cylinders that were created with 12s 8000 VPM showed penetration that exceeded the upper limit. Penetration also seemed to be more substantial for cylinders created with 2L 50R.

Segregation was also investigated based on the visual appearance of the concrete immediately after the cylinder was created. This is a qualitative and somewhat subjective assessment; however, it was useful in identifying trends. Every time cylinders were created and visual signs of segregation, such as bleeding or a large amount of paste on the surface of the cylinder, were present, it was recorded. A matrix was created in which the

cylinders affected were highlighted. This matrix can be found in Appendix B, and an abbreviated form of it can be seen in Table 5.4. This matrix revealed that visual signs of segregation were only identified on cylinders that had been vibrated. Signs of segregation were observed on five of the sets of cylinders that had been vibrated in Mixture 5 and three sets in Mixture 6. Seven out of the 14 mixtures had signs of segregation when cylinders were consolidated with 6s 8000 VPM. Furthermore, nine exhibited signs of segregation on cylinders consolidated with 12s 8000 VPM.

Table 5.4 Consolidation methods showing visual signs of bleeding. Values highlighted in red represent the affected sets.

	Paste Vol	w/c	3s, 6000 vpm	3s, 8000 vpm	6s, 8000 vpm	3s, 12000 vpm	12s, 8000 vpm
Mix 10	25%	0.45	0.0	0.0	0.0	0.0	0.0
Mix 3	25%	0.45	0.0	0.0	0.0	0.0	0.7
Mix 4	30%	0.45	0.0	0.0	0.0	0.0	0.0
Mix 9	30%	0.45	0.3	0.8	1.0	0.2	1.5
Mix 6	32.50%	0.4	0.0	0.0	0.0	0.0	0.0
Mix 13	32.50%	0.4	0.2	0.0	0.0	0.0	0.0
Mix 14	32.50%	0.4	0.0	0.2	0.3	0.2	0.5
Mix 5	32.50%	0.45	0.3	0.2	0.2	0.0	0.5
Mix 1	39%	0.5	0.0	0.0	0.3	0.0	0.7
Mix 8	32.50%	0.5	0.3	0.8	1.0	0.2	1.5
Mix 2	35%	0.45	0.3	0.3	0.7	0.3	0.7
Mix 12	32.50%	0.4	0.0	0.3	0.2	0.0	0.0
Mix 7	32.50%	0.45	0.3	0.2	0.5	0.7	1.0
Mix 11	35%	0.45	1.8	3.7	4.7	1.7	6.3

5.3.3. Comparison of Mixtures. The deltas of the average penetration of the sets were then directly compared to similar mixtures. When the mixtures were compared based on cement paste viscosities, many mixtures experienced more penetration on vibrated sets. Low-viscosity mixtures seem to be slightly more sensitive to vibration

duration and high-viscosity mixtures seem to be more sensitive to frequency. This is illustrated in Table 5.5.

Table 5.5 Penetration deltas of vibrated mixtures. Orange highlighted values represent sets that exceeded the 90% confidence interval. Mixtures 8, 11, and 7 are low-viscosity mixtures, Mixture 5 is a mid-level viscosity mixture, and Mixtures 12, 6, 14, and 13 are high-viscosity mixtures.

	Paste Vol	w/c	1s, 8000 vpm	3s, 6000 vpm	3s, 8000 vpm	6s, 8000 vpm	3s, 12000 vpm	12s, 8000 vpm
Mix 8	32.50%	0.5	-0.1	-0.4	-0.2	0.1	-0.5	0.7
Mix 11	35%	0.45	-1.3	-1.9	-1.7	0.1	-1.7	2.2
Mix 7	32.50%	0.45	-0.1	-0.3	-0.9	-0.3	0.2	0.3
Mix 5	32.50%	0.45	-0.2	0.2	-0.2	-0.1	-0.1	0.3
Mix 12	32.50%	0.4	-0.8	-0.3	-0.5	-0.5	-0.2	-0.4
Mix 6	32.50%	0.4	0.0	0.0	0.0	0.0	0.0	0.0
Mix 14	32.50%	0.4	0.0	-0.1	0.0	0.2	0.1	0.4
Mix 13	32.50%	0.4	0.0	0.2	0.0	0.0	0.0	0.0

When mixtures were compared based on paste volume, higher deltas, and therefore more penetration, were seen as paste volume increased. Higher paste volumes seemed to show more penetration on under-consolidated procedures such as the 1L 25 R. This may be due to entrapped air still being present in the cylinder and the pressure of the apparatus forcing it out. Higher deltas were also seen on mixtures with higher w/c, while plasticizer and fly ash seem to have little effect.

5.4. RESULTS OF SATURATED SURFACE DRY RELATIVE DENSITY

5.4.1. Analysis Procedure. The first step in determining if any of the consolidation methods had a significant impact on SSD relative density values was to analyze each set of cylinders for excessive variations. ASTM C127 Standard Test

Method for Relative Density (Specific Gravity) and Absorption of Coarse Aggregate has a table based on the results from the AASHTO Materials Reference Laboratory Proficiency Sample Program for determining precision. This standard states that the standard deviation of the SSD relative density should be under 0.007 [94]. It is important to note that the table in this standard was intended to be applied to coarse aggregates, not concrete. Therefore, a different value of standard deviation for this application may be more appropriate. However, this was the most suitable value that could be located and is sufficient in helping to identify trends. A matrix was made of all cylinder sets that fell outside of this acceptable range. This matrix can be seen in Table 5.6.

Table 5.6 Sets that exceeded the standard deviation limit for SSD relative densities.

	Paste Vol	w/c	2L, 0R	2L, 5R	2L, 10R	1L, 25R	2L, 15R	2L, 20R	2L, 25R	2L, 25R	2L, 25R	2L, 25R	2L 30R	2L 40R	2L, 50R	4L 25R	1s, 8000 vpm	3s, 6000 vpm	3s, 8000 vpm	6s, 8000 vpm	3s, 12000 vpm	12s, 8000 vpm
Mix 10	25%	0.45	0.003		0.001	0.004		0.026	0.007	0.050	0.004	0.005	0.014	0.012	0.202	0.004	0.004	0.005	0.002	0.003	0.003	0.015
Mix 3	25%	0.45	0.008		0.003	0.011		0.005	0.003	0.006	0.004	0.003	0.002	0.005	0.001	0.003	0.003	0.007	0.006	0.007	0.011	0.006
Mix 4	30%	0.45	0.007		0.002	0.005		0.005	0.001	0.005	0.003	0.003	0.008	0.002	0.004	0.005	0.004	0.007	0.004	0.005	0.008	0.005
Mix 9	30%	0.45	0.007		0.001	0.006		0.006	0.008	1.555	0.006	0.004	0.006	0.001	0.004	0.005	0.003	0.007	0.006	0.008	0.004	0.003
Mix 6	32.50%	0.4	0.005		0.001	0.002		0.005	0.003	0.006	0.001	0.002	0.005	0.001	0.005	0.006	0.001	0.005	0.003	0.005	0.004	0.006
Mix 13	32.50%	0.4	0.006		0.003	0.004		0.003	0.002	0.004	0.005	0.007	0.002	0.003	0.003	0.004	0.003	0.004	0.004	0.004	0.003	0.001
Mix 14	32.50%	0.4	0.001	0.002	0.004	0.006	0.025	0.008	0.001	0.002	0.004	0.006			0.003	0.004	0.004	0.025	0.005	0.006	0.004	0.005
Mix 5	32.50%	0.45	0.009	0.003	0.007	0.005	0.001	0.010	0.009	0.005	0.009	0.013			0.007	0.011	0.005	0.004	0.004	0.005	0.002	0.005
Mix 1	39%	0.5	0.043	0.004	0.001	0.008	0.003	0.006	0.006	0.005	0.006				0.004		0.003	0.007	0.006	0.012	0.003	0.001
Mix 8	32.50%	0.5	0.005	0.006	0.005	0.005	0.006	0.005	0.001	0.003	0.006	0.004			0.003	0.012	0.006	0.005	0.005	0.002	0.004	0.004
Mix 2	35%	0.45	0.004	0.000	0.008	0.014	0.007	0.005	0.001	0.014	0.005					0.009	0.005	0.006	0.007	0.004	0.009	0.002
Mix 12	32.50%	0.4	0.008	0.004	0.002	0.004	0.001	0.002	0.008	0.005	0.007	0.006			0.009	0.006	0.003	0.001	0.009	0.003	0.002	0.004
Mix 7	32.50%	0.45	0.005	0.004	0.002	0.004	0.005	0.005	0.007	0.003	0.001	0.003			0.005	0.003	0.007	0.008	0.001	0.007	0.002	0.003
Mix 11	35%	0.45	0.006	0.002	0.003	0.007	0.006	0.008	0.010	0.003	0.013	0.003			0.019	0.007	0.006	0.004	0.013	0.011	0.006	0.009
Total % below limit			36	0	14	21	7	29	36	21	21	8	14	7	31	23	7	29	21	29	21	14
Stiff mix % below limit			33		0	17		33	33	33	0	0	33	17	17	0	0	33	0	17	33	17
Fluid mix % below limit			38	0	25	25	13	25	38	13	38	17			43	43	13	25	38	38	13	13

When the standard deviation of the SSD relative density within each set was calculated, some consolidation methods showed more frequent deviations above .007 than others. Sets consolidated with 2L 0R, exceeded the allowed standard deviation in

five out of the 14 sets. However, the first reference set did as well. Therefore, this was not deemed to be significant.

The next step was to determine if the SSD relative density of the cylinders from each consolidation method was significantly lower than the densities of the reference sets. The same method used for determining if the penetration was significant was employed. For each batch, the SSD relative densities of the cylinders of each consolidation method were averaged and plotted on a density versus time graph, as can be seen in Figure 5.4. A trendline between the two references was inserted, and the equation was used to determine the deltas of each consolidation method.

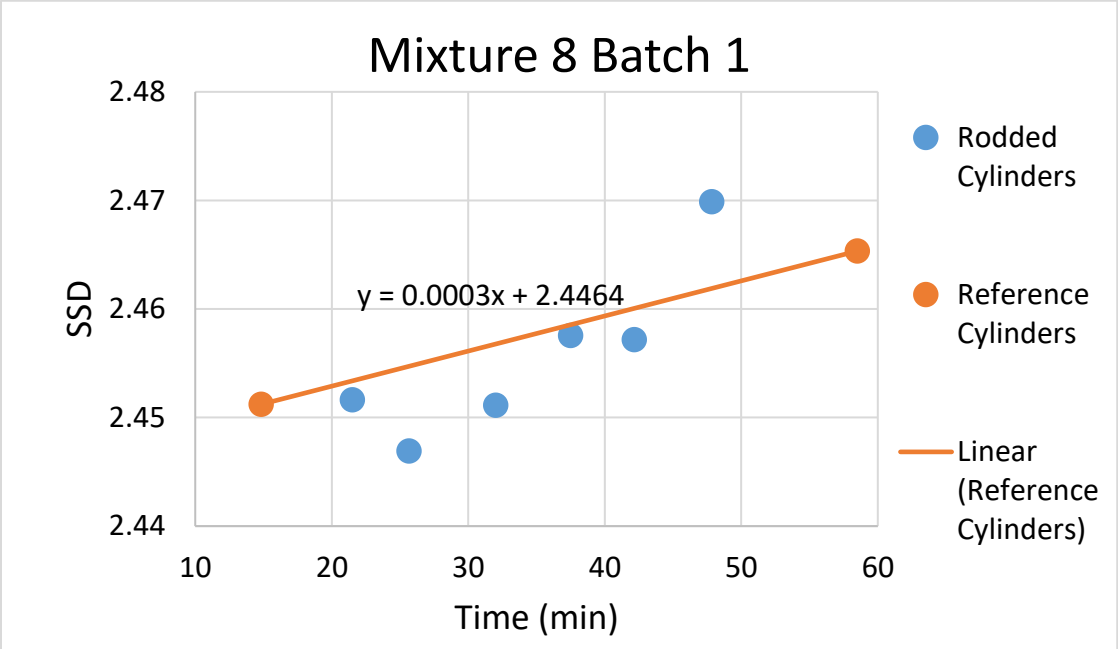

Figure 5.4 SSD Relative Density Reference Trendline

The standard deviation was then calculated. A t-value of 1.886 was used to calculate the 90% confidence interval. This value corresponded with one-tail and two degrees of freedom for the three cylinders in the reference sets. The confidence interval was used to find the upper and lower limits of the SSD relative density delta values. These limits, along with the delta of each consolidation method, were plotted to better visualize the data. This can be seen in Figure 5.5.

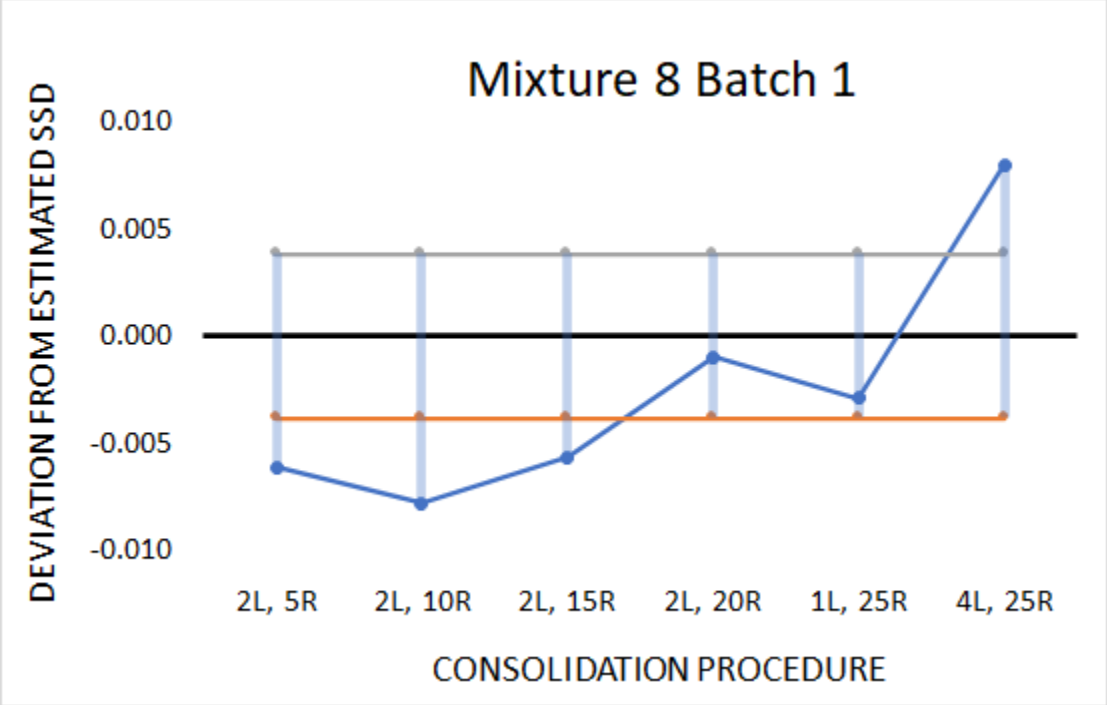

Figure 5.5 SSD Relative Density Deviation from Reference

The sets of cylinders and the corresponding consolidation method that fell outside of the limits were identified. Because the SSD relative density was being used to evaluate for under-consolidation, only cylinders that were less dense than the references, and were

under the lower limit were considered. These graphs for each mixture can be found in Appendix A.

When all points below the lower limit were identified, a matrix was created. This can be found in Appendix B. The percentage of sets of each consolidation method that exceeded the limit was calculated. The mix designs were split into two groups based on if the cylinders were created with the fluid or stiff procedure. The percentage of sets of each consolidation method that were below the limit was also calculated. This can be seen in Table 5.7.

Table 5.7 SSD relative density deltas. Orange highlighted values fall below the 90% confidence interval.

	Paste Vol	w/c	2L, 0R	2L, 5R	2L, 10R	1L, 25R	2L, 15R	2L, 20R	2L 30R	2L 40R	2L, 50R	4L, 25R	1s, 8000 vpm	3s, 6000 vpm	3s, 8000 vpm	6s, 8000 vpm	3s, 12000 vpm	12s, 8000 vpm
Mix 10	25%	0.45	-0.043		-0.037	-0.008		-0.014	0.021	0.033	0.157	0.060	-0.006	0.008	-0.001	0.016	0.014	0.033
Mix 3	25%	0.45	-0.034		-0.007	0.002		0.002	0.003	0.001	0.010	0.004	0.006	0.006	0.025	0.016	0.007	0.022
Mix 4	30%	0.45	-0.045		0.002	0.007		0.002	0.003	0.005	0.005	-0.002	-0.004	-0.006	0.005	0.007	0.007	0.007
Mix 9	30%	0.45	-0.024		-0.007	-0.008		-0.004	0.000	0.001	0.001	0.003	-0.006	-0.008	0.005	0.004	0.007	0.013
Mix 6	32.50%	0.4	-0.022		-0.003	-0.005		0.002	0.007	0.007	0.011	0.001	-0.007	-0.010	-0.003	-0.004	-0.002	0.004
Mix 13	32.50%	0.4	0.002		-0.003	-0.003		0.002	0.002	0.002	0.005	0.001	0.000	0.004	0.002	0.005	0.011	0.014
Mix 14	32.50%	0.4	-0.017	-0.002	-0.001	-0.003	-0.001	0.001			-0.003	0.000	-0.007	0.004	-0.006	0.000	0.004	0.010
Mix 5	32.50%	0.45	-0.023	-0.009	-0.013	-0.006	-0.004	-0.003			-0.003	-0.002	-0.008	-0.006	-0.003	0.000	0.008	0.017
Mix 1	39%	0.5	0.010	0.003	0.019	0.003	0.023	0.018			0.006		0.000	-0.003	0.010	0.010	0.001	0.015
Mix 8	32.50%	0.5	-0.013	-0.006	-0.008	-0.003	-0.006	-0.001			0.001	0.008	0.000	-0.003	-0.002	0.010	0.004	0.019
Mix 2	35%	0.45	-0.013	0.002	0.010	-0.018	0.010	0.017				-0.011	-0.004	-0.018	-0.010	-0.010	0.010	0.011
Mix 12	32.50%	0.4	-0.011	-0.002	0.006	0.010	0.009	0.013			-0.002	0.007	-0.003	0.002	0.003	0.015	0.012	0.020
Mix 7	32.50%	0.45	-0.014	-0.010	-0.009	-0.007	0.000	-0.008			0.003	-0.002	-0.007	-0.011	-0.001	0.009	-0.004	0.010
Mix 11	35%	0.45	-0.002	-0.001	0.003	0.009	0.003	0.011			-0.019	0.012	0.006	0.015	0.015	0.015	0.020	0.019
Total % below limit			79	38	50	29	25	14	0	0	8	15	29	21	7	7	0	0
Stiff mix % below limit			83	0	50	17	0	17	0	0	0	17	17	17	0	0	0	0
Fluid mix % below limit			75	38	50	38	25	13	0	0	14	14	38	25	13	13	0	0

5.4.2. Discussion of Results. After analyzing the matrix, it was determined that the cylinders created with 2L 0R were below the SSD relative density lower limit 79% of the time. The cylinders made with 2L 5R were below the acceptable level 38% of the time, and the cylinders made with 2L 10 R were below the acceptable level 50% of the

time. This suggests these consolidation methods provide an insufficient amount of consolidation for both fluid and stiff mixtures.

Cylinders made with 1L 25R and 1s 8000 both exceeded the lower limit for fluid mixtures 38% of the time and 17% for stiff mixtures. This is indicative of a trend that was repeatedly seen of stiff mixtures having fewer sets exceeding the lower limit. Mixture 10, which had an initial slump of 0 inches, only had one consolidation method, 2L 0R, exceed the lower limit of the 90% confidence interval. However, Mixture 7, which had an initial slump of 8.5 inches, had seven out of the 14 consolidation methods exceed the lower limit. Furthermore, the SSD relative density deltas of the three stiffest mixtures, Mixtures 10, 3, and 4, on average had 1.7 out of the 14 consolidation methods exceed the lower limit of their corresponding confidence intervals. However, the three most fluid mixtures, Mixtures 12, 7, and 11, on average, had three out of the 14 exceed the lower limit. To ensure that this trend was not due to the change in the confidence intervals, the strictest confidence interval was applied to all of the mixtures. When this was done, the three stiffest mixtures had, on average, 3.3 consolidation methods exceed the limit, while the three most fluid mixtures had 4.7 exceed the limit. This can be seen in Table 5.8.

Table 5.8 SSD relative density deltas of most stiff and fluid mixtures. Highlighted values fall below the lower limit when the same confidence interval was used throughout.

	Paste Vol	w/c	2L, 5R	2L, 10R	2L, 15R	2L, 20R	1L, 25R	2L, 50R	4L, 25R	3s, 8000 vpm	1s, 8000 vpm	3s, 6000 vpm	3s, 12000 vpm	2L, 0R	All	Vib	Rod
10	25%	0.45		-0.037		-0.014	-0.008	0.157	0.060	-0.001	-0.006	0.008	0.014	-0.043	5	1	4
3	25%	0.45		-0.007		0.002	0.002	0.010	0.004	0.025	0.006	0.006	0.007	-0.034	2	0	2
4	30%	0.45		0.002		0.002	0.007	0.005	-0.002	0.005	-0.004	-0.006	0.007	-0.045	4	2	2
12	32.50%	0.4	-0.002	0.006	0.009	0.013	0.010	-0.002	0.007	0.003	-0.003	0.002	0.012	-0.011	3	0	3
7	32.50%	0.45	-0.010	-0.009	0.000	-0.008	-0.007	0.003	-0.002	-0.001	-0.007	-0.011	-0.004	-0.014	9	3	6
11	35%	0.45	-0.001	0.003	0.003	0.011	0.009	-0.019	0.012	0.015	0.006	0.015	0.020	-0.002	2	0	2

While in the majority of the batch, stiff mixtures were less sensitive to the consolidation procedure, this was not true for the last set, 2L 0R, which repeatedly had higher negative deltas than the fluid mixtures. For every mixture, 2L 0R was the last set created. At this point in the process, all mixtures were experiencing some degree of slump loss, which may be particularly detrimental for stiff mixtures. For Mixtures 10, 3, and 4, the second reference set in the batch, which was created immediately before the set 2L 0R, was as dense or denser than the first. This suggests that while 2L 25R is still as effective at consolidating the concrete at the end of the batch as it is at the beginning, the effect of slump loss on stiff mixtures exaggerated the negative effects of under-consolidation.

Notably, in none of the mix designs did cylinders made with high amounts of vibration, such as 12s 8000 VPM and 3s 12000 VPM fall below the lower limit. This suggests a high amount of vibration does not lead to under-consolidation.

5.4.3. Comparison of Mixtures. To determine how the various consolidation methods impacted mixtures when only a few variables were changed, the deltas of similar mix designs were compared. The viscosities of the cement pastes were the first parameter analyzed. There seemed to be little variation as the paste viscosity increased. However, all mixtures in this group had a paste volume of 32.5% or above. Regardless of paste viscosity, consolidation methods such as 2L 0R, 2L 5R, 2L 10R, 1L 25R, and 1s 8000 VPM all routinely exceeded the lower limit. This can be seen in Table 5.9.

Table 5.9 SSD relative density deltas of mixtures with increasing viscosities. Mixtures 8, 11, and 7 are low-viscosity mixtures, Mixture 5 is a mid-level viscosity mixture, and Mixtures 12, 6, 14, and 13 are high-viscosity mixtures. Orange highlighted values are below the 90% confidence interval.

	Paste Vol	w/c	2L, 0R	2L, 5R	2L, 10R	1L, 25R	2L, 15R	2L, 20R	2L, 50R	1s, 8000 vpm	3s, 6000 vpm
Mix 8	32.50%	0.5	-0.013	-0.006	-0.008	-0.003	-0.006	-0.001	0.001	0.000	-0.003
Mix 11	35%	0.45	-0.002	-0.001	0.003	0.009	0.003	0.011	-0.019	0.006	0.015
Mix 7	32.50%	0.45	-0.014	-0.010	-0.009	-0.007	0.000	-0.008	0.003	-0.007	-0.011
Mix 5	32.50%	0.45	-0.023	-0.009	-0.013	-0.006	-0.004	-0.003	-0.003	-0.008	-0.006
Mix 12	32.50%	0.4	-0.011	-0.002	0.006	0.010	0.009	0.013	-0.002	-0.003	0.002
Mix 6	32.50%	0.4	-0.022		-0.003	-0.005		0.002	0.011	-0.007	-0.010
Mix 14	32.50%	0.4	-0.017	-0.002	-0.001	-0.003	-0.001	0.001	-0.003	-0.007	0.004
Mix 13	32.50%	0.4	0.002		-0.003	-0.003		0.002	0.005	0.000	0.004

Mixtures 2, 5, and 4 were then directly compared. These mix designs were nearly the same, but the paste volume was decreased from 35%, 32.5%, to 30% respectively. Although not a strong trend, as paste volume decreases, there seem to be fewer sets falling below the lower limit. Similarly, Mixtures 9 and 10 are comparable, with 9 having a paste volume of 30% and 10 a paste volume of 25%. These mixtures show a similar trend of stiffer mixtures being less sensitive to the consolidation procedure. To evaluate if this is occurring because of the changing need of the consolidation procedure or simply because the standard deviation changed, the deltas were reevaluated based on the narrowest confidence interval within the group. For example, between Mixtures 2, 5, and 4, Mixture 5 had the narrowest confidence interval. It allowed for a delta of -76 in the first batch and -152 in the second batch. All three mixtures were then reevaluated based on this criterion. Between Mixtures 2, 5, and 4 there were no changes. However, more sets fell below the new limit in Mixture 10. The consolidation methods that do repeatedly fall below the lower limit are 2L 0R, 2L 10R, and 1L 25R. Tables 5.10 and 5.11, seen

below, are condensed versions of the matrix found in Appendix B. It depicts only the consolidation methods within the groups that exceeded the lower limit.

Table 5.10 SSD relative density deltas of similar mixtures, decreasing paste volume. Orange highlighted values are below the 90% confidence interval.

	Paste Vol	w/c	2L, 0R	2L, 5R	2L, 10R	1L, 25R	2L, 15R	4L, 25R	1s, 8000 vpm	3s, 6000 vpm	3s, 8000 vpm	6s, 8000 vpm
Mix 2	35%	0.45	-0.013	0.002	0.010	-0.018	0.010	-0.011	-0.004	-0.018	-0.010	-0.010
Mix 5	32.50%	0.45	-0.023	-0.009	-0.013	-0.006	-0.004	-0.002	-0.008	-0.006	-0.003	0.000
Mix 4	30%	0.45	-0.045		0.002	0.007		-0.002	-0.004	-0.006	0.005	0.007

Table 5.11 SSD relative density deltas of similar mixtures, decreasing paste volume. Orange highlighted values are below the 90% confidence interval. Green highlighted values would have been below the 90% confidence interval if the narrowest interval of the group was applied.

	Paste Vol	w/c	2L, 0R	2L, 10R	1L, 25R	2L, 20R	3s, 6000 vpm
Mix 9	30%	0.45	-0.024	-0.007	-0.008	-0.004	-0.008
Mix 10	25%	0.45	-0.043	-0.037	-0.008	-0.014	0.008

Between Mixtures 5, 6, and 8 the w/c was increased from 0.4, 0.45, to 0.5. These mixtures exhibited deltas falling below the lower limit on repeated consolidation methods, such as the 2L 0R, 2L 5R, 2L 10R, 2L 15R, 1L 25 R, and 1s 8000 VPM, which all had a low amount of consolidation energy applied. It was observed that unlike when the paste volume was decreased, a decrease in w/c did not lead to fewer sets exceeding the lower limit of the 90% confidence interval.

Between Mixtures 4 and 9 the only change was the gradation, with more coarse aggregates and less sand being incorporated in Mixture 9. Throughout Mixture 9, the deltas were lower, and the mixture seemed to have more sets falling under the confidence

interval, particularly when a low amount of consolidation energy was applied. This could be because additional coarse aggregates create more aggregate interlock, and therefore more friction within the concrete. As the level of friction within the concrete increases, additional consolidation is required. This trend did not change when the narrowest confidence intervals of the group were applied. Because the sample size is small, it is difficult to know if this change was due to the change in gradation or another unknown factor. This can be seen in Table 5.12.

Table 5.12 SSD relative density deltas of similar mixtures, changing gradation. Orange highlighted values are below the 90% confidence interval.

	Paste Vol	w/c	2L, 0R	2L, 10R	1L, 25R	2L, 20R	4L, 25R	1s, 8000 vpm	3s, 6000 vpm
Mix 4	30%	0.45	-0.045	0.002	0.007	0.002	-0.002	-0.004	-0.006
Mix 9	30%	0.45	-0.024	-0.007	-0.008	-0.004	0.003	-0.006	-0.008

Mixtures 12, 13, and 14 only had the dosage of the plasticizer altered. This did not seem to impact the consolidation methods that fell below the lower limit; however, the SSD relative density values did increase as the plasticizer was added. There also did not seem to be a change in density between Mixtures 5 and 7, when fly ash was incorporated.

5.5. RESULTS OF COMPRESSIVE STRENGTH

5.5.1. Analysis Procedure. To determine if the compaction method had a significant impact on the repeatability within each set, the coefficient of variation within the set was determined. This is simply the standard deviation of the set divided by the average value. ASTM C39 states that the acceptable coefficient of variation is 3.2% [95].

The reference sets, on average, exceeded this 35% of the time. The sets made with 2L 0R exceeded it 79% of the time. However, all other rodded sets exceeded it 36% of the time or less. The sets made with 1s 8000 VPM, 3s 8000 VPM, and 6s 8000 VPM all exceeded the acceptable coefficient of variation 43% of the time. Sets consolidated with 12s 8000 VPM, and 3s 12000 VPM both exceeded it 50% of the time. This demonstrates the high degree of variability vibration adds. This information is summarized in Table 5.13.

Table 5.13 Sets that exceeded the coefficient of variation limit for compressive strengths.

	Paste Vol	w/c	2L, 0R	2L, 5R	2L, 10R	1L, 25R	2L, 15R	2L, 20R	2L, 25R	2L, 25R	2L, 25R	2L, 25R	2L 30R	2L 40R	2L, 50R	4L, 25R	1s, 8000 vpm	3s, 6000 vpm	3s, 8000 vpm	6s, 8000 vpm	3s, 12000 vpm	12s, 8000 vpm
Mix 10	25%	0.45	11.60		1.98	1.95		10.29	5.79	11.54	1.49	3.33	18.19	16.26	37.96	2.22	5.66	2.69	2.62	0.82	1.56	1.38
Mix 3	25%	0.45	5.92		3.71	11.03		3.51	3.99	2.68	5.07	1.72	2.08	4.10	2.39	3.75	6.63	17.04	4.06	9.27	6.59	10.53
Mix 4	30%	0.45	36.20		2.22	2.82		3.08	6.39	3.90	3.69	0.55	2.46	1.13	2.17	1.06	6.58	3.33	2.03	1.56	2.28	3.65
Mix 9	30%	0.45	13.63		0.59	1.91		1.98	0.53	4.11	1.21	4.01	2.61	0.19	2.33	4.34	5.96	2.96	3.99	5.92	4.04	0.80
Mix 6	32.50%	0.4	4.00		1.43	1.03		1.20	1.89	3.02	1.42	2.02	2.57	5.73	3.97	2.09	1.65	2.51	1.73	2.10	1.40	5.06
Mix 13	32.50%	0.4	5.76		3.95	2.64		3.89	0.91	3.81	6.28	1.68	3.19	5.71	1.78	2.00	3.46	3.70	1.43	2.40	2.37	7.20
Mix 14	32.50%	0.4	2.25	4.66	2.70	0.63	1.70	1.79	3.53	3.35	2.80	0.39			1.86	2.10	2.70	3.97	5.66	3.95	2.70	3.51
Mix 5	32.50%	0.45	3.80	2.83	1.61	7.34	4.78	0.92	1.50	2.32	2.28	2.97			2.02	3.88	1.80	3.25	0.71	6.34	4.69	1.68
Mix 1	39%	0.5	28.88	2.93	8.40	3.26	1.85	1.46	2.93	2.06	0.71				3.82		5.33	1.84	1.43	4.18	6.10	0.87
Mix 8	32.50%	0.5	2.66	2.27	3.31	1.63	2.86	1.25	2.31	3.17	2.75	3.45			1.23	3.00	2.62	2.33	0.82	4.01	1.43	0.33
Mix 2	35%	0.45	5.17	1.08	2.65	1.44	2.99	0.37	3.89	1.51	5.38					2.94	1.97	2.33	3.23	2.86	3.59	1.59
Mix 12	32.50%	0.4	4.42	1.51	0.34	0.86	2.92	2.85	2.27	1.27	2.67	1.66			2.66	0.57	2.46	1.43	3.62	1.24	4.91	1.09
Mix 7	32.50%	0.45	2.29	1.12	9.90	1.98	2.05	3.80	2.14	4.87	2.70	2.30			3.06	1.25	2.26	2.90	1.82	2.36	2.41	5.25
Mix 11	35%	0.45	3.57	1.99	2.44	2.66	5.85	0.43	1.48	1.00	6.34	0.36			4.95	1.22	2.73	1.72	4.56	2.22	6.93	8.60
Total % above limit			78.6	12.5	35.7	21.4	25.0	28.6	35.7	42.9	33.3	28.6	7.1	28.6	30.8	23.1	42.9	35.7	42.9	42.9	50.0	50.0
Stiff mixtures above limit			100.0	0.0	33.3	16.7	0.0	50.0	50.0	66.7	50.0	33.3	16.7	66.7	33.3	33.3	83.3	50.0	33.3	50.0	33.3	66.7
Fluid mixtures above limit			62.5	12.5	37.5	25.0	25.0	12.5	25.0	25.0	14.3	25.0	0.0	0.0	28.6	14.3	12.5	25.0	50.0	37.5	62.5	37.5

The method used to analyze the compressive strength data was identical to that of the SSD relative density. For each batch, the compressive strengths of each cylinder, in a given set, were averaged and plotted on a graph with compressive strength on the y-axis and time on the x-axis. This can be seen in Figure 5.6. A trendline between the two references was inserted, and the equation of the trendline was used to determine the deltas of each consolidation method.

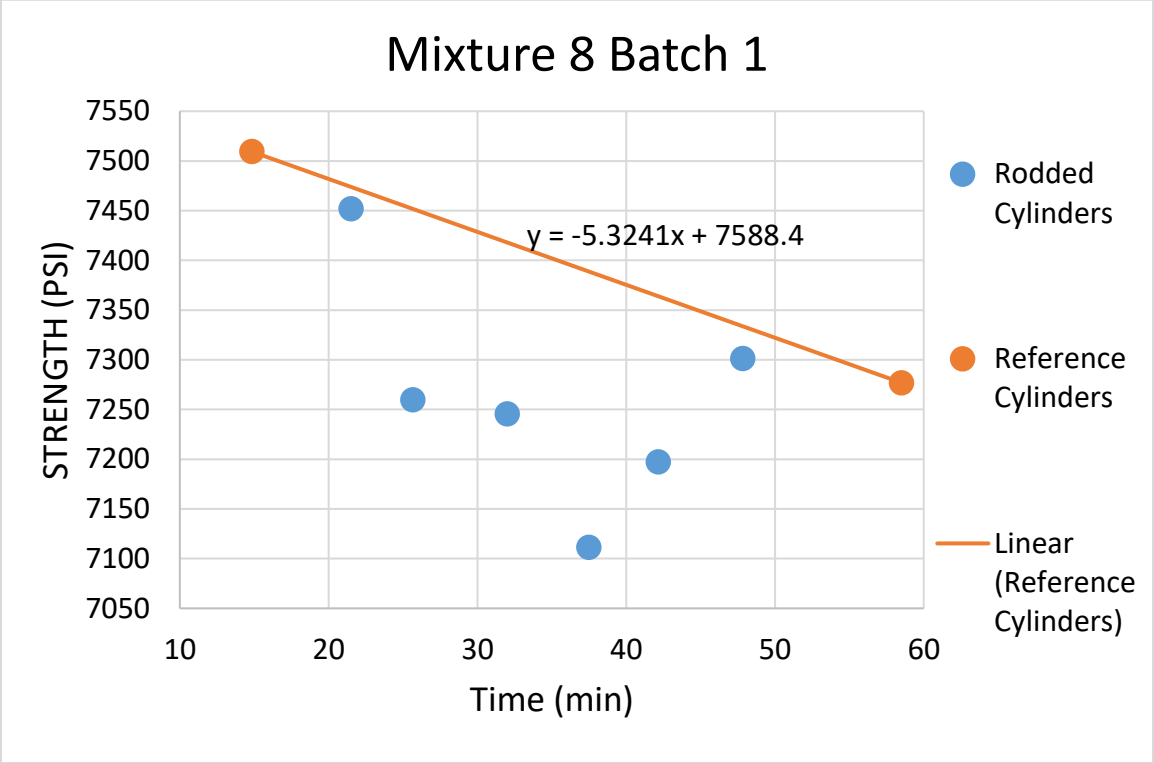

Figure 5.6 Compressive Strength Reference Trendline

The standard deviation was then calculated. A t-value of 1.886 was used to calculate the 90% confidence interval. This value corresponded with one-tail and two degrees of freedom for the three cylinders in the reference sets. The confidence interval was then used to find the upper and lower limits. These values were plotted to better enable visualization of the data. A sample of this can be seen in Figure 5.7. The consolidation methods that fell outside of the limits were identified. The compressive strengths were to evaluate the cylinders for under-consolidation. Therefore, only cylinders that had a lower compressive strength and fell under the lower limit were considered.

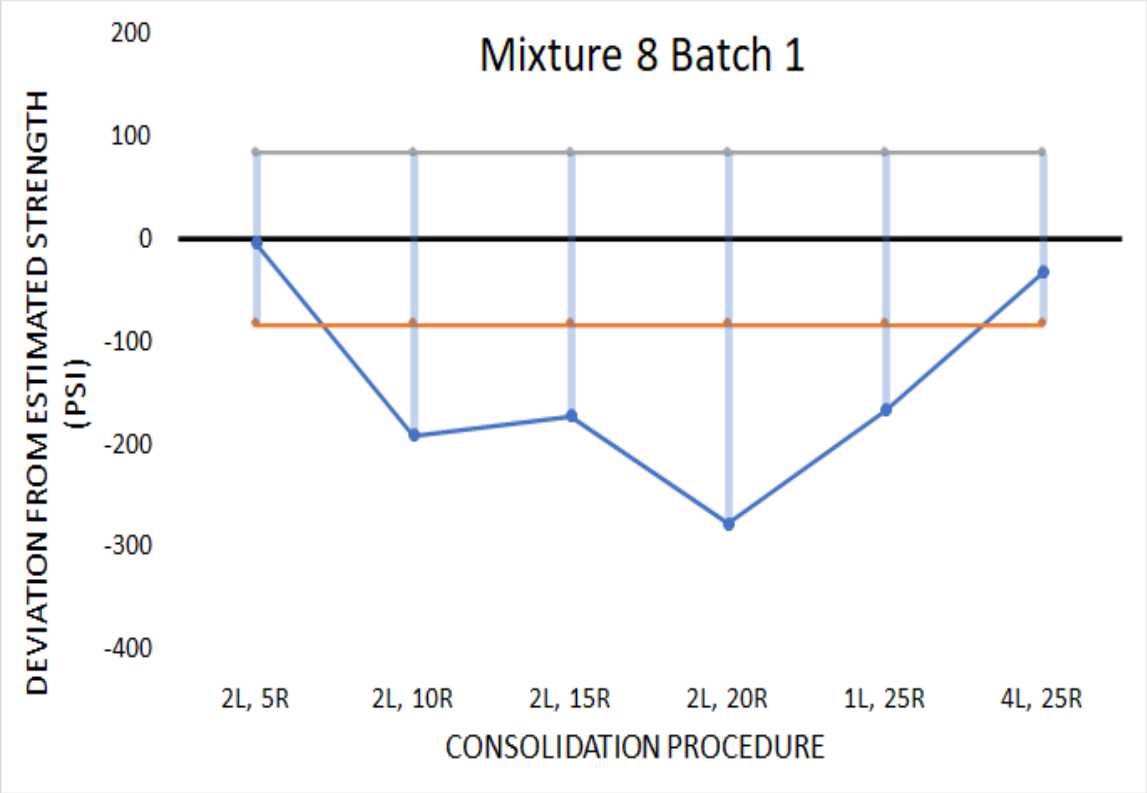

Figure 5.7 Deviation from Reference Strengths

All the points that fell below the lower limit of the 90% confidence interval were identified, and a matrix was created. This can be found in Appendix A and an abbreviated form can be seen in Table 5.14.

5.5.2. Discussion of Results. After analyzing the matrix, it was determined that sets consolidated with 2L 10R fell below the acceptable level 50% of the time for fluid mixtures. For stiff mixtures, cylinders consolidated with 2L 20R, broke below the confidence interval 50% of the time. This implies that too little consolidation has a negative impact on compressive strength.

Table 5.14 Compressive strength deltas. Orange highlighted values are below the 90% confidence interval.

	Paste Vol	w/c	2L, 0R	2L, 5R	2L, 10R	1L, 25R	2L, 15R	2L, 20R	2L 30R	2L 40R	2L, 50R	4L, 25R	1s, 8000 vpm	3s, 6000 vpm	3s, 8000 vpm	6s, 8000 vpm	3s, 12000 vpm	12s, 8000 vpm
Mix 10	25%	0.45	-1126		-2425	-611		-937	242	328	-1515	1901	-311	-12	-21	413	-247	370
Mix 3	25%	0.45	9		184	-1401		-2081	874	1027	903	601	1256	-163	2628	431	32	716
Mix 4	30%	0.45	-640		108	-11		-99	140	166	-24	-114	-416	-402	107	-83	46	-31
Mix 9	30%	0.45	-862		-56	-194		-214	108	-101	-176	68	-478	-500	-517	-683	-16	-542
Mix 6	32.50%	0.4	-1425		41	-183		86	291	507	771	788	-363	-552	-347	-532	-363	-390
Mix 13	32.50%	0.4	-1686		-2	-346		-108	187	14	579	783	-218	-1020	-362	-680	-771	-708
Mix 14	32.50%	0.4	-1029	297	390	197	183	272			-146	266	-149	-264	-360	-374	-368	-131
Mix 5	32.50%	0.45	194	7	-182	31	-119	130			-57	-98	-14	-313	-186	-389	97	-340
Mix 1	39%	0.5	-1396	-313	-59	35	68	-18			7		-193	-76	60	-41	-175	91
Mix 8	32.50%	0.5	-91	-4	-192	-167	-172	-277			-4	-32	-530	-426	-272	-429	-217	-769
Mix 2	35%	0.45	-257	208	149	-39	-17	378				-271	-400	-728	-250	-427	-370	20
Mix 12	32.50%	0.4	-1357	45	254	-43	180	46			-133	-45	-193	-519	-183	-605	-355	-502
Mix 7	32.50%	0.45	-86	-55	-512	-284	20	-225			179	131	-159	-454	-191	-450	-123	-503
Mix 11	35%	0.45	-125	7	-103	-265	-312	-47			62	-158	-326	-436	-949	-995	-666	-1881
Total % below limit			64.3	12.5	35.7	35.7	37.5	35.7	0.0	16.7	15.4	30.8	35.7	64.3	57.1	71.4	50.0	57.1
Stiff mix % below limit			83.3	0.0	16.7	33.3	0.0	50.0	0.0	16.7	33.3	16.7	50.0	66.7	33.3	50.0	33.3	50.0
Fluid mix % below limit			50.0	12.5	50.0	37.5	37.5	25.0	0.0	0.0	0.0	42.9	25.0	62.5	75.0	87.5	62.5	62.5

More workable mixtures showed increased sensitivity to the consolidation procedure. For example, Mixture 3, which had a starting slump of 3 inches, had two out of the 14 consolidation procedures exceeding the lower limit of the 90% confidence interval for compressive strength. However, Mixture 8, which had a starting slump of 7.5 inches, had 10 out of the 14 consolidation procedures fall below the confidence interval. Moreover, the compressive strength deltas of the three stiffest mixtures, Mixtures 10, 3, and 4, on average had five out of the 14 consolidation methods exceed the lower limit of their corresponding confidence intervals. The three most fluid mixtures, Mixtures 12, 7, and 11 had seven out of the 14 exceed the lower limit. To verify this trend was not due to the confidence intervals varying in magnitude across the mixtures, the narrowest confidence interval was selected and applied to all mixtures. When this was done, on average, five out of the 14 consolidation procedures exceeded the lower limit for stiff

mixtures, and nine out of the 14 exceeded it for fluid mixtures. However, it should be considered that the vibrated sets strongly contributed to this. This information can be seen in Table 5.15 below.

Table 5.15 Compressive strength deltas of most stiff and fluid mixtures. Highlighted values fall below the lower limit when the same confidence interval was used throughout.

	Paste Vol	w/c	2L, 0R	2L, 10R	1L, 25R	2L, 15R	2L, 20R	2L, 50R	4L, 25R	1s, 8000 vpm	3s, 6000 vpm	3s, 8000 vpm	6s, 8000 vpm	3s, 12000 vpm	12s, 8000 vpm	All	Vib	Rod
10	25%	0.45	-1126	-2425	-611		-937	-1515	1901	-311	-12	-21	413	-247	370	7	2	5
3	25%	0.45	9	184	-1401		-2081	903	601	1256	-163	2628	431	32	716	3	1	2
4	30%	0.45	-640	108	-11		-99	-24	-114	-416	-402	107	-83	46	-31	5	2	3
12	32.50%	0.4	-1357	254	-43	180	46	-133	-45	-193	-519	-183	-605	-355	-502	8	6	2
7	32.50%	0.45	-86	-512	-284	20	-225	179	131	-159	-454	-191	-450	-123	-503	8	5	3
11	35%	0.45	-125	-103	-265	-312	-47	62	-158	-326	-436	-949	-995	-666	-1881	10	6	4

The sets consolidated with 2L 0R routinely broke at lower compressive strengths than the references, falling below the lower limit 64% of the time. This consolidation method seemed particularly detrimental for stiff mixtures, falling below the lower limit 83% of the time. For 2L 0R, the average delta of the seven stiffest mixtures was -966, while the average delta for the seven most fluid mixtures was -445. Stiff mixtures seem to be less sensitive to the consolidation method, throughout the majority of the batch, however, this is reversed for this consolidation method in particular. This may be because it was systematically created at the end of the batch when all mixtures were experiencing slump loss. The second reference sets typically broke as high or higher than the first. This implied that 2L 25R is as effective at consolidating concrete before the slump loss as after. However, some consolidation is required to remove the entrapped air from the concrete, particularly for stiff mixtures.

When cylinders that had been created with low degrees of consolidation energy, and had low corresponding SSD relative density values, broke at strength values below the lower limit of the 90% confidence interval, it was clear that the cylinders were insufficiently consolidated. However, a phenomenon presented itself, in which vibrated cylinders that had been created with a high degree of consolidation energy, and had high SSD relative density values, were breaking at low strength values. For example, cylinders created with the consolidation method of 3s 8000 VPM surpassed the lower limit 57% of the time. Cylinders consolidated at 6s 8000 VPM exceeded the lower limit 71% of the time with 88% of the fluid mixtures being impacted. Sets consolidated for 12s 8000, 3s 6000 VMP, and 3s 12000 VPM also routinely exceeded the lower limit. The majority of these sets had SSD relative density values above or comparable to the references. This data can be seen in Figures 5.8, 5.9, and 5.10.

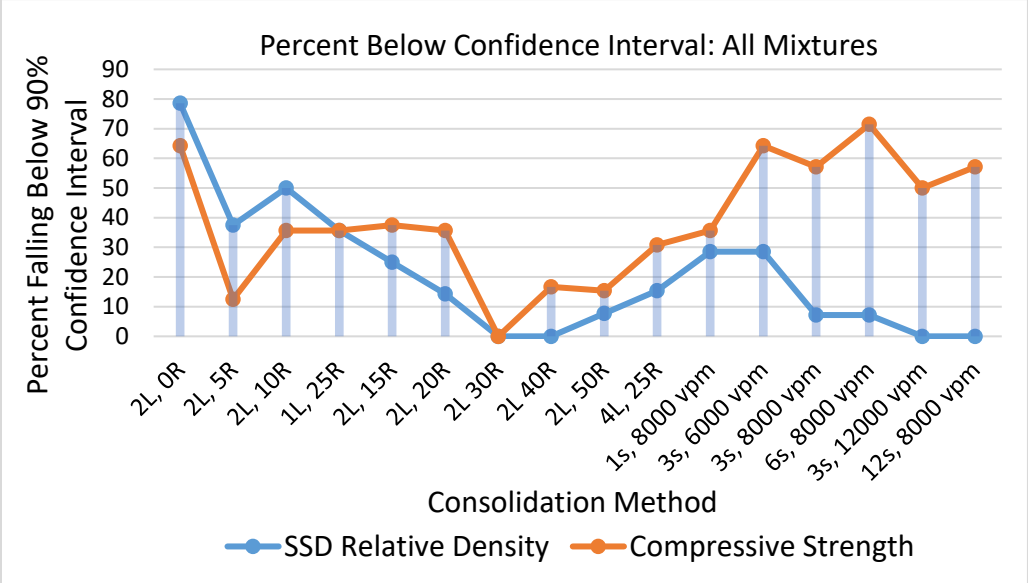

Figure 5.8 Percent Falling Below Confidence Interval for all Mixtures

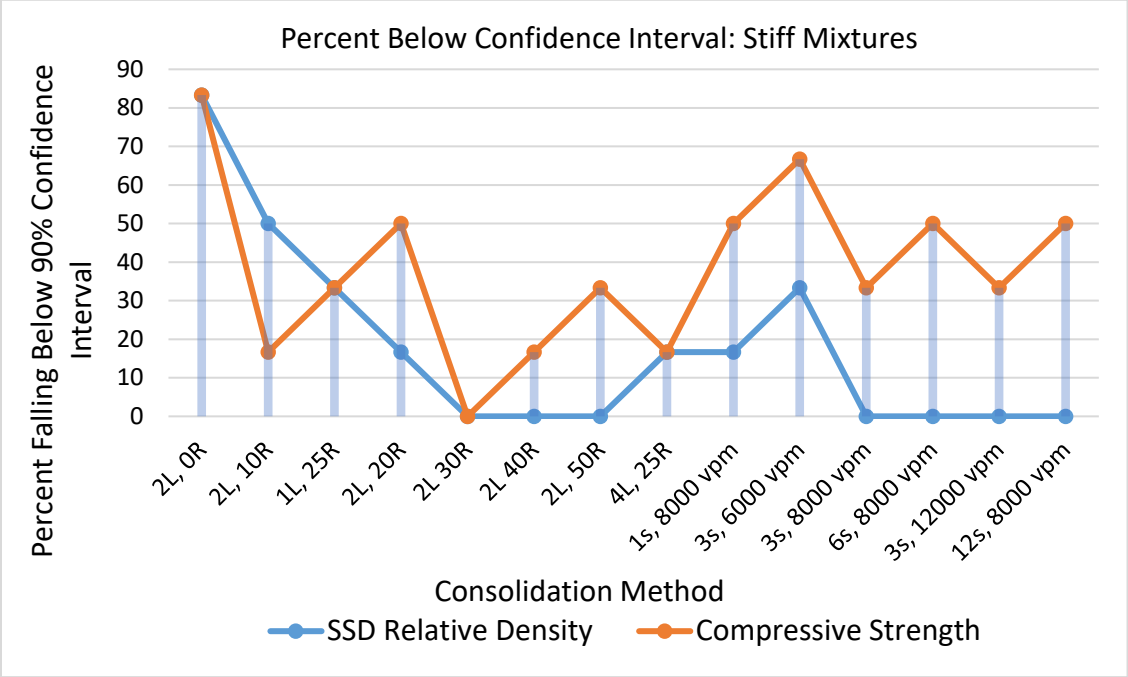

Figure 5.9 Percent Falling Below Confidence Interval for Stiff Mixtures

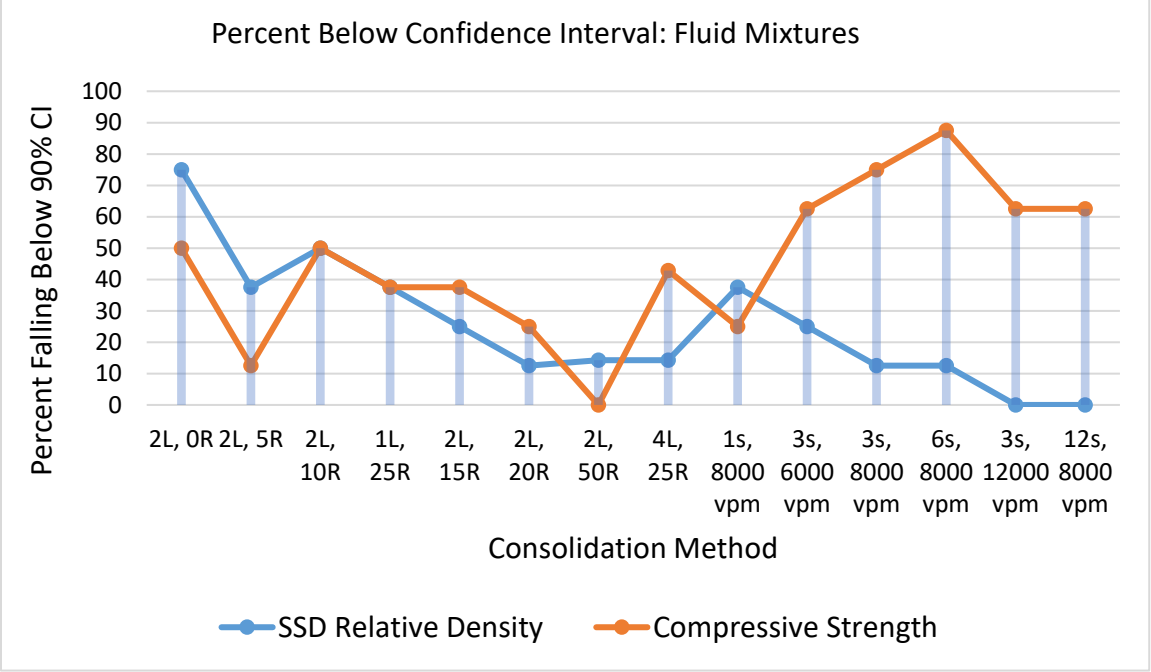

Figure 5.10 Percent Falling Below Confidence Interval for Fluid Mixtures

The conclusion that can be drawn from this is that vibration has a negative impact on compressive strength. However, the low breaks are not the result of being under-consolidated. To further explore this, the break patterns were analyzed. A sample of the break-type pie charts from Mixture 8 can be seen below in Figures 5.11 and 5.12. The remaining pie charts can be found in Appendix C.

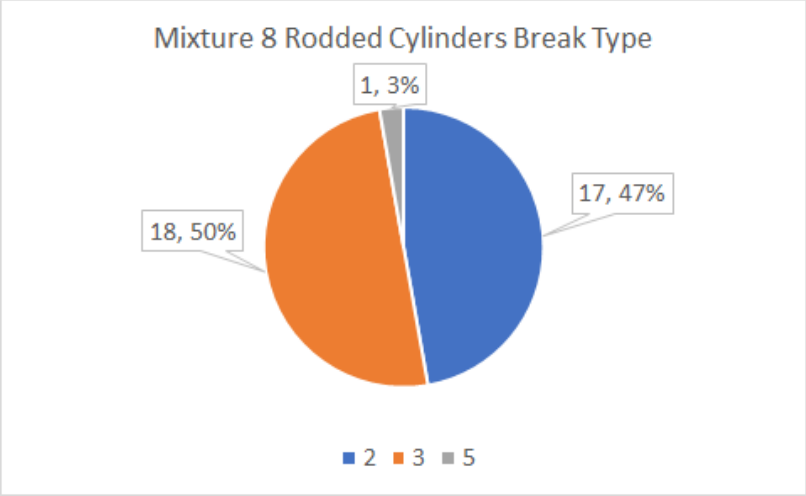

Figure 5.11 Break Types of Rodded Sets

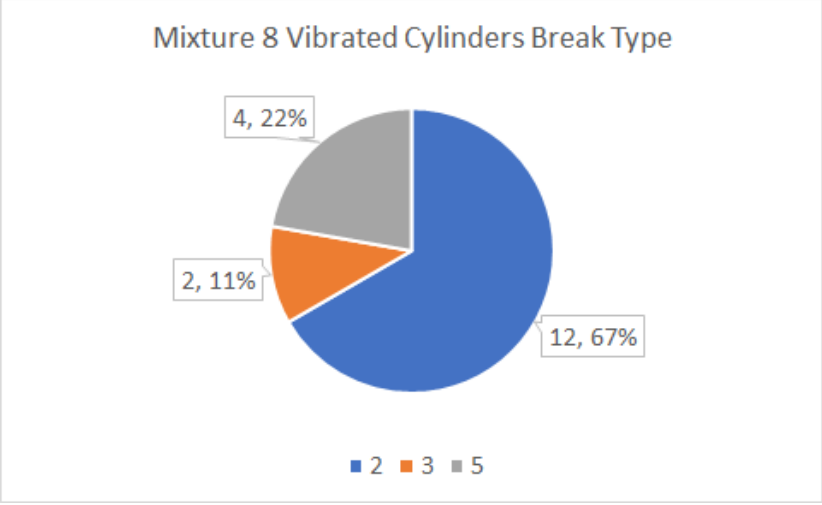

Figure 5.12 Break Types of Vibrated Sets

From these charts, it can be seen that vibrated cylinders exhibit far more type 5 and 6 breaks according to Table 1 from ASTM C39 [84]. When a type 5 or 6 break occurs, only a corner of the cylinder breaks off and the potential strength of the cylinder is unknown. Looking at the results from the penetration analysis, it can be seen that cylinders consolidated at 12s 8000 VPM showed the highest degree of penetration. Furthermore, it was the vibrated cylinders, particularly the sets 6s 8000 VPM and 12s 8000 VPM that showed the most visual signs of segregation.

As previously discussed, segregation is one of the risks of over-consolidation. The components in concrete all have different densities, which makes more dense components such as coarse aggregate more prone to sinking into the concrete than less dense components, such as water or paste. Typically, the yield stress of the concrete prevents coarse aggregates from sinking into the concrete. However, when concrete is subjected to vibration the yield stress is diminished [74]. Ideally, during vibration, the entrapped air, having the lowest density, rises out of the cylinder, at which point the vibration should cease. However, if vibration continues, the aggregates, which have higher densities, tend to move downward. Paste, which has a lower density, tends to move upward. If this segregation occurs, it can lead to the top of the cylinder having a dramatically higher degree of porosity than the rest of the cylinder, leading to the top section of the cylinder having a higher potential for failure [12]. This could explain why the vibrated cylinders in this research project showed a higher percentage of type 5 and 6 breaks than the rodded cylinders. It is possible that these types of breaks are potentially causing low compressive strength in the cylinders. Although the compressive strengths were intended

to show under-consolidation, these low breaks in the vibrated cylinders combined with the normal densities imply they are over-consolidated.

To further explore this, when the next set of cylinders was broken, the cylinders were examined. Below, in Figure 5.13 is an image of cylinder 42 of Mixture 13, immediately before it was tested for compressive strength. It was consolidated with 12s 8000 VPM. As can be seen, it has a flat and level top and does not lean to one side. Figure 5.14 shows the cylinder after being broken. It exhibits a type 5 break.

Figure 5.13 Unbroken Cylinder

Figure 5.14 Cylinder Broken Once

The cylinder was then cleaned off and placed back in the machine to be tested again. The second time it broke, it had a slightly lower compressive strength. It again exhibited a type 5 break in a new location, which can be seen in Figure 5.15.

Figure 5.15 Cylinder Broken Twice

Again, the cylinder was cleaned off, and for a third time tested for compressive strength. The cylinder broke at a much lower compressive strength but finally split down the middle. This can be seen in Figure 5.16. After visually inspecting the cylinder, it was determined there was significantly more mortar near the top of the cylinder and coarse aggregate near the bottom.

Figure 5.16 Cylinder Completely Broken

5.5.3. Comparison of Mixtures. To determine how the various consolidation methods impacted mixtures, the deltas of similar mix designs were compared. The mixtures that were outside of the granular flow regime, having a paste volume of 32.5% or greater, were compared based on the viscosity of the cement paste. The mixtures were listed in ascending order according to the viscosity. In this configuration, it could be seen

that as the cement paste became more viscous, sets that were created with a low amount of consolidation energy, such as the 2L 10R, 2L 15R, 2L 20R, and 1L 25 R, seemed to fall under the 90% confidence interval less frequently. This trend was not changed when the narrowest confidence intervals of the group were applied to all mixtures.

Sets consolidated with 2L 0R continued to be under the limit and had larger and larger negative deltas as viscosity increased. This could have to do with the fact that the 2L 0R was consistently the last cylinders in the batch made. All mixtures were impacted by slump loss, but mixtures that already had a low w/c may be particularly vulnerable to its negative effects. Furthermore, Mixtures 12, 13, and 14 all contained HRWRA. As discussed in Section 4, HRWRA is only effective at reducing slump for 30-60 minutes. Typically, by the time set 2L 0R was created over 60 minutes had elapsed. To illustrate the dramatic effect this can have, Mixture 8 had a starting slump of 7.5 inches and a final slump of 6.5 inches. However, Mixture 12 had a starting slump of 8.5 inches and a final slump of 3.75 inches. This makes the properties of the concrete with HRWRA when set 2L 0R was created very different from when the 2L 10R cylinders were created.

What could also be seen from this group of high paste volume mixtures, was that the effect of vibration was particularly detrimental to strength. Sets consolidated with 6s 8000 VPM exceeded the lower limit 100% of the time. Sets with 3s 8000 VPM exceeded the limit 75% of the time and 12s 8000 VPM exceeded it 87.5% of the time. Sets created with 3s 6000 and 3s 12000 VPM were also under the lower limit 75% of the time. This can be seen in Table 5.16.

Table 5.16 Compressive strength deltas of increasing viscosity. Mixtures 8, 11, and 7 are low-viscosity mixtures, Mixture 5 is a mid-level viscosity mixture, and Mixtures 12, 6, 14, and 13 are high-viscosity mixtures. Orange highlighted values exceed the lower 90% confidence interval. Greed highlighted values exceed the lower 90% confidence interval when the narrowest confidence intervals were applied.

	Paste Vol	w/c	2L, 0R	2L, 10R	1L, 25R	2L, 15R	2L, 20R	4L, 25R	1s, 8000 vpm	3s, 6000 vpm	3s, 8000 vpm	6s, 8000 vpm	3s, 12000 vpm	12s, 8000 vpm
Mix 8	32.50%	0.5	-91	-192	-167	-172	-277	-32	-530	-426	-272	-429	-217	-769
Mix 11	35%	0.45	-125	-103	-265	-312	-47	-158	-326	-436	-949	-995	-666	-1881
Mix 7	32.50%	0.45	-86	-512	-284	20	-225	131	-159	-454	-191	-450	-123	-503
Mix 5	32.50%	0.45	194	-182	31	-119	130	-98	-14	-313	-186	-389	97	-340
Mix 12	32.50%	0.4	-1357	254	-43	180	46	-45	-193	-519	-183	-605	-355	-502
Mix 6	32.50%	0.4	-1425	41	-183		86	788	-363	-552	-347	-532	-363	-390
Mix 14	32.50%	0.4	-1029	390	197	183	272	266	-149	-264	-360	-374	-368	-131
Mix 13	32.50%	0.4	-1686	-2	-346		-108	783	-218	-1020	-362	-680	-771	-708

Mixtures with similar compositions were then compared. This can be seen in Table 5.17. Mixtures 2, 5, and 4 were similar but had varying paste volumes, which decreased from 35%, 32.5% to 30%. Within these mixtures, vibrated cylinders seemed less prone to failure as the paste volume was decreased. The set that was consolidated with 4L 25R fell below the lower limit for each mixture, bringing into question if it too was over-consolidated and experiencing the same phenomena as the vibrated cylinders. Similarly, mixtures 9 and 10 are comparable with 9 having a paste volume of 30% and 10 having a volume of 25%. These mixtures showed a similar trend of stiffer mixtures being less prone to experiencing over-consolidation from vibration. While five of the vibrated sets in Mixture 9 were below the lower limit, none of the sets in Mixture 10 were. For both mixtures, the cylinders consolidated with 2L 50R exceeded the lower limit, possibly also experiencing the over-consolidation phenomenon. In both sets, the cylinders consolidated with 2L 0R also exceeded the lower limit. Given the density results from these sets, it can be assumed they are under-consolidated. To ensure this trend was not

due to a change in standard deviation, the narrowest confidence intervals of the group were applied to the mixtures. This did not affect the results between Mixtures 2, 5, and 6. The narrower confidence interval did affect Mixture 10, but not enough to alter the trend. This information can be seen in Table 5.18.

Table 5.17 Compressive strength deltas of similar mixtures but decreasing paste volume. Orange highlighted values exceed the lower 90% confidence interval.

	Paste Vol	w/c	2L, 0R	2L, 10R	2L, 15R	2L, 20R	4L, 25R	1s, 8000 vpm	3s, 6000 vpm	3s, 8000 vpm	6s, 8000 vpm	3s, 12000 vpm	12s, 8000 vpm
Mix 2	35%	0.45	-257	149	-17	378	-271	-400	-728	-250	-427	-370	20
Mix 5	32.50%	0.45	194	-182	-119	130	-98	-14	-313	-186	-389	97	-340
Mix 4	30%	0.45	-640	108		-99	-114	-416	-402	107	-83	46	-31

Table 5.18 Compressive strength deltas of similar mixtures but decreasing paste volume. Orange highlighted values exceed the lower 90% confidence interval of the mixture. Greed highlighted values exceed the lower 90% confidence interval when the narrowest confidence intervals were applied.

	Paste Vol	w/c	2L, 0R	2L, 10R	1L, 25R	2L, 20R	2L 40R	2L, 50R	1s, 8000 vpm	3s, 6000 vpm	3s, 8000 vpm	6s, 8000 vpm	12s, 8000 vpm
Mix 9	30%	0.45	-862	-56	-194	-214	-101	-176	-478	-500	-517	-683	-542
Mix 10	25%	0.45	-1126	-2425	-611	-937	328	-1515	-311	-12	-21	413	370

Mixtures 5, 6, and 8 were similar other than the w/c, which increased from 0.4, 0.45, to 0.5. These mixtures all showed very similar types of failures. This implies that over-consolidation due to vibration is far more dependent on paste volume than the w/c. As far as the rodded sets go, there were slightly more failures in the 2L 10 R, 2L 15R, and 1L 25R sets as the w/c increased. However, the increase was not significant enough to be considered a trend. An abbreviated version of the matrix focusing on this can be

seen in Table 5.19. Between Mixtures 12 and 11, the w/c was increased from 0.40 to 0.45, with both having the same amount of plasticizer. Mixture 11 had more samples falling outside of the limit when created with a low degree of consolidation energy, such as 2L 10 R, 2 L 15R, and 1L 25 R. It also exhibited lower deltas on the vibrated sets. However, between Mixtures 12 and 11, the paste volume also increased from 32.5% to 35%, so this effect could also be attributed to the change in paste volume. An abbreviated version of the matrix focusing on this can be seen in Table 5.20.

Table 5.19 Compressive strength deltas of similar mixtures but increasing w/c. Orange highlighted values exceed the lower 90% confidence interval.

	Paste Vol	w/c	2L, 0R	2L, 10R	1L, 25R	2L, 15R	2L, 20R	4L, 25R	1s, 8000 vpm	3s, 6000 vpm	3s, 8000 vpm	6s, 8000 vpm	3s, 12000 vpm	12s, 8000 vpm
Mix 6	32.50%	0.4	-1425	41	-183		86	788	-363	-552	-347	-532	-363	-390
Mix 5	32.50%	0.45	194	-182	31	-119	130	-98	-14	-313	-186	-389	97	-340
Mix 8	32.50%	0.5	-91	-192	-167	-172	-277	-32	-530	-426	-272	-429	-217	-769

Table 5.20 Compressive strength deltas of similar mixtures but increasing w/c. Orange highlighted values exceed the lower 90% confidence interval.

	Paste Vol	w/c	2L, 0R	2L, 10R	1L, 25R	2L, 15R	4L, 25R	3s, 6000 vpm	3s, 8000 vpm	6s, 8000 vpm	3s, 12000 vpm	12s, 8000 vpm
Mix 12	32.50%	0.4	-1357	254	-43	180	-45	-519	-183	-605	-355	-502
Mix 11	35%	0.45	-125	-103	-265	-312	-158	-436	-949	-995	-666	-1881

Between Mixtures 4 and 9, only the gradation was changed, with more coarse aggregates and less sand being incorporated in Mixture 9. As the coarse aggregate content increased, the negative effects of vibration became more pronounced. This could be because the larger, and therefore, heavier coarse aggregates sink faster when vibrated, increasing the chance of a failure plane forming at the top of the cylinder. Although the

deltas did not always fall below the lower limit, Mixture 9 did have more negative deltas on sets created with low consolidation energies. This could be because additional coarse aggregates created more aggregate interlock, and therefore more friction within the concrete. When this occurs, additional consolidation is needed. The 90% confidence intervals for the two mixtures are similar. However, this is an extremely small sample size, making it difficult to determine if this is a trend. This section of the matrix can be seen in Table 5.21.

Table 5.21 Compressive strength deltas of similar mixtures but changing gradation. Orange highlighted values exceed the lower 90% confidence interval.

	Paste Vol	w/c	2L, 0R	2L, 10R	1L, 25R	2L, 20R	2L 30R	2L 40R	2L, 50R	4L, 25R	1s, 8000 vpm	3s, 6000 vpm	3s, 8000 vpm	6s, 8000 vpm	12s, 8000 vpm
Mix 4	30%	0.45	-640	108	-11	-99	140	166	-24	-114	-416	-402	107	-83	-31
Mix 9	30%	0.45	-862	-56	-194	-214	108	-101	-176	68	-478	-500	-517	-683	-542

Only the dosage of the plasticizer was changed between Mixtures 12, 13, and 14. This had very little effect on compressive strength, with the deltas following the same trends, and the raw values being relatively close. In all mixtures, none of the rodded cylinders, aside from the 2L 0R, were under the lower limit. However, for each mixture, three to four of the vibrated sets were under the limit. Similarly, the addition of fly ash between Mixtures 5 and 7 seemed to have very little impact on compressive strength outcomes. However, it should be noted these are extremely small sample sizes.

6. CONCLUSIONS AND FUTURE WORK

6.1. CONCLUSION

The main conclusion that can be drawn from this research project is that concrete mixtures are impacted by the consolidation procedure differently based on the paste volume, paste viscosity, and gradation. Mixtures with high paste volumes generally had more signs of segregation than their lower paste volume counterparts. As paste volume decreases, there seem to be fewer sets falling below the lower limit for SSD relative density, and vibrated cylinders seem less vulnerable to the negative effects of over-consolidation. The viscosity of the cement pastes also played a role. As cement paste became more viscous, the compressive strengths of sets that were created with a low amount of consolidation energy seemed to fall under the 90% confidence interval less frequently. Gradation also influenced the outcomes of the consolidation methods. When more coarse aggregates and less sand were incorporated sets were more prone to falling under the 90% confidence interval for both SSD relative density and compressive strength when a low degree of consolidation energy was applied.

Mixtures with low workability exhibited fewer signs of segregation than mixtures with high workability, even when created with a high amount of consolidation energy. As the concrete mixtures become stiffer, not only do the cylinders become less likely to show signs of segregation, but the SSD relative density values and compressive strength values also become less sensitive to the consolidation procedure. The relationship between workability and both SSD relative density values as well as compressive strength values seems to be more dependent on paste volume than w/c.

In general, sets created with a low amount of consolidation energy showed lower SSD relative density values and lower compressive strengths. However, many of the vibrated sets created with a high amount of consolidation energy had compressive strengths that fell below the 90% confidence interval. On the same sets with low compressive strengths, such as the sets consolidated with 12s 8000 VPM and 3s 12000 VPM, the SSD relative density values were above or comparable to the reference sets for all mixtures. In 50% of the mixtures, cylinders that were consolidated with 12s 8000 VPM had a penetration depth that exceeded the upper limit. Furthermore, the visual signs of segregation were only seen on cylinders that had been vibrated. When a consolidation procedure of 6s 8000 VPM was used, seven out of the 14 mixtures had visible signs of segregation, and when 12s 8000 VPM was used, nine of the mixtures had visible signs of segregation.

The conclusion that was drawn from this is that many of the vibrated cylinders were over-consolidated. During vibration, the yield stress of the concrete is exceeded. Without the yield stress, the denser components of the concrete such as the coarse aggregate begin to sink to the bottom of the cylinder. The cement paste, which has a lower density, tends to move upward. This leads to the top section of the cylinder having a higher potential for failure. This theory is supported by the fact that a disproportionate amount of type 5 and 6 breaks come from the vibrated cylinders. This theory was also supported by fully breaking one of these cylinders and inspecting the core visually. It appeared as though there was more mortar at the top of the cylinder and more aggregate near the bottom. Both in terms of penetration depth and compressive strength sets impacted by this phenomenon seem to be more dramatically impacted by the duration of

the vibration than by the frequency, possibly because it takes time for coarse aggregates to sink to the bottom. Although it did not have a drastic impact, the viscosity of the cement paste did influence the degree to which the penetration depth increased, and the amount the compressive strength was diminished by the vibration. For example, for the sets consolidated for 12s 8000 VPM, the three low-viscosity mixtures, 8, 11, and 7, had an average compressive strength delta of -1051 psi. The four high-viscosity mixtures, 12, 6, 13, and 14, had an average compressive strength delta of -433 psi. The penetration depths of the low-viscosity mixtures were also more heavily impacted by increased vibration duration. However, when the duration was lower, and the frequency was high, the effect was reversed. On 3s 12000 VPM, the average strength delta of the low viscosity mixtures was -336 psi, while for the high viscosity mixtures, it was -464 psi. The penetration depths of the high-viscosity mixtures were also more severely impacted by frequency. The negative impact of over-consolidation due to vibration seemed to be much more pronounced on high-paste volume mixtures. For example, none of the vibrated sets in Mixture 10 or 3, which both had a paste volume of 25%, were under the 90% confidence interval for compressive strength.

6.2. LIMITATIONS OF THE PROJECT

There were several factors that limited how deeply this topic could be explored during this project, one of which was the short duration. If there had been time for more batches to have been created, a reference mixture that was repeated multiple times could have been established. Furthermore, creating more mix designs would also have been beneficial when attempting to identify trends. For example, only two gradations were

used, and fly ash was only used once, making it difficult to determine with certainty that changes in SSD relative density and compressive strength values were in fact trends due to a given variable change, or if they were rooted in other causes.

Another limitation was that all of the analysis is dependent on the assumption that 2L 25R has an adequate amount of consolidation for every mix design evaluated. This should be further explored, especially given the fact that the mix designs exhibited different reactions to the consolidation methods. Another possible flaw with this method of analysis is that if the reference set breaks particularly high or low it can change the criteria for which consolidation methods were considered inadequate. When looking into the precision evaluation of the SSD relative density values, it was revealed that the reference mixtures exceeded the allowed standard deviation in five out of the 14 sets. The only other consolidation method that had this degree of standard deviation was the sets that were consolidated with 2L 0R. This trend was slightly different when considering the precision analysis for the compressive strengths, but only because the vibrated cylinders showed such a high degree of variation. The reference sets still exceeded the 3.2% coefficient of variation limit 35% of the time. This may be for a variety of reasons, such as the reference sets being created more confidently and, therefore, more quickly than other sets.

6.3. FUTURE WORK

If this project is continued, it would benefit from the establishment of a repeatability mix design. This would give more context to what a normal deviation in test results is. The project would also benefit from the creation of more similar mix designs

with a single variable change. Doing so would allow for the trends to be more confidently established. A better understanding of these trends could, in the future, enable the recommendation of an ideal consolidation method based on the mix design of the concrete. Furthermore, the data should undergo a statistical analysis and be compared to standards to determine if in fact, 2L 25R is an adequate amount of consolidation for all mix designs.

The phenomena around the over-consolidation of the vibrated cylinders should also be further explored. A large-scale study that determines the acceptable amount of vibration duration and frequency should be investigated. It should also be confirmed that segregation is the reason behind the lower compressive strengths. One additional evaluation method that could be put in place would be to create an extra cylinder for every consolidation procedure for the sole purpose of studying the aggregate distribution within the cylinder.

APPENDIX A.

DEVIATION FROM REFERENCES

OVERVIEW

This appendix presents the amount each consolidation procedure differed from the expected values based on the reference mixtures. These values are also referred to as the deltas.

PENETRATION

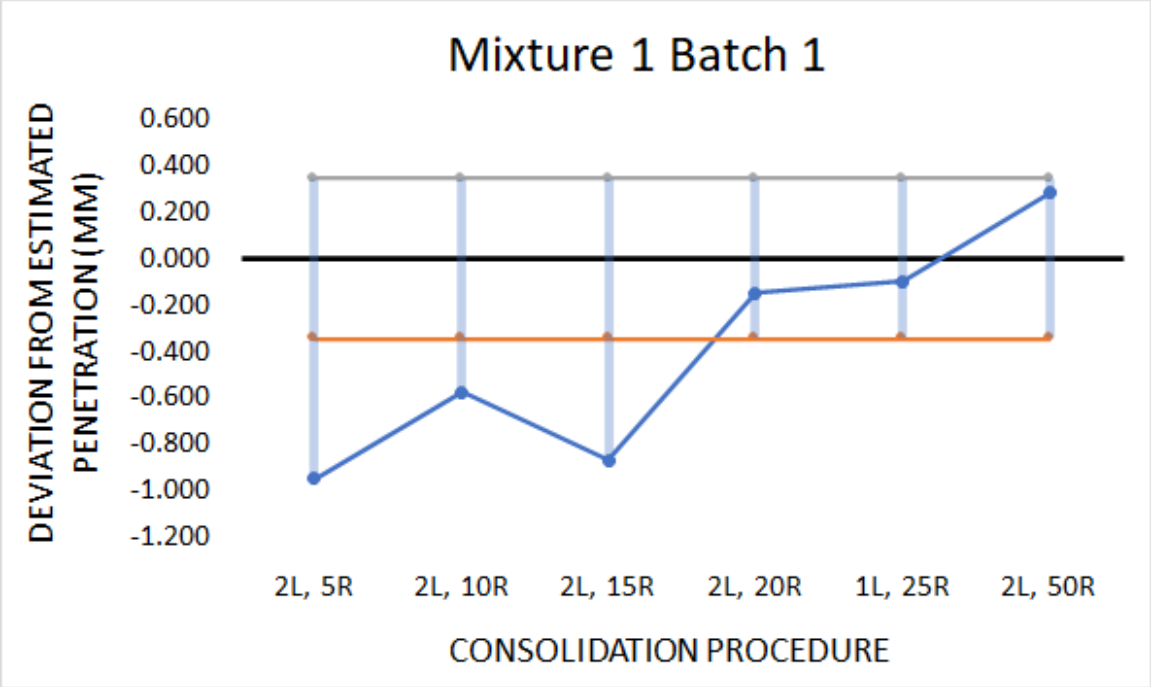

Figure A.1. Mixture 1 Batch 1 Deltas of Penetration

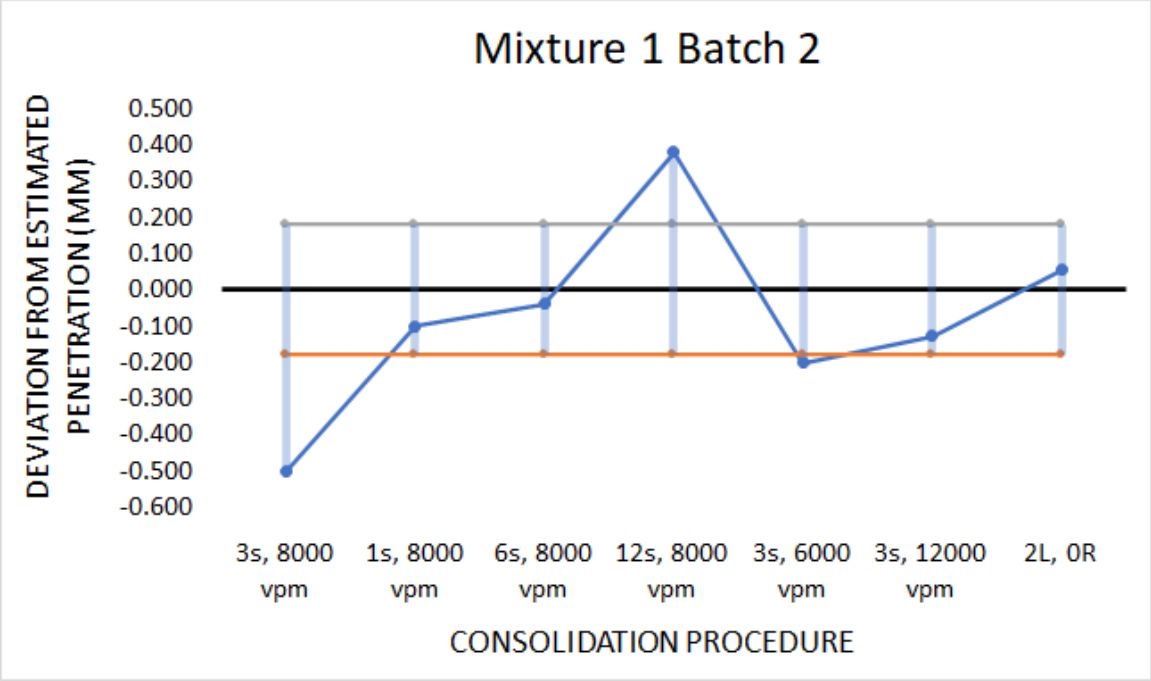

Figure A.2. Mixture 1 Batch 2 Deltas of Penetration

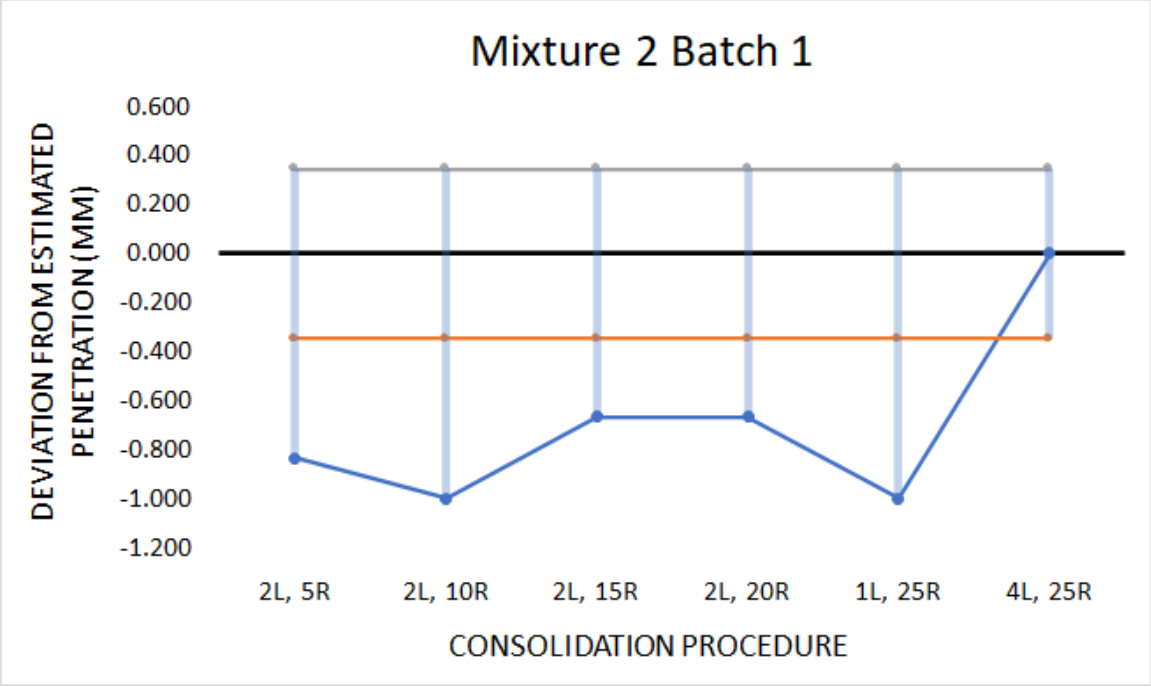

Figure A.3. Mixture 2 Batch 1 Deltas of Penetration

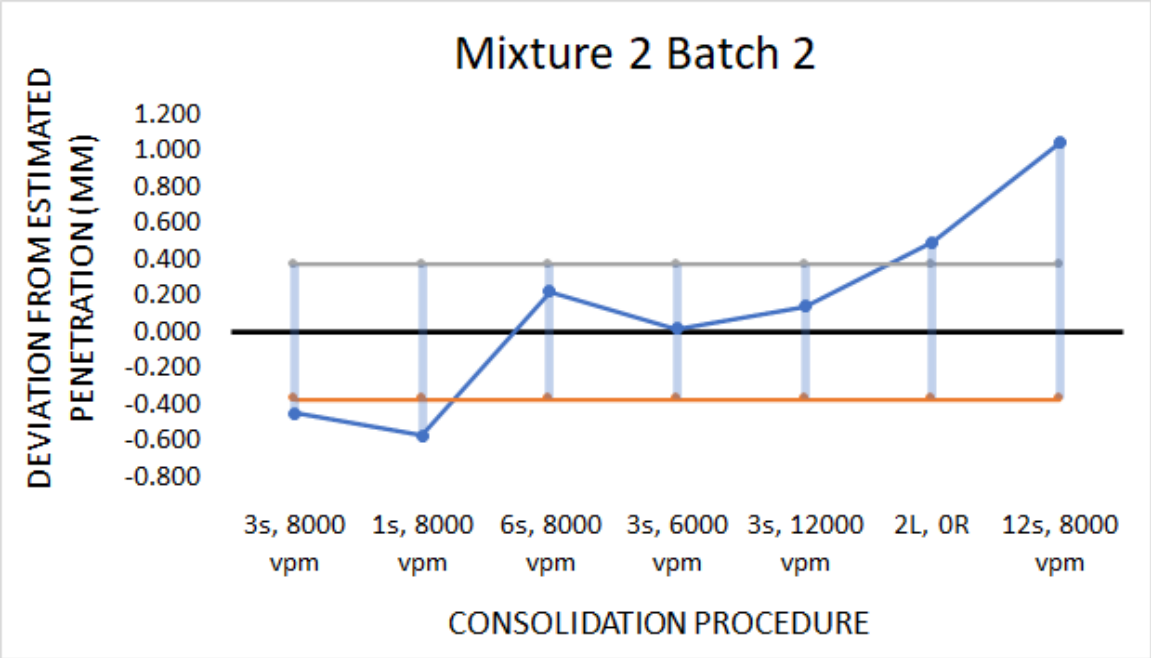

Figure A.4. Mixture 2 Batch 2 Deltas of Penetration

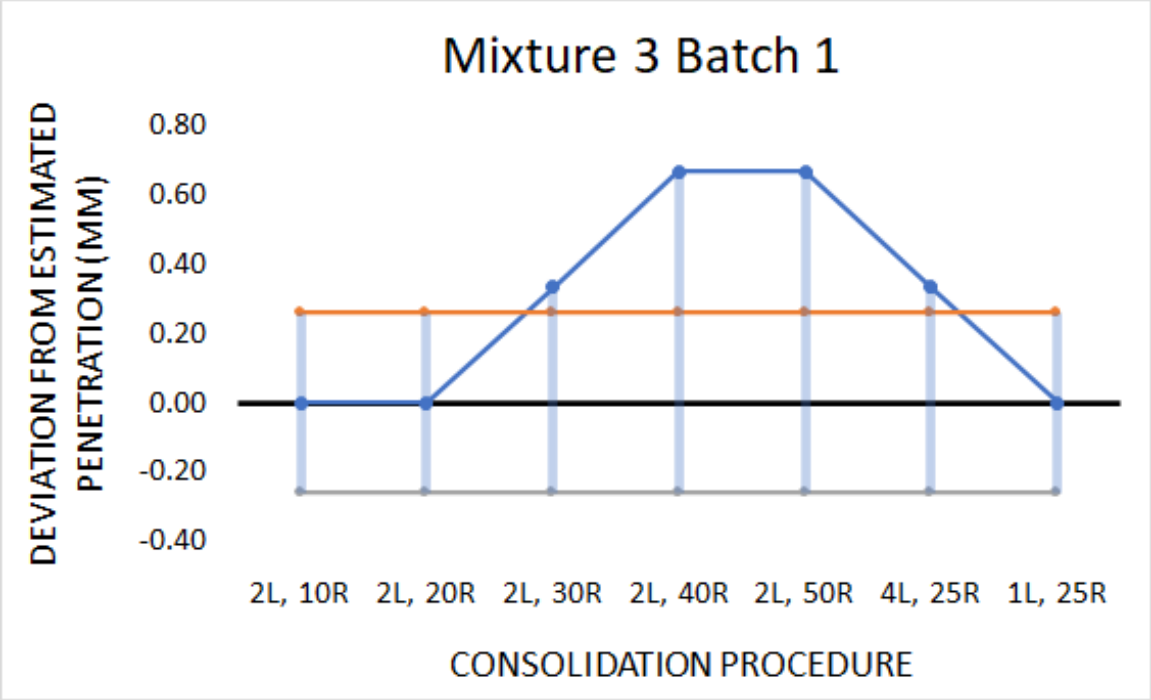

Figure A.5. Mixture 3 Batch 1 Deltas of Penetration

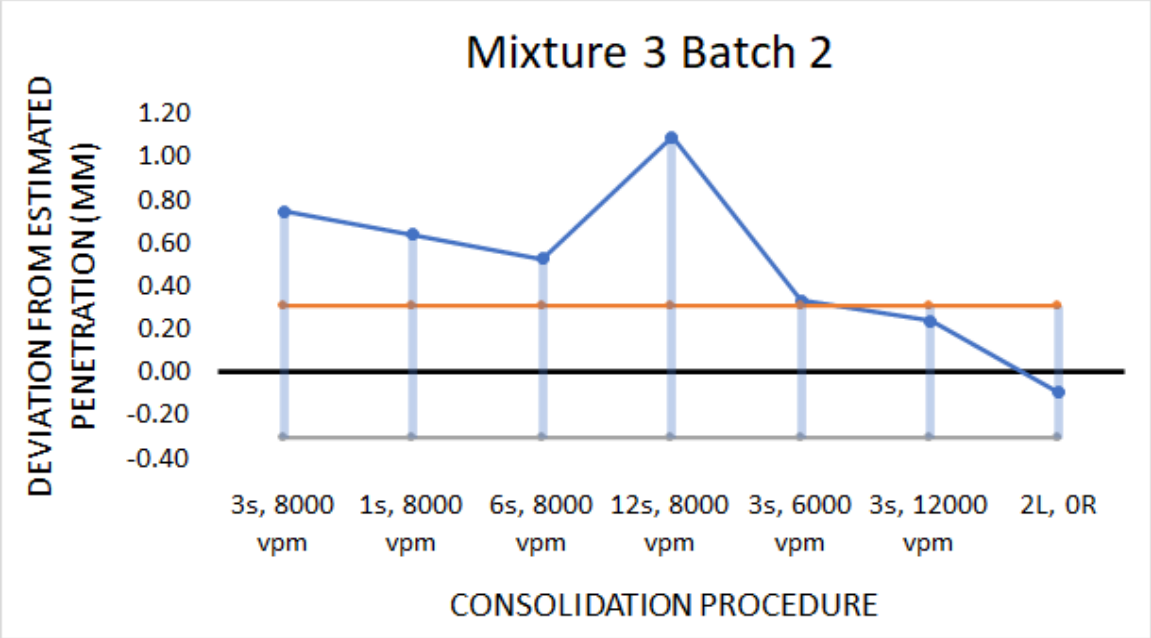

Figure A.6. Mixture 3 Batch 2 Deltas of Penetration

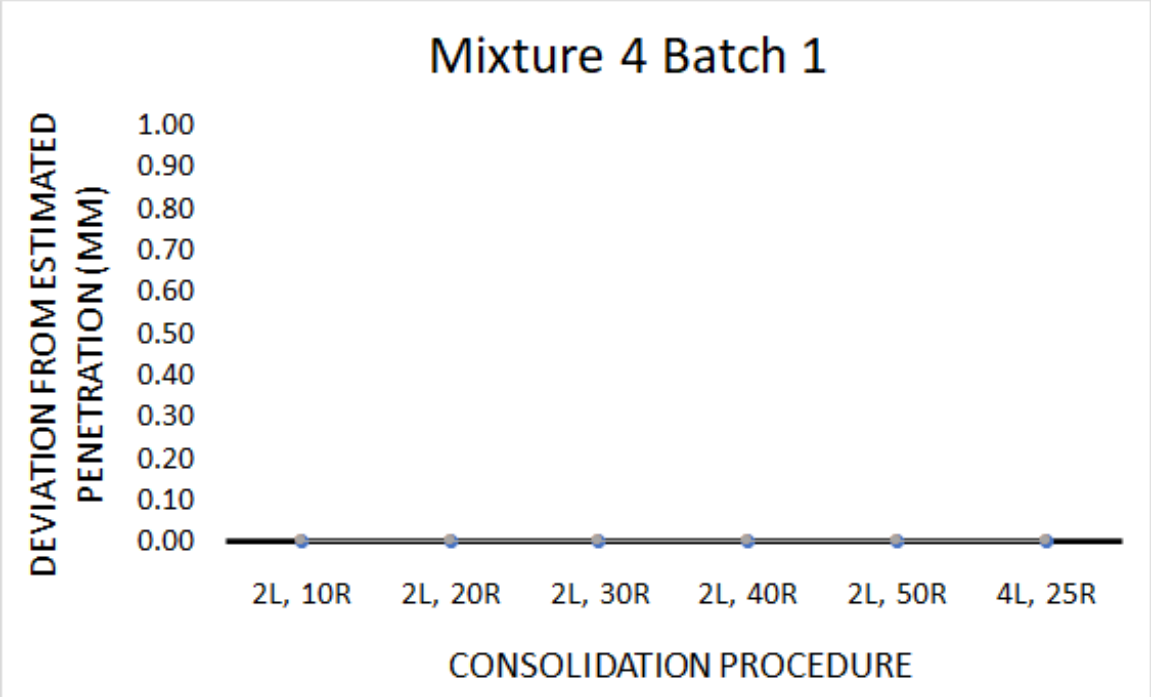

Figure A.7. Mixture 4 Batch 1 Deltas of Penetration

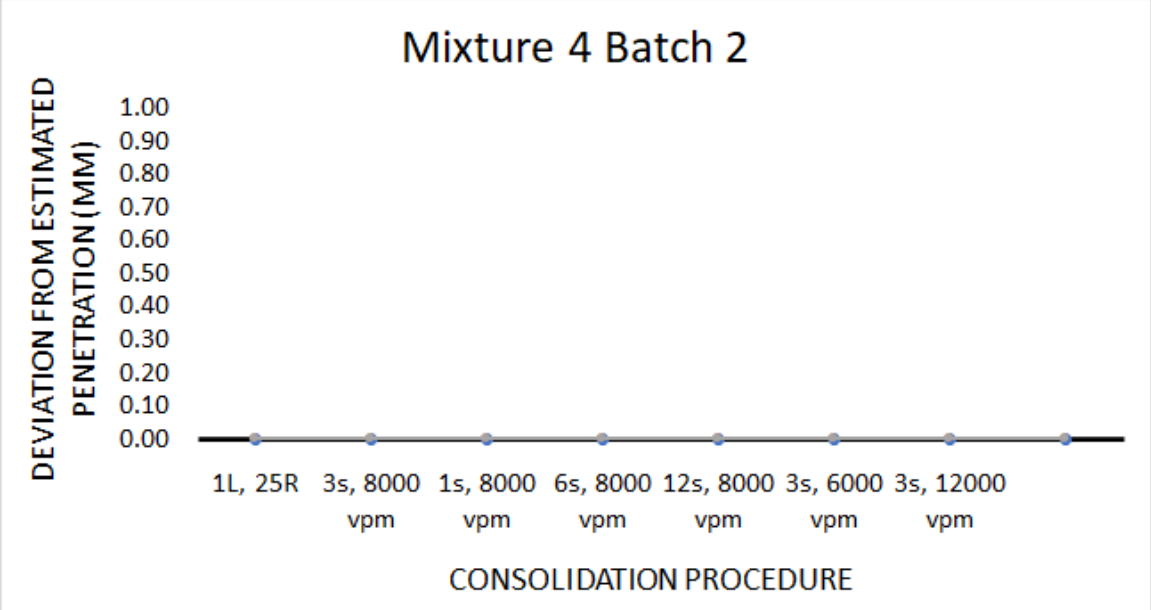

Figure A.8. Mixture 4 Batch 2 Deltas of Penetration

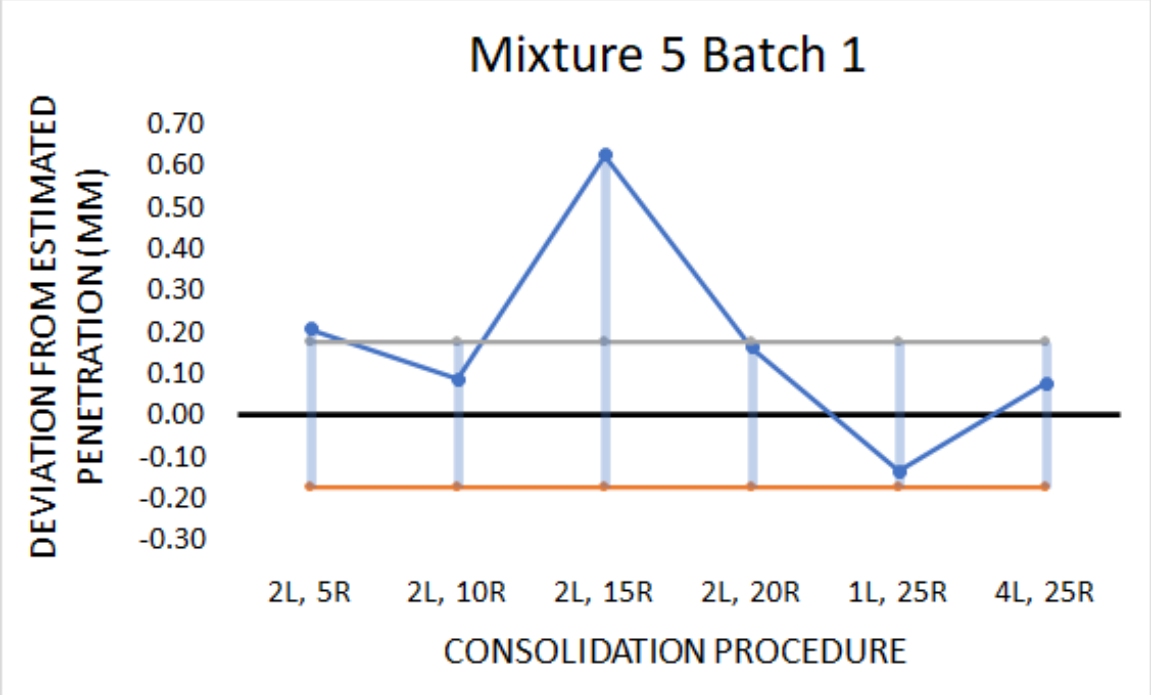

Figure A.9. Mixture 5 Batch 1 Deltas of Penetration

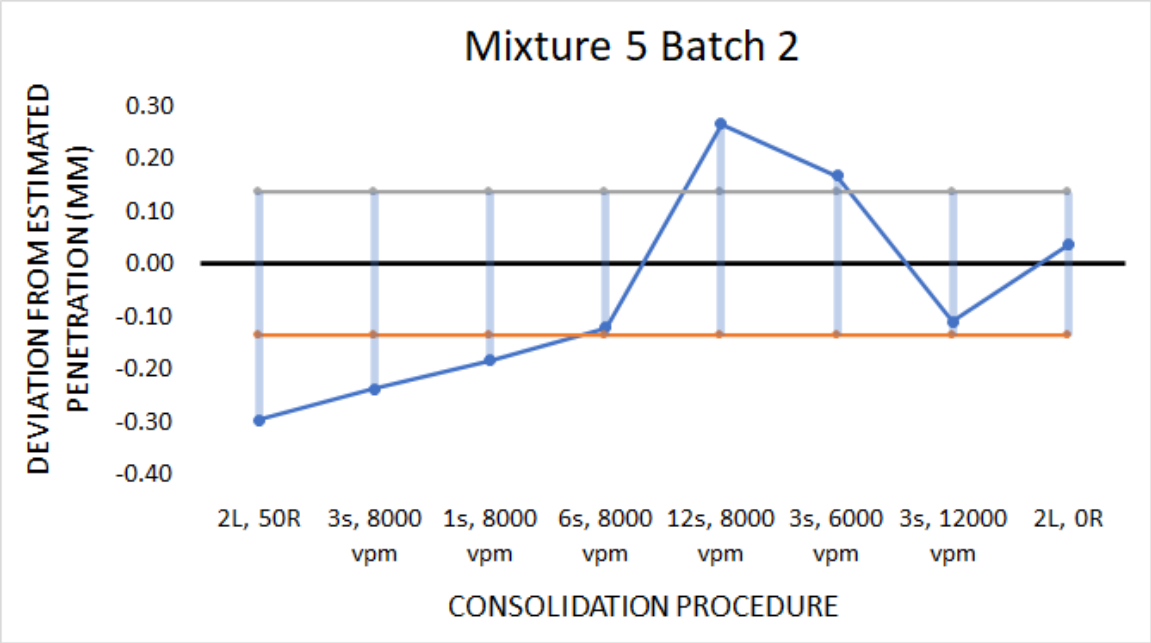

Figure A.10. Mixture 5 Batch 2 Deltas of Penetration

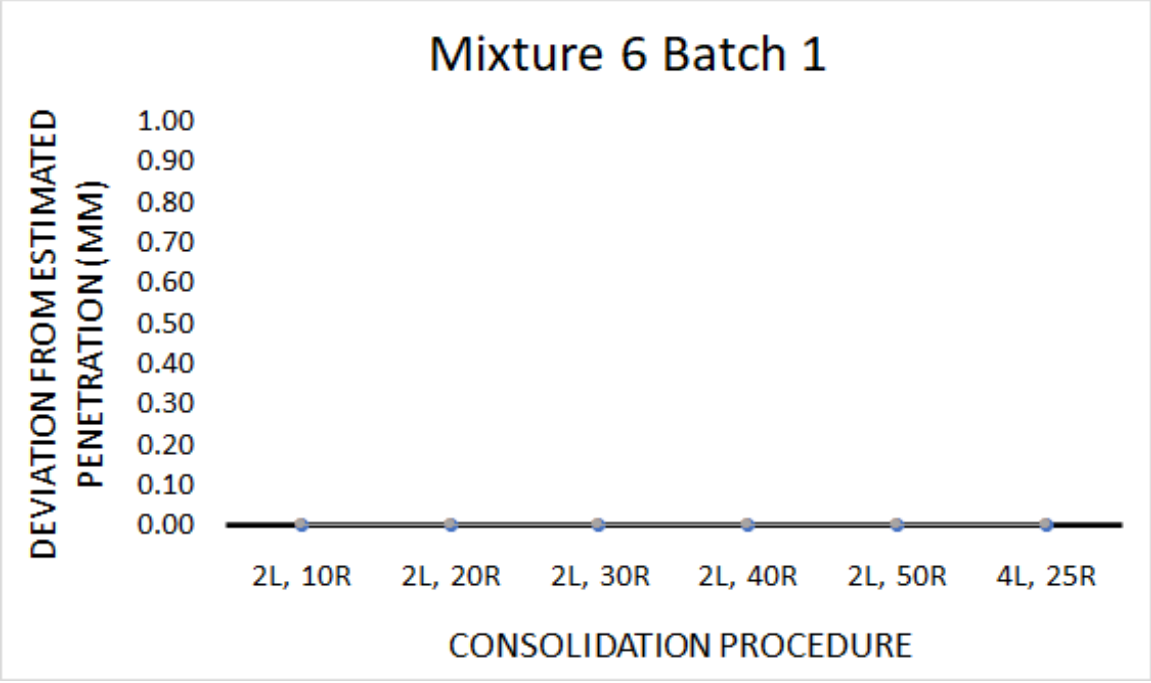

Figure A.11. Mixture 5 Batch 1 Deltas of Penetration

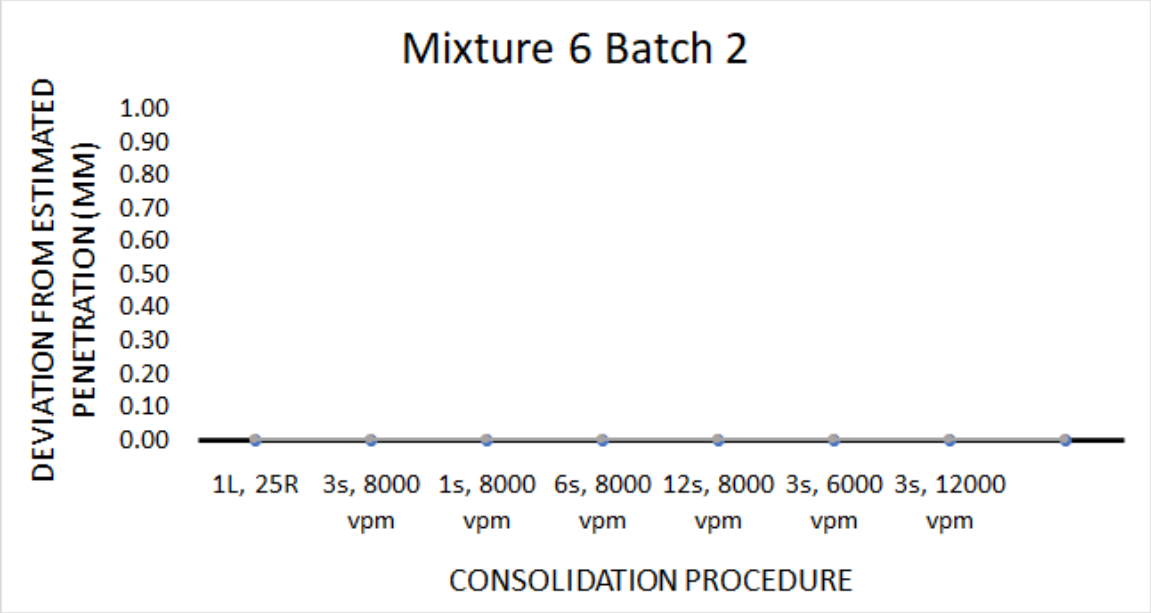

Figure A.12. Mixture 6 Batch 2 Deltas of Penetration

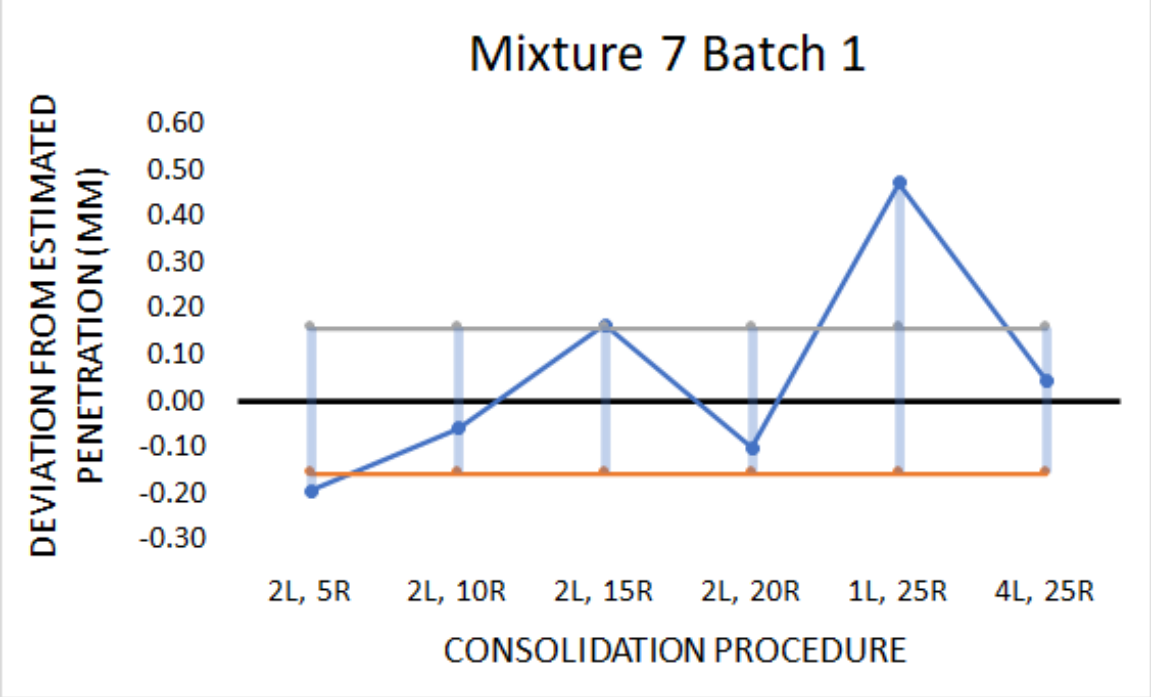

Figure A.13. Mixture 7 Batch 1 Deltas of Penetration

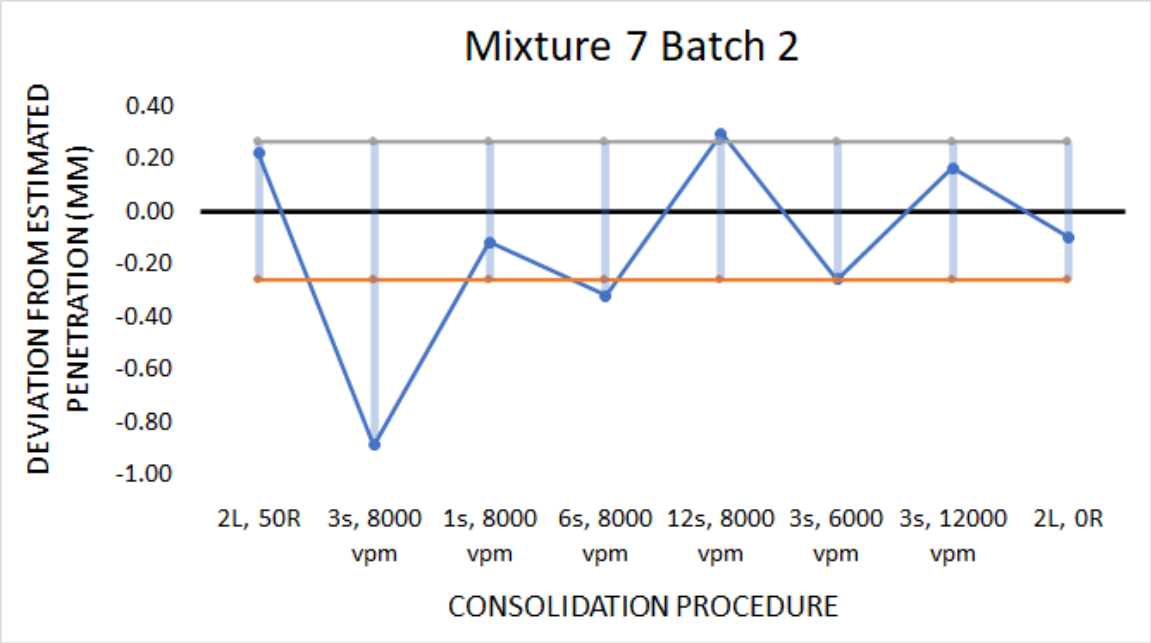

Figure A.14. Mixture 7 Batch 2 Deltas of Penetration

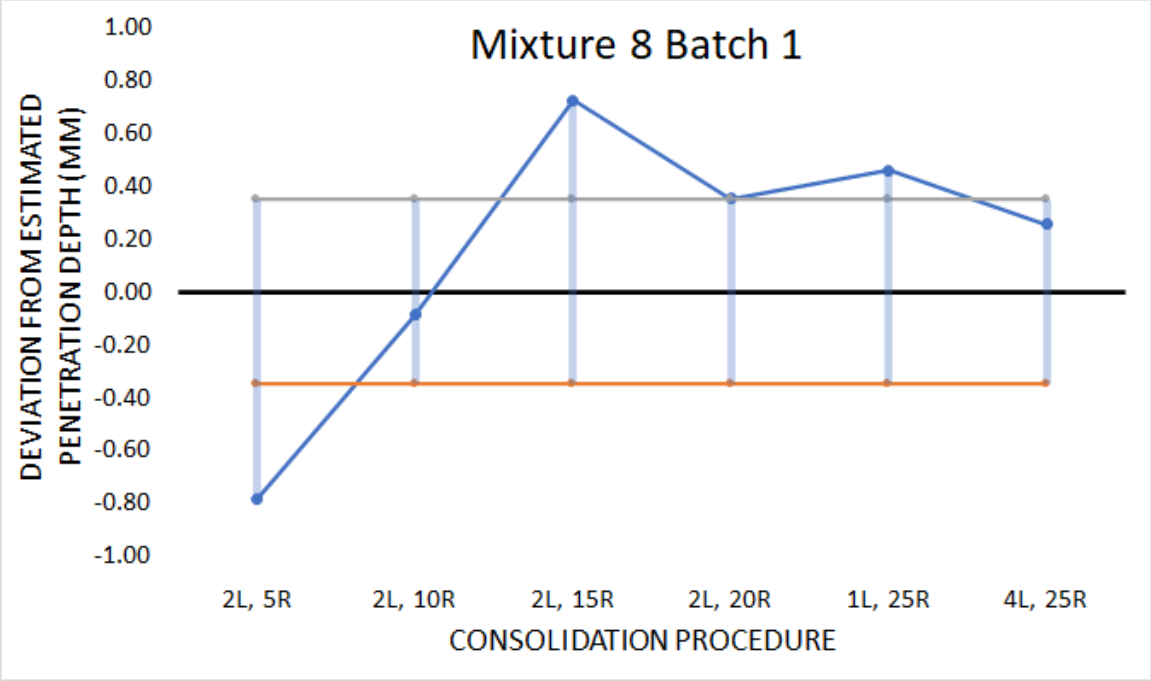

Figure A.15. Mixture 8 Batch 1 Deltas of Penetration

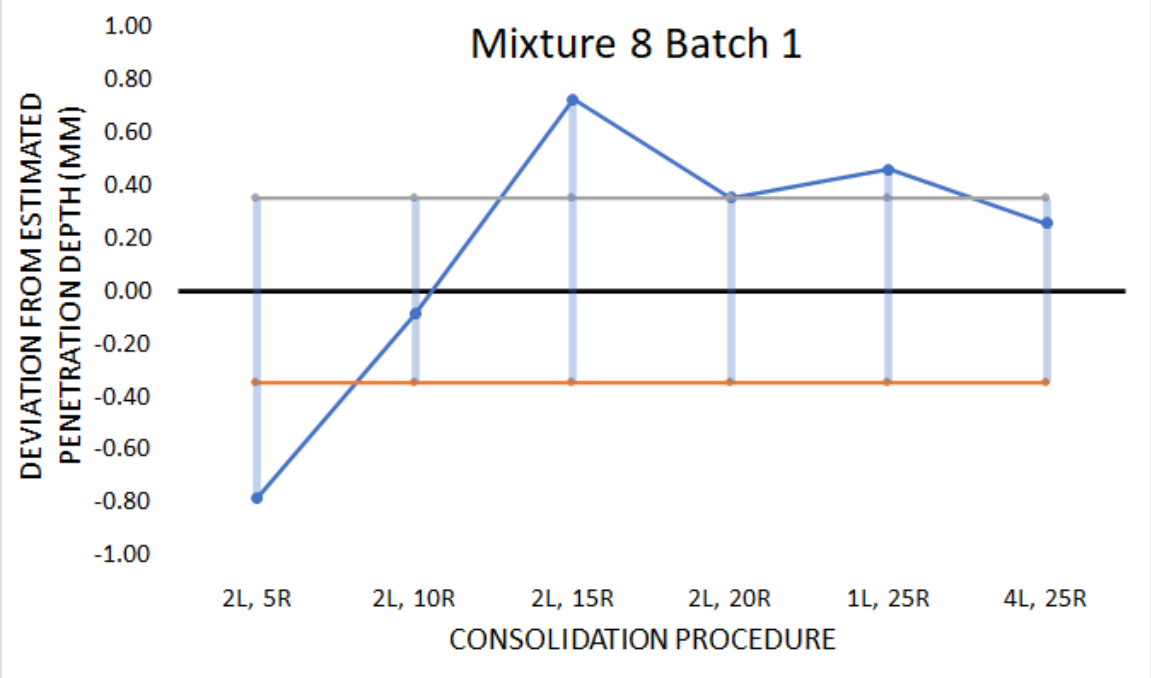

Figure A.16. Mixture 8 Batch 1 Deltas of Penetration

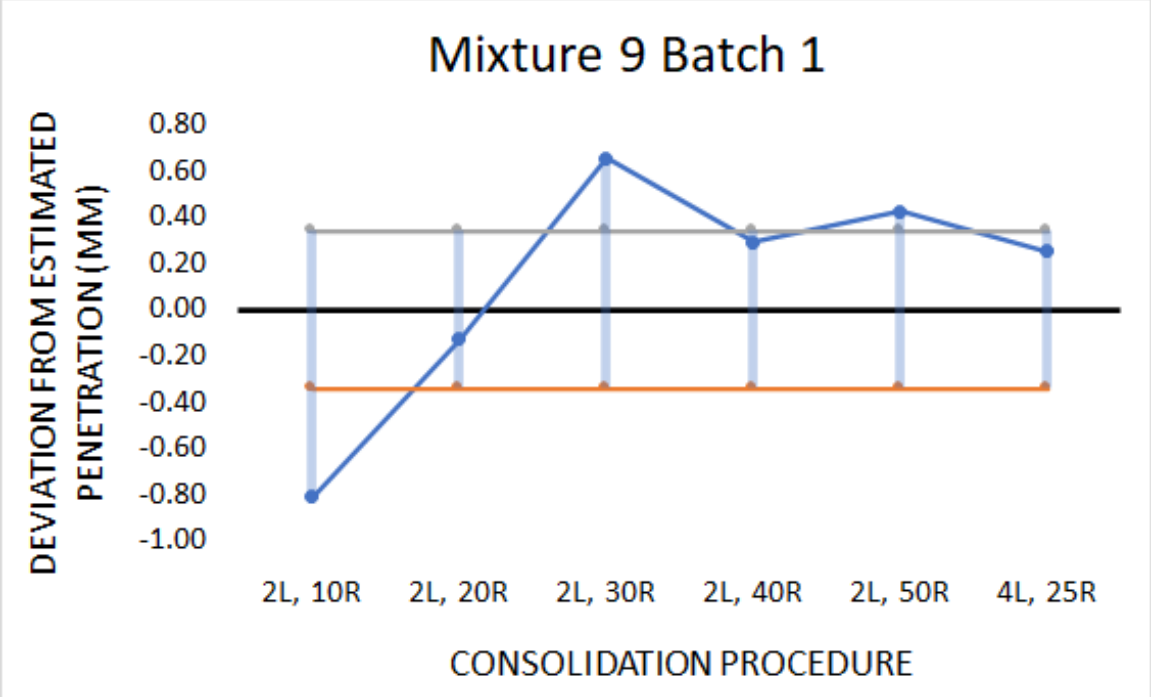

Figure A.17. Mixture 9 Batch 1 Deltas of Penetration

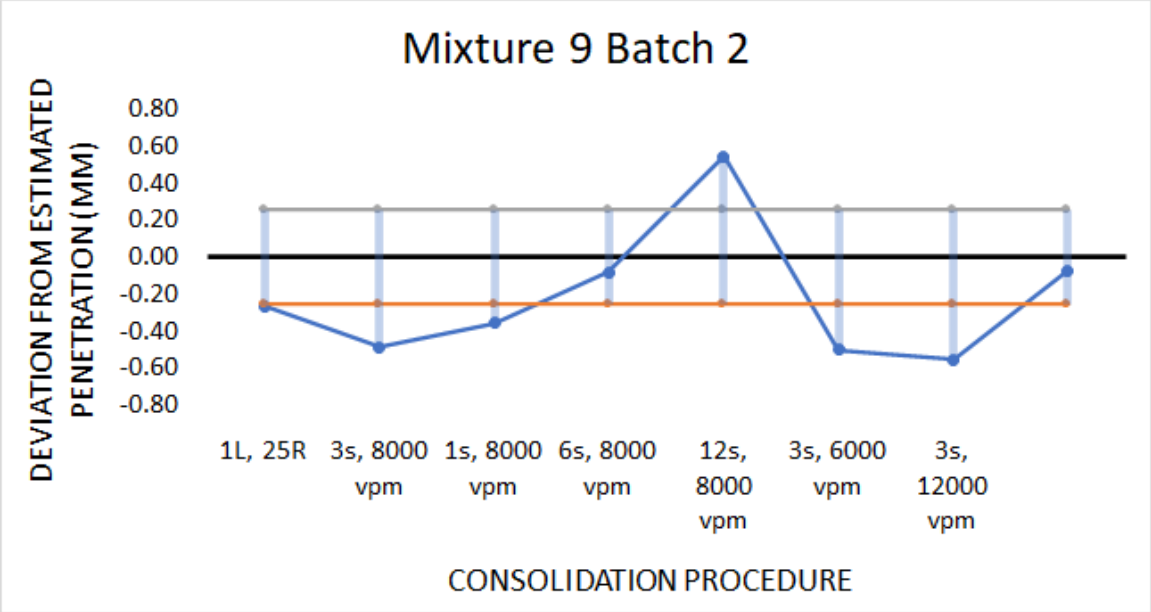

Figure A.18. Mixture 9 Batch 2 Deltas of Penetration

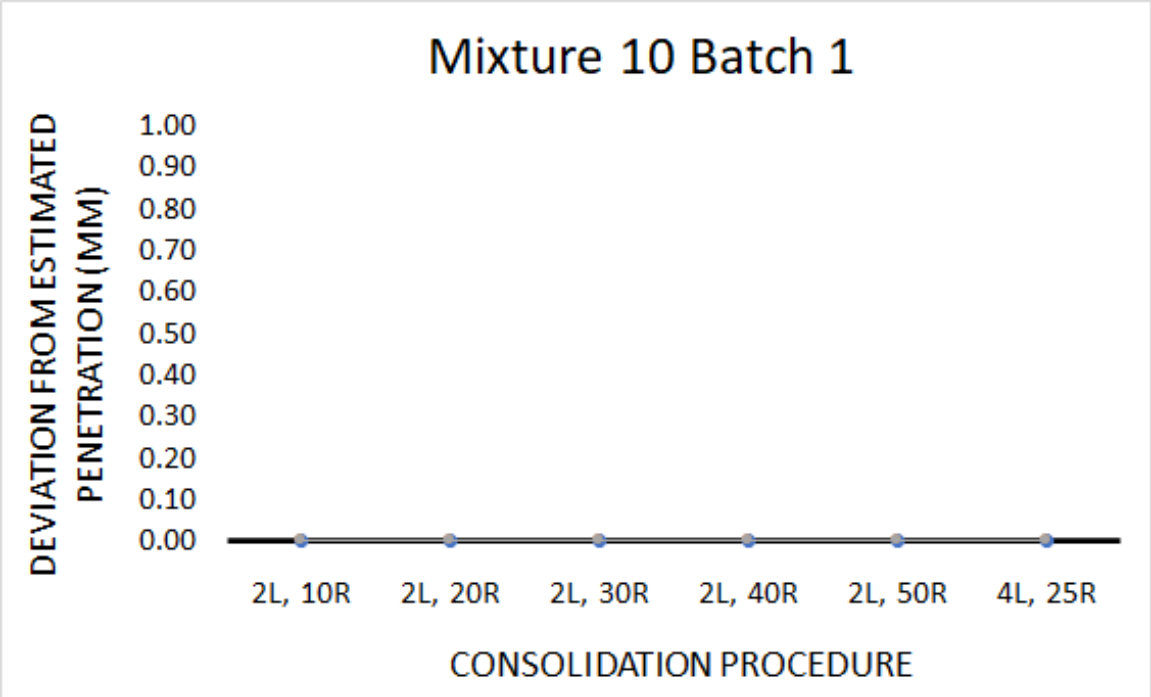

Figure A.19. Mixture 10 Batch 1 Deltas of Penetration

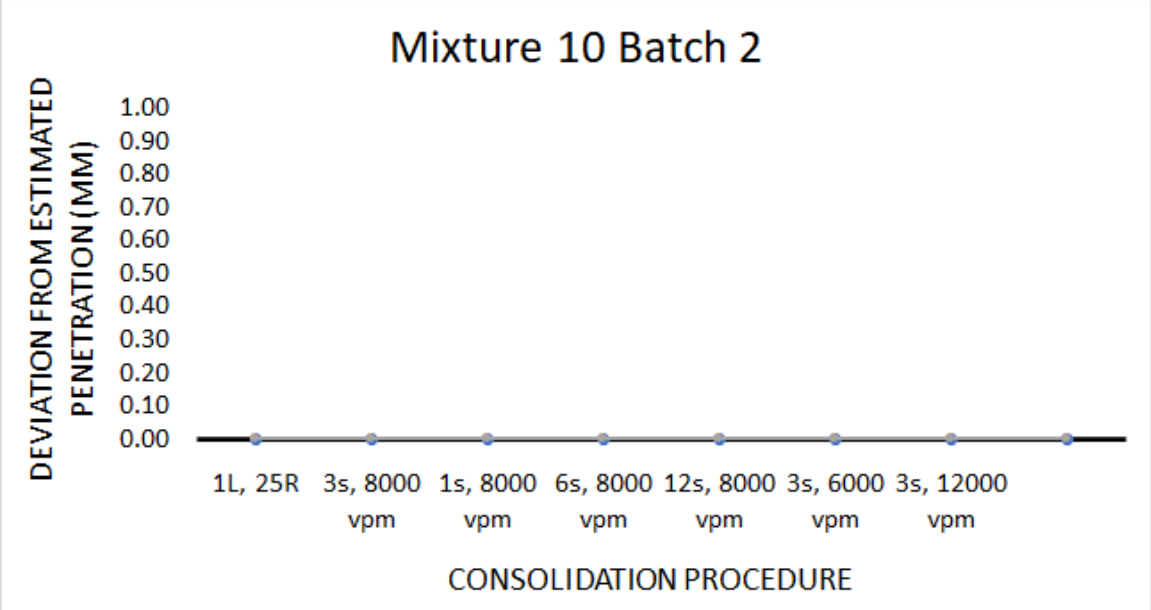

Figure A.20. Mixture 10 Batch 2 Deltas of Penetration

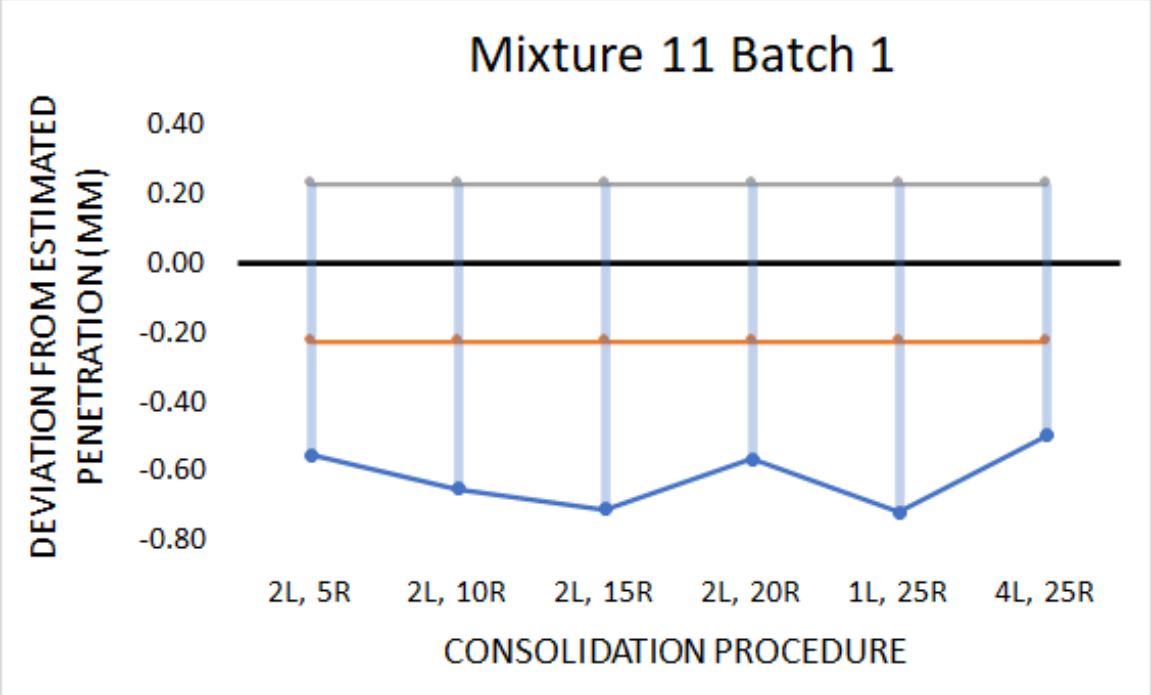

Figure A.21. Mixture 11 Batch 1 Deltas of Penetration

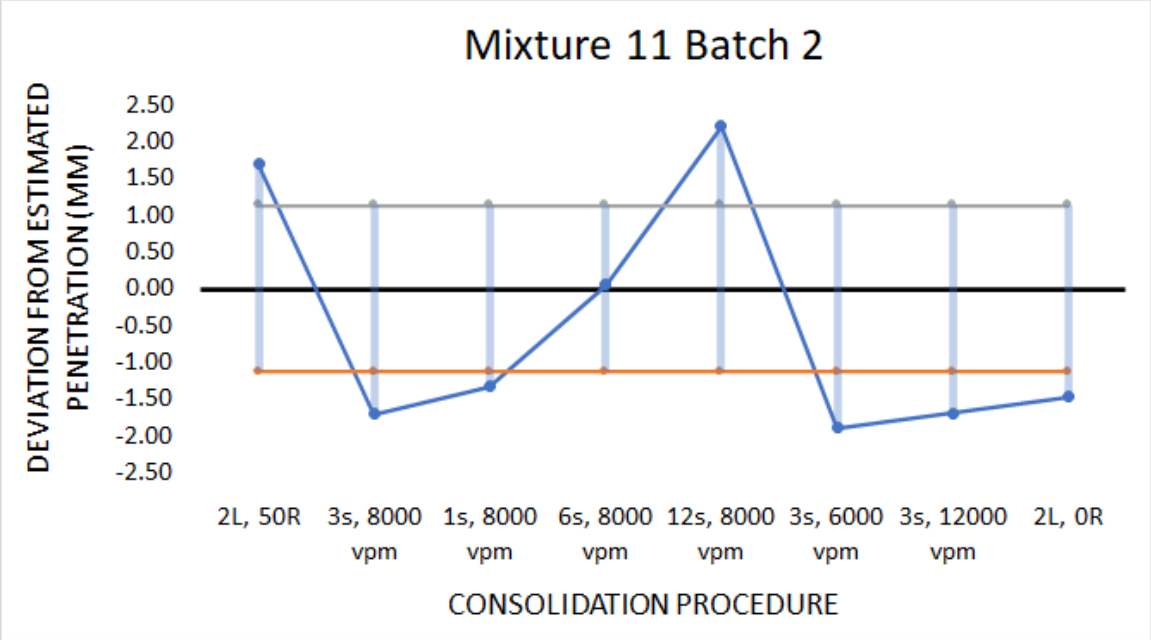

Figure A.22. Mixture 11 Batch 2 Deltas of Penetration

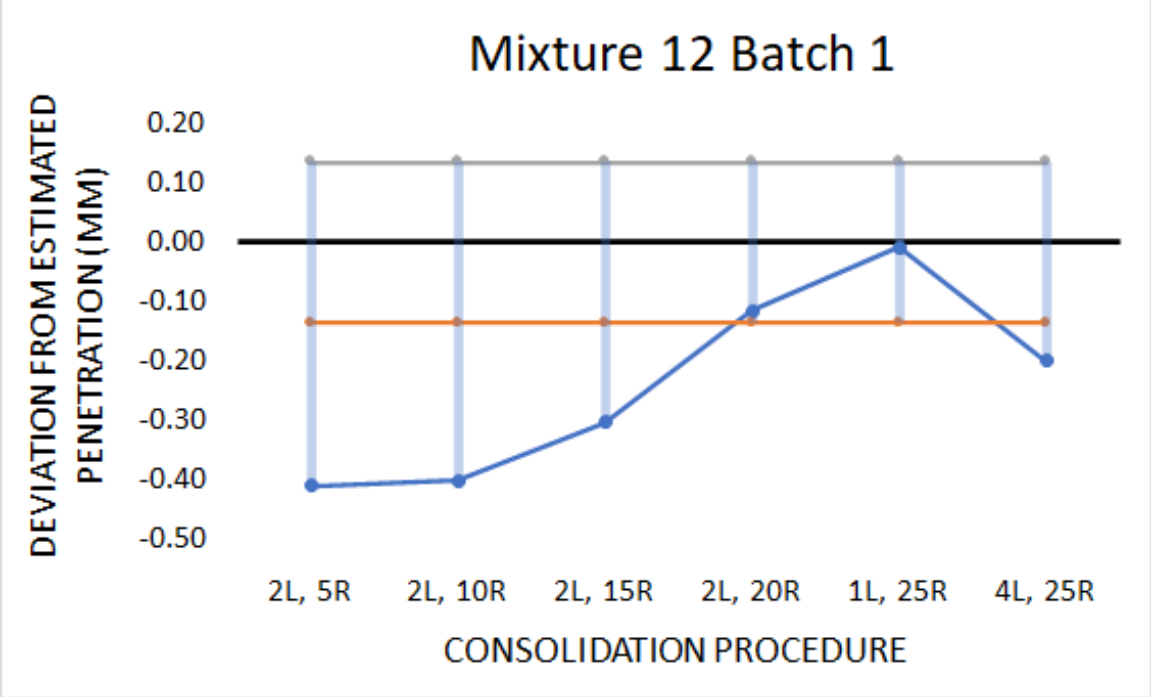

Figure A.23. Mixture 12 Batch 1 Deltas of Penetration

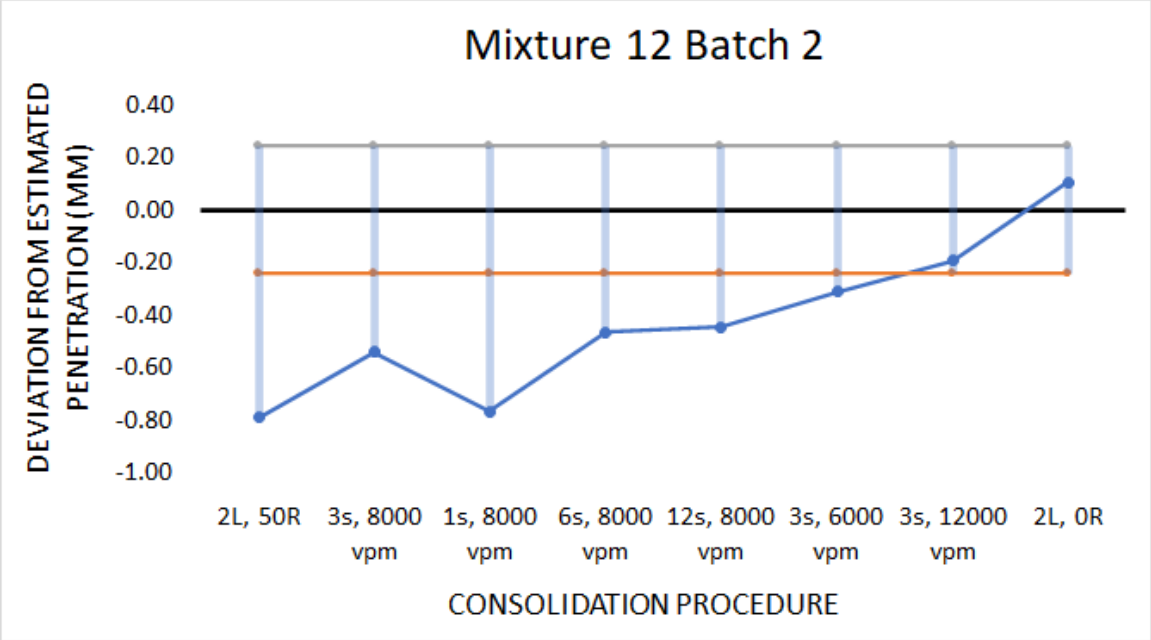

Figure A.24. Mixture 12 Batch 2 Deltas of Penetration

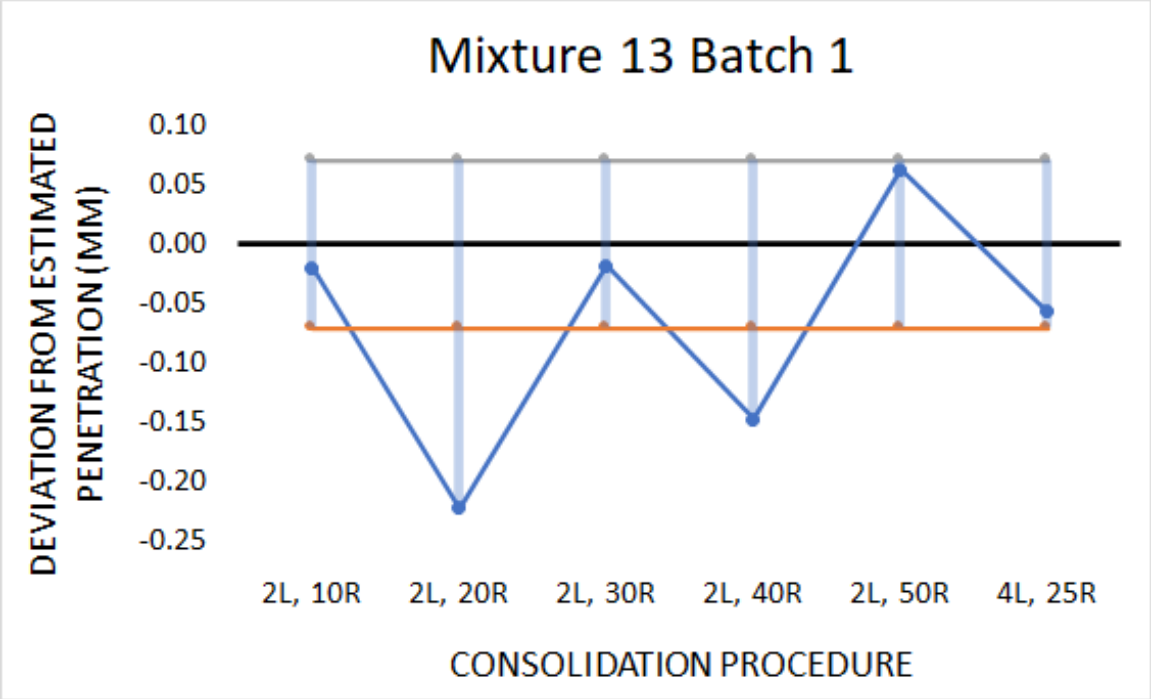

Figure A.25. Mixture 13 Batch 1 Deltas of Penetration

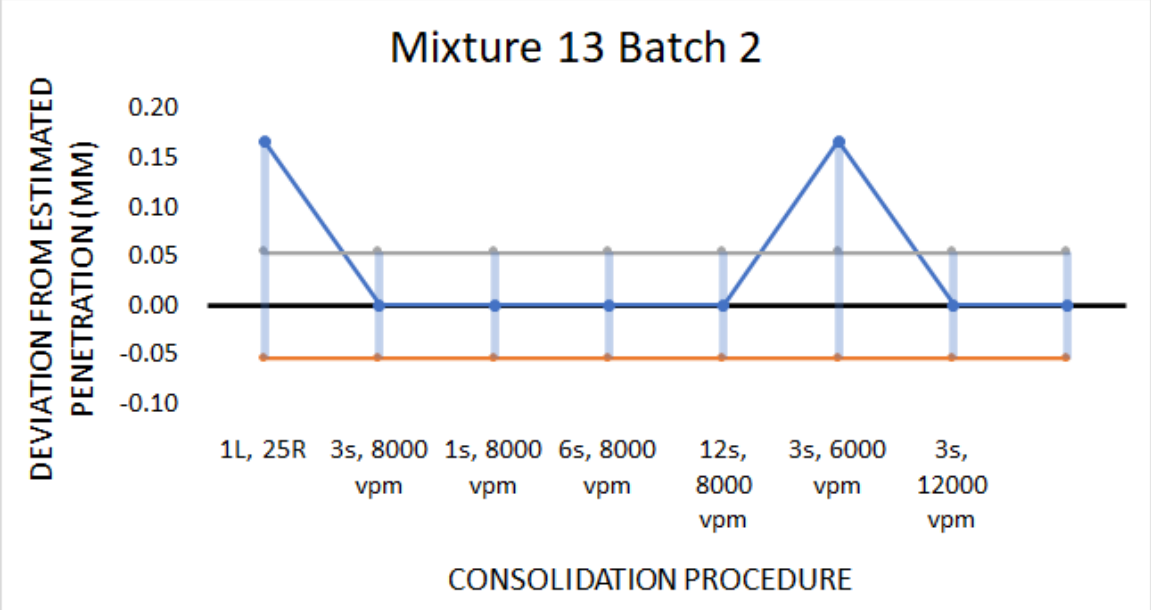

Figure A.26. Mixture 13 Batch 2 Deltas of Penetration

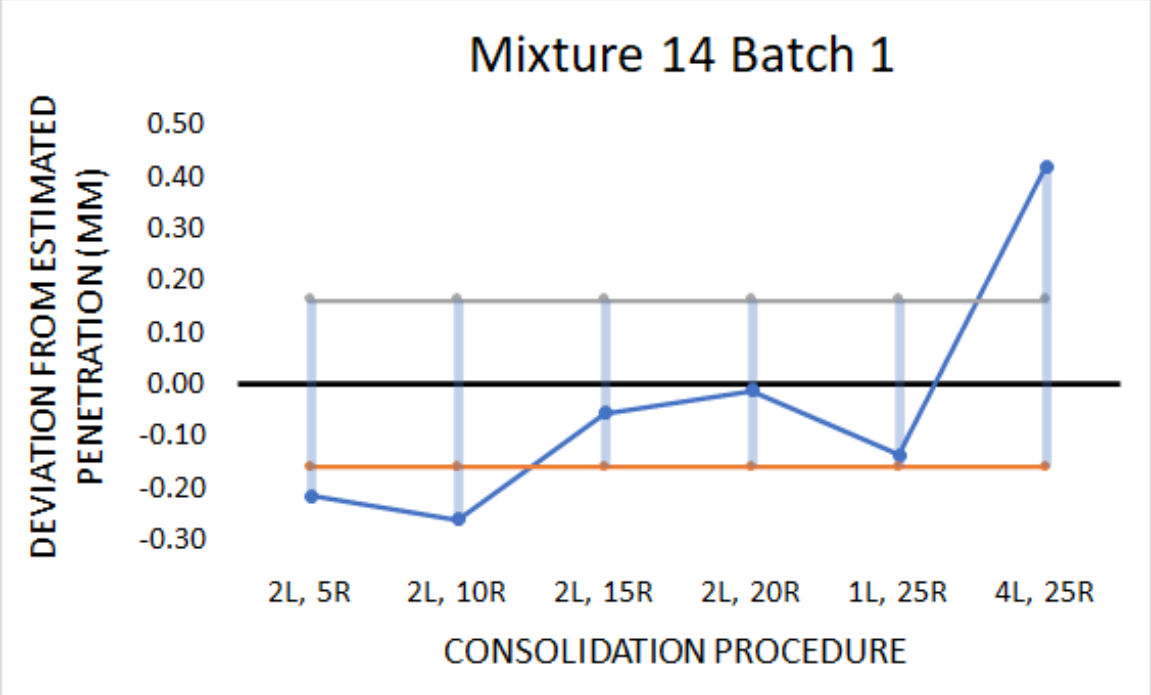

Figure A.27. Mixture 14 Batch 1 Deltas of Penetration

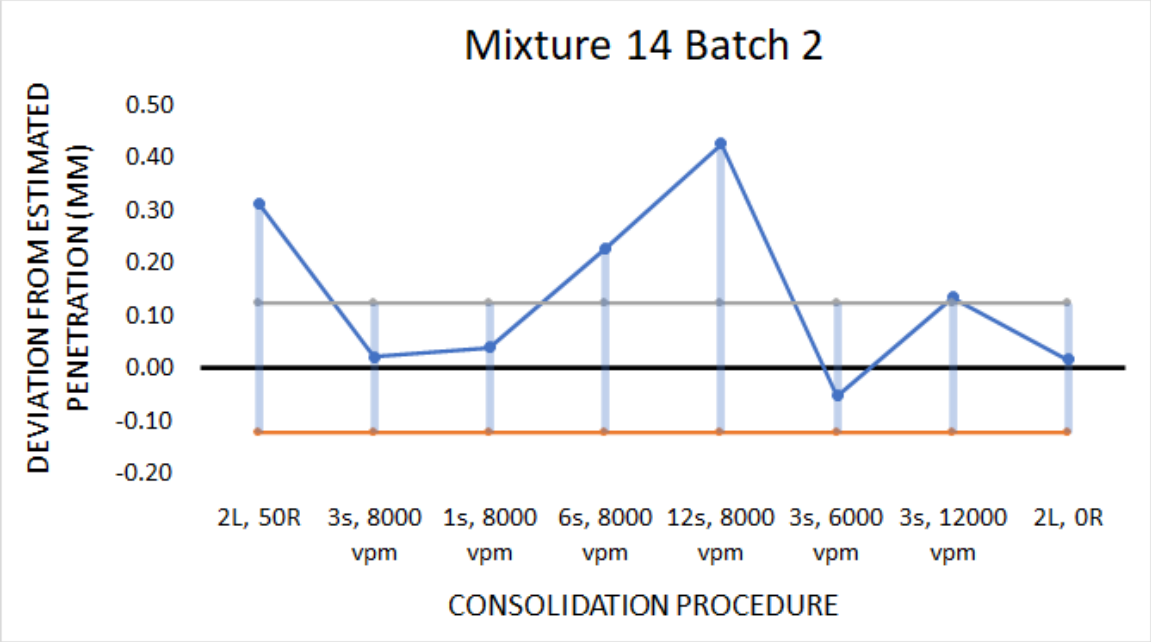

Figure A.28. Mixture 14 Batch 2 Deltas of Penetration

SATURATED SURFACE DRY DENSITIES

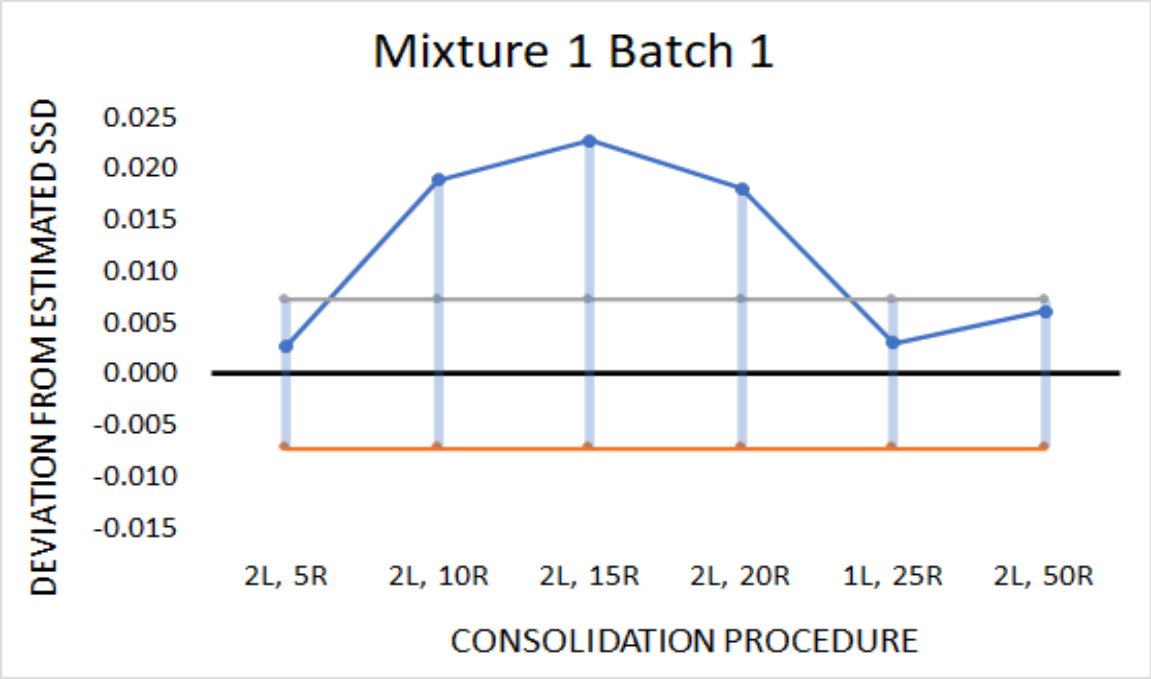

Figure A.29. Mixture 1 Batch 1 Deltas of SSD Relative Density

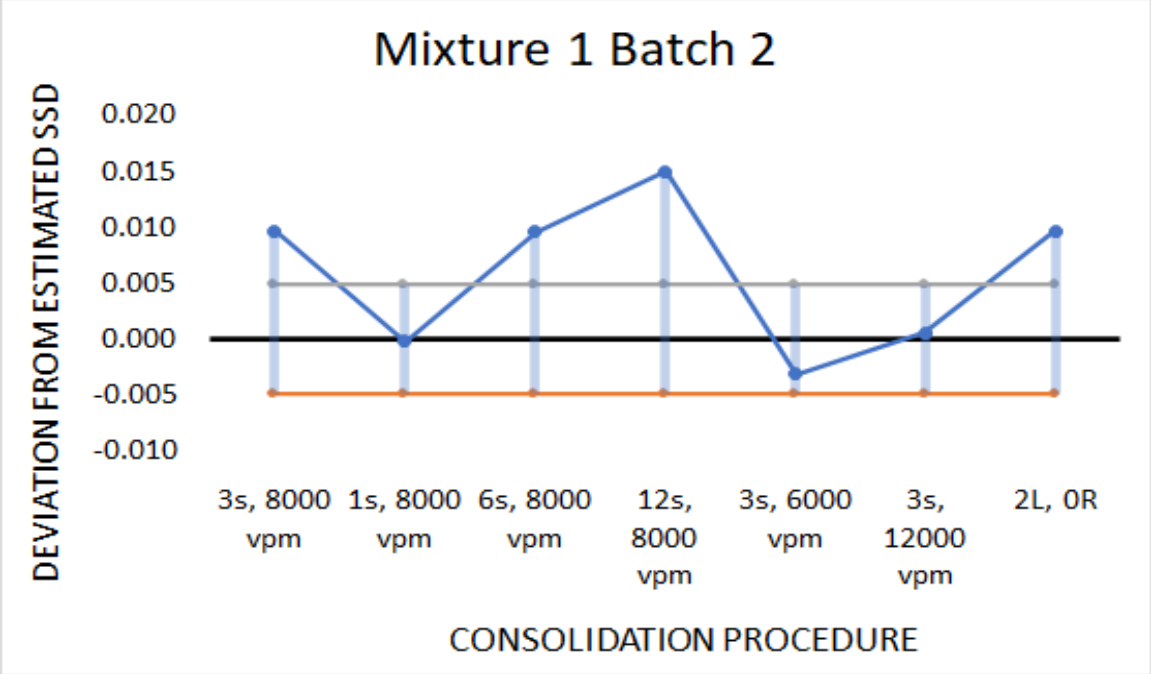

Figure A.30. Mixture 1 Batch 2 Deltas of SSD Relative Density

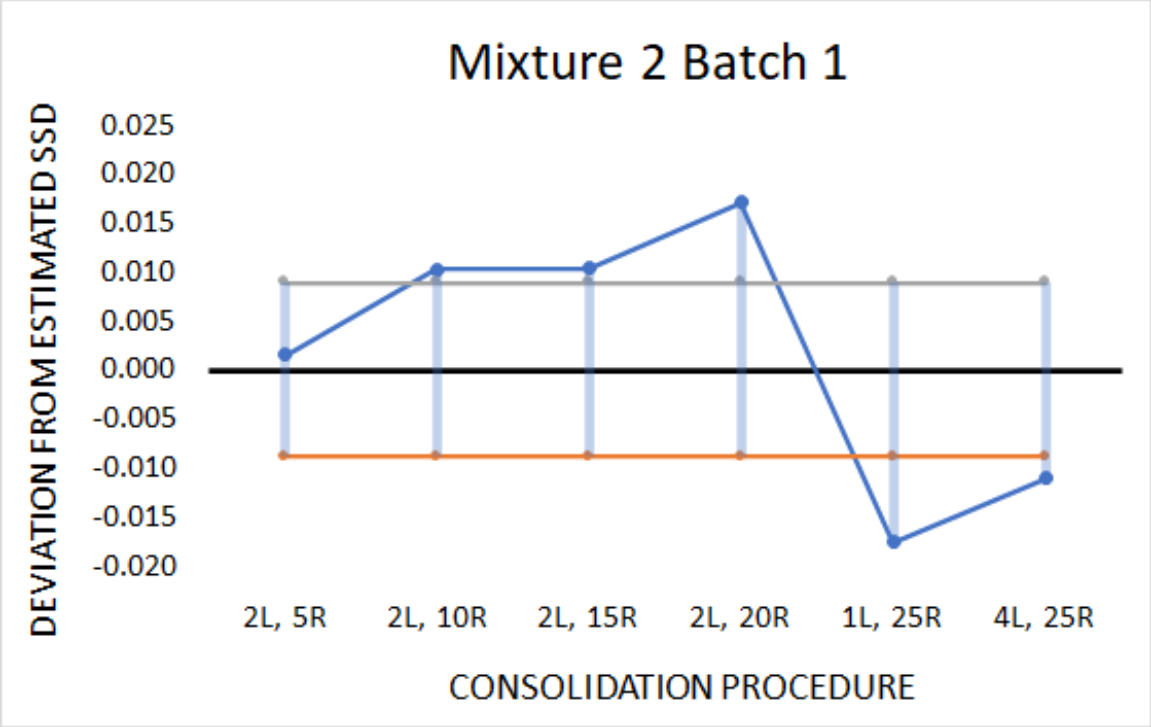

Figure A.31. Mixture 2 Batch 1 Deltas of SSD Relative Density

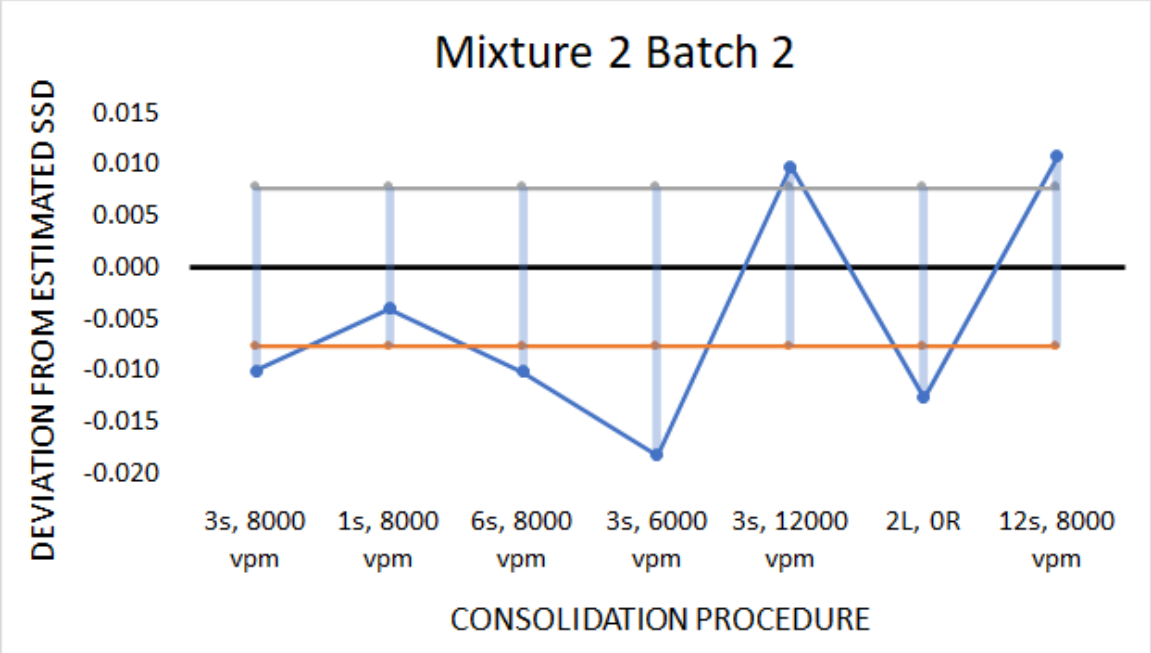

Figure A.32. Mixture 2 Batch 2 Deltas of SSD Relative Density

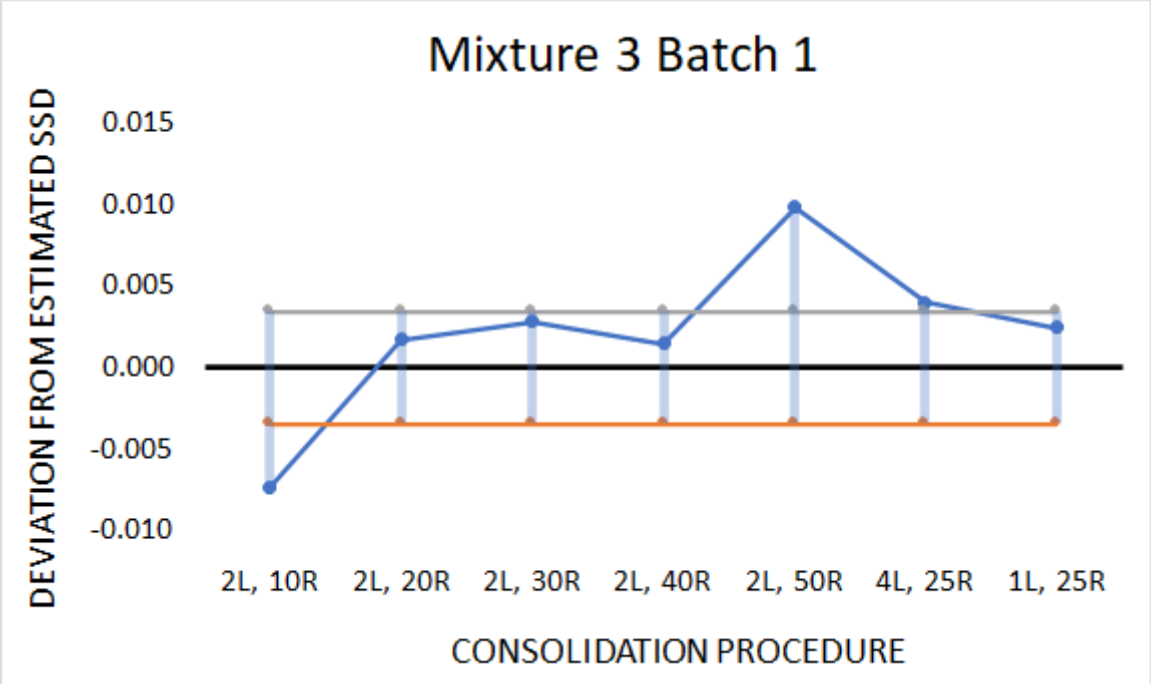

Figure A.33. Mixture 3 Batch 1 Deltas of SSD Relative Density

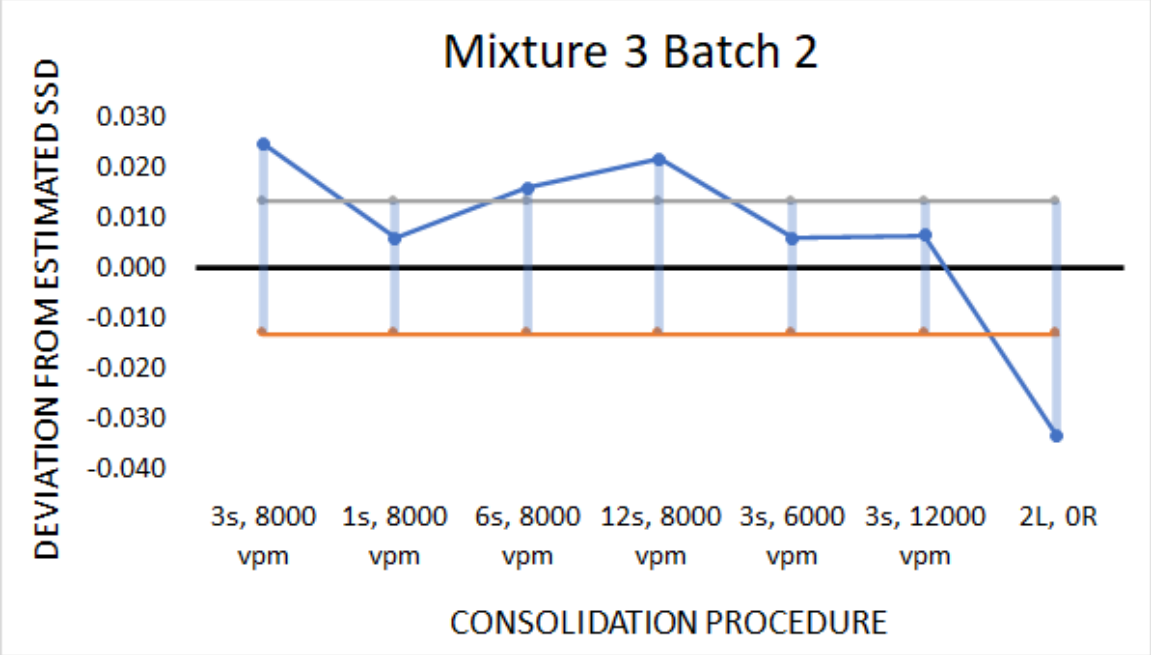

Figure A.34. Mixture 3 Batch 2 Deltas of SSD Relative Density

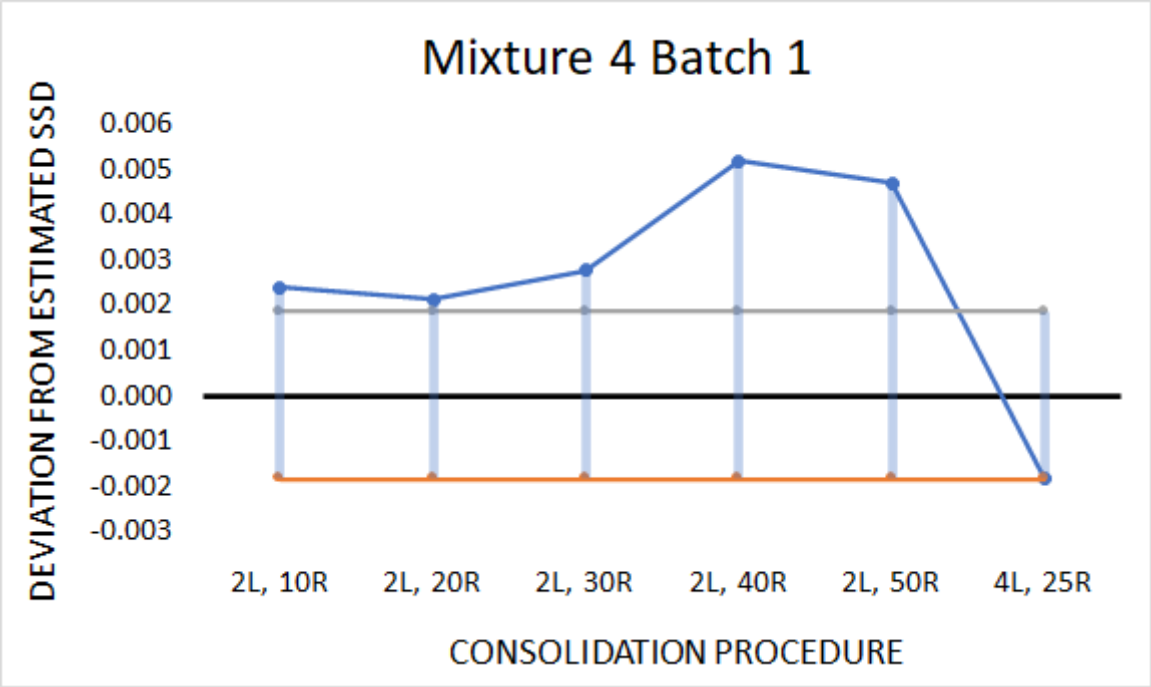

Figure A.35. Mixture 4 Batch 1 Deltas of SSD Relative Density

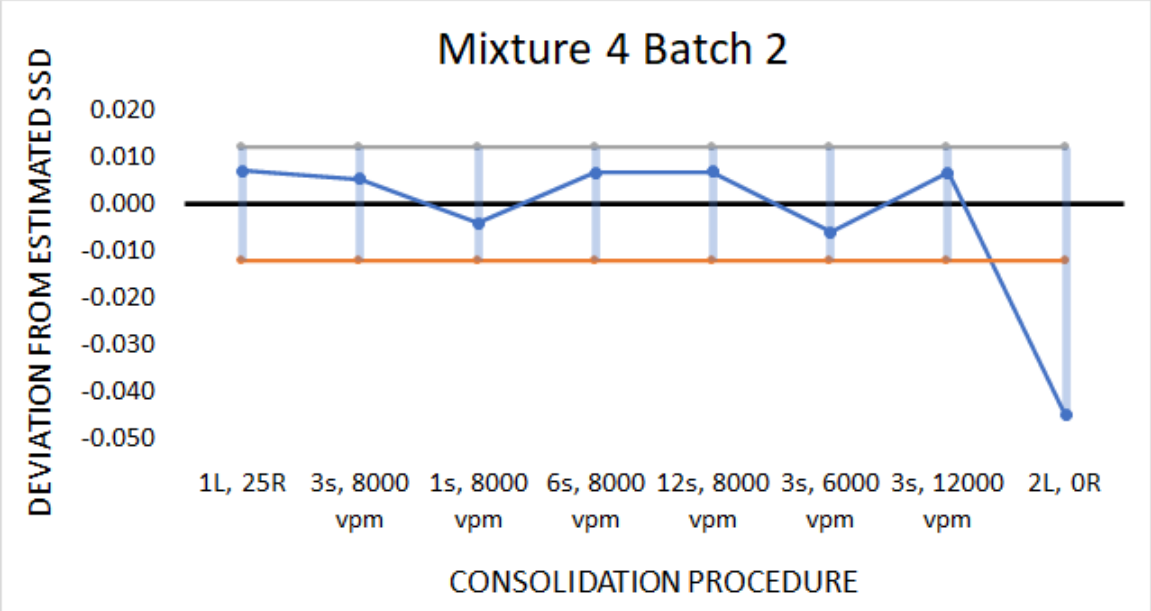

Figure A.36. Mixture 4 Batch 2 Deltas of SSD Relative Density

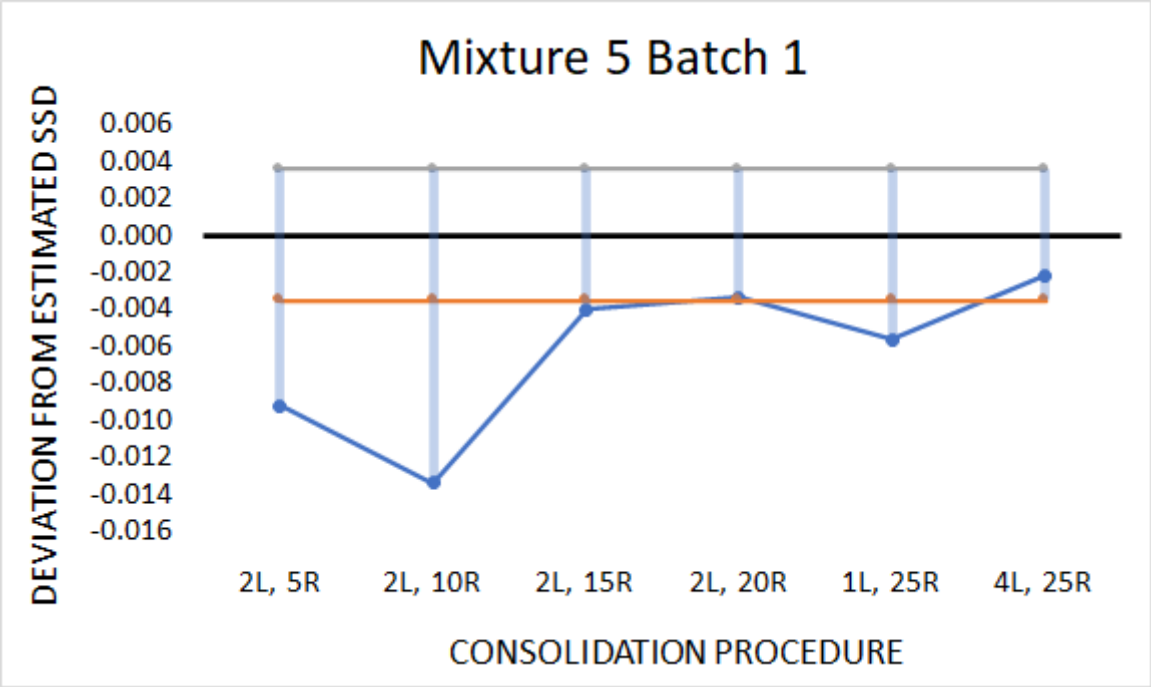

Figure A.37. Mixture 5 Batch 1 Deltas of SSD Relative Density

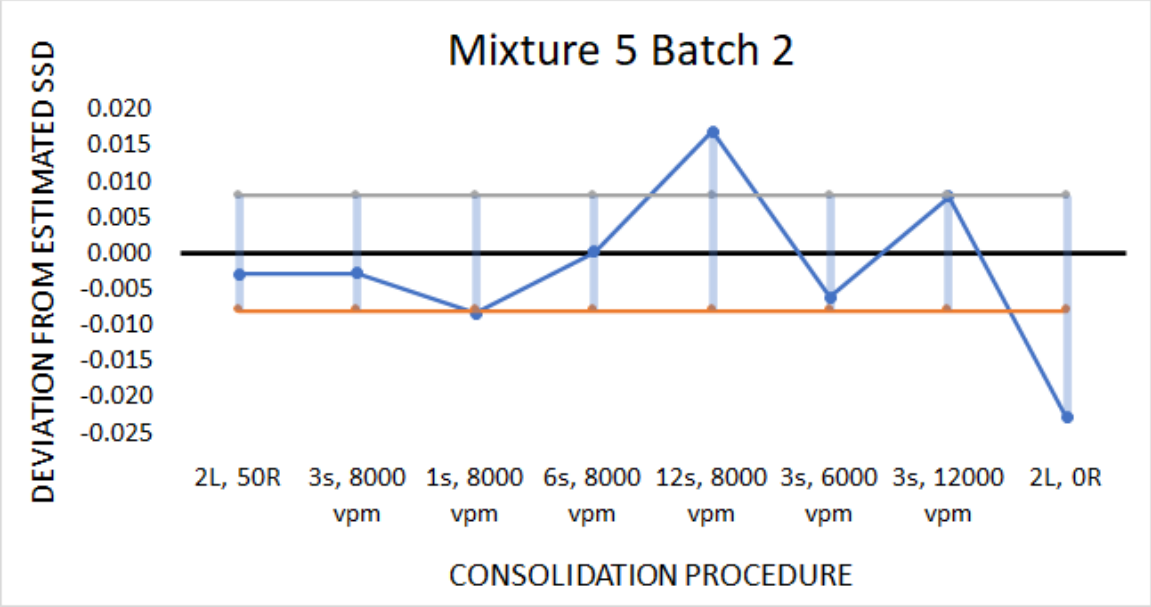

Figure A.38. Mixture 5 Batch 2 Deltas of SSD Relative Density

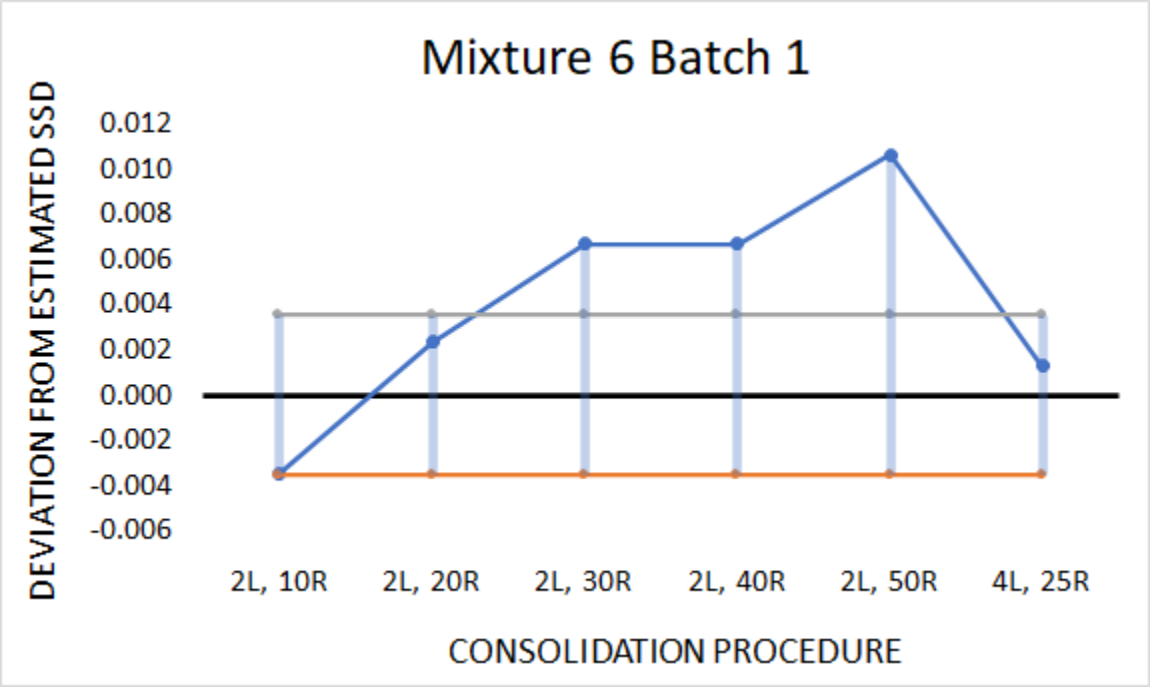

Figure A.39. Mixture 6 Batch 1 Deltas of SSD Relative Density

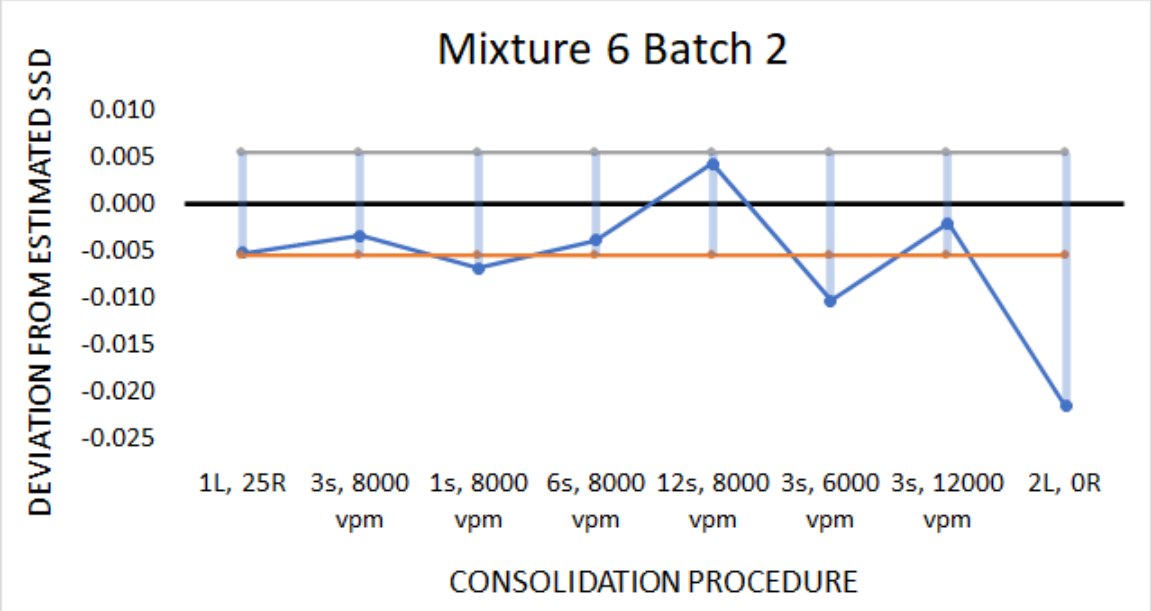

Figure A.40. Mixture 6 Batch 2 Deltas of SSD Relative Density

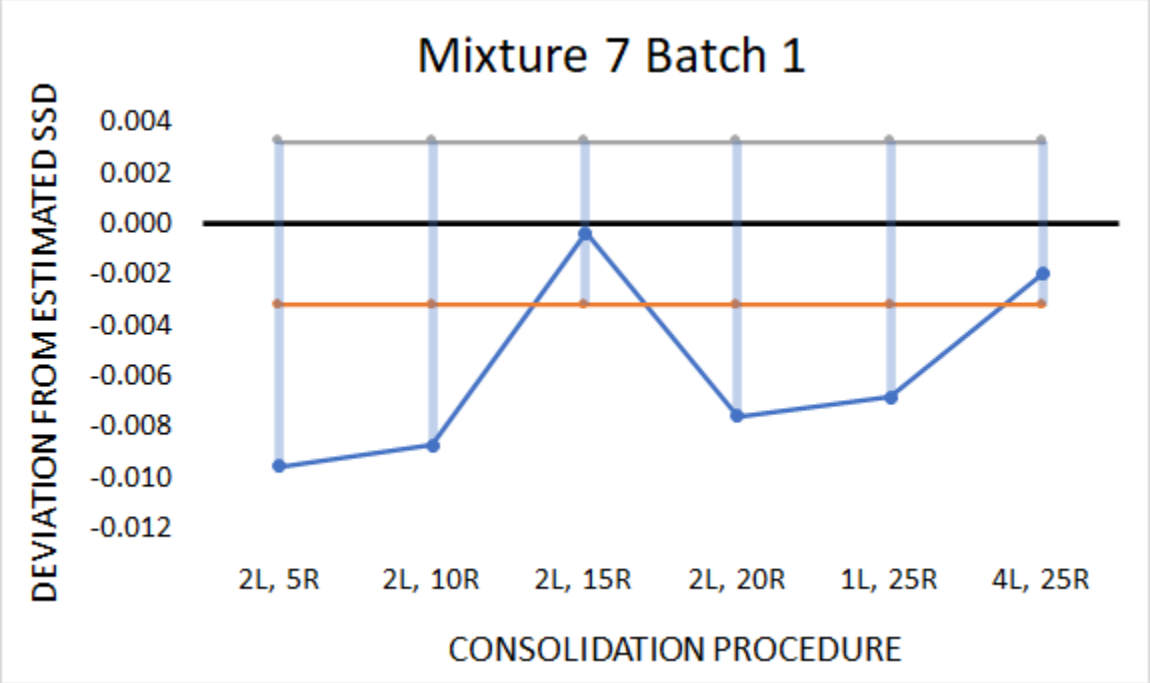

Figure A.41. Mixture 7 Batch 1 Deltas of SSD Relative Density

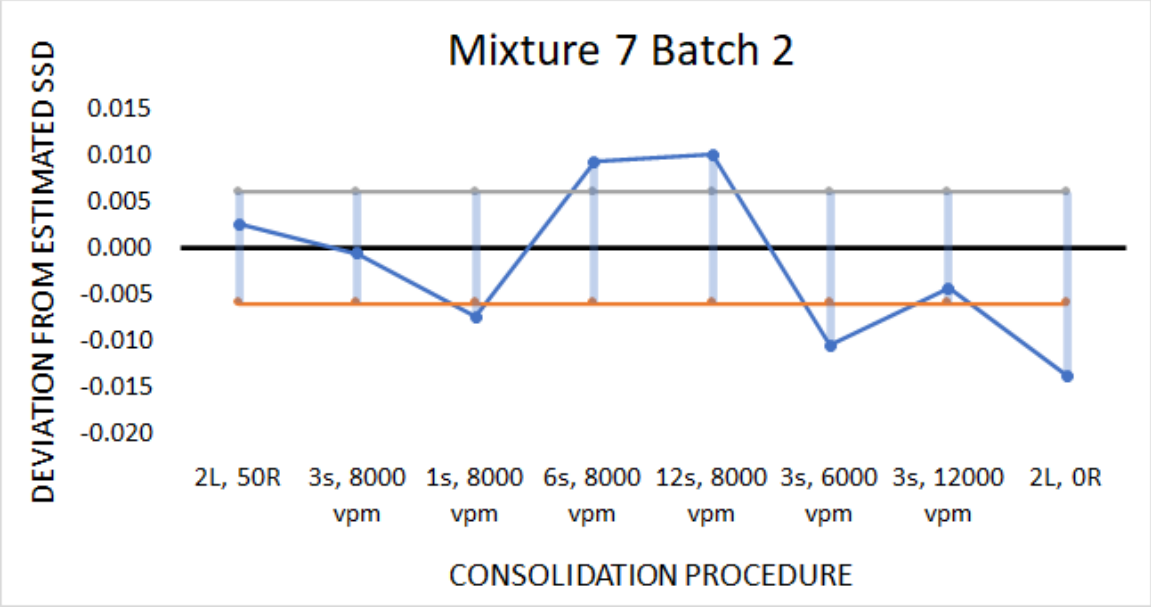

Figure A.42. Mixture 7 Batch 2 Deltas of SSD Relative Density

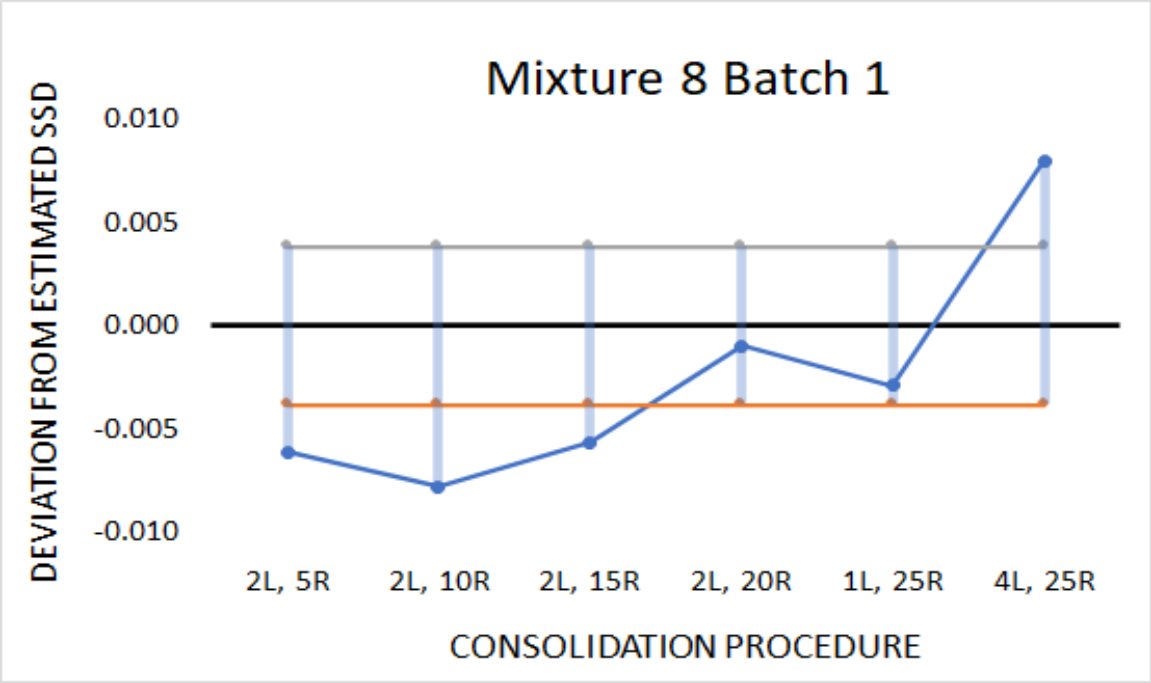

Figure A.43. Mixture 8 Batch 1 Deltas of SSD Relative Density

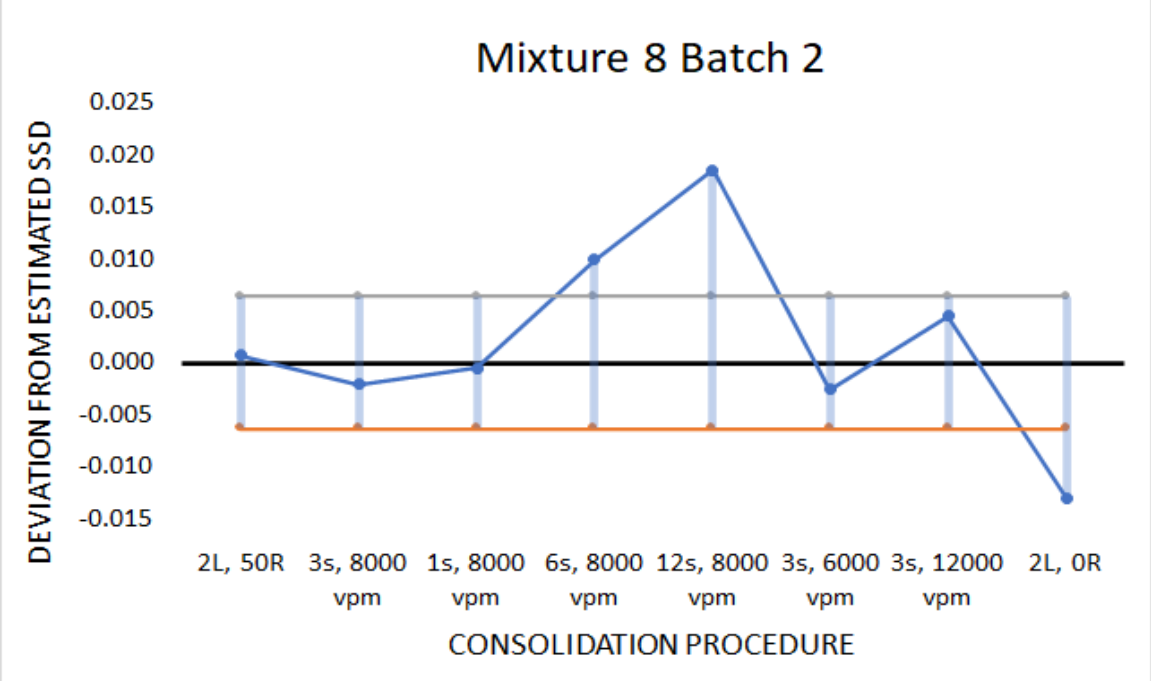

Figure A.44. Mixture 8 Batch 2 Deltas of SSD Relative Density

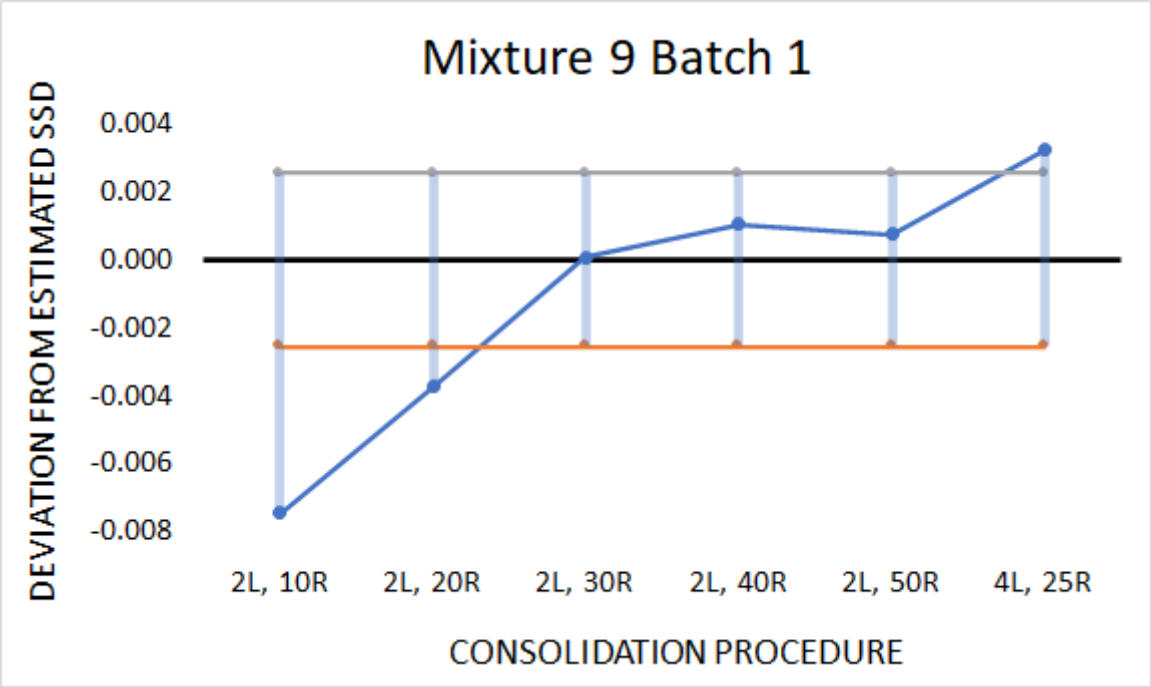

Figure A.45. Mixture 9 Batch 1 Deltas of SSD Relative Density

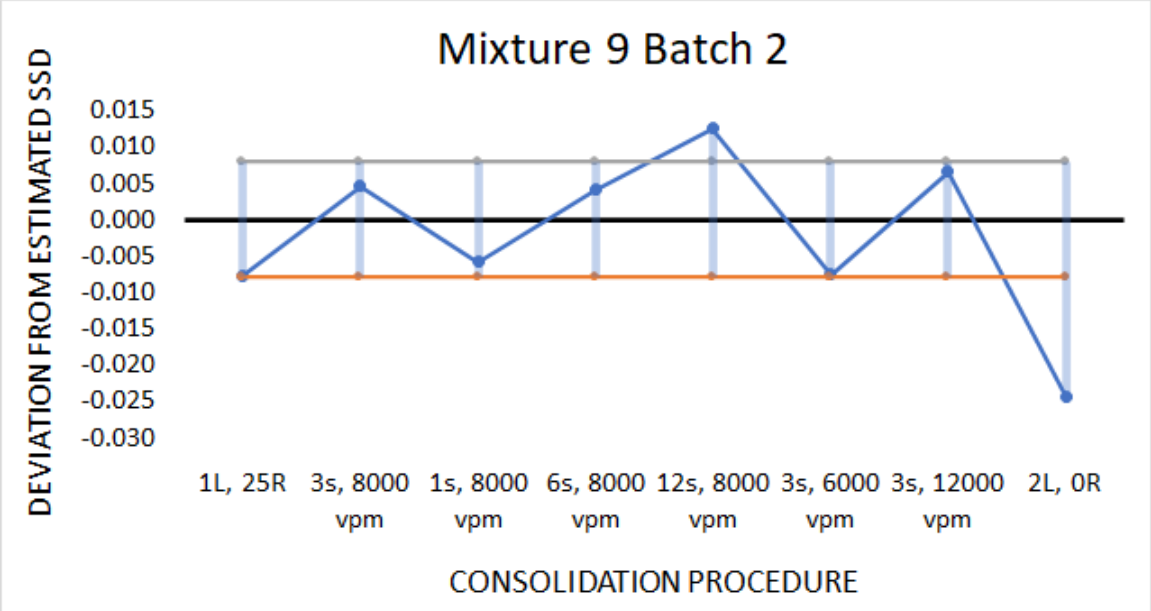

Figure A.46. Mixture 9 Batch 2 Deltas of SSD Relative Density

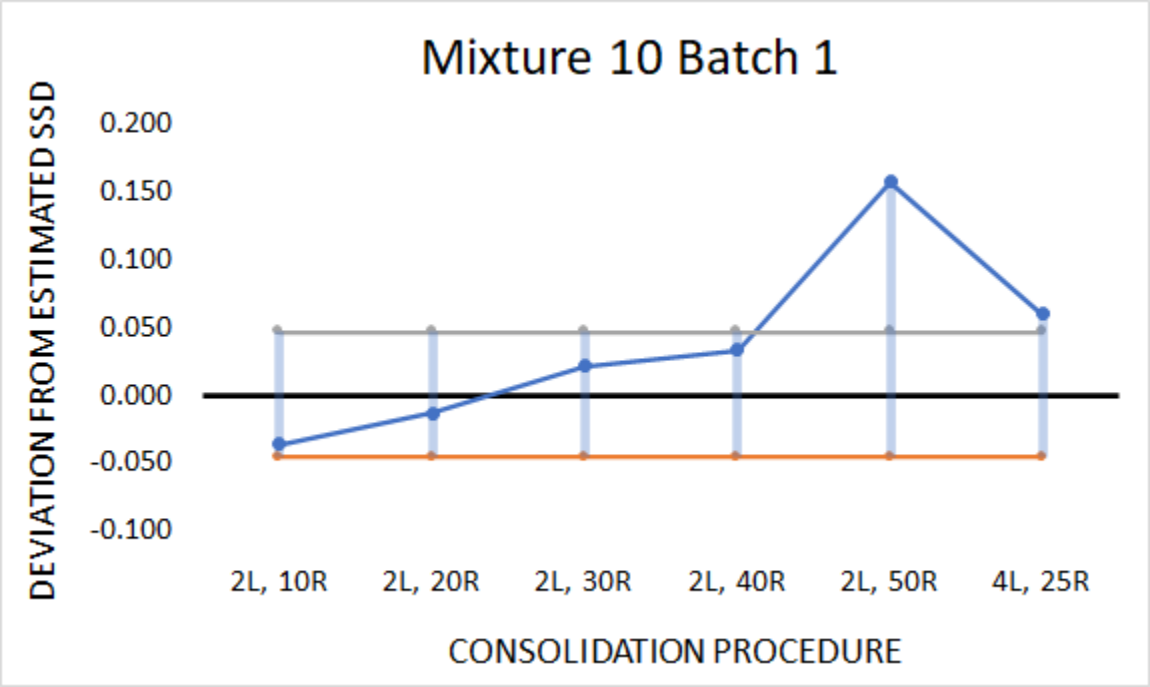

Figure A.47. Mixture 10 Batch 1 Deltas of SSD Relative Density

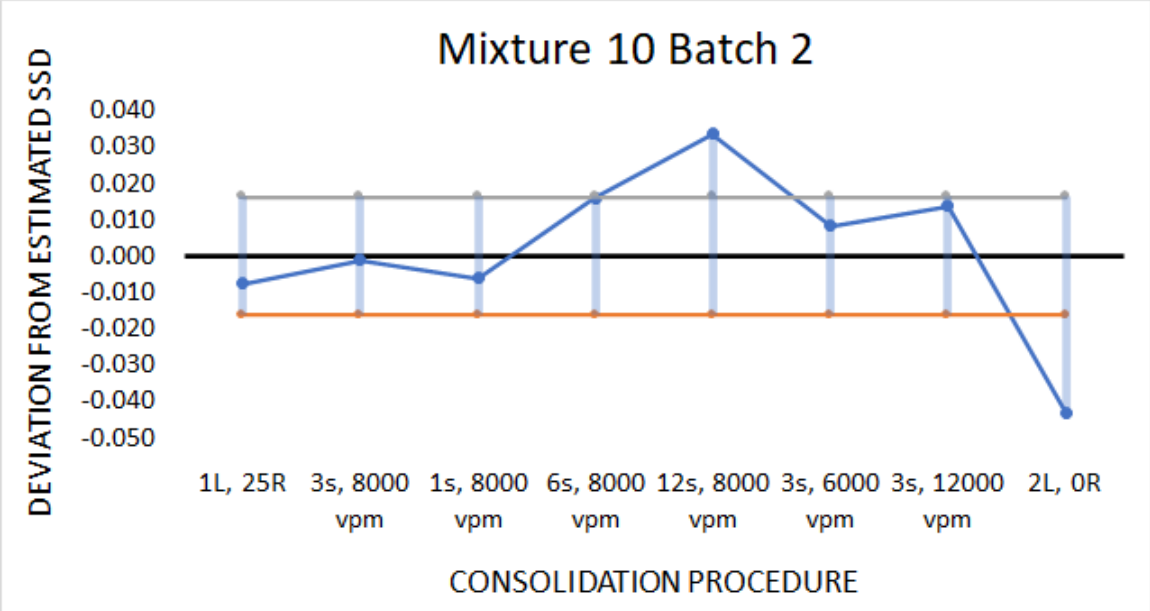

Figure A.48. Mixture 10 Batch 2 Deltas of SSD Relative Density

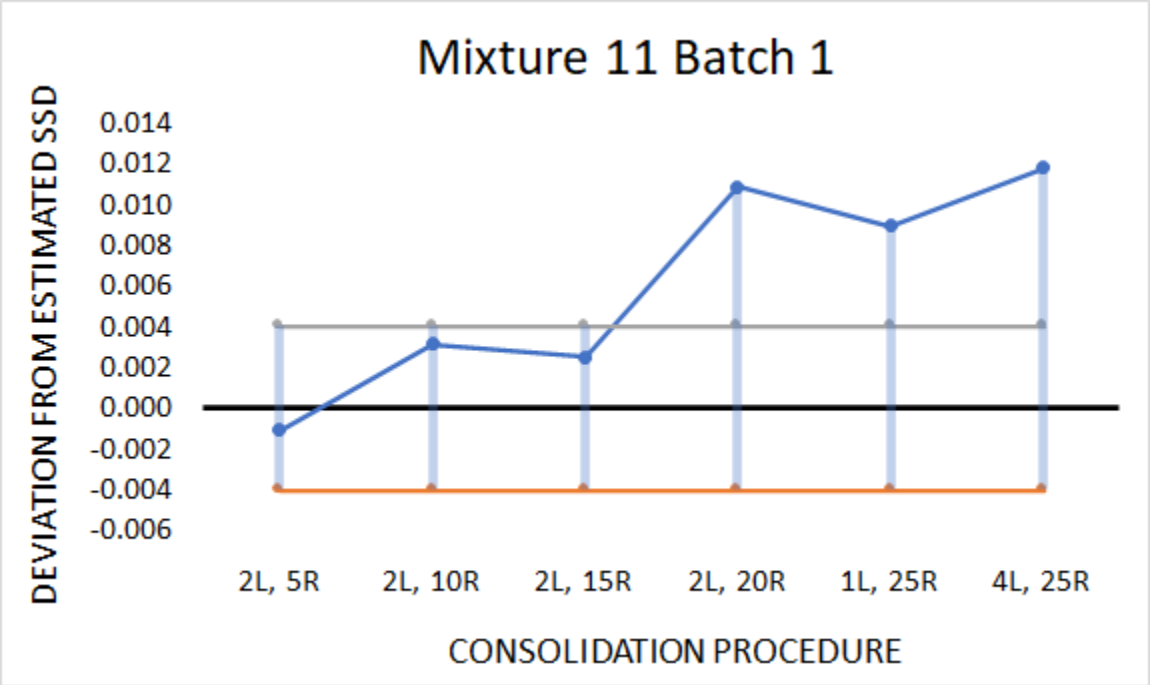

Figure A.49. Mixture 11 Batch 1 Deltas of SSD Relative Density

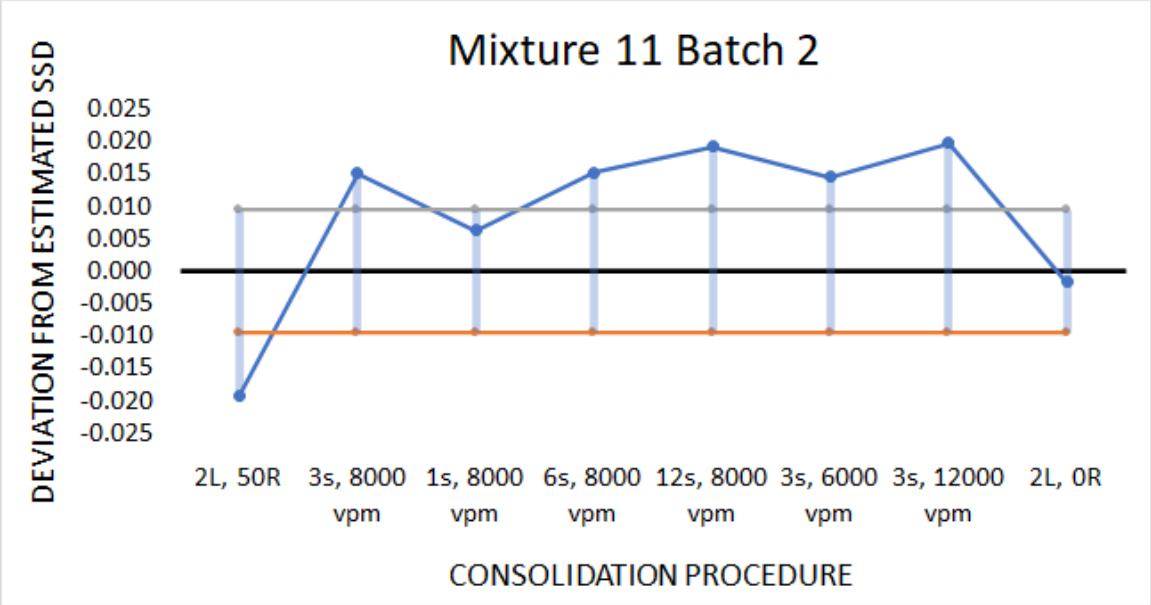

Figure A.50. Mixture 11 Batch 2 Deltas of SSD Relative Density

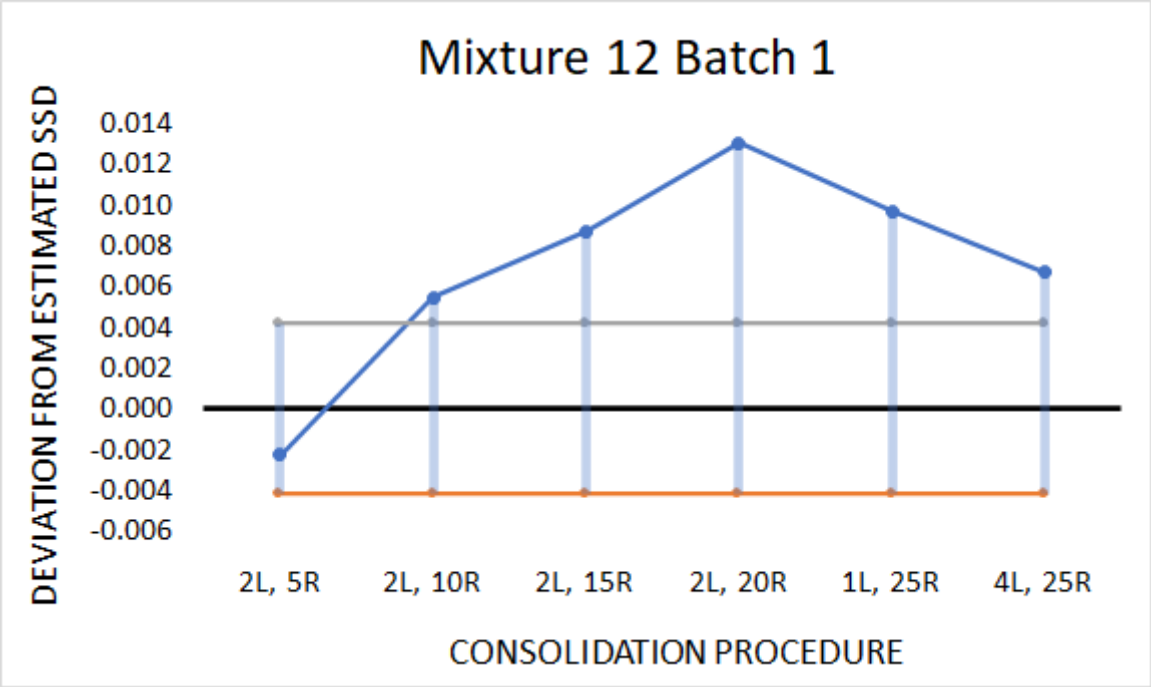

Figure A.51. Mixture 12 Batch 1 Deltas of SSD Relative Density

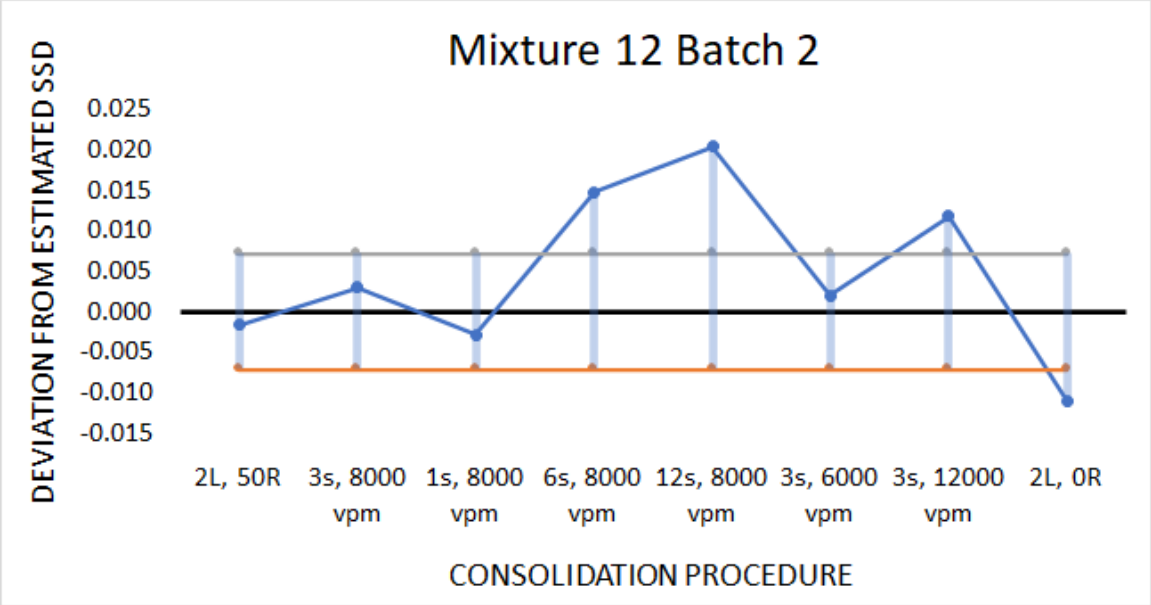

Figure A.52. Mixture 12 Batch 2 Deltas of SSD Relative Density

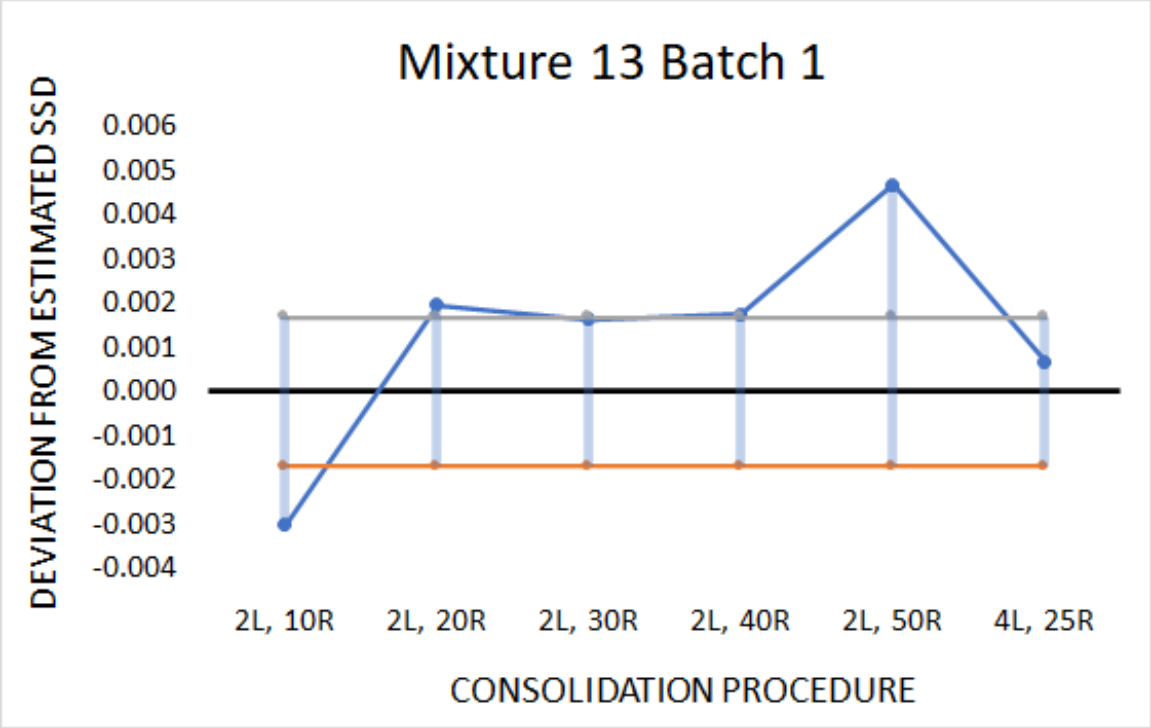

Figure A.53. Mixture 13 Batch 1 Deltas of SSD Relative Density

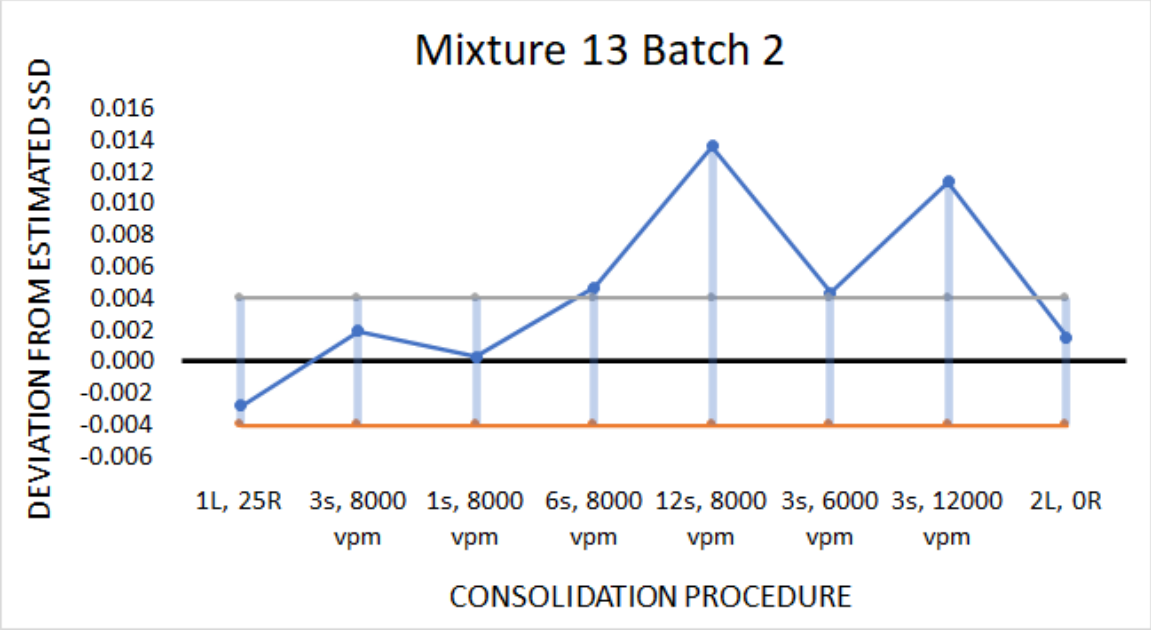

Figure A.54. Mixture 13 Batch 2 Deltas of SSD Relative Density

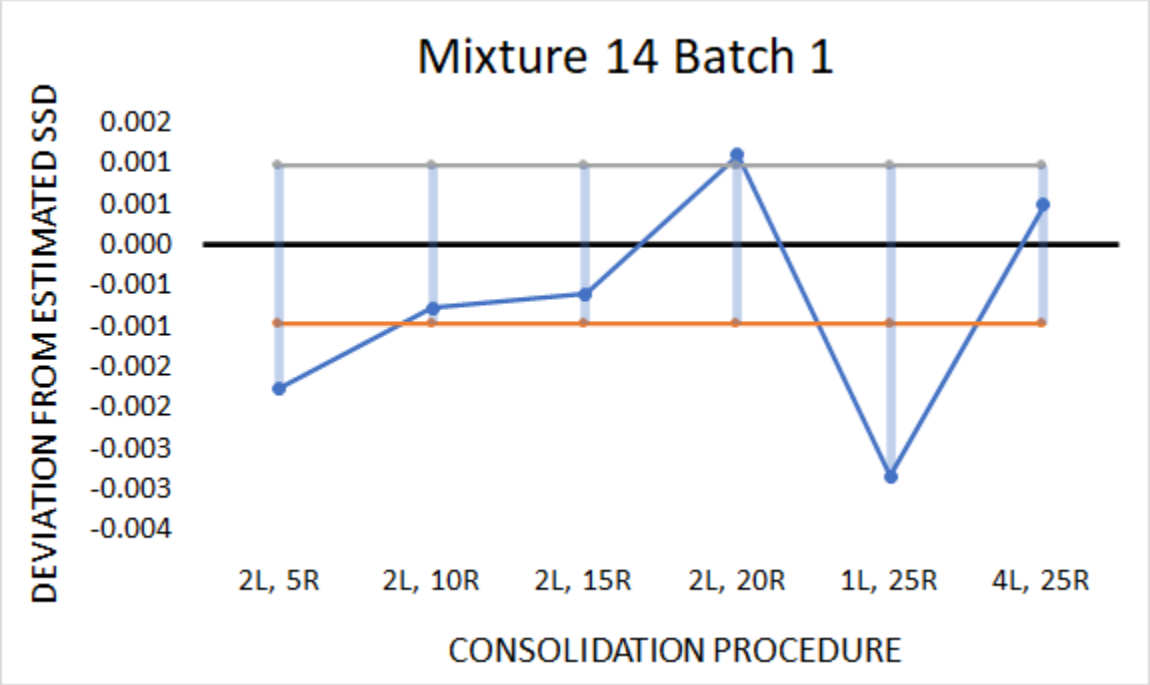

Figure A.55. Mixture 14 Batch 1 Deltas of SSD Relative Density

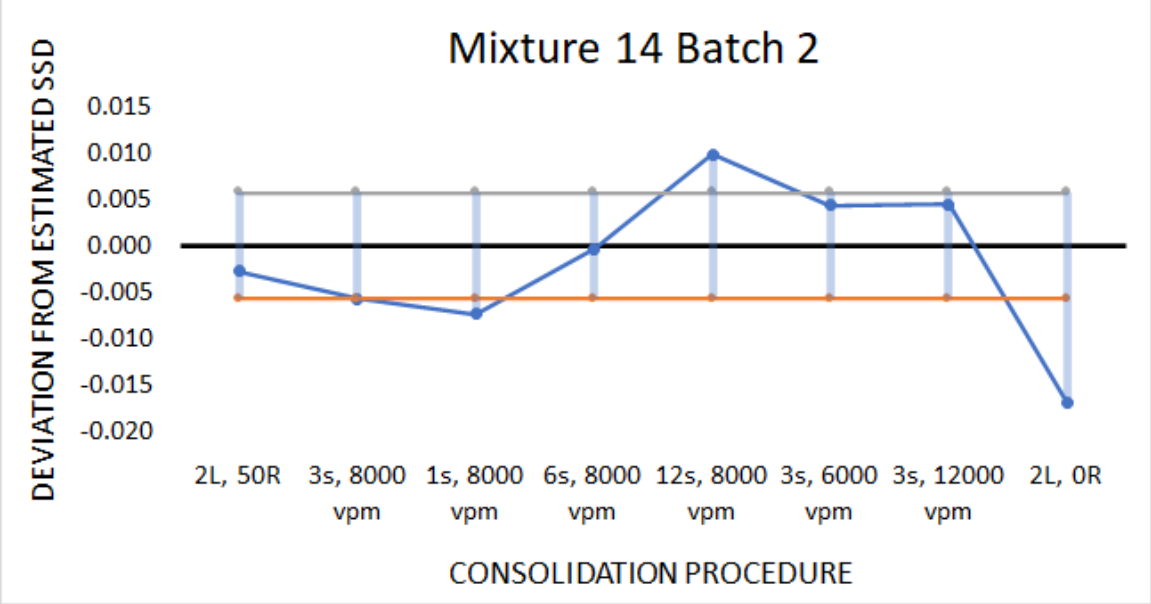

Figure A.56. Mixture 14 Batch 2 Deltas of SSD Relative Density

STRENGTH

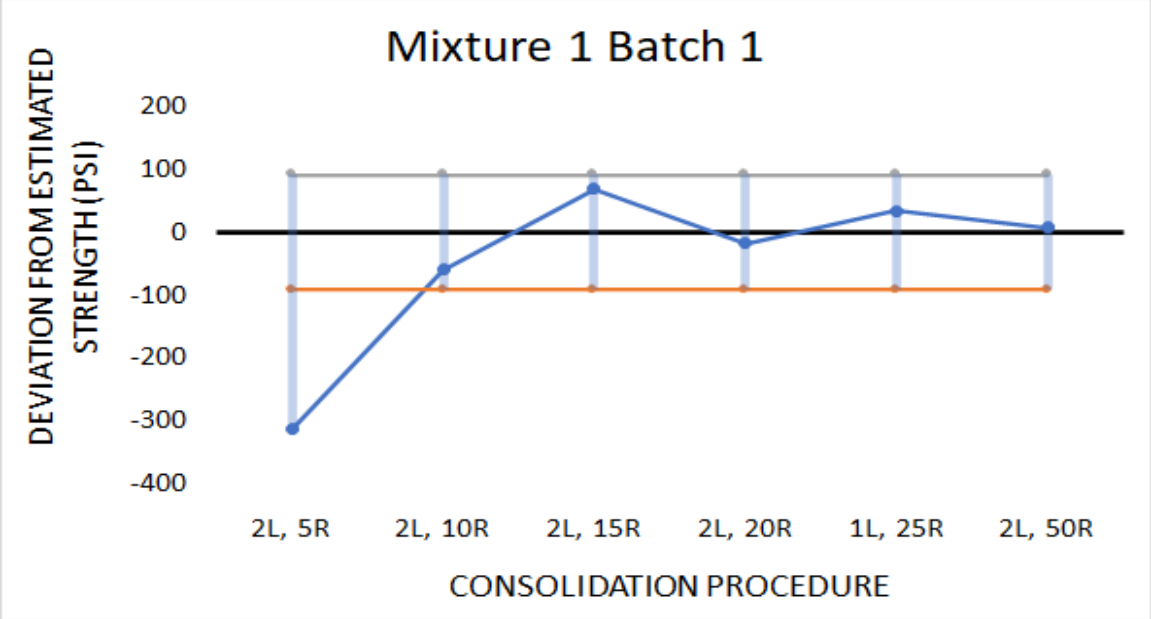

Figure A.57. Mixture 1 Batch 1 Deltas of Compressive Strength

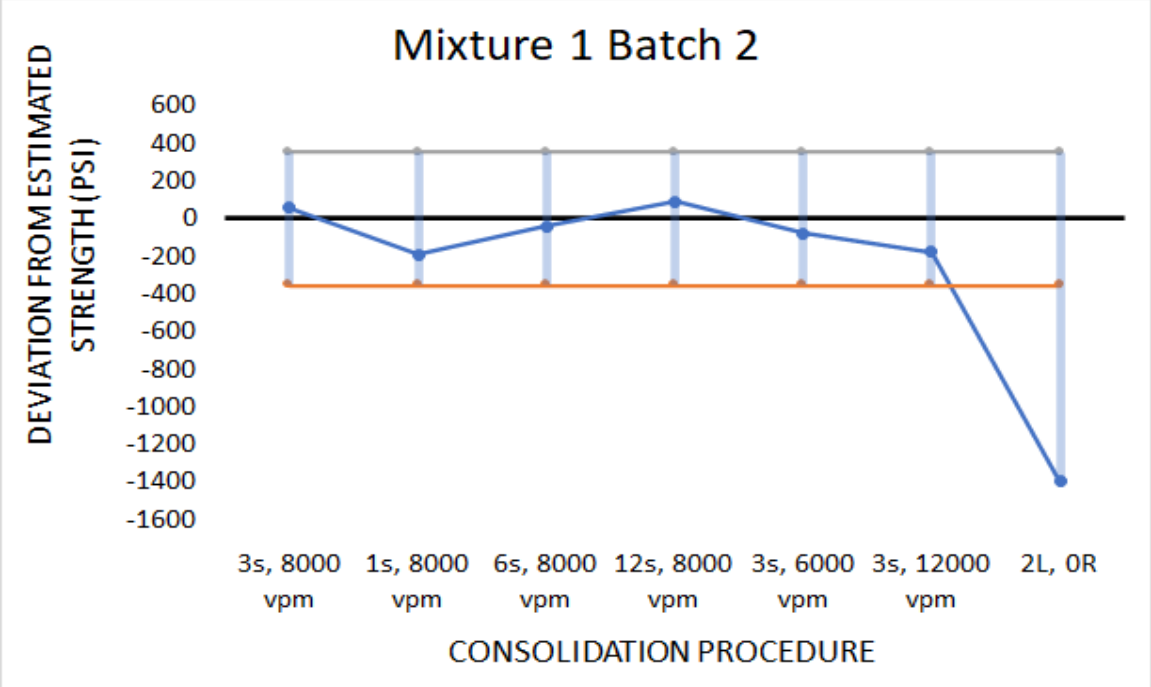

Figure A.58. Mixture 1 Batch 2 Deltas of Compressive Strength

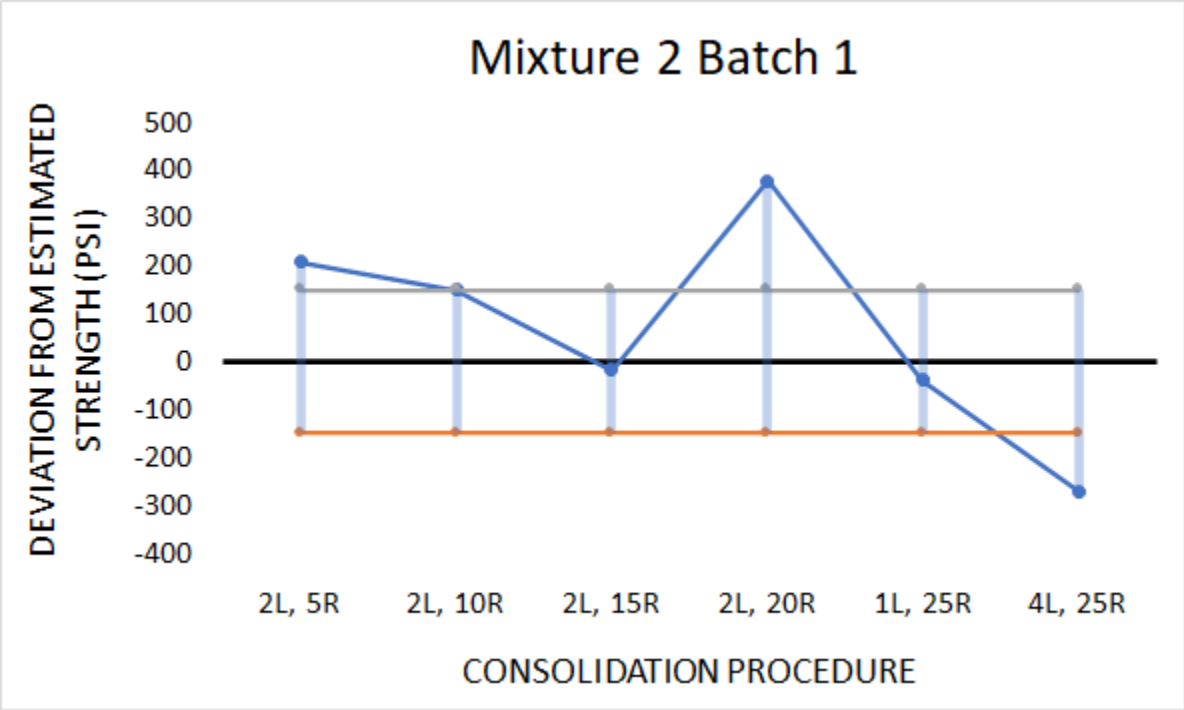

Figure A.59. Mixture 2 Batch 1 Deltas of Compressive Strength

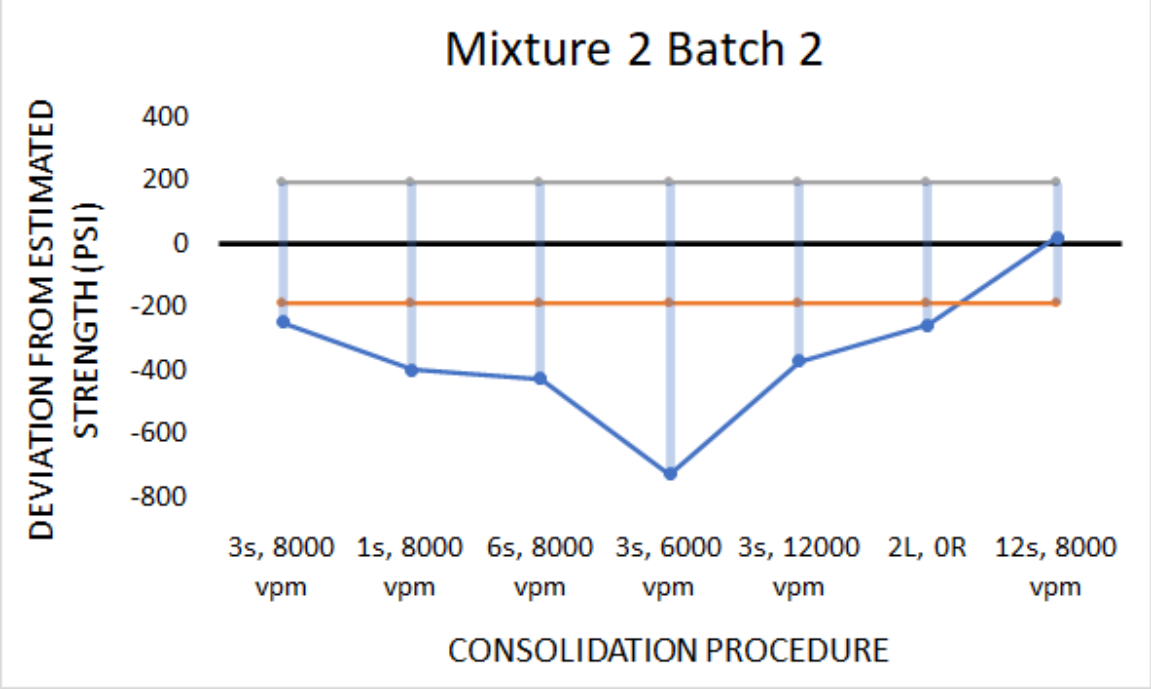

Figure A.60. Mixture 2 Batch 2 Deltas of Compressive Strength

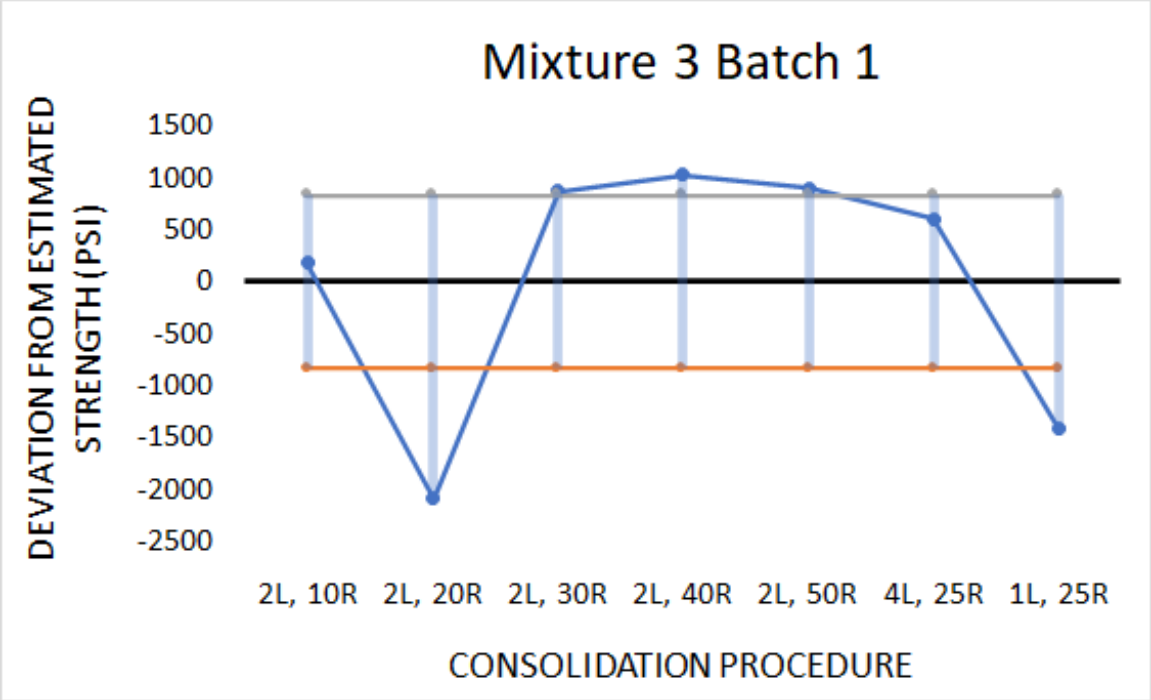

Figure A.61. Mixture 3 Batch 1 Deltas of Compressive Strength

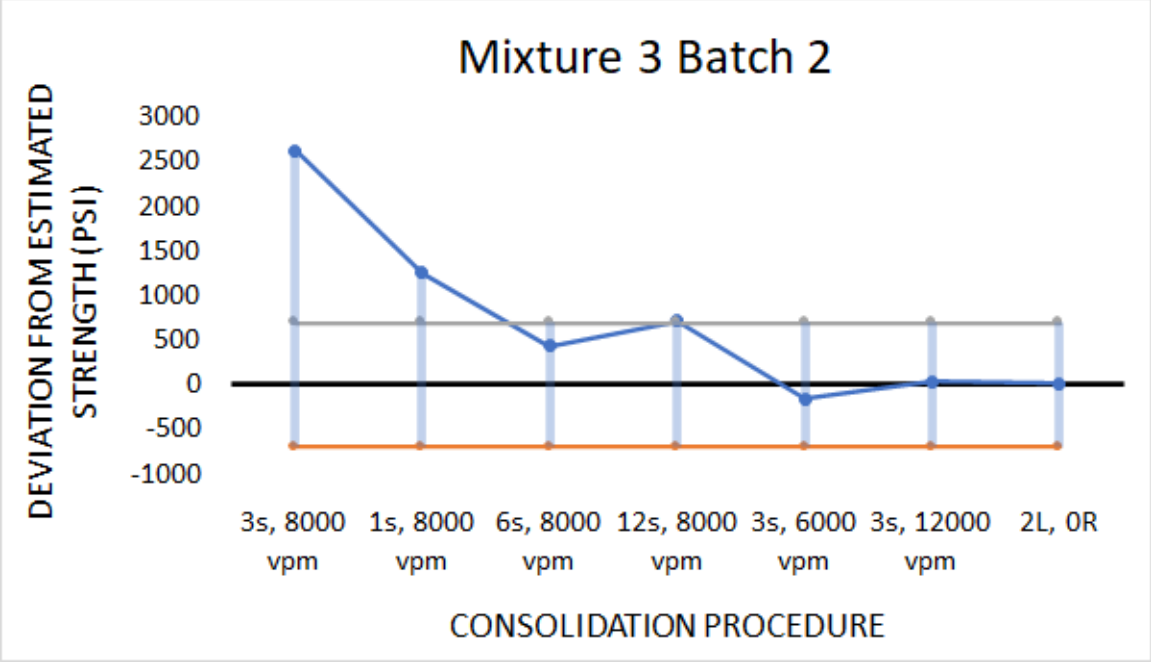

Figure A.62. Mixture 3 Batch 2 Deltas of Compressive Strength

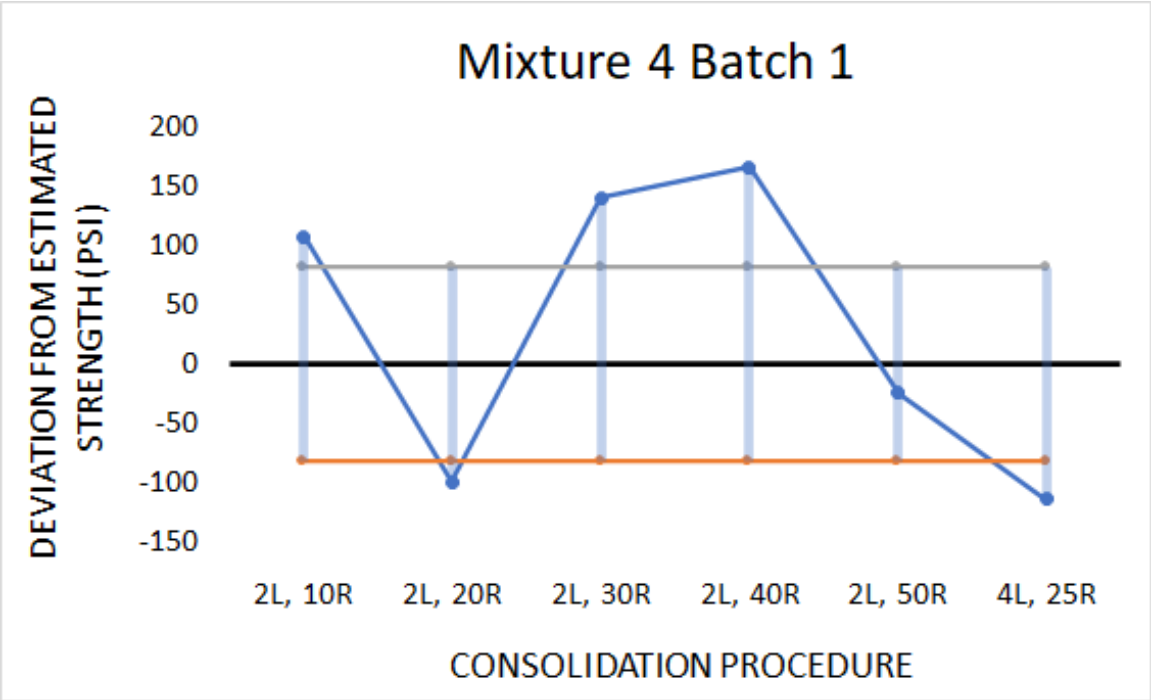

Figure A.63. Mixture 4 Batch 1 Deltas of Compressive Strength

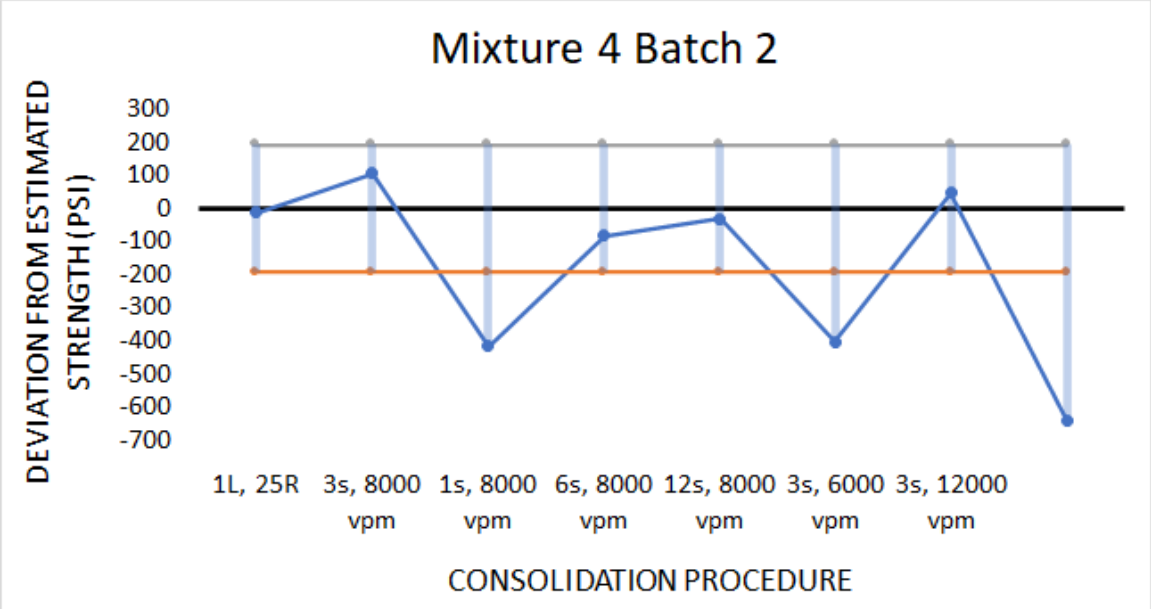

Figure A.64. Mixture 4 Batch 2 Deltas of Compressive Strength

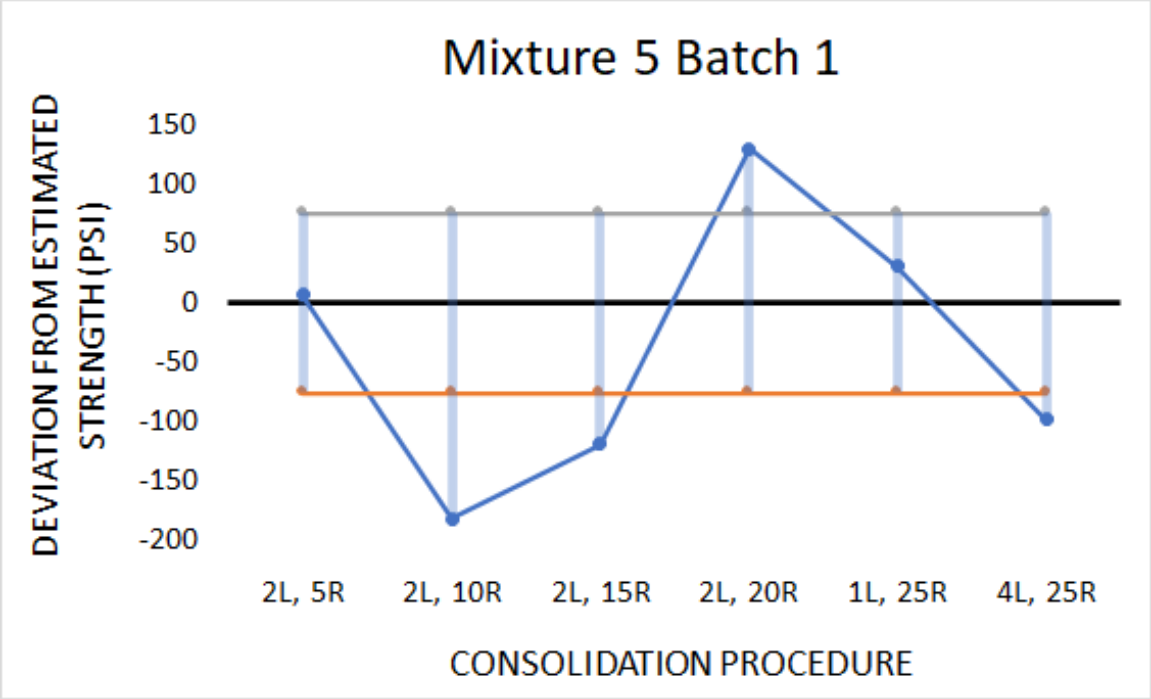

Figure A.65. Mixture 5 Batch 1 Deltas of Compressive Strength

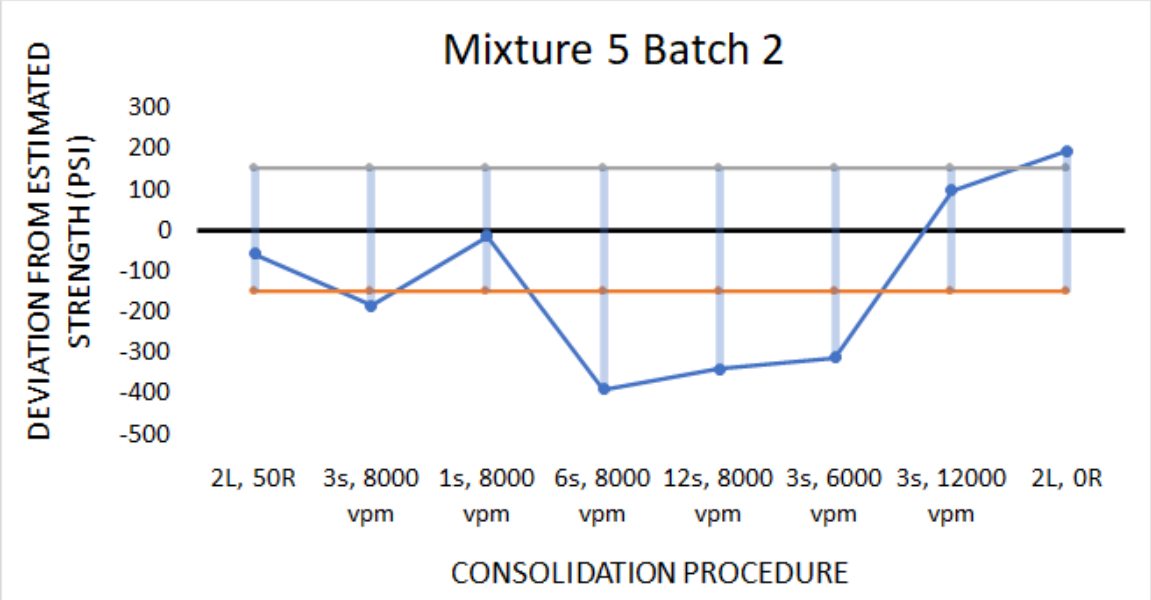

Figure A.66. Mixture 5 Batch 2 Deltas of Compressive Strength

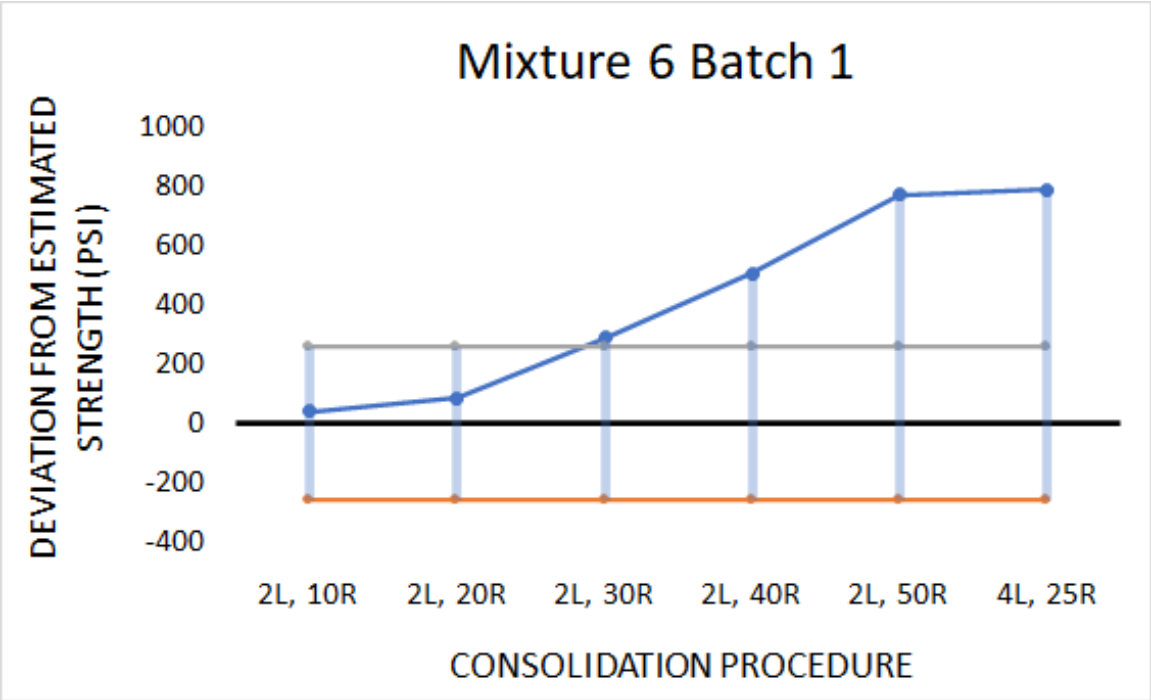

Figure A.67. Mixture 6 Batch 1 Deltas of Compressive Strength

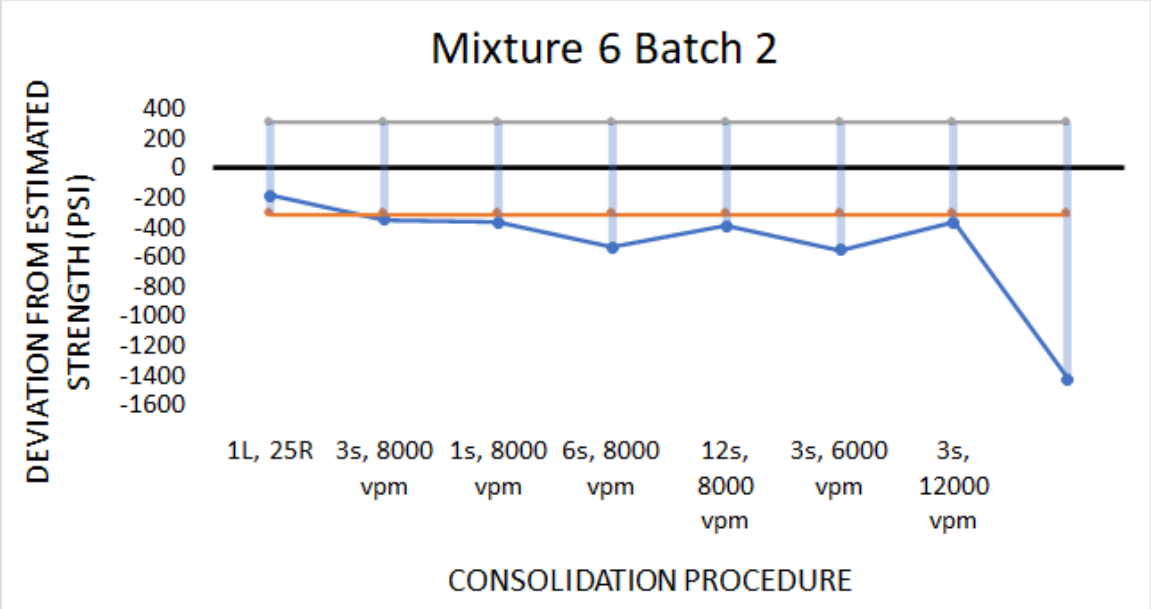

Figure A.68. Mixture 6 Batch 2 Deltas of Compressive Strength

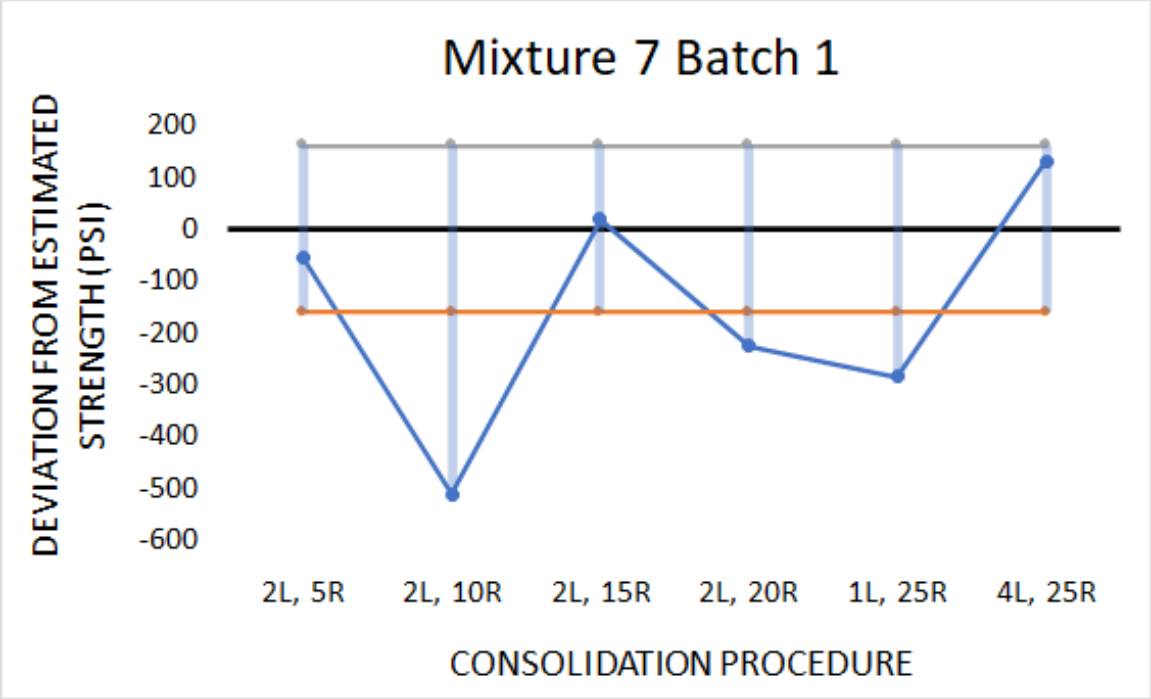

Figure A.69. Mixture 7 Batch 1 Deltas of Compressive Strength

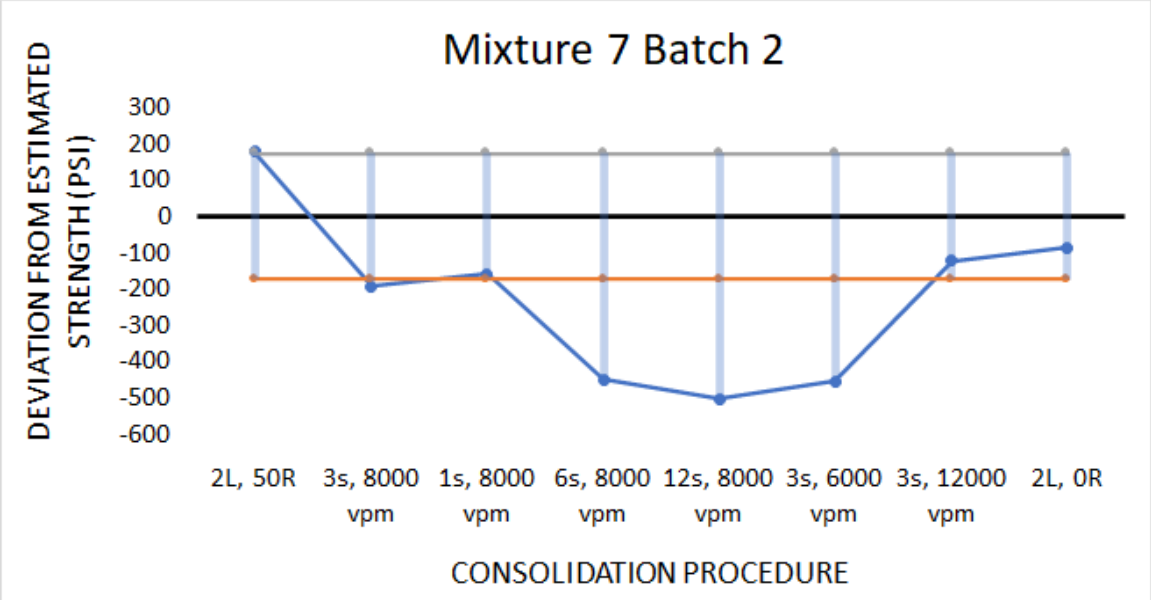

Figure A.70. Mixture 7 Batch 2 Deltas of Compressive Strength

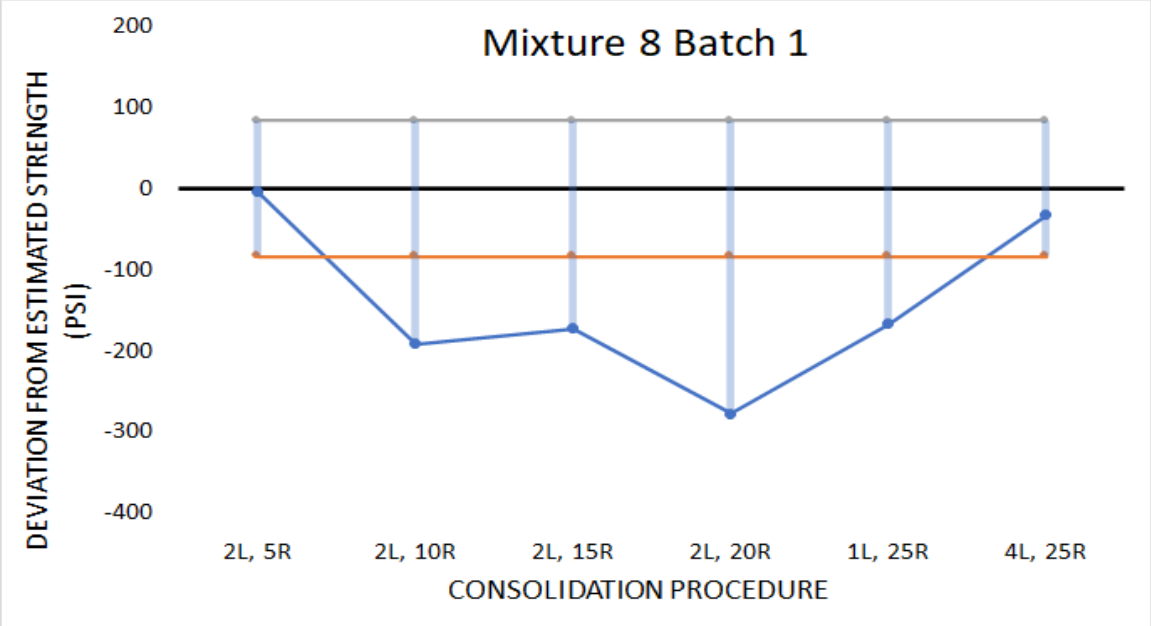

Figure A.71. Mixture 8 Batch 1 Deltas of Compressive Strength

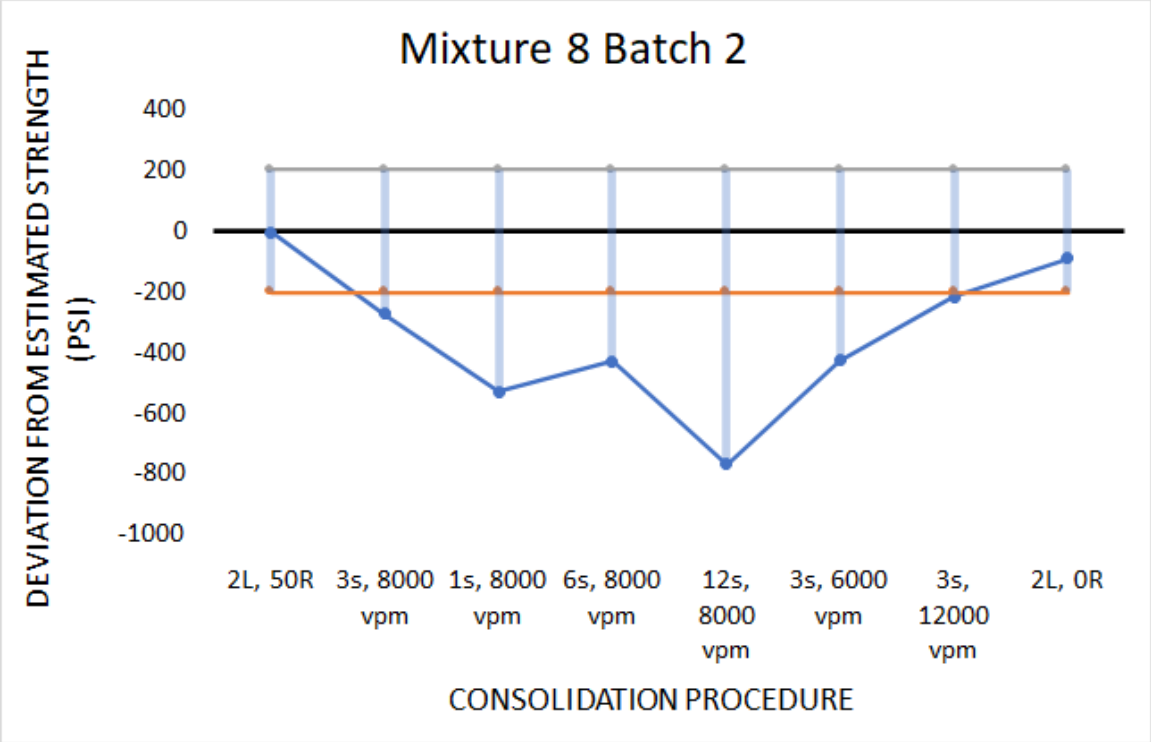

Figure A.72. Mixture 8 Batch 2 Deltas of Compressive Strength

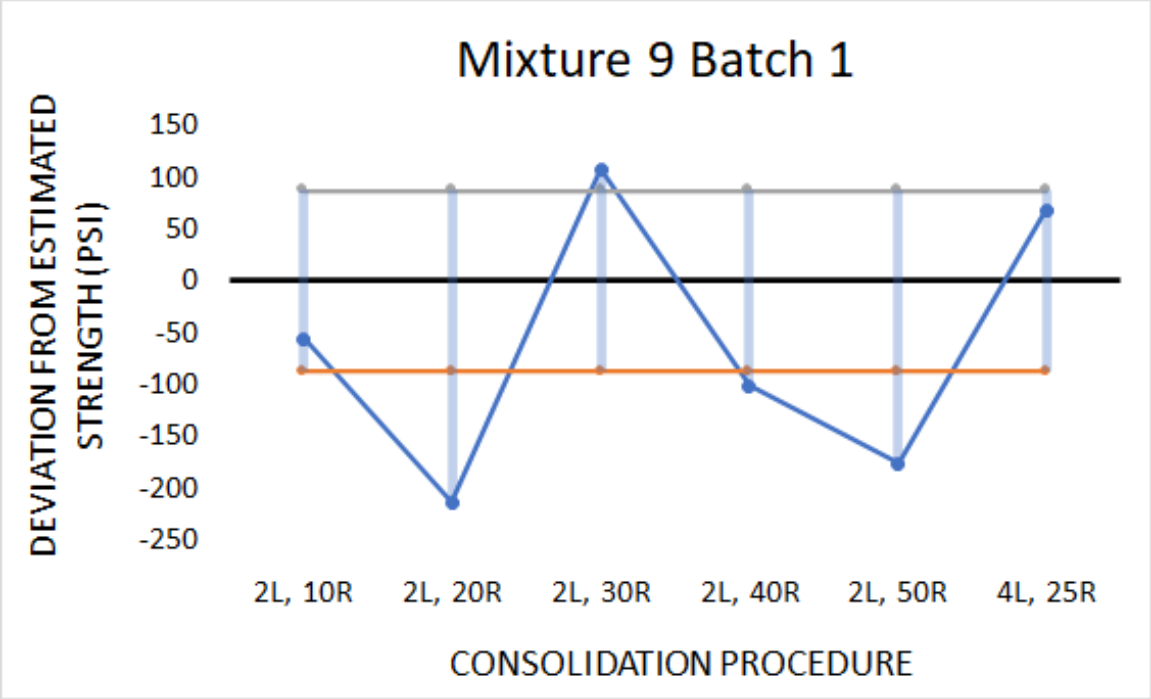

Figure A.73. Mixture 9 Batch 1 Deltas of Compressive Strength

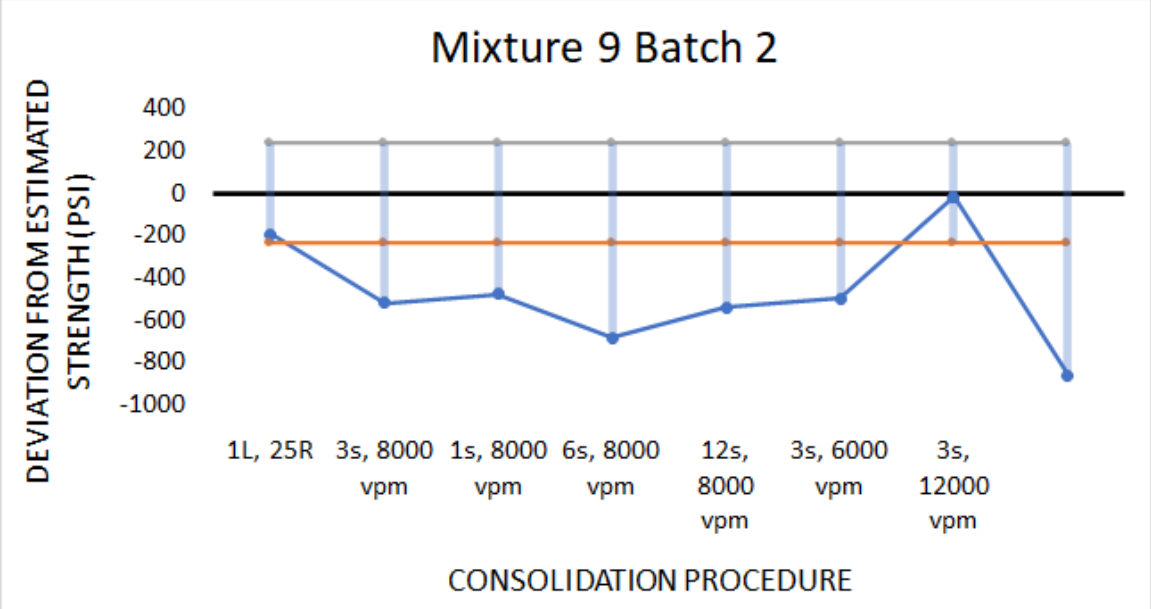

Figure A.74. Mixture 9 Batch 2 Deltas of Compressive Strength

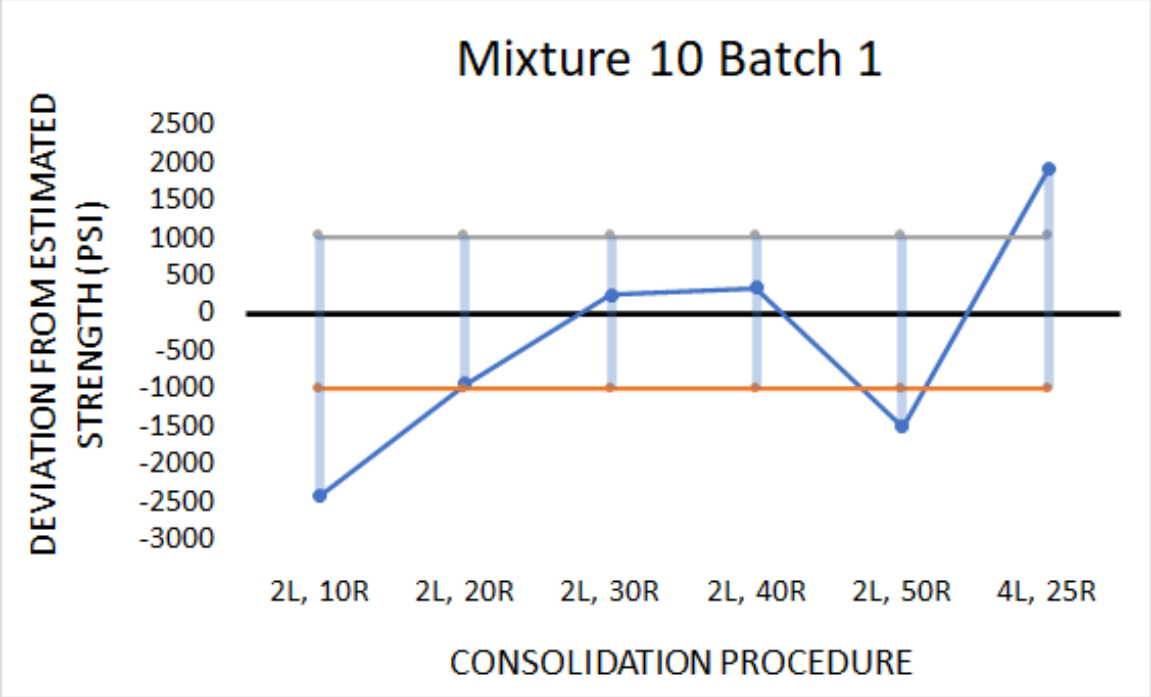

Figure A.75. Mixture 10 Batch 1 Deltas of Compressive Strength

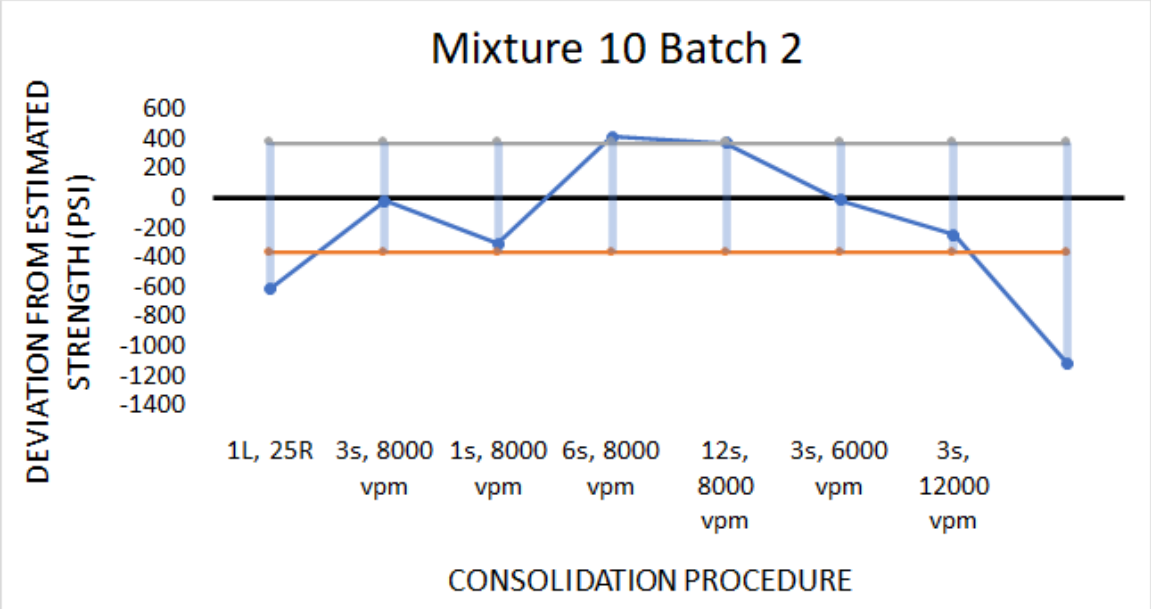

Figure A.76. Mixture 10 Batch 2 Deltas of Compressive Strength

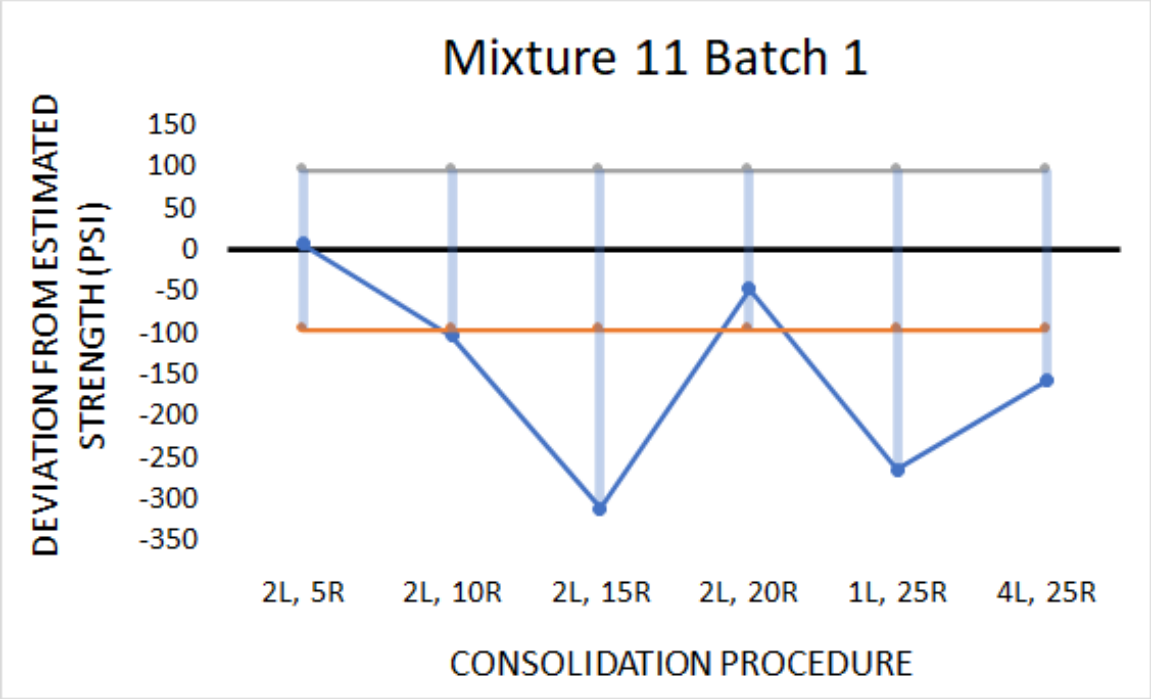

Figure A.77. Mixture 11 Batch 1 Deltas of Compressive Strength

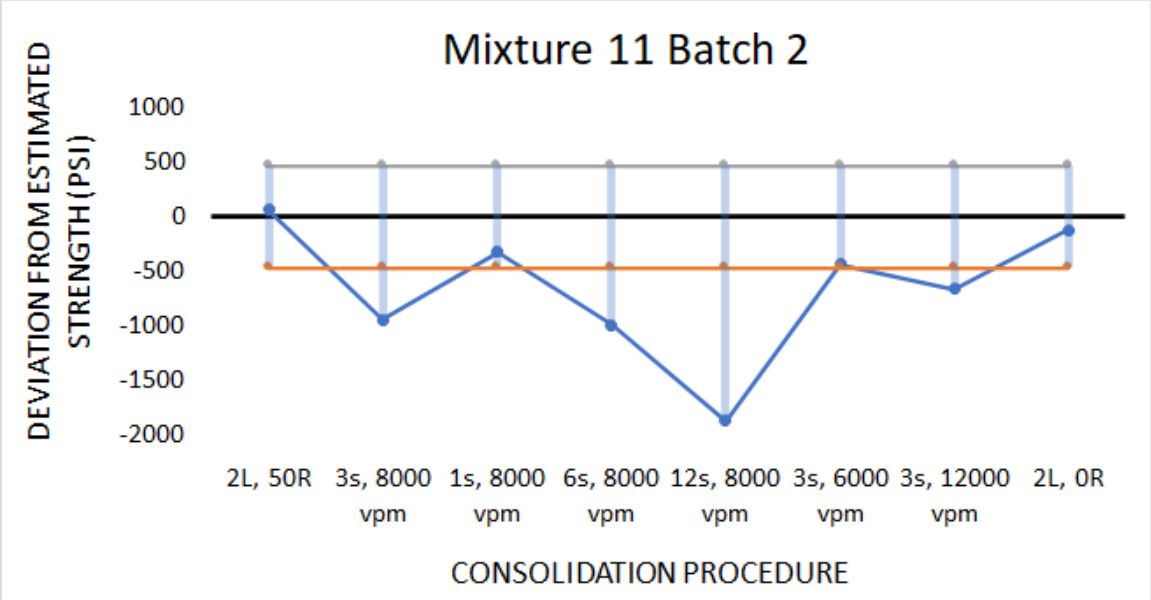

Figure A.78. Mixture 11 Batch 2 Deltas of Compressive Strength

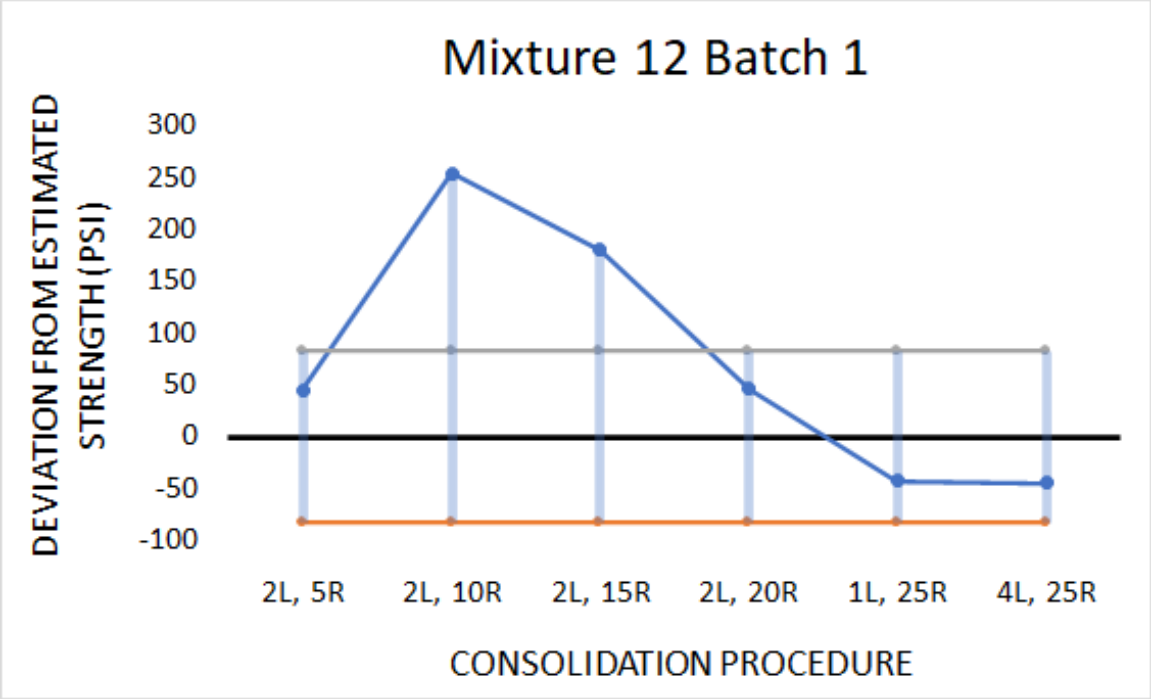

Figure A.79. Mixture 12 Batch 1 Deltas of Compressive Strength

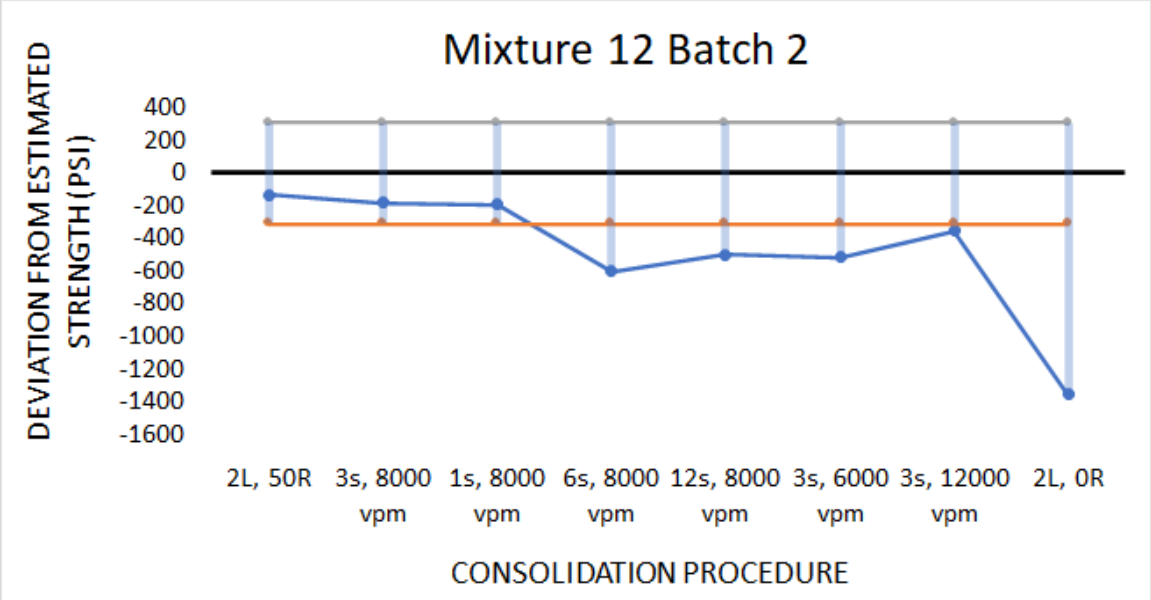

Figure A.80. Mixture 12 Batch 2 Deltas of Compressive Strength

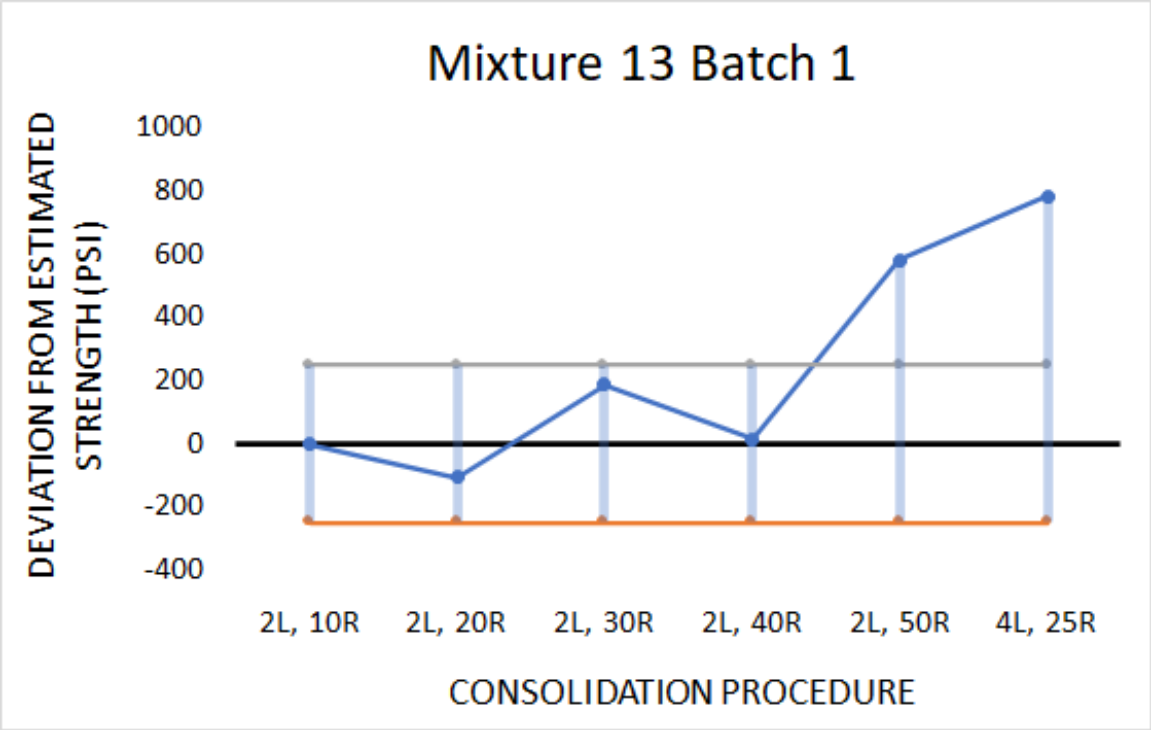

Figure A.81. Mixture 13 Batch 1 Deltas of Compressive Strength

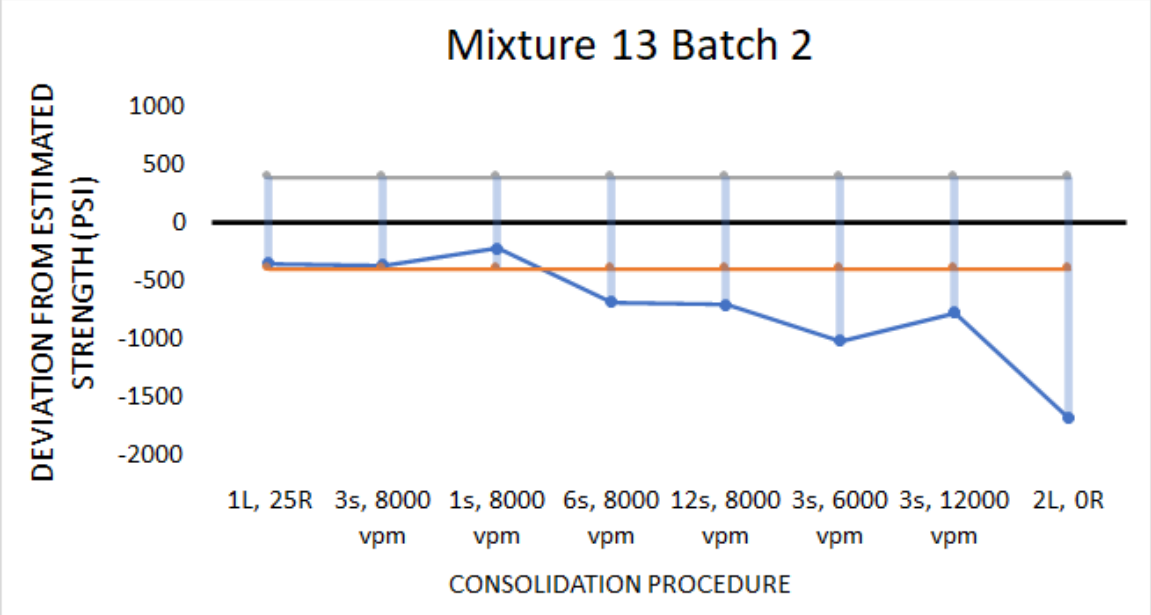

Figure A.82. Mixture 13 Batch 2 Deltas of Compressive Strength

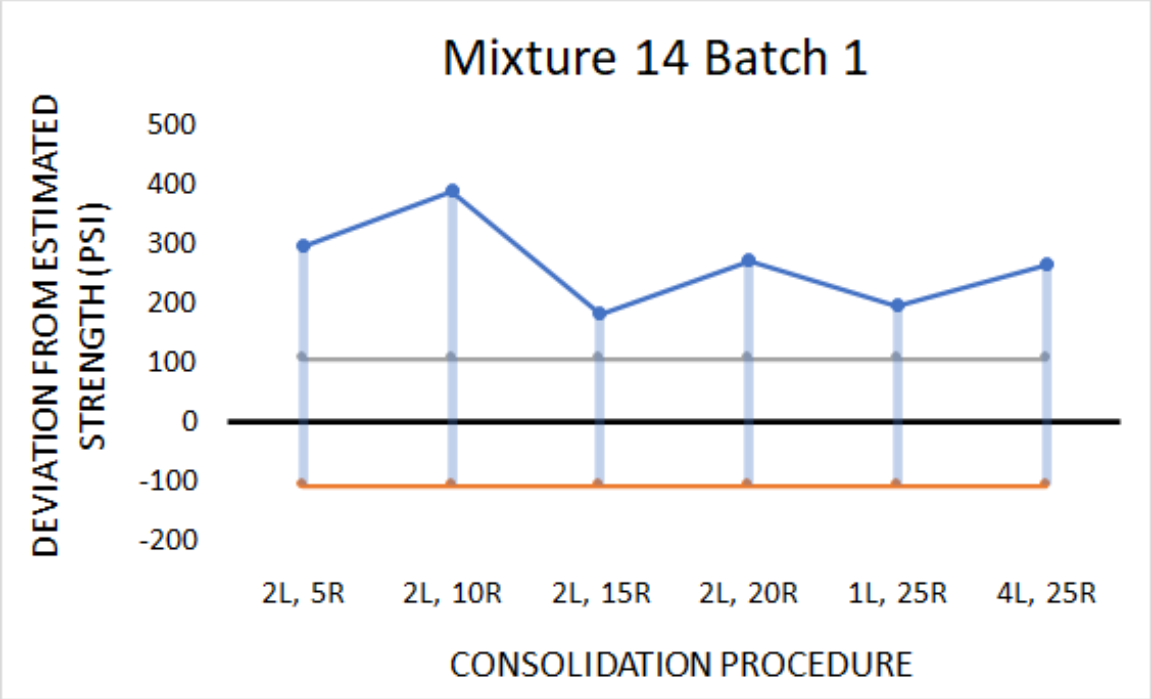

Figure A.83. Mixture 14 Batch 1 Deltas of Compressive Strength

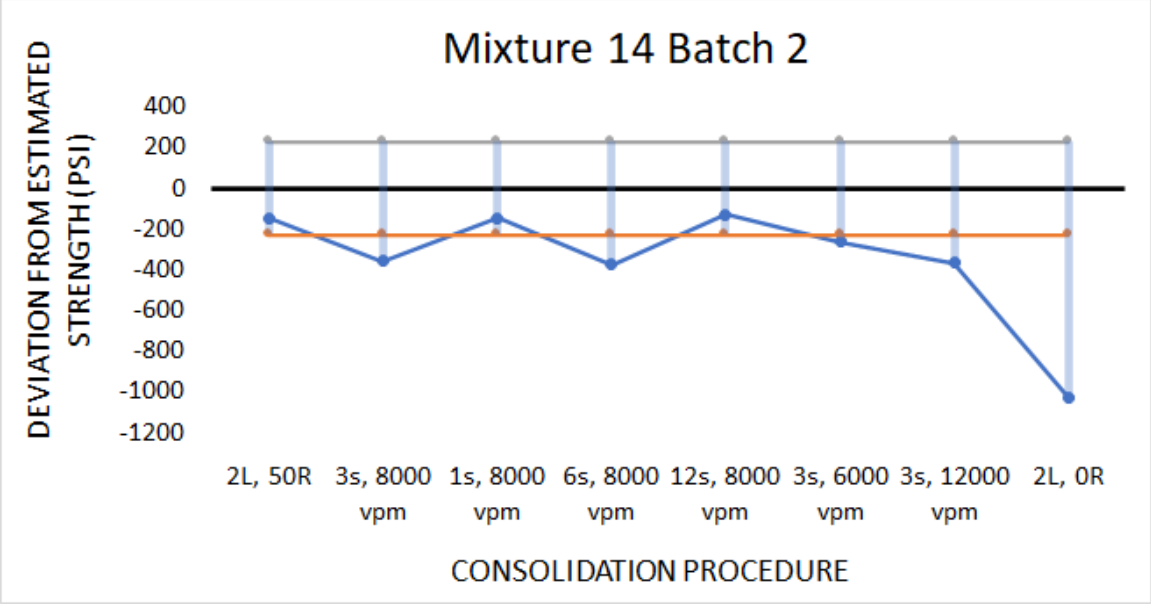

Figure A.84. Mixture 14 Batch 2 Deltas of Compressive Strength

APPENDIX B.

MATRICES OF DATA ON PENETRATION DEPTH, SURFACE SATURATED DRY DENSITY, AND COMPRESSIVE STRENGTH

OVERVIEW

This section contains the data on segregation, in the form of average and deltas of penetration depth. It also contains the average values and deltas of SSD densities and compressive strengths.

Table B.1. Average penetration depth of rodded sets, highlighted sets displayed visual indications of segregation.

	Paste Vol	w/c	2L, 25R	2L, 5R	2L, 10R	2L, 15R	2L, 20R	2L 30R	2L 40R	1L, 25R	2L, 50R	4L 25R	2L, 25R	2L, 25R	2L, 25R	2L, 0R
Mix 10	25%	0.45	0.0		0.0		0.0	0.0	0.0	0.0	0.0	0.0	0.0	0.0	0.0	0.0
Mix 3	25%	0.45	0.0		0.0		0.0	0.3	0.7	0.0	0.7	0.3	0.0	0.3	0.0	0.0
Mix 4	30%	0.45	0.0		0.0		0.0	0.0	0.0	0.0	0.0	0.0	0.0	0.0	0.0	0.0
Mix 9	30%	0.45	1.2		0.3		0.8	1.5	1.0	1.2	1.0	0.7	0.2	1.5	0.5	0.3
Mix 6	32.50%	0.4	0.0		0.0		0.0	0.0	0.0	0.0	0.0	0.0	0.0	0.0	0.0	0.0
Mix 13	32.50%	0.4	0.3		0.3		0.0	0.2	0.0	0.0	0.2	0.0	0.0	0.2	0.0	0.0
Mix 14	32.50%	0.4	0.5	0.3	0.2	0.3	0.3			0.2	0.5	0.7	0.2	0.2	0.0	0.0
Mix 5	32.50%	0.45	0.3	0.5	0.3	0.8	0.3			0.0	0.2	0.2	0.0	0.5	0.0	0.0
Mix 1	39%	0.5	1.0	0.0	0.3	0.0	0.7			0.7	1.0		0.7		0.0	0.0
Mix 8	32.50%	0.5	1.2	0.3	0.8	1.5	1.0			1.0	1.5	0.7	0.2	1.2	0.5	0.3
Mix 2	35%	0.45	1.3	0.3	0.3	0.7	0.7			0.3		1.3	1.3		0.0	0.3
Mix 12	32.50%	0.4	1.0	0.5	0.4	0.4	0.5			0.5	0.3	0.2	0.2	1.0	0.0	0.0
Mix 7	32.50%	0.45	1.0	0.8	0.8	1.0	0.7			1.2	0.7	0.7	0.5	1.2	0.3	0.2
Mix 11	35%	0.45	2.7	1.8	1.3	1.0	0.8			0.4	4.3	0.3	0.3	5.7	2.7	1.0

Table B.2. Average penetration depth of vibrated sets, highlighted sets displayed visual indications of segregation.

	Paste Vol	w/c	3s, 8000 vpm	1s, 8000 vpm	6s, 8000 vpm	12s, 8000 vpm	3s, 6000 vpm	3s, 12000 vpm
Mix 10	25%	0.45	0.0	0.0	0.0	0.0	0.0	0.0
Mix 3	25%	0.45	0.0	0.0	0.0	0.7	0.0	0.0
Mix 4	30%	0.45	0.0	0.0	0.0	0.0	0.0	0.0
Mix 9	30%	0.45	0.8	0.8	1.0	1.5	0.3	0.2
Mix 6	32.50%	0.4	0.0	0.0	0.0	0.0	0.0	0.0
Mix 13	32.50%	0.4	0.0	0.0	0.0	0.0	0.2	0.0
Mix 14	32.50%	0.4	0.2	0.2	0.3	0.5	0.0	0.2
Mix 5	32.50%	0.45	0.2	0.2	0.2	0.5	0.3	0.0
Mix 1	39%	0.5	0.0	0.3	0.3	0.7	0.0	0.0
Mix 8	32.50%	0.5	0.8	0.8	1.0	1.5	0.3	0.2
Mix 2	35%	0.45	0.3	0.0	0.7	0.7	0.3	0.3
Mix 12	32.50%	0.4	0.3	0.0	0.2	0.0	0.0	0.0
Mix 7	32.50%	0.45	0.2	0.8	0.5	1.0	0.3	0.7
Mix 11	35%	0.45	3.7	3.7	4.7	6.3	1.8	1.7

Table B.3. Penetration depth deltas of rodded sets, highlighted sets exceed the upper limit of the 90% confidence interval.

	Paste Vol	w/c	2L, 25R	2L, 5R	2L, 10R	2L, 15R	2L, 20R	2L 30R	2L 40R	1L, 25R	2L, 50R	4L 25R	2L, 25R	2L, 25R	2L, 25R	2L, 0R
Mix 10	25%	0.45	0.0		0.0		0	0.0	0.0	0.0	0.0	0.0	0.0	0.0	0.0	0.0
Mix 3	25%	0.45	0.0		0.0		0	0.3	0.7	0.0	0.7	0.3	0.0	0.0	0.0	-0.1
Mix 4	30%	0.45	0.0		0.0		0	0.0	0.0	0.0	0.0	0.0	0.0	0.0	0.0	0.0
Mix 9	30%	0.45	0.0		-0.8		-0.13	0.7	0.3	-0.3	0.4	0.3	0.0	0.0	0.0	-0.1
Mix 6	32.50%	0.4	0.0		0.0		0	0.0	0.0	0.0	0.0	0.0	0.0	0.0	0.0	0.0
Mix 13	32.50%	0.4	0.0		0.0		-0.22	0.0	-0.1	0.2	0.1	-0.1	0.0	0.0	0.0	0.0
Mix 14	32.50%	0.4	0.0	-0.2	-0.3	-0.1	-0.01			-0.1	0.3	0.4	0.0	0.0	0.0	0.0
Mix 5	32.50%	0.45	0.0	0.2	0.1	0.6	0.16			-0.1	-0.3	0.1	0.0	0.0	0.0	0.0
Mix 1	39%	0.5	0.0	-1.0	-0.6	-0.9	-0.15			-0.1	0.3		0.0	0.0	0.0	0.1
Mix 8	32.50%	0.5	0.0	-0.8	-0.1	0.7	0.35			0.5	0.2	0.3	0.0	0.0	0.0	-0.1
Mix 2	35%	0.45	0.0	-0.8	-1.0	-0.7	-0.67			-1.0		0.0	0.0	0.0	0.0	0.5
Mix 12	32.50%	0.4	0.0	-0.4	-0.4	-0.3	-0.12			0.0	-0.8	-0.2	0.0	0.0	0.0	0.1
Mix 7	32.50%	0.45	0.0	-0.2	-0.1	0.2	-0.1			0.5	0.2	0.0	0.0	0.0	0.0	-0.1
Mix 11	35%	0.45	0.0	-0.6	-0.7	-0.7	-0.57			-0.7	1.7	-0.5	0.0	0.0	0.0	-1.5

Table B.4. Penetration depth deltas of vibrated sets, highlighted sets exceed the upper limit of the 90% confidence interval.

	Paste Vol	w/c	3s, 8000 vpm	1s, 8000 vpm	6s, 8000 vpm	12s, 8000 vpm	3s, 6000 vpm	3s, 12000 vpm
Mix 10	25%	0.45	0.0	0.0	0.0	0.0	0.0	0.0
Mix 3	25%	0.45	0.7	0.6	0.5	0.7	0.3	0.2
Mix 4	30%	0.45	0.0	0.0	0.0	0.0	0.0	0.0
Mix 9	30%	0.45	-0.5	-0.4	-0.1	0.5	-0.5	-0.6
Mix 6	32.50%	0.4	0.0	0.0	0.0	0.0	0.0	0.0
Mix 13	32.50%	0.4	0.0	0.0	0.0	0.0	0.2	0.0
Mix 14	32.50%	0.4	0.0	0.0	0.2	0.4	-0.1	0.1
Mix 5	32.50%	0.45	-0.2	-0.2	-0.1	0.3	0.2	-0.1
Mix 1	39%	0.5	-0.5	-0.1	0.0	0.4	-0.2	-0.1
Mix 8	32.50%	0.5	-0.2	-0.1	0.1	0.7	-0.4	-0.5
Mix 2	35%	0.45	-0.4	-0.6	0.2	1.0	0.0	0.1
Mix 12	32.50%	0.4	-0.5	-0.8	-0.5	-0.4	-0.3	-0.2
Mix 7	32.50%	0.45	-0.9	-0.1	-0.3	0.3	-0.3	0.2
Mix 11	35%	0.45	-1.7	-1.3	0.1	2.2	-1.9	-1.7

Table B.5. Standard deviation of SSD relative density within each set of rodded cylinders, highlighted cells exceed the limit set in ASTM C127.

	Paste Vol	w/c	2L, 0R	2L, 5R	2L, 10R	1L, 25R	2L, 15R	2L, 20R	2L, 25R	2L, 25R	2L, 25R	2L, 25R	2L 30R	2L 40R	2L, 50R	4L 25R
Mix 10	25%	0.45	0.003		0.001	0.004		0.026	0.007	0.050	0.004	0.005	0.014	0.012	0.202	0.004
Mix 3	25%	0.45	0.008		0.003	0.011		0.005	0.003	0.006	0.004	0.003	0.002	0.005	0.001	0.003
Mix 4	30%	0.45	0.007		0.002	0.005		0.005	0.001	0.005	0.003	0.003	0.008	0.002	0.004	0.005
Mix 9	30%	0.45	0.007		0.001	0.006		0.006	0.008	1.555	0.006	0.004	0.006	0.001	0.004	0.005
Mix 6	32.50%	0.4	0.005		0.001	0.002		0.005	0.003	0.006	0.001	0.002	0.005	0.001	0.005	0.006
Mix 13	32.50%	0.4	0.006		0.003	0.004		0.003	0.002	0.004	0.005	0.007	0.002	0.003	0.003	0.004
Mix 14	32.50%	0.4	0.001	0.002	0.004	0.006	0.025	0.008	0.001	0.002	0.004	0.006			0.003	0.004
Mix 5	32.50%	0.45	0.009	0.003	0.007	0.005	0.001	0.010	0.009	0.005	0.009	0.013			0.007	0.011
Mix 1	39%	0.5	0.043	0.004	0.001	0.008	0.003	0.006	0.006	0.005	0.006				0.004	
Mix 8	32.50%	0.5	0.005	0.006	0.005	0.005	0.006	0.005	0.001	0.003	0.006	0.004			0.003	0.012
Mix 2	35%	0.45	0.004	0.000	0.008	0.014	0.007	0.005	0.001	0.014	0.005					0.009
Mix 12	32.50%	0.4	0.008	0.004	0.002	0.004	0.001	0.002	0.008	0.005	0.007	0.006			0.009	0.006
Mix 7	32.50%	0.45	0.005	0.004	0.002	0.004	0.005	0.005	0.007	0.003	0.001	0.003			0.005	0.003
Mix 11	35%	0.45	0.006	0.002	0.003	0.007	0.006	0.008	0.010	0.003	0.013	0.003			0.019	0.007
Total % below limit			36	0	14	21	7	29	36	21	21	8	14	7	31	23
Stiff mix % below limit			33		0	17		33	33	33	0	0	33	17	17	0
Fluid mix % below limit			38	0	25	25	13	25	38	13	38	17			43	43

Table B.6. Standard deviation of SSD relative density within each set of vibrated cylinders, highlighted cells exceed the limit set in ASTM C127.

	Paste Vol	w/c	1s, 8000 vpm	3s, 6000 vpm	3s, 8000 vpm	6s, 8000 vpm	3s, 12000 vpm	12s, 8000 vpm
Mix 10	25%	0.45	0.004	0.005	0.002	0.003	0.003	0.015
Mix 3	25%	0.45	0.003	0.007	0.006	0.007	0.011	0.006
Mix 4	30%	0.45	0.004	0.007	0.004	0.005	0.008	0.005
Mix 9	30%	0.45	0.003	0.007	0.006	0.008	0.004	0.003
Mix 6	32.50%	0.4	0.001	0.005	0.003	0.005	0.004	0.006
Mix 13	32.50%	0.4	0.003	0.004	0.004	0.004	0.003	0.001
Mix 14	32.50%	0.4	0.004	0.025	0.005	0.006	0.004	0.005
Mix 5	32.50%	0.45	0.005	0.004	0.004	0.005	0.002	0.005
Mix 1	39%	0.5	0.003	0.007	0.006	0.012	0.003	0.001
Mix 8	32.50%	0.5	0.006	0.005	0.005	0.002	0.004	0.004
Mix 2	35%	0.45	0.005	0.006	0.007	0.004	0.009	0.002
Mix 12	32.50%	0.4	0.003	0.001	0.009	0.003	0.002	0.004
Mix 7	32.50%	0.45	0.007	0.008	0.001	0.007	0.002	0.003
Mix 11	35%	0.45	0.006	0.004	0.013	0.011	0.006	0.009
Total % below limit			7	29	21	29	21	14
Stiff mix % below limit			0	33	0	17	33	17
Fluid mix % below limit			13	25	38	38	13	13

Table B.7. SSD relative density values of rodded sets, highlighted sets exceed the lower limit of the 90% confidence interval.

	Paste Vol	w/c	2L, 25R	2L, 5R	2L, 10R	2L, 15R	2L, 20R	2L 30R	2L 40R	1L, 25R	2L, 50R	4L, 25R	2L, 25R	2L, 25R	2L, 25R	2L, 0R
Mix 10	25%	0.45	2.48		2.43		2.45	2.47	2.48	2.48	2.59	2.49	2.42	2.49	2.51	2.46
Mix 3	25%	0.45	2.47		2.46		2.47	2.47	2.48	2.48	2.49	2.48	2.49	2.46	2.47	2.44
Mix 4	30%	0.45	2.44		2.45		2.45	2.45	2.45	2.45	2.45	2.44	2.45	2.44	2.46	2.42
Mix 9	30%	0.45	2.47		2.47		2.47	2.48	2.48	2.47	2.48	2.49	1.59	2.47	2.49	2.47
Mix 6	32.50%	0.4	2.46		2.45		2.46	2.47	2.47	2.43	2.47	2.46	2.46	2.44	2.45	2.43
Mix 13	32.50%	0.4	2.46		2.46		2.47	2.47	2.47	2.45	2.47	2.47	2.47	2.45	2.46	2.47
Mix 14	32.50%	0.4	2.45	2.47	2.47	2.47	2.47			2.46	2.45	2.47	2.47	2.46	2.47	2.45
Mix 5	32.50%	0.45	2.45	2.44	2.44	2.45	2.45			2.45	2.43	2.45	2.46	2.44	2.45	2.43
Mix 1	39%	0.5	2.39	2.39	2.41	2.41	2.40			2.38	2.39		2.38		2.40	2.41
Mix 8	32.50%	0.5	2.45	2.45	2.45	2.45	2.46			2.46	2.45	2.47	2.47	2.45	2.46	2.45
Mix 2	35%	0.45	2.43	2.43	2.44	2.44	2.44			2.41		2.42	2.43		2.43	2.42
Mix 12	32.50%	0.4	2.47	2.48	2.49	2.48	2.49			2.49	2.48	2.49	2.49	2.48	2.48	2.47
Mix 7	32.50%	0.45	2.45	2.44	2.44	2.45	2.45			2.45	2.46	2.45	2.46	2.44	2.46	2.45
Mix 11	35%	0.45	2.45	2.45	2.46	2.47	2.48			2.48	2.45	2.49	2.48	2.45	2.47	2.47
Total falling below limit			0	38	50	25	14	0	0	29	8	15	0	0	0	79
Stiff mix falling below limit			0	0	50	0	17	0	0	17	0	17	0	0	0	83
Fluid mix falling below limit			0	38	50	25	13	0	0	38	14	14	0	0	0	75

Table B.8. SSD relative density values of vibrated sets, highlighted sets exceed the lower limit of the 90% confidence interval.

	Paste Vol	w/c	3s, 8000 vpm	1s, 8000 vpm	6s, 8000 vpm	12s, 8000 vpm	3s, 6000 vpm	3s, 12000 vpm
Mix 10	25%	0.45	2.49	2.49	2.51	2.53	2.51	2.52
Mix 3	25%	0.45	2.46	2.45	2.46	2.47	2.46	2.47
Mix 4	30%	0.45	2.45	2.45	2.46	2.46	2.45	2.46
Mix 9	30%	0.45	2.48	2.47	2.48	2.49	2.48	2.49
Mix 6	32.50%	0.4	2.43	2.43	2.44	2.45	2.43	2.44
Mix 13	32.50%	0.4	2.46	2.46	2.46	2.47	2.47	2.47
Mix 14	32.50%	0.4	2.45	2.45	2.46	2.47	2.47	2.47
Mix 5	32.50%	0.45	2.44	2.43	2.44	2.46	2.44	2.45
Mix 1	39%	0.5	2.39	2.38	2.40	2.40	2.39	2.39
Mix 8	32.50%	0.5	2.45	2.45	2.46	2.47	2.45	2.46
Mix 2	35%	0.45	2.42	2.42	2.42	2.44	2.41	2.44
Mix 12	32.50%	0.4	2.48	2.48	2.49	2.50	2.48	2.49
Mix 7	32.50%	0.45	2.45	2.44	2.46	2.46	2.44	2.45
Mix 11	35%	0.45	2.47	2.46	2.47	2.48	2.47	2.48
Total falling below limit			7	29	7	0	21	0
Stiff mix falling below limit			0	17	0	0	17	0
Fluid mix falling below limit			13	38	13	0	25	0

Table B.9. SSD relative density deltas of rodded sets, highlighted sets exceed the lower limit of the 90% confidence interval.

	Paste Vol	w/c	2L, 0R	2L, 5R	2L, 10R	1L, 25R	2L, 15R	2L, 20R	2L 30R	2L 40R	2L, 50R	4L, 25R
Mix 10	25%	0.45	-0.043		-0.037	-0.008		-0.014	0.021	0.033	0.157	0.060
Mix 3	25%	0.45	-0.034		-0.007	0.002		0.002	0.003	0.001	0.010	0.004
Mix 4	30%	0.45	-0.045		0.002	0.007		0.002	0.003	0.005	0.005	-0.002
Mix 9	30%	0.45	-0.024		-0.007	-0.008		-0.004	0.000	0.001	0.001	0.003
Mix 6	32.50%	0.4	-0.022		-0.003	-0.005		0.002	0.007	0.007	0.011	0.001
Mix 13	32.50%	0.4	0.002		-0.003	-0.003		0.002	0.002	0.002	0.005	0.001
Mix 14	32.50%	0.4	-0.017	-0.002	-0.001	-0.003	-0.001	0.001			-0.003	0.000
Mix 5	32.50%	0.45	-0.023	-0.009	-0.013	-0.006	-0.004	-0.003			-0.003	-0.002
Mix 1	39%	0.5	0.010	0.003	0.019	0.003	0.023	0.018			0.006	
Mix 8	32.50%	0.5	-0.013	-0.006	-0.008	-0.003	-0.006	-0.001			0.001	0.008
Mix 2	35%	0.45	-0.013	0.002	0.010	-0.018	0.010	0.017				-0.011
Mix 12	32.50%	0.4	-0.011	-0.002	0.006	0.010	0.009	0.013			-0.002	0.007
Mix 7	32.50%	0.45	-0.014	-0.010	-0.009	-0.007	0.000	-0.008			0.003	-0.002
Mix 11	35%	0.45	-0.002	-0.001	0.003	0.009	0.003	0.011			-0.019	0.012
Total % below limit			79	38	50	29	25	14	0	0	8	15
Stiff mix % below limit			83	0	50	17	0	17	0	0	0	17
Fluid mix % below limit			75	38	50	38	25	13	0	0	14	14

Table B.10. SSD relative density deltas of vibrated sets, highlighted sets exceed the lower limit of the 90% confidence interval.

	Paste Vol	w/c	1s, 8000 vpm	3s, 6000 vpm	3s, 8000 vpm	6s, 8000 vpm	3s, 12000 vpm	12s, 8000 vpm
Mix 10	25%	0.45	-0.006	0.008	-0.001	0.016	0.014	0.033
Mix 3	25%	0.45	0.006	0.006	0.025	0.016	0.007	0.022
Mix 4	30%	0.45	-0.004	-0.006	0.005	0.007	0.007	0.007
Mix 9	30%	0.45	-0.006	-0.008	0.005	0.004	0.007	0.013
Mix 6	32.50%	0.4	-0.007	-0.010	-0.003	-0.004	-0.002	0.004
Mix 13	32.50%	0.4	0.000	0.004	0.002	0.005	0.011	0.014
Mix 14	32.50%	0.4	-0.007	0.004	-0.006	0.000	0.004	0.010
Mix 5	32.50%	0.45	-0.008	-0.006	-0.003	0.000	0.008	0.017
Mix 1	39%	0.5	0.000	-0.003	0.010	0.010	0.001	0.015
Mix 8	32.50%	0.5	0.000	-0.003	-0.002	0.010	0.004	0.019
Mix 2	35%	0.45	-0.004	-0.018	-0.010	-0.010	0.010	0.011
Mix 12	32.50%	0.4	-0.003	0.002	0.003	0.015	0.012	0.020
Mix 7	32.50%	0.45	-0.007	-0.011	-0.001	0.009	-0.004	0.010
Mix 11	35%	0.45	0.006	0.015	0.015	0.015	0.020	0.019
Total % below limit			29	21	7	7	0	0
Stiff mix % below limit			17	17	0	0	0	0
Fluid mix % below limit			38	25	13	13	0	0

Table B.11. Coefficient of variation within each set of rodded cylinders, highlighted cells exceed the limit set in ASTM C39.

	Paste Vol	w/c	2L, 25R	2L, 5R	2L, 10R	2L, 15R	2L, 20R	2L 30R	2L 40R	1L, 25R	2L, 50R	4L, 25R	2L, 25R	2L, 25R	2L, 25R	2L, 0R
Mix 10	25%	0.45	5.79		1.98		10.29	18.19	16.26	1.95	37.96	2.22	11.54	1.49	3.33	11.60
Mix 3	25%	0.45	3.99		3.71		3.51	2.08	4.10	11.03	2.39	3.75	2.68	5.07	1.72	5.92
Mix 4	30%	0.45	6.39		2.22		3.08	2.46	1.13	2.82	2.17	1.06	3.90	3.69	0.55	36.20
Mix 9	30%	0.45	0.53		0.59		1.98	2.61	0.19	1.91	2.33	4.34	4.11	1.21	4.01	13.63
Mix 6	32.50%	0.4	1.89		1.43		1.20	2.57	5.73	1.03	3.97	2.09	3.02	1.42	2.02	4.00
Mix 13	32.50%	0.4	0.91		3.95		3.89	3.19	5.71	2.64	1.78	2.00	3.81	6.28	1.68	5.76
Mix 14	32.50%	0.4	3.53	4.66	2.70	1.70	1.79			0.63	1.86	2.10	3.35	2.80	0.39	2.25
Mix 5	32.50%	0.45	1.50	2.83	1.61	4.78	0.92			7.34	2.02	3.88	2.32	2.28	2.97	3.80
Mix 1	39%	0.5	2.93	0.03	8.40	1.85	1.46			3.26	3.82		2.06		0.71	28.88
Mix 8	32.50%	0.5	2.31	2.27	3.31	2.86	1.25			1.63	1.23	3.00	3.17	2.75	3.45	2.66
Mix 2	35%	0.45	3.89	1.08	2.65	2.99	0.37			1.44		2.94	1.51		5.38	5.17
Mix 12	32.50%	0.4	2.27	1.51	0.34	2.92	2.85			0.86	2.66	0.57	1.27	2.67	1.66	4.42
Mix 7	32.50%	0.45	2.14	1.12	9.90	2.05	3.80			1.98	3.06	1.25	4.87	2.70	2.30	2.29
Mix 11	35%	0.45	1.48	1.99	2.44	5.85	0.43			2.66	4.95	1.22	1.00	6.34	0.36	3.57
Total % below limit			35.7	12.5	35.7	25.0	28.6	7.1	28.6	21.4	30.8	23.1	42.9	33.3	28.6	78.6
Stiff mix % below limit			50.0	0.0	33.3	0.0	50.0	16.7	66.7	16.7	33.3	33.3	66.7	50.0	33.3	100.0
Fluid mix % below limit			25.0	12.5	37.5	25.0	12.5	0.0	0.0	25.0	28.6	14.3	25.0	14.3	25.0	62.5

Table B.12. Coefficient of variation within each set of vibrated cylinders, highlighted cells exceed the limit set in ASTM C39.

	Paste Vol	w/c	3s, 8000 vpm	1s, 8000 vpm	6s, 8000 vpm	12s, 8000 vpm	3s, 6000 vpm	3s, 12000 vpm
Mix 10	25%	0.45	2.62	5.66	0.82	1.38	2.69	1.56
Mix 3	25%	0.45	4.06	6.63	9.27	10.53	17.04	6.59
Mix 4	30%	0.45	2.03	6.58	1.56	3.65	3.33	2.28
Mix 9	30%	0.45	3.99	5.96	5.92	0.80	2.96	4.04
Mix 6	32.50%	0.4	1.73	1.65	2.10	5.06	2.51	1.40
Mix 13	32.50%	0.4	1.43	3.46	2.40	7.20	3.70	2.37
Mix 14	32.50%	0.4	5.66	2.70	3.95	3.51	3.97	2.70
Mix 5	32.50%	0.45	0.71	1.80	6.34	1.68	3.25	4.69
Mix 1	39%	0.5	1.43	5.33	4.18	0.87	1.84	6.10
Mix 8	32.50%	0.5	0.82	2.62	4.01	0.33	2.33	1.43
Mix 2	35%	0.45	3.23	1.97	2.86	1.59	2.33	3.59
Mix 12	32.50%	0.4	3.62	2.46	1.24	1.09	1.43	4.91
Mix 7	32.50%	0.45	1.82	2.26	2.36	5.25	2.90	2.41
Mix 11	35%	0.45	4.56	2.73	2.22	8.60	1.72	6.93
Total % below limit			42.9	42.9	42.9	50.0	35.7	50.0
Stiff mix % below limit			33.3	83.3	50.0	66.7	50.0	33.3
Fluid mix % below limit			50.0	12.5	37.5	37.5	25.0	62.5

Table B.13. Compressive strength values of rodded sets, highlighted sets exceed the lower limit of the 90% confidence interval.

	Paste Vol	w/c	2L, 25R	2L, 5R	2L, 10R	2L, 15R	2L, 20R	2L 30R	2L 40R	1L, 25R	2L, 50R	4L, 25R	2L, 25R	2L, 25R	2L, 25R	2L, 0R
Mix 10	25%	0.45	7774		5110		6062	6869	6571	7835	5444	7486	5160	8457	103972	4057
Mix 3	25%	0.45	7453		7670		8229	8511	8736	6575	8695	8483	8137	6694	84416	5394
Mix 4	30%	0.45	7888		7978		7688	7865	7814	7642	7551	7386	7390	7639	97530	1945
Mix 9	30%	0.45	8422		8380		8170	8470	8236	8116	8136	8351	8237	8331	100833	6121
Mix 6	32.50%	0.4	9372		9224		9063	9038	8959	8455	9025	8817	7634	8645	107645	5427
Mix 13	32.50%	0.4	8468		8296		8078	8277	8009	7933	8463	8548	7621	8229	8751	7670
Mix 14	32.50%	0.4	7872	8246	8311	8130	8247			8200	8013	8307	8094	8159	102546	7996
Mix 5	32.50%	0.45	7383	7311	7152	7194	7422			7303	7110	7148	7197	7184	87388	6804
Mix 1	39%	0.5	6683	6315	6522	6604	6455			6453	6371		6303		6154	4746
Mix 8	32.50%	0.5	7509	7452	7260	7246	7111			7197	7133	7301	7277	7146	90661	7132
Mix 2	35%	0.45	7107	7327	7278	7122	7528			7124		6916	7156		7045	6774
Mix 12	32.50%	0.4	8450	8600	8680	8591	8444			8340	8137	8318	8335	8292	106448	7795
Mix 7	32.50%	0.45	7391	7236	6815	7311	7025			6921	7357	7293	7086	7021	90518	6875
Mix 11	35%	0.45	8133	8172	7883	7615	7813			7537	7332	7578	7629	7501	91388	7025
Total % below limit			0.0	12.5	35.7	37.5	35.7	0.0	16.7	35.7	15.4	30.8	0.0	0.0	0.0	64.3
Stiff mix % below limit			0.0	0.0	16.7	0.0	50.0	0.0	16.7	33.3	33.3	16.7	0.0	0.0	0.0	83.3
Fluid mix % below limit			0.0	12.5	50.0	37.5	25.0	0.0	0.0	37.5	0.0	42.9	0.0	0.0	0.0	50.0

Table B.14. Compressive strength values of vibrated sets, highlighted sets exceed the lower limit of the 90% confidence interval.

	Paste Vol	w/c	3s, 8000 vpm	1s, 8000 vpm	6s, 8000 vpm	12s, 8000 vpm	3s, 6000 vpm	3s, 12000 vpm
Mix 10	25%	0.45	8410	8096	8801	8733	8327	8068
Mix 3	25%	0.45	6157	5246	4895	5619	5135	5736
Mix 4	30%	0.45	7780	7280	7625	7686	7329	7793
Mix 9	30%	0.45	7758	7758	7520	7621	7627	8076
Mix 6	32.50%	0.4	8285	8260	8082	8214	8041	8219
Mix 13	32.50%	0.4	8001	8256	7834	7857	7597	7890
Mix 14	32.50%	0.4	7799	8010	7785	8028	7896	7792
Mix 5	32.50%	0.45	6955	7102	6698	6722	6718	7102
Mix 1	39%	0.5	6327	6059	6197	6309	6123	6008
Mix 8	32.50%	0.5	6885	6636	6743	6411	6763	6984
Mix 2	35%	0.45	6861	6693	6655	7034	6344	6691
Mix 12	32.50%	0.4	8132	8141	7753	7889	7897	8081
Mix 7	32.50%	0.45	6854	6908	6646	6618	6693	7044
Mix 11	35%	0.45	6530	7124	6426	5504	6917	6659
Total % below limit			57.1	35.7	71.4	57.1	64.3	50.0
Stiff mix % below limit			33.3	50.0	50.0	50.0	66.7	33.3
Fluid mix % below limit			75.0	25.0	87.5	62.5	62.5	62.5

Table B.15. Compressive strength deltas of rodded sets, highlighted sets exceed the lower limit of the 90% confidence interval.

	Paste Vol	w/c	2L, 0R	2L, 5R	2L, 10R	1L, 25R	2L, 15R	2L, 20R	2L 30R	2L 40R	2L, 50R	4L, 25R
Mix 10	25%	0.45	-1126		-2425	-611		-937	242	328	-1515	1901
Mix 3	25%	0.45	9		184	-1401		-2081	874	1027	903	601
Mix 4	30%	0.45	-640		108	-11		-99	140	166	-24	-114
Mix 9	30%	0.45	-862		-56	-194		-214	108	-101	-176	68
Mix 6	32.50%	0.4	-1425		41	-183		86	291	507	771	788
Mix 13	32.50%	0.4	-1686		-2	-346		-108	187	14	579	783
Mix 14	32.50%	0.4	-1029	297	390	197	183	272			-146	266
Mix 5	32.50%	0.45	194	7	-182	31	-119	130			-57	-98
Mix 1	39%	0.5	-1396	-313	-59	35	68	-18			7	
Mix 8	32.50%	0.5	-91	-4	-192	-167	-172	-277			-4	-32
Mix 2	35%	0.45	-257	208	149	-39	-17	378				-271
Mix 12	32.50%	0.4	-1357	45	254	-43	180	46			-133	-45
Mix 7	32.50%	0.45	-86	-55	-512	-284	20	-225			179	131
Mix 11	35%	0.45	-125	7	-103	-265	-312	-47			62	-158
Total % below limit			64.3	12.5	35.7	35.7	37.5	35.7	0.0	16.7	15.4	30.8
Stiff mix % below limit			83.3	0.0	16.7	33.3	0.0	50.0	0.0	16.7	33.3	16.7
Fluid mix % below limit			50.0	12.5	50.0	37.5	37.5	25.0	0.0	0.0	0.0	42.9

Table B.16. Compressive strength deltas of vibrated sets, highlighted sets exceed the lower limit of the 90% confidence interval.

	Paste Vol	w/c	1s, 8000 vpm	3s, 6000 vpm	3s, 8000 vpm	6s, 8000 vpm	3s, 12000 vpm	12s, 8000 vpm
Mix 10	25%	0.45	-311	-12	-21	413	-247	370
Mix 3	25%	0.45	1256	-163	2628	431	32	716
Mix 4	30%	0.45	-416	-402	107	-83	46	-31
Mix 9	30%	0.45	-478	-500	-517	-683	-16	-542
Mix 6	32.50%	0.4	-363	-552	-347	-532	-363	-390
Mix 13	32.50%	0.4	-218	-1020	-362	-680	-771	-708
Mix 14	32.50%	0.4	-149	-264	-360	-374	-368	-131
Mix 5	32.50%	0.45	-14	-313	-186	-389	97	-340
Mix 1	39%	0.5	-193	-76	60	-41	-175	91
Mix 8	32.50%	0.5	-530	-426	-272	-429	-217	-769
Mix 2	35%	0.45	-400	-728	-250	-427	-370	20
Mix 12	32.50%	0.4	-193	-519	-183	-605	-355	-502
Mix 7	32.50%	0.45	-159	-454	-191	-450	-123	-503
Mix 11	35%	0.45	-326	-436	-949	-995	-666	-1881
Total % below limit			35.7	64.3	57.1	71.4	50.0	57.1
Stiff mix % below limit			50.0	66.7	33.3	50.0	33.3	50.0
Fluid mix % below limit			25.0	62.5	75.0	87.5	62.5	62.5

APPENDIX C.

PIE CHARTS OF CYLINDER BREAK PATTERNS

OVERVIEW

This appendix presents the percentage of break types according to if the consolidation method used to create the cylinders was rodding or vibration.

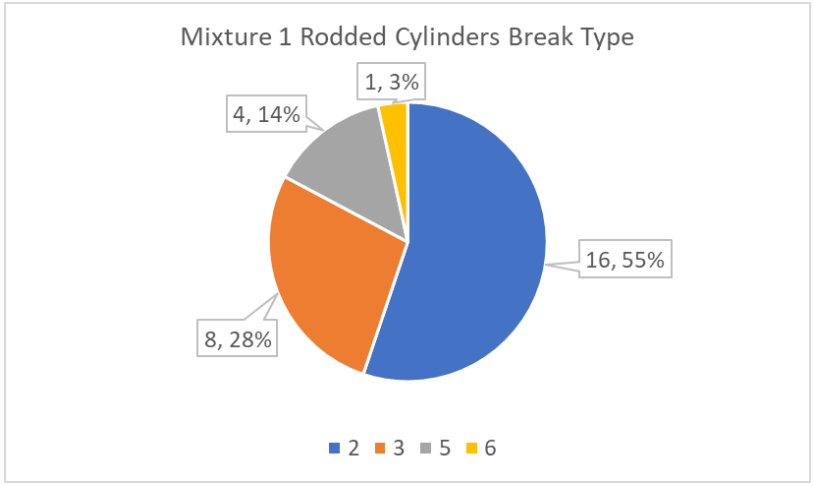

Figure C.1. Mixture 1 Rodded Cylinder Breaks

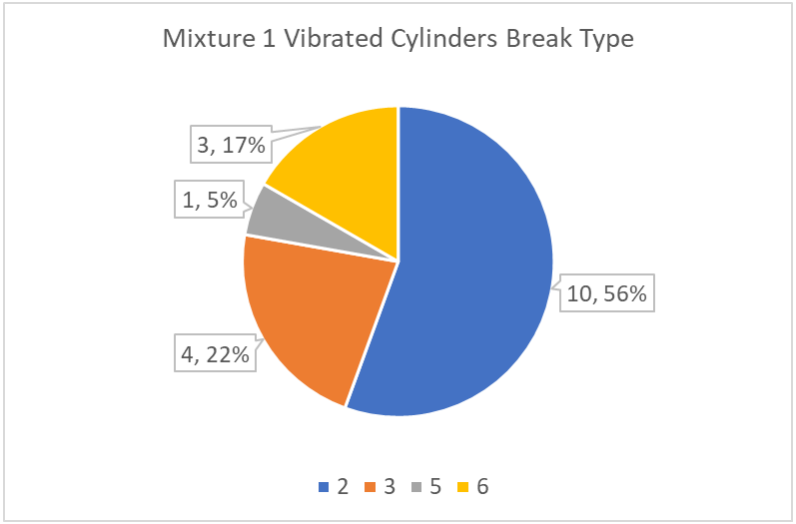

Figure C.2. Mixture 1 Vibrated Cylinder Breaks

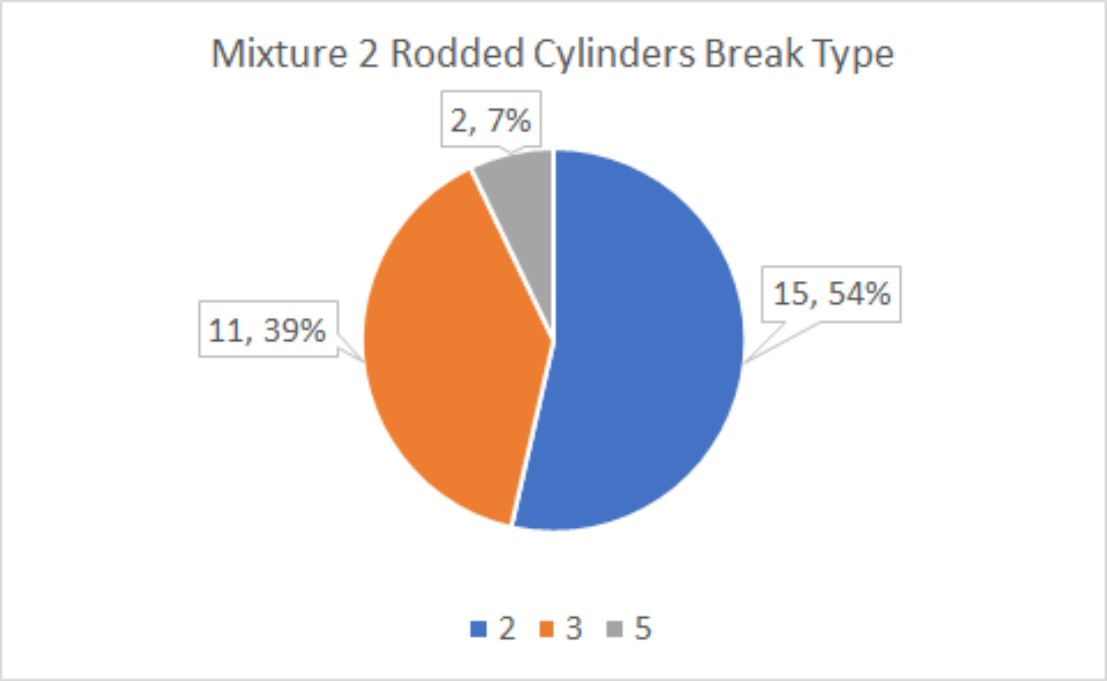

Figure C.3. Mixture 2 Rodded Cylinder Breaks

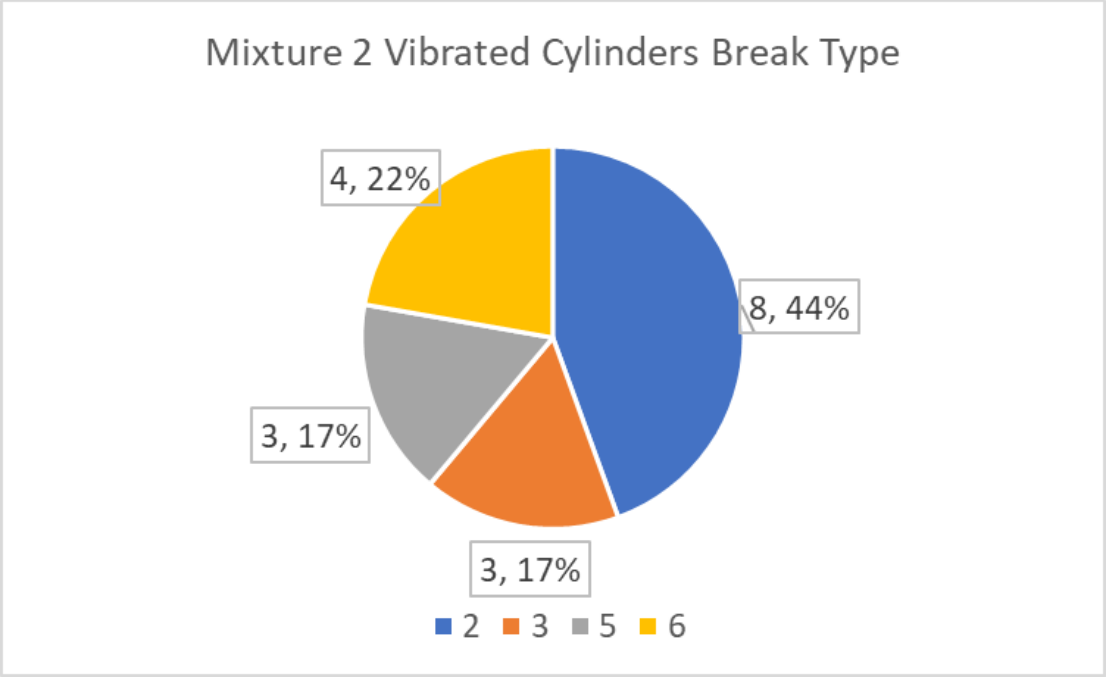

Figure C.4. Mixture 2 Vibrated Cylinder Breaks

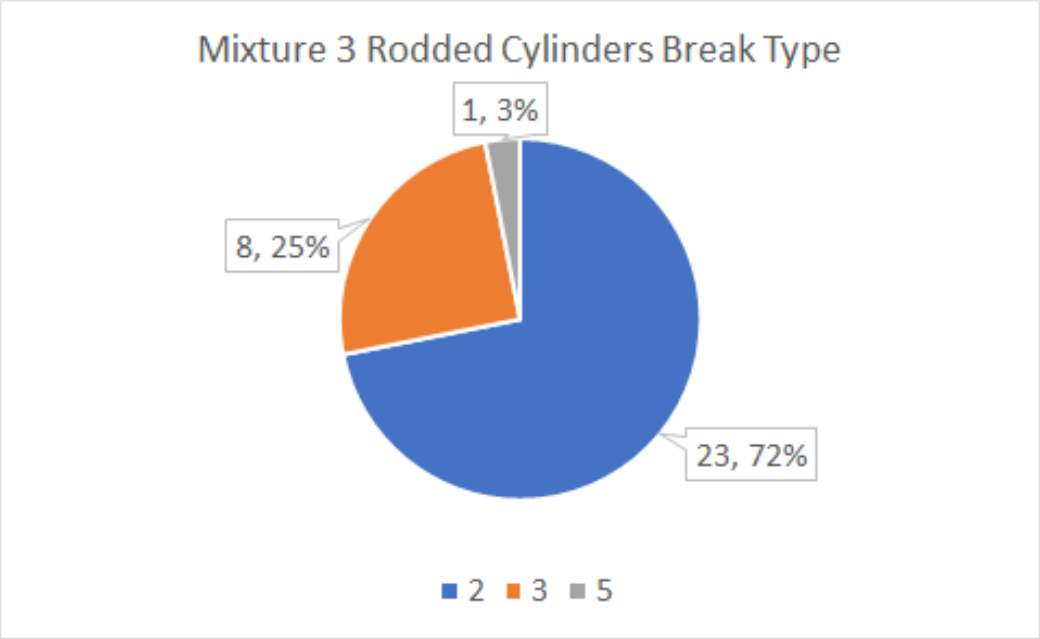

Figure C.5. Mixture 3 Rodded Cylinder Breaks

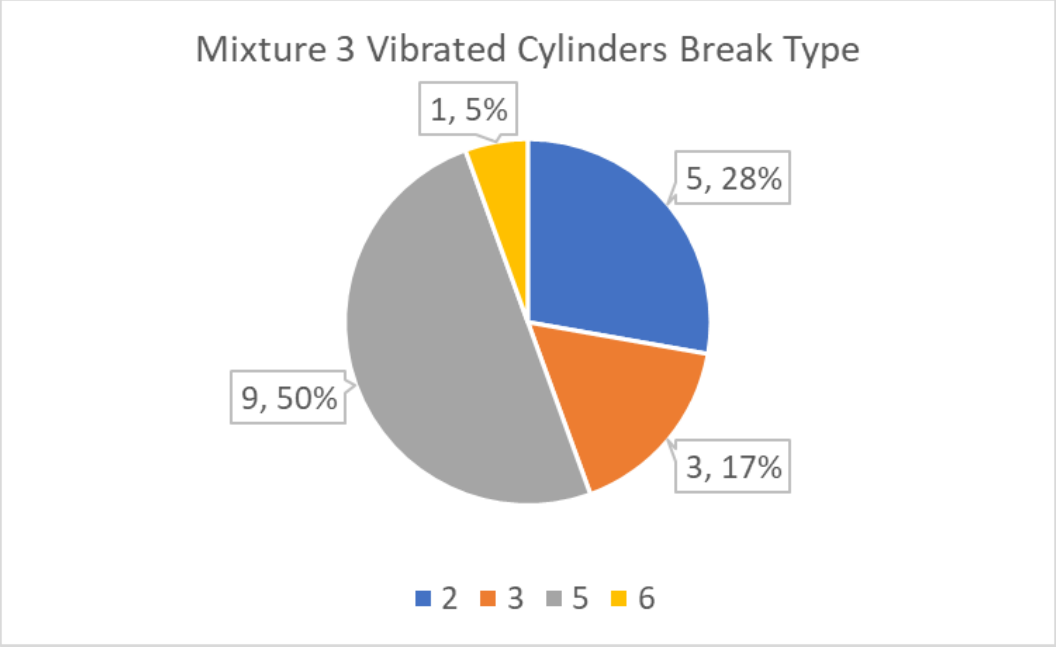

Figure C.6. Mixture 3 Vibrated Cylinder Breaks

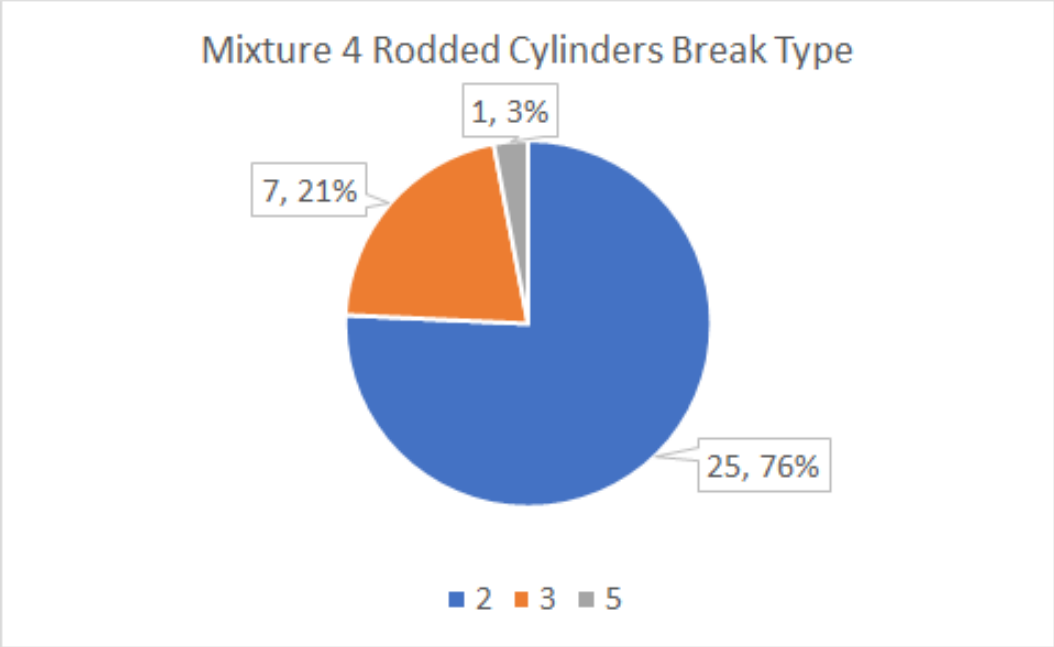

Figure C.7. Mixture 4 Rodded Cylinder Breaks

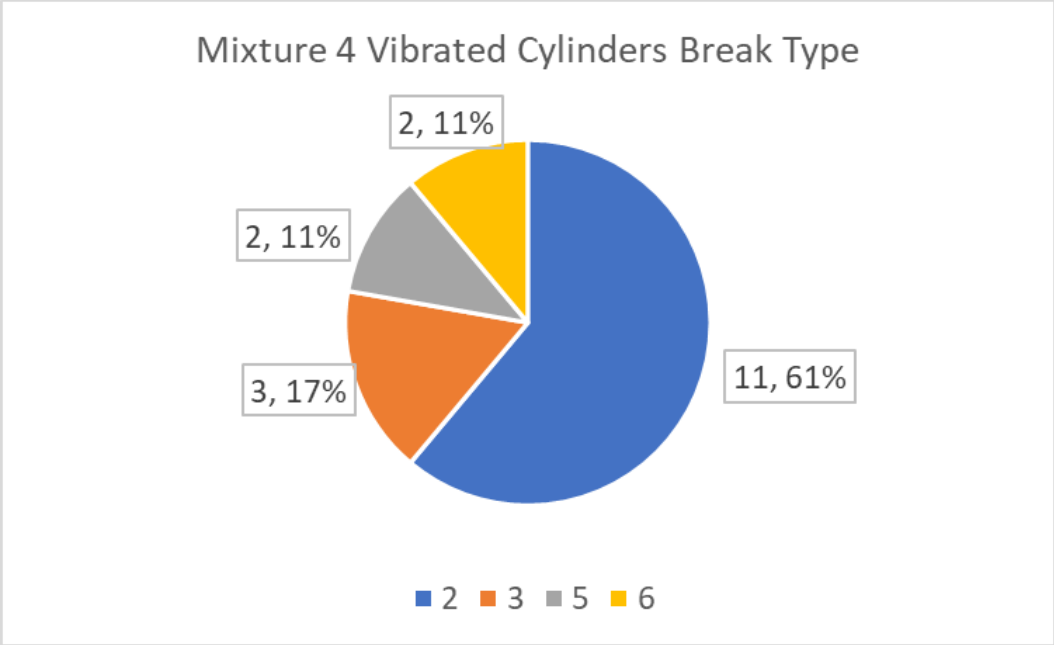

Figure C.8. Mixture 4 Vibrated Cylinder Breaks

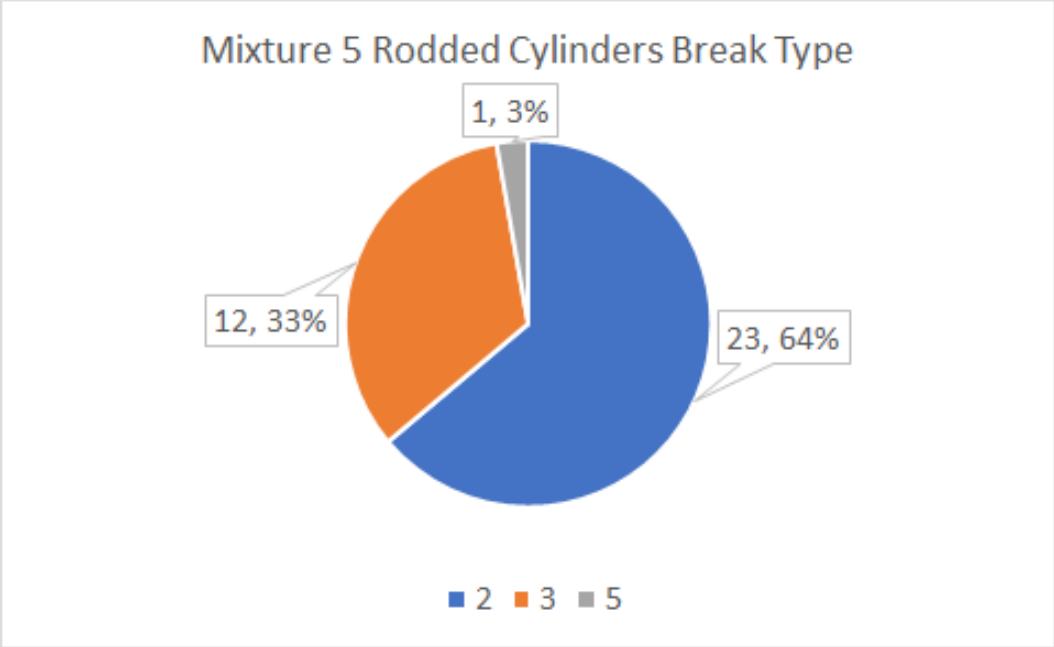

Figure C.9. Mixture 5 Rodded Cylinder Breaks

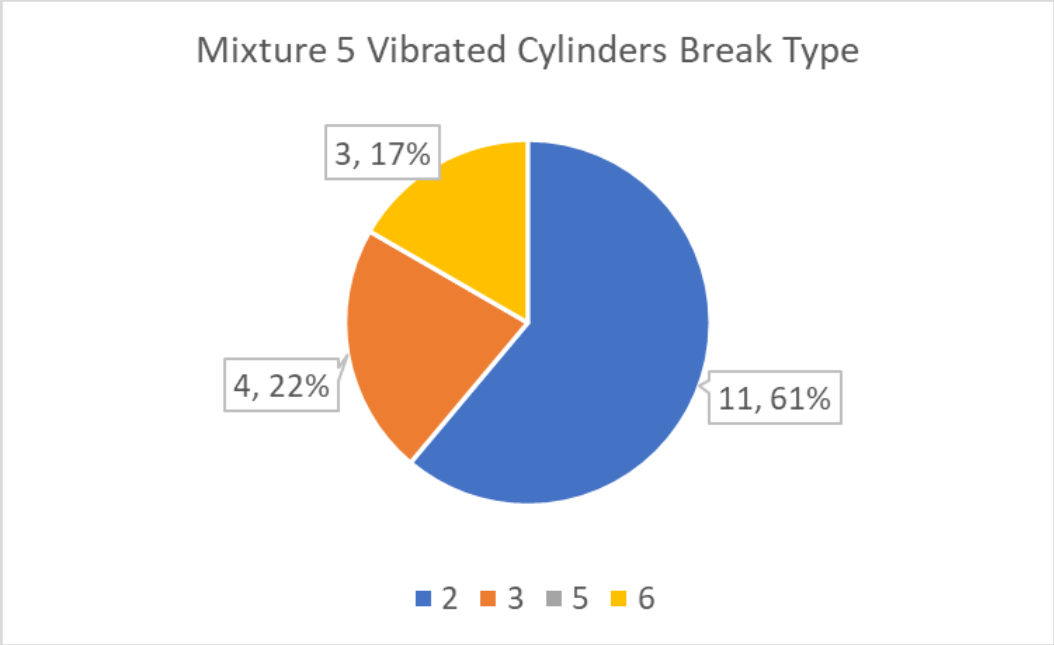

Figure C.10. Mixture 5 Vibrated Cylinder Breaks

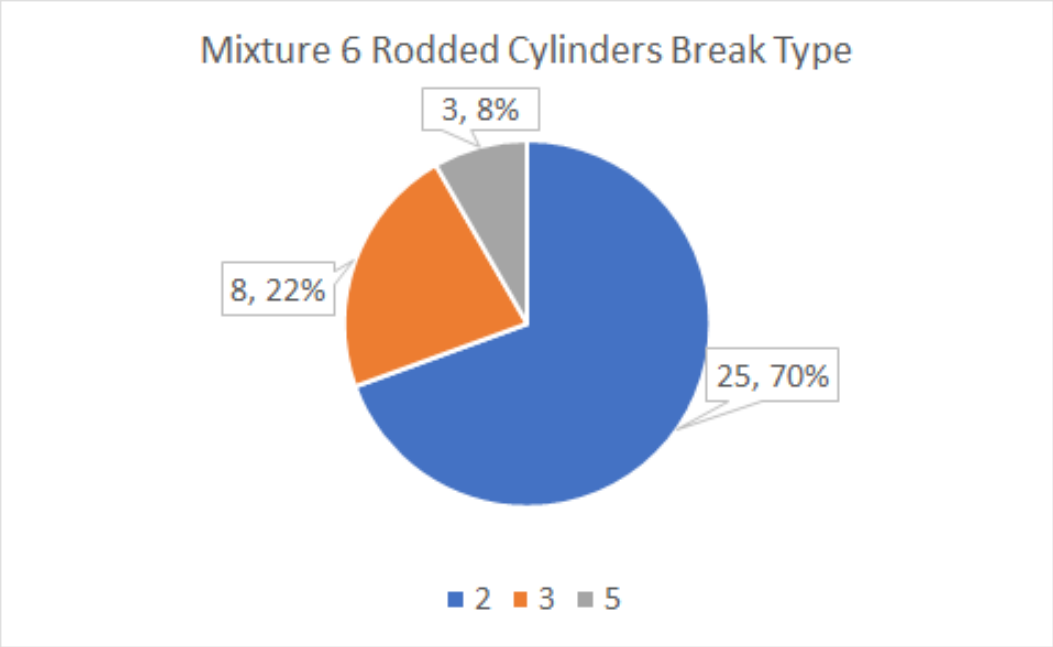

Figure C.11. Mixture 6 Rodded Cylinder Breaks

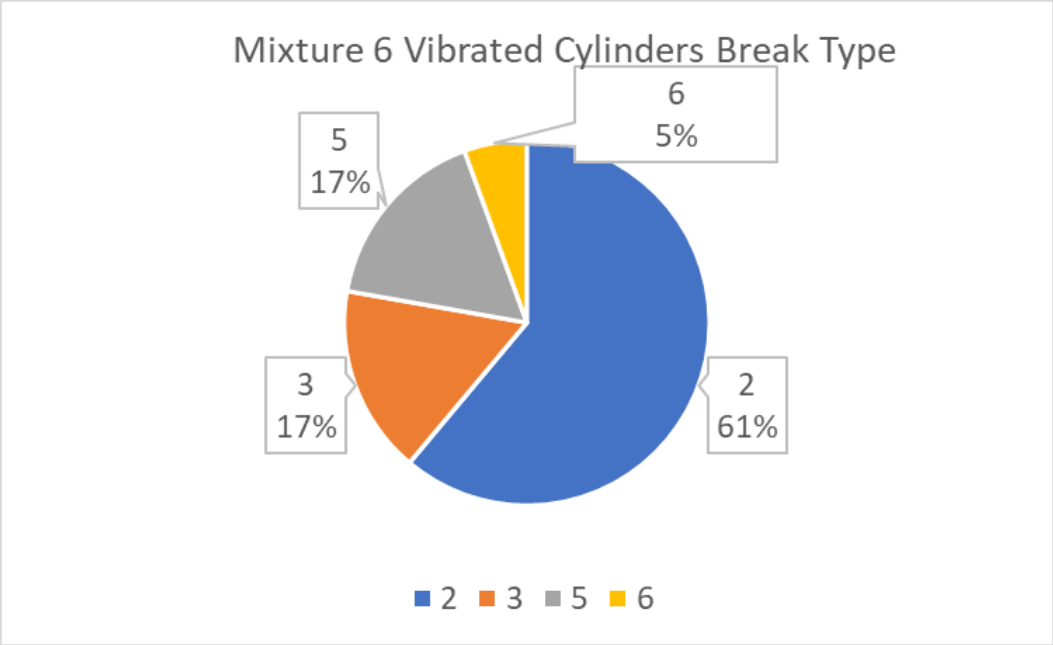

Figure C.12. Mixture 6 Vibrated Cylinder Breaks

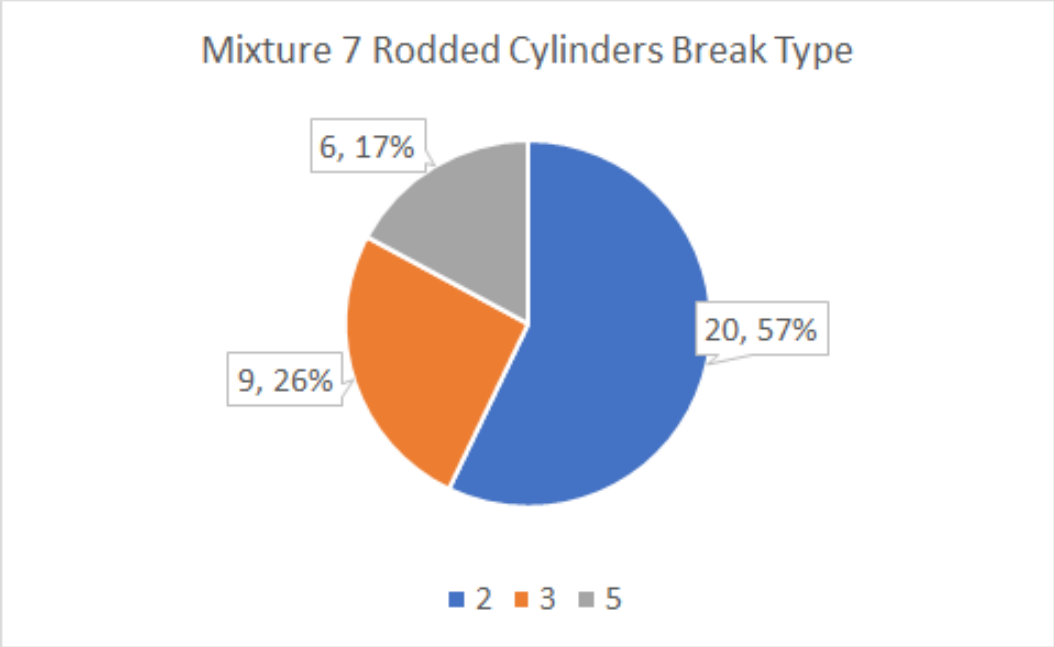

Figure C.13. Mixture 7 Rodded Cylinder Breaks

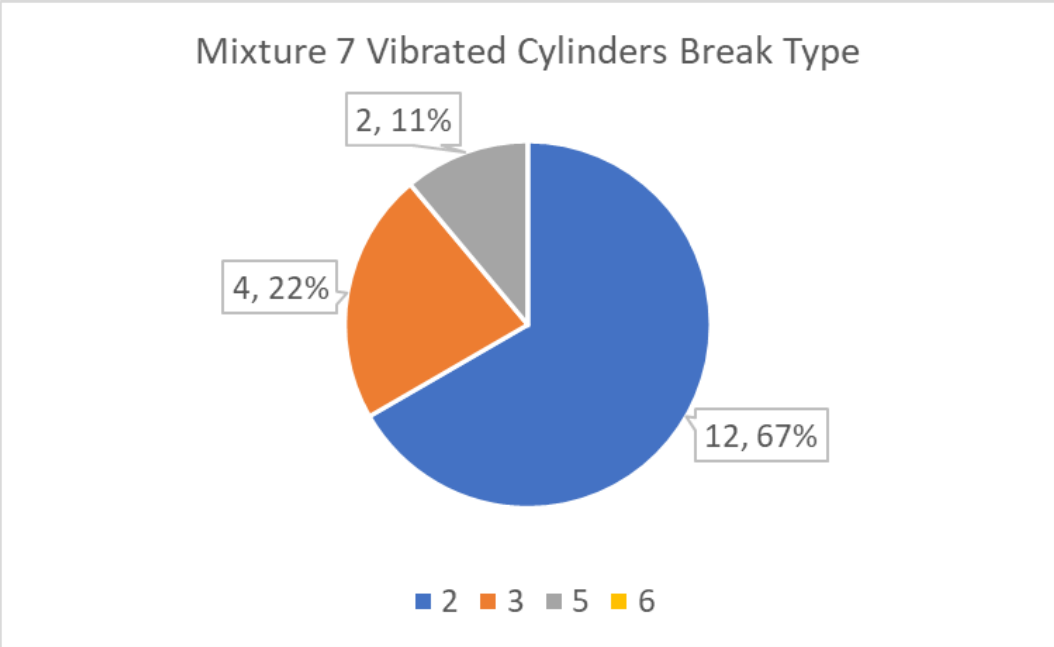

Figure C.14. Mixture 7 Vibrated Cylinder Breaks

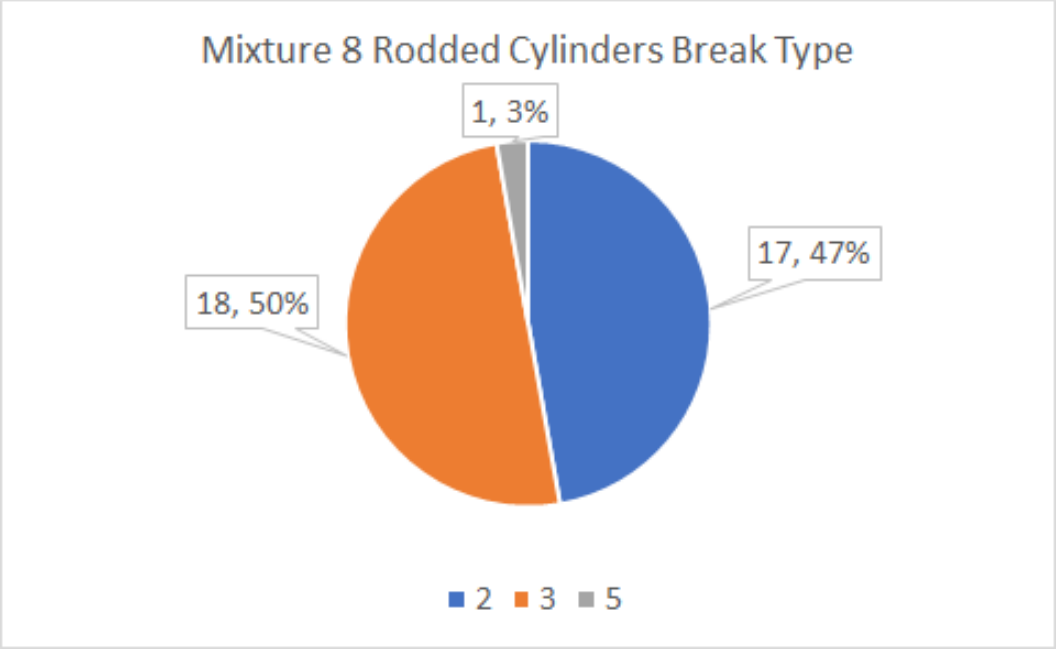

Figure C.15. Mixture 8 Rodded Cylinder Breaks

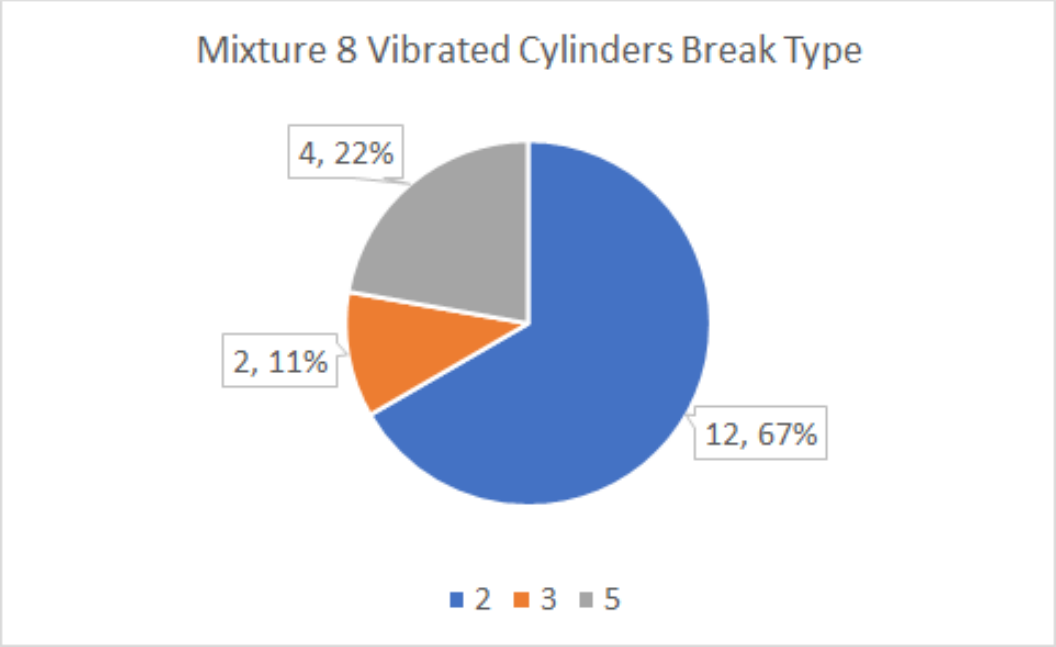

Figure C.16. Mixture 8 Vibrated Cylinder Breaks

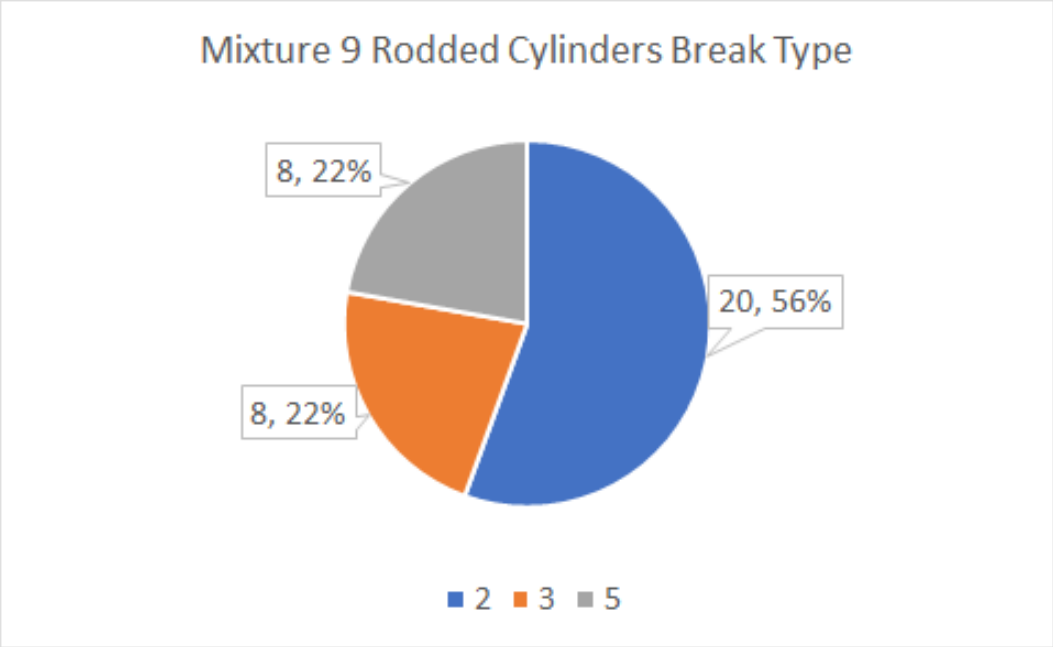

Figure C.17. Mixture 9 Rodded Cylinder Breaks

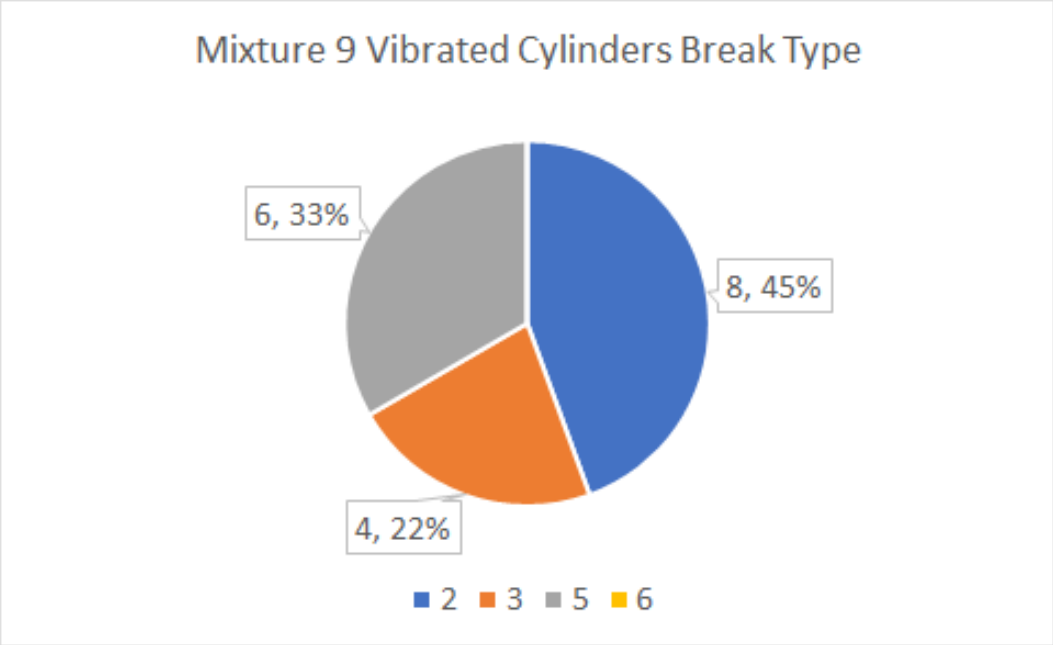

Figure C.18. Mixture 9 Vibrated Cylinder Breaks

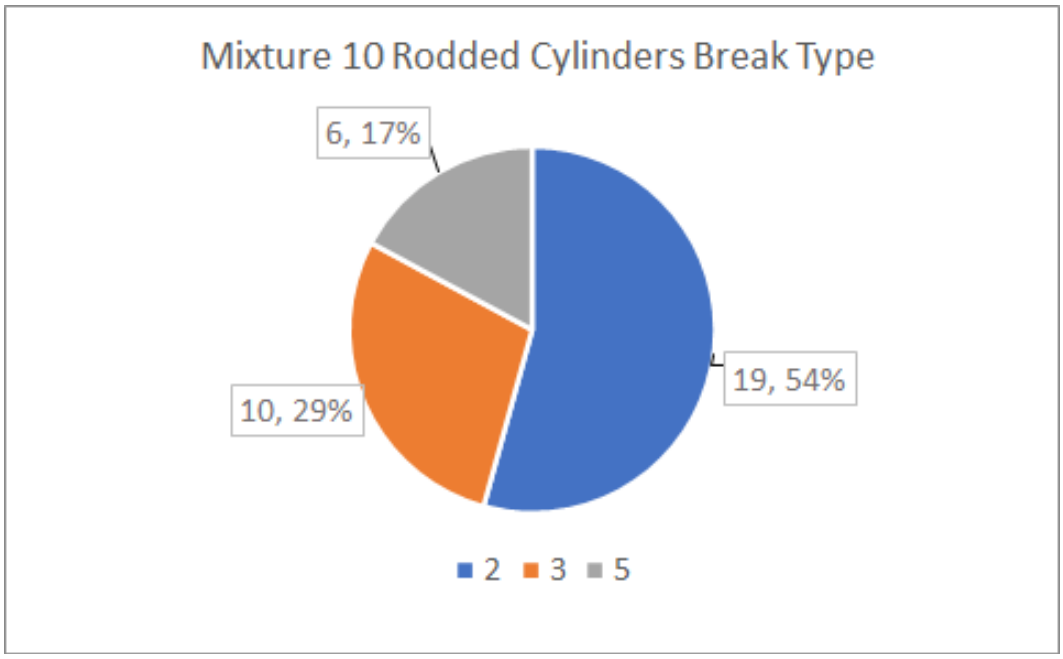

Figure C.19. Mixture 10 Rodded Cylinder Breaks

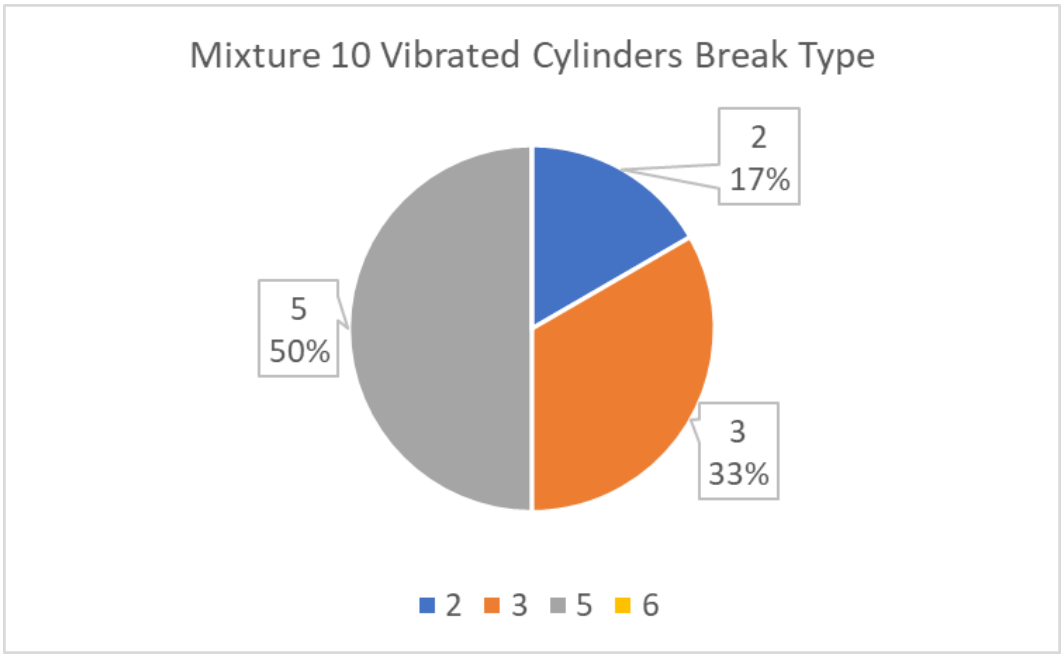

Figure C.20. Mixture 10 Vibrated Cylinder Breaks

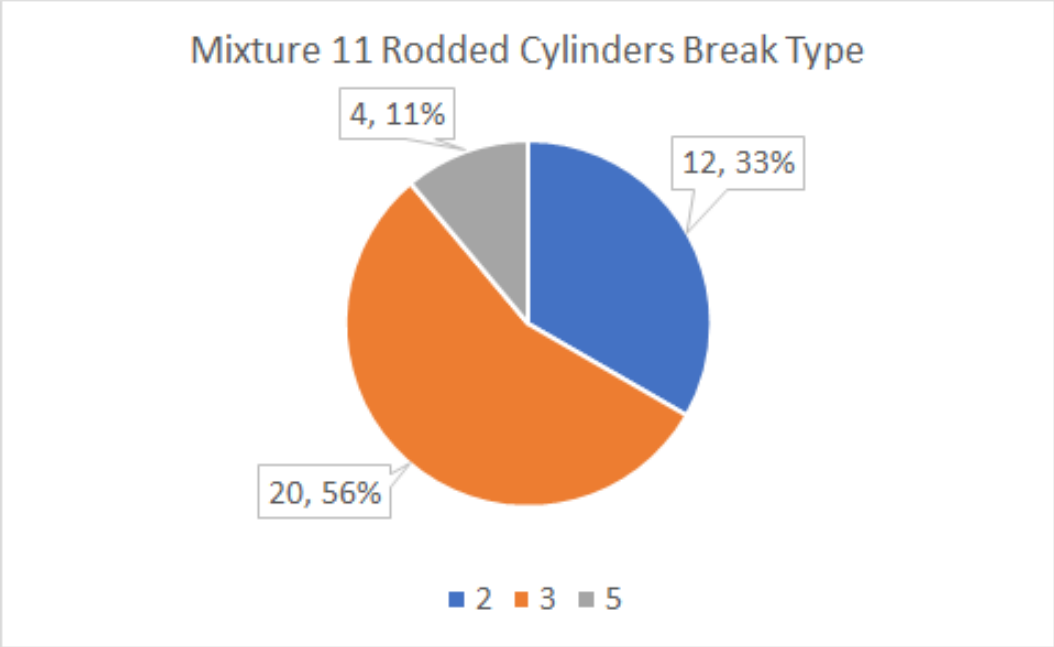

Figure C.21. Mixture 11 Rodded Cylinder Breaks

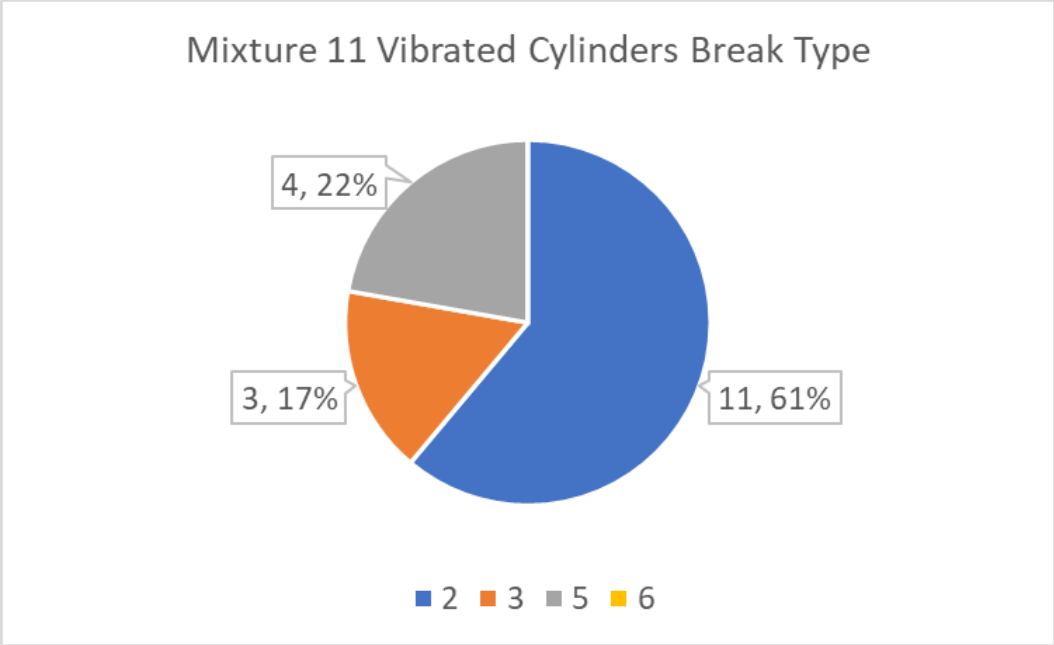

Figure C.22. Mixture 11 Vibrated Cylinder Breaks

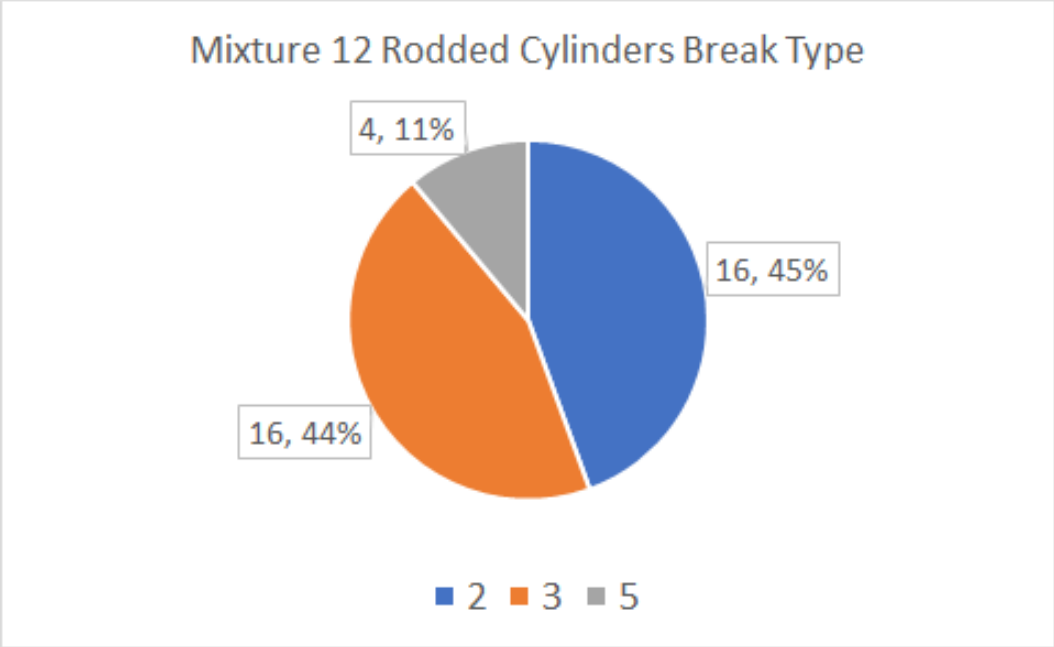

Figure C.23. Mixture 12 Rodded Cylinder Breaks

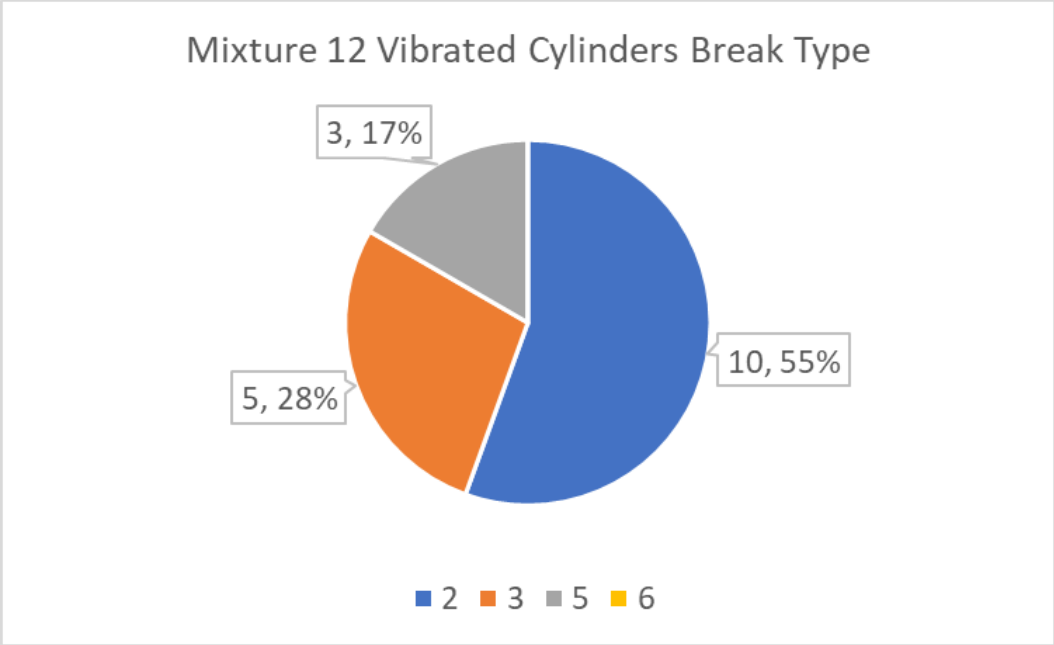

Figure C.24. Mixture 12 Vibrated Cylinder Breaks

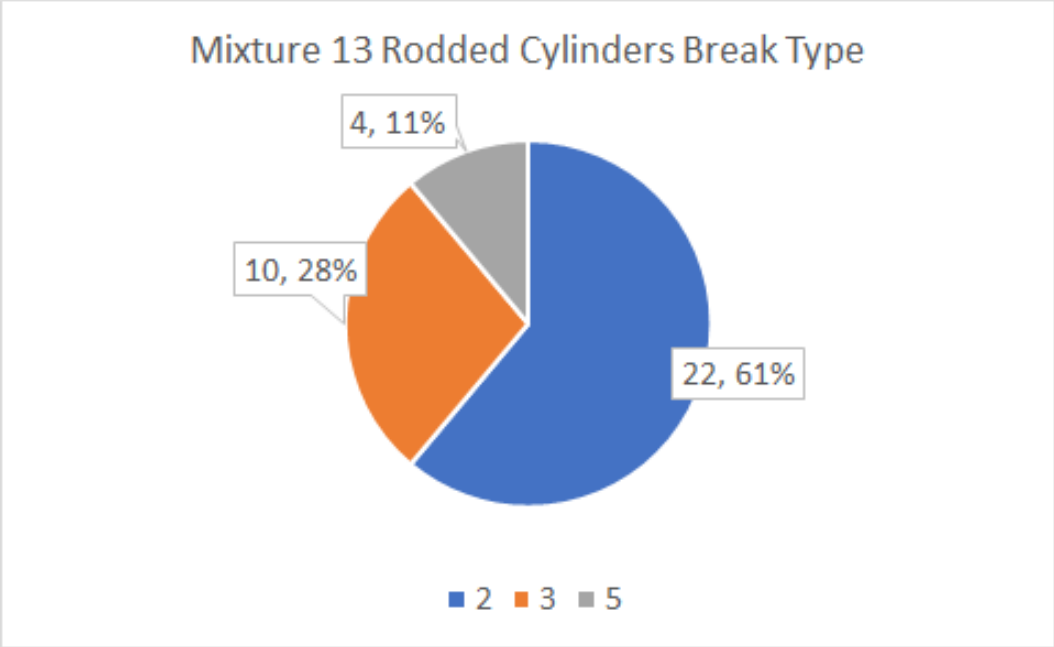

Figure C.25. Mixture 13 Rodded Cylinder Breaks

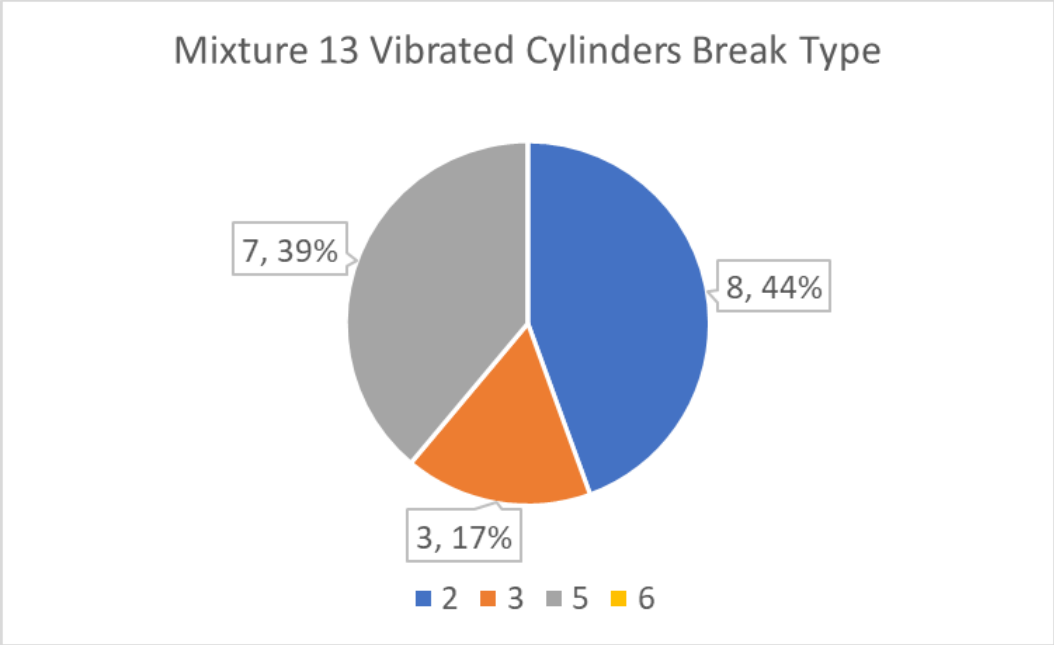

Figure C.26. Mixture 13 Vibrated Cylinder Breaks

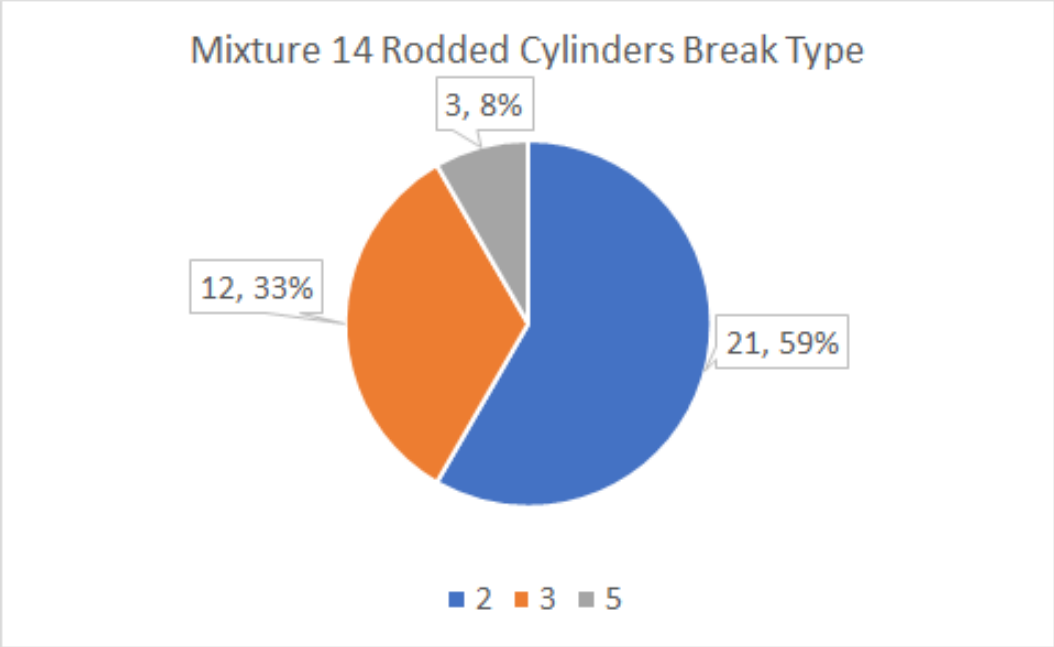

Figure C.27. Mixture 14 Rodded Cylinder Breaks

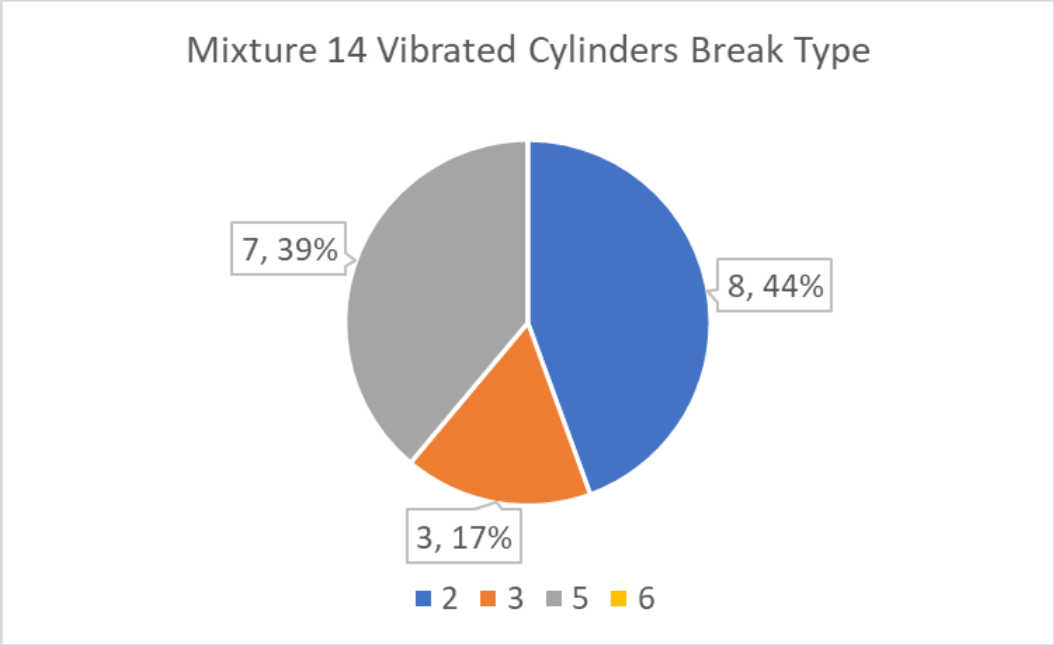

Figure C.28. Mixture 14 Vibrated Cylinder Breaks

BIBLIOGRAPHY

[1] Yumpu.com. (n.d.). ASTM Construction Standards: Supporting the Building Industry. yumpu.com. Retrieved March 6, 2023, from https://www.yumpu.com/en/document/read/16494 242/astm-construction-standards-supporting-the-building-industry

[2] Published by the American Society for Testing Materials. (1921). Standard Test Methods for Making and Storing Specimens of Concrete in the Field. In ASTM standards 1921: Issued triennially (pp. 641–644). essay.

[3] American Society for Testing and Materials. ASTM Standards In Building Codes: Specifications, Methods of Test, Definitions. 6th ed. Philadelphia, 1967.

[4] ASTM C1758 Practice for fabricating test specimens with self-consolidating concrete. (n.d.). https://doi.org/10.1520/c1758_c1758m-13

[5] ASTM C1435 Practice for molding roller-compacted concrete in cylinder molds using a vibrating hammer. (n.d.). https://doi.org/10.1520/c1435_c1435m

[6] Dukare, P., Khan, M., Raut, S., & Godbole, K. (n.d.). WORKABILITY OF FRESH CONCRETE BY COMPACTION FACTOR. International Research Journal of Engineering and Technology (IRJET).

[7] Wallevik, O. H., & Wallevik, J. E. (2011). Rheology as a tool in concrete science: The use of rheographs and workability boxes. Cement and Concrete Research, 41(12), 1279–1288. https://doi.org/10.1016/j.cemconres.2011.01.009

[8] Lamond, J. F. (2006). Significance of tests and properties of concrete and concrete-making materials. ASTM.

[9] Khaled Marar and Özgür Eren. Effect of cement content and water/cement ratio on fresh concrete ... (n.d.). Retrieved October 8, 2022, from https://www.researchgate.net/publication/266602831_Effect_of_cement_content_and_watercement_ratio_on_fresh_concrete_properties_without_admixtures

[10] Rasekh, H., Joshaghani, A., Jahandari, S., Aslani, F., & Ghodrat, M. (2020). Rheology and workability of SCC. Self-Compacting Concrete: Materials, Properties and Applications, 31–63. https://doi.org/10.1016/b978-0-12-817369-5.00002-7

[11] Ferraris, C. F. (2018, April 6). Role of rheology in achieving successful concrete performance. NIST. Retrieved January 8, 2023, from https://www.nist.gov/publications/role-rheology-achieving-successful-concrete-performance

[12] Ojala, T., Ahmed, H., Vehmas, T., Chen, Y., Tauqir, A., Oey, T., Al-Neshawy, F., Leivo, M., & Punkki, J. (1970, January 1). Factors for compactibility and risk of segregation for concrete - report for Contract Research Project "Compact Air". Aaltodoc. Retrieved October 6, 2022, from https://aaltodoc.aalto.fi/handle/123456789/108491

[13] Lachemi, M., Hossain, K. M. A., Lambros, V., Nkinamubanzi, P.-C., & Bouzoubaâ, N. (2004). Performance of new viscosity modifying admixtures in enhancing the rheological properties of cement paste. Cement and Concrete Research, 34(2), 185–193. https://doi.org/10.1016/s0008-8846(03)00233-3

[14] Ferraris, C. F., Billberg, P., Ferron, R., Feys, D., Hu, J., Kawashima, S., Koehler, E., Sonebi, M., Tanesi, J., & Tregger, N. (2017, June 1). Home. Concrete International. Retrieved April 20, 2023, from https://www.concrete.org/publications/internationalconcreteabstractsportal.aspx?m=details&i=51700809

[15] Wong, G. S. (2001). Portland-Cement Concrete Rheology and workability: Final report. U.S. Dept. of Transportation, Federal Highway Administration, Research Development and Technology, Turner-Fairbank Highway Research Center.

[16] Roussel, N., Ovarlez, G., Garrault, S., & Brumaud, C. (2012). The origins of thixotropy of fresh cement pastes. Cement and Concrete Research, 42(1), 148–157. https://doi.org/10.1016/j.cemconres.2011.09.004

[17] Yuan, Q., Lu, X., Khayat, K. H., Feys, D., & Shi, C. (2016). Small amplitude oscillatory shear technique to evaluate structural build-up of cement paste. Materials and Structures, 50(2). https://doi.org/10.1617/s11527-016-0978-2

[18] Reiter, L., Wangler, T., Anton, A., & Flatt, R. J. (2020). Setting on demand for Digital Concrete – principles, measurements, chemistry, Validation. Cement and Concrete Research, 132, 106047. https://doi.org/10.1016/j.cemconres.2020.106047

[19] Jarny S, Roussel N, Rodts S, Le Roy R, Coussot P (2005) Rheological behavior of cement pastes from MRI velocimetry. Cem Concr Res 35:1873–1881

[20] Quiroga, P. N., & Fowler, D. W. (2003, December 1). The effects of the aggregates characteristics on the performance of Portland Cement Concrete. TexasScholarWorks. Retrieved March 23, 2023, from https://repositories.lib.utexas.edu/handle/2152/35333

[21] Powers, T. C. (1968). The properties of fresh concrete. Wiley.

[22] Trautwine, J. C., & Trautwine, J. C. (1904). The Civil Engineer's pocket-book, of mensuration, trigonometry, surveying, hydraulics ... etc. .. J. Wiley & Sons.

[23] O. Graf, Experiments of the behavior of reinforcement in concrete of various compositions, Dtsch. Aussch. Eisenbeton 71 (1933) 37–60.

[24] Tattersall, G. H., & G., B. P. F. (1983). The rheology of fresh concrete. Pitman.

[25] Development of concrete rheometers an overview - schleibinger. (n.d.). Retrieved April 15, 2023, from http://www.schleibinger.com/cmsimple/downloads/k2021_Keller.pdf

[26] Bogner, A., Link, J., Baum, M., Mahlbacher, M., Gil-Diaz, T., Lützenkirchen, J., Sowoidnich, T., Heberling, F., Schäfer, T., Ludwig, H.-M., Dehn, F., Müller, H. S., & Haist, M. (2020). Early hydration and microstructure formation of Portland cement paste studied by oscillation rheology, isothermal calorimetry, 1H NMR relaxometry, conductance and saxs. Cement and Concrete Research, 130, 105977. https://doi.org/10.1016/j.cemconres.2020.105977

[27] Bellotto, M. (2013). Cement paste prior to setting: A rheological approach. Cement and Concrete Research, 52, 161–168. https://doi.org/10.1016/j.cemconres.2013.07.002

[28] John, E., Matschei, T., & Stephan, D. (2018). Nucleation seeding with calcium silicate hydrate – A Review. Cement and Concrete Research, 113, 74–85. https://doi.org/10.1016/j.cemconres.2018.07.003

[29] A.K.H. Kwan, S.K. Ling, Lowering paste volume of SCC through aggregate proportioning to reduce carbon footprint, Constr. Build. Mater. 93 (2015) 584–594.

[30] Plassard, C., Lesniewska, E., Pochard, I., & Nonat, A. (2005). Nanoscale Experimental Investigation of Particle Interactions at the origin of the cohesion of Cement. Langmuir, 21(16), 7263–7270. https://doi.org/10.1021/la050440+

[31] John, E., Matschei, T., & Stephan, D. (2018). Nucleation seeding with calcium silicate hydrate – A Review. Cement and Concrete Research, 113, 74–85. https://doi.org/10.1016/j.cemconres.2018.07.003

[32] Ioannidou, K., Kanduč, M., Li, L., Frenkel, D., Dobnikar, J., & Del Gado, E. (2016). The crucial effect of early-stage gelation on the mechanical properties of cement hydrates. Nature Communications, 7(1). https://doi.org/10.1038/ncomms12106

[33] Ramachandran, V.S. 1995, Concrete Admixtures Handbook – Properties, Science, and Technology.

[34] Effects of mineral admixtures on the workability of fresh concrete. (2016). Cement and Concrete Mineral Admixtures, 96–125. https://doi.org/10.1201/b20093-12

[35] Struble, L.J., Jiang, Qingye effects of Air Entrainment on Rheology - Researchgate. (n.d.). Retrieved February 9, 2023, from https://www.researchgate.net/publication/288569745_Effects_of_air_entrainment_on_rheology

[36] Asghari, Hernandez, Feys, De Schutter (2016), Which parameters, other than the water content, influence the robustness of cement paste with SCC consistency?. Construction and Building Materials, 124, 95-103

[37] S.H. Chu, Effect of paste volume on fresh and hardened properties of concrete. Construction and Building Materials. Retrieved February 7, 2023, from https://www.sciencedirect.com/science/article/pii/S0950061819313005

[38] A.M. Neville, Properties of concrete, Longman, London, 1995.

[39] Alhozaimy, A. M. (2009). Effect of absorption of limestone aggregates on strength and s lump loss of concrete. Cement and Concrete Composites, 31(7), 470–473. https://doi.org/10.1016/j.cemconcomp.2009.04.010

[40] Guide for curing portland cement concrete pavements, II. FHWA. (n.d.). Retrieved April 15, 2023, from https://www.fhwa.dot.gov/publications/research/infrastructure/pavements/pccp/05038/005.cfm

[41] Chu, S. H. (2019). Effect of paste volume on fresh and hardened properties of concrete. Construction and Building Materials, 218, 284–294. https://doi.org/10.1016/j.conbuildmat.2019.05.131

[42] Kolias, S., & Georgiou, C. (2005). The effect of paste volume and of water content on the strength and water absorption of concrete. Cement and Concrete Composites, 27(2), 211–216. https://doi.org/10.1016/j.cemconcomp.2004.02.009

[43] Jiong Hu a, a, b, & study, A. I. the present. (2010, September 27). Effect of coarse aggregate characteristics on concrete rheology. Construction and Building Materials. Retrieved February 6, 2023, from https://www.sciencedirect.com/science/article/pii/S095006181000468X

[44] Jamkar, S. S., & Rao, C. B. K. (2004). Index of aggregate particle shape and texture of coarse aggregate as a parameter for concrete mix proportioning. Cement and Concrete Research, 34(11), 2021–2027. https://doi.org/10.1016/j.cemconres.2004.03.010

[45] Controlling three-dimensional-printable concrete with vibration. (2021). ACI Materials Journal, 118(6). https://doi.org/10.14359/51734150

[46] Hooton, R. D., Geiker, M. R., Brandl, M., Thrane, L. N., & Nielsen, L. F. (2002). On the effect of coarse aggregate fraction and shape on the rheological properties of self-compacting concrete. Cement, Concrete and Aggregates, 24(1), 3. https://doi.org/10.1520/cca10484j

[47] Roberto Cesar de Oliveira Romano, & Rafael Giuliano Pileggi. (n.d.). Use of rheological models for the evaluation of cement pastes with air entraining agent in different temperatures. Retrieved February 11, 2023, from https://nrs.blob.core.windows.net/pdfs/nrspdf-a0760e90-fee4-4f44-a193-e6b90c2c1728.pdf

[48] Gálvez-Moreno, D., Feys, D., & Riding, K. (2019). Characterization of air dissolution and reappearance under pressure in cement pastes by means of rheology. Frontiers in Materials, 6. https://doi.org/10.3389/fmats.2019.00073

[49] Edmeades, R., and Hewlett, P., 1999, “Cement Admixtures,” Lea’s Chemistry of Cement and Concrete, 4th Edition, Chemical Publishing Co., pp. 837-901.

[50] Puertas, F., Santos, H., Palacios, M., & Martinez-Ramirez, S. (n.d.). Polycarboxylate superplasticiser admixtures: Effect on hydration, microstructure and rheological behaviour in cement pastes. Advances in Cement Research. Retrieved February 8, 2023, from https://www.icevirtuallibrary.com/doi/10.1680/adcr.2005.17.2.77

[51] Yan, Z., & Zhang, Q. (n.d.). Impact of water reducing agent on concrete strength. Chemical Engineering Transactions. Retrieved March 26, 2023, from https://www.cetjournal.it/index.php/cet/article/view/CET1866182

[52] Wallevik, O. H., & Wallevik, J. E. (2011). Rheology as a tool in concrete science: The use of rheographs and workability boxes. Cement and Concrete Research, 41(12), 1279–1288. https://doi.org/10.1016/j.cemconres.2011.01.009

[53] ACI Education Bulletin E4-12 - CHEMICAL ADMIXTURES FOR CONCRETE. American Concrete Institute. (n.d.). Retrieved March 24, 2023, from https://www.concrete.org/Portals/0/Files/PDF/fE4-12.pdf

[54] Sugiyama T., Ohta A. and Uomoto T. The dispersing mechanism and applications of polycarboxylate-based super plasticizers. Proceedings of the XI International Conference on the Chemistry of Cement, Durban, 2003, pp. 560–568.

[55] Asghari, Hernandez, Feys, De Schutter (2016), Which parameters, other than the water content, influence the robustness of cement paste with SCC consistency?. Construction and Building Materials, 124, 95-103

[56] Hanehara, S., & Yamada, K. (1999). Interaction between cement and chemical admixture from the point of cement hydration, absorption behavior of admixture, and Paste Rheology. Cement and Concrete Research, 29(8), 1159–1165. https://doi.org/10.1016/s0008-8846(99)00004-6

[57] Rossington, D. R., & Struble, L. J. (1989). Adsorption of high-range water-reducing agents on selected Portland cement phases and related materials. https://doi.org/10.6028/nist.ir.89-4172

[58] Kosmatka, S. H., & Wilson, M. L. (2016). Chapter 6 Admixtures for Concrete. In Design and control of concrete mixtures. essay, Portland Cement Association.

[59] Feys, Verhoeven, De Schutter (2009), Why is fresh self-compacing concrete shear thickening?, Cem. Conc. Res. 39, 510-523

[60] Brito Prado Vieira, L., & Domingues Figueiredo, A. (2020). Implementation of the use of hydration stabilizer admixtures at a ready-mix concrete plant. Case Studies in Construction Materials, 12. https://doi.org/10.1016/j.cscm.2020.e00334

[61] TB-1301 - recover® hydration stabilizer applications and Performance Review Technical Bulletin: GCP Applied Technologies. TB-1301 - RECOVER® Hydration Stabilizer Applications and Performance Review Technical Bulletin | Resource | GCP Applied Technologies. (n.d.). Retrieved March 23, 2023, from https://gcpat.com/en/solutions/products/recover-hydration-stabilizer/tb-1301-recover-hydration-stabilizer-applications

[62] Nath, P., & Sarker, P. (2011, October 01). Effect of fly ash on the durability properties of high strength concrete. Retrieved February 7, 2023, from https://www.sciencedirect.com/science/article/pii/S1877705811012215

[63] Silica fume topic - american concrete institute. (n.d.). Retrieved February 15, 2023, from https://www.concrete.org/topicsinconcrete/topicdetail/silica%20fume

[64] Coa, C., Sun, W., & Quin, H. (2000, February 25). The analysis on strength and fly ash effect of roller-compacted concrete with high volume fly ash. Retrieved February 7, 2023, from https://www.sciencedirect.com/science/article/pii/S0008884699002033

[65] American Concrete Institute. (2021). 2021 Aci Collection Of Concrete codes, specifications, and practices.

[66] Federal Highway Administration. (1997). Petrographic Methods of Examining Hardened Concrete: A Petrographic Manual. Retrieved February 25, 2021, from https://www.fhwa.dot.gov/publications/research/infrastructure/pavements/pccp/97146/index.cfm#toc

[67] Balasubramanian, K. (2019). Compaction of Concrete. Retrieved May 13, 2021, from https://www.constrofacilitator.com/compaction-of-concrete

[68] Cement Concrete and Aggregates Australia. (2006). Compaction of Concrete (Issue June). Retrieved February 26, 2021, from https://www.boral.com.au/sites/default/files/media/field_document/Compaction of Concrete.pdf

[69] Dr. Peter Taylor, Effects of vibration on concrete mixtures - Institute for Transportation. (n.d.). Retrieved March 7, 2023, from https://intrans.iastate.edu/app/uploads/2021/09/MAPbriefFall2021.pdf

[70] Ling, Y., & Taylor, P. (2021). Effect of controlled vibration dynamics on concrete mixtures. ACI Materials Journal, 118(5). https://doi.org/10.14359/51732981

[71] Hanotin, C.; Kiesgen de Richter, S.; Michot, L. J.; and Marchal, P., "Viscoelasticity of Vibrated Granular Suspensions," Journal of Rheology, V. 59, No. 1, 2015, pp. 253-273. doi: 10.1122/1.4904421

[72] Banfill, P. F. G.; Yongmo, X.; and Domone, P. L. J., "Relationship between the Rheology of Unvibrated Fresh Concrete and Its Flow under Vibration in a Vertical Pipe Apparatus," Magazine of Concrete Research, V. 51, No. 3, 1999, pp. 181-190. doi: 10.1680/macr.1999.51.3.181

[73] Hou, Z. Y., Yuan, Y. Z., Yuan, Z. G., Liang, Y. D., & Zhou, Z. H. (2013). Study on vibrational liquefaction behavior of air-entrained concrete. Advanced Materials Research, 857, 20–26. https://doi.org/10.4028/www.scientific.net/amr.857.20

[74] Pang Qiangte. Concrete Product Technology [M]. Wuhan University of Technology Press, Wuhan, 1990: 51-56.

[75] Kisaku, T., Yoshida, Y., Muto, K., Kurosawa, T., Ito, Y., & Fujiyama, C. (2022). Prediction of effective vibration condition under air void reduction using mortar rheological constant. Engineering Reports, 4(9). https://doi.org/10.1002/eng2.12484

[76] L'Hermite, R., Winterkorn, H. F., & Tournon, G. (1948). The vibration of fresh concrete: Theoretical and experimental investigations. Princeton University, Winterkorn Road Research Institute.

[77] R.L. Hemite, G. Tournnon, Vibration of Fresh Concrete, John Wiley & Sons Inc., 1968, pp. 501–503.

[78] Smith, J., Rampit, R., & Parey, R. (n.d.). Characterization of vibration effects on the internal structure and strength of regular and high strength recycled concrete. Purdue e-Pubs. Retrieved March 7, 2023, from https://docs.lib.purdue.edu/icdcs/2018/mid/9/

[79] Arslan, M., Yozgat, E., Pul, S., & Husem, M. (2011). Effects of vibration time on strength of ordinary and high performance concrete (pp. 270–274).

[80] Tymkowicz, S., and Steffes, R., "Vibration Study for Consolidation of Portland Cement Concrete (Project Research Report No. MLR-95-4)," Iowa Department of Transportation, Ames, IA, Mar. 1999, 96 pp.

[81] Crawley, W. O. (1953). Effect of Vibration on Air Content of Mass Concrete. Journal Proceedings, 49(6), 909–920. https://doi.org/10.14359/11862

[82] Portable vane test to assess structural buildup at rest of self-consolidating concrete. (2011). ACI Materials Journal, 108(6). https://doi.org/10.14359/51683466

[83] Bauer, E., de Sousa, J. G. G., Guimarães, E. A., & Silva, F. G. (2007). Study of the laboratory vane test on mortars. Building and Environment, 42(1), 86–92. https://doi.org/10.1016/j.buildenv.2005.08.016

[84] Test method for compressive strength of cylindrical concrete specimens. (n.d.). https://doi.org/10.1520/c0039_c0039m-11a

[85] How to read a cement mill certificate: Part 2. Go to National Precast Concrete Association. (n.d.). Retrieved April 1, 2023, from https://precast.org/2013/09/how-to-read-a-cement-mill-certificate-part-2/

[86] Oey, T., Kumar, A., Bullard, J. W., Neithalath, N., & Sant, G. (2013). The filler effect: The influence of filler content and surface area on cementitious reaction rates. Journal of the American Ceramic Society, 96(6), 1978–1990. https://doi.org/10.1111/jace.12264

[87] Says, D., & Deepak. (n.d.). How to read a cement mill certificate: Part 1. Go to National Precast Concrete Association. Retrieved April 1, 2023, from https://precast.org/2013/06/how-to-read-a-cement-mill-certificate-part-1/

[88] What is PLC or type il? - euclid chemical. (n.d.). Retrieved April 1, 2023, from https://www.euclidchemical.com/fileshare/Literature/Technical_Bulletins/AD-08-What_Is_PLC_or_Type_IL.pdf

[89] Whiting, D., & Dziedzic, W. (1992). Effects of conventional and high-range water reducers on concrete properties. Portland Cement Association.

[90] Abudawaba, F. & ElGawady, M. (2023). Table 1: Chemical composition of the FA using X-ray fluorescence (XRF). Missouri University of Science and Technology

[91] Haist, M., Link, J., Nicia, D., Leinitz, S., Baumert, C., von Bronk, T., Cotardo, D., Eslami Pirharati, M., Fataei, S., Garrecht, H., Gehlen, C., Hauschildt, I., Ivanova, I., Jesinghausen, S., Klein, C., Krauss, H.-W., Lohaus, L., Lowke, D., Mazanec, O., … Mechtcherine, V. (2020). Interlaboratory study on rheological properties of cement pastes and reference substances: Comparability of measurements performed with different rheometers and measurement geometries. Materials and Structures, 53(4). https://doi.org/10.1617/s11527-020-01477-w

[92] Feys, D., Asghari, A., Ghafari, E., Hernandez, A. M. L., Van Der Vurst, F., De Schutter, G., & Missouri University of Science and Technology. Center for Transportation Infrastructure and Safety. (2014, August 1). Influence of mixing procedure on robustness of self-consolidating concrete. Welcome to ROSA P. Retrieved April 20, 2023, from https://rosap.ntl.bts.gov/view/dot/27962

[93] ASTM C 1712 Test method for rapid assessment of static segregation resistance of self-consolidating concrete using penetration test. (n.d.). https://doi.org/https://www.astm.org/c1712-20.html

[94] ASTM C127 Test method for relative density (specific gravity) and absorption of coarse aggregate. (n.d.).https://ensayosdelaboratoriosuelos.files.wordpress.com/2015/12/astm-c-127.pdf

[95] ASTM C39 Test method for compressive strength of cylindrical concrete specimens. (n.d.). https://doi.org/https://www.astm.org/astm-tpt-174.html

VITA

Paige Marie Toebben was born in Jefferson City, Missouri and raised in Frankenstein, Missouri. She enlisted in the Missouri National Guard in 2013 and graduated from Fatima High School in 2014. She received the degree of Bachelor of Science in Civil Engineering from Missouri University of Science and Technology in May 2021. She was commissioned as a Second Lieutenant in the Missouri Air National Guard in 2023. She received the degree of Master of Science in Civil Engineering from Missouri University of Science and Technology in July 2023.